



# MARTIN-LUTHER-UNIVERSITÄT HALLE-WITTENBERG

Investigations of Anti-infective Agents From  
*Camellia sinensis* and *Kniphofia foliosa*  
and Development of a Microbiological Tool to Study  
Antimycobacterial Activity Under Hypoxic Conditions

## **Kumulative Dissertation**

Zur Erlangung des akademischen Grades  
*Doctor rerum naturalium* (Dr. rer. nat.)

Vorgelegt der  
Naturwissenschaftlichen Fakultät I – Biowissenschaften  
Martin-Luther-Universität Halle-Wittenberg

Von  
Ruth Feilcke, geb. Ilchmann





1. Gutachter/in: Prof. Dr. Peter Imming
2. Gutachter/in: Prof. Dr. Kaleab Asres
3. Gutachter/in: Prof. Dr. Björn Junker

Verteidigung der vorliegenden Arbeit am 12.08.2025



“Am Fluss machten der kleine Tiger und der kleine Bär Rast. Denn  
wer einen Weg zu laufen hat,  
der muss auch mal eine Pause machen.  
Und wer eine Pause macht,  
bekommt mehr mit vom Leben”

JANOSCH

in

„Als Tiger und Bär beinahe das Beste verpassten“



In memory of my grandfather  
and his collection of dried medicinal plants



---

# Acknowledgements

The support of many people has been the cornerstone in finalizing this thesis after working on a variety of projects over some years of my life. Therefore, I would like to begin this thesis by expressing my deep gratitude to these people.

First of all, I want to thank my supervisor PROF. DR. PETER IMMING for offering the opportunity to work on these projects. Our discussions regarding my ideas as well as his tremendous support when I resumed my project after a long break were the backbone of my time as a PhD student. I would also like to thank him very much for giving me the opportunity to contribute to the launch of the TriSusTain project and for his encouragement to contribute to conferences in our field whenever there was the chance to do so. I thank PROF. DR. DR. HC. REINHARD NEUBERT who drew PROF. IMMING'S attention to a young diploma student, interested in medicinal plants from Sub-Saharan Africa. I also thank PROF. DR. KALEAB ASRES and PROF. DR. BJÖRN JUNKER for taking the time to review my work and give their expert opinion on it. I thank DR. MARKUS LANG and DR. ANNELIESE REITER for proof reading the manuscript and their helpful suggestions to improve my English skills.

I would like to express my deep gratitude to my colleagues for shaping an inspiring and fruitful atmosphere to work in: DR. ADRIAN RICHTER, that I shared the longest time with in the lab and who taught me many things in chemistry as well as in microbiology. DR. MARKUS LANG, LEA MANN, DR. RÜDIGER SEIDEL, PAUL R. PALME, FRANZISKA FLESCH, DR. RANA ABDELAZIZ, DR. HENOK ASFAW, DR. LISA LAMPP, DR. THOMAS WETZLAR and MARCEL KLEMM all contributed to the friendship like atmosphere in our working group. Moreover, I thank SABINE DOBBERSTEIN, ILONA FRITSCHKE, JULIA SEISER, DIRK STOLZENHEIN, ANTJE HERBRICH-PETERS and NICOLE GLAUBITZ for their scientific and technical support. I thank the master and diploma students who worked with me on these projects: GEORGETTE ARNOUK and SIMONE WAPPLER. I thank PROF. DR. IAN TIETJEN for helpful discussions on our knipholone anthrone project.

I thank my parents, ESTHER and REINHOLD, my grandmother MARGOT (who supported me with lots of letters from afar) and my parents in law SUSANNE and GERHARD. They all supported us as a family so I could complete my doctoral thesis.

Most of all I would like to thank my husband, ERNST-ULRICH FEILCKE, who's boundless support has accompanied me over all these years. Without him, taking care of our two wonderful children in such a devoted way, I would not have been free to go on with my projects and my thesis. Thank you for your understanding and your open arms, into which I was able to take refuge. KASIMIR and OPHELIA, I am grateful that you have endured my absence from family life on long working days so patiently over the last few months.





# Table of Contents

<b>Acknowledgements .....</b>	<b>I</b>
<b>Table of Contents.....</b>	<b>III</b>
<b>List of Tables.....</b>	<b>VI</b>
<b>List of Figures.....</b>	<b>VI</b>
<b>List of Abbreviations.....</b>	<b>VIII</b>
<b>1) Introduction.....</b>	<b>1</b>
<b>1.1) Plants and Their Secondary Metabolites as Medicines .....</b>	<b>1</b>
<b>1.2) The Prominent Role of Phytopharmaceuticals in Sub-Saharan-Africa .....</b>	<b>2</b>
<b>1.3) Investigated Plants and Secondary Plant Metabolites.....</b>	<b>4</b>
1.3.1) Kniphofia foliosa Hochst.....	4
1.3.2) Camellia sinensis.....	7
<b>1.4) Common Infectious Diseases in Sub-Saharan-Africa.....</b>	<b>9</b>
1.4.1) HIV Infections.....	10
1.4.1.1) General Information on Epidemiology, Disease and Therapy.....	10
1.4.1.2) The Latent Reservoir: A Major Hurdle to an HIV-Cure.....	11
1.4.1.3) Limitations of Current Treatment and Strategies Towards a Cure .....	12
1.4.1.4) Latency Reversal and the Method of Shock and Kill .....	13
1.4.2) Malaria .....	16
1.4.2.1) The life cycle of the parasite .....	17
1.4.3) Tuberculosis and Infections with Non-tuberculous Mycobacteria .....	19
1.4.3.1) General Information on Origin, Epidemiology and Treatment.....	19
1.4.3.2) The Role of Granulomas in Mycobacterial Infections.....	24
1.4.3.3) Non-replicating Persisters of Mycobacteria.....	25
1.4.3.4) Models to Mimic NRPs in Vitro .....	25
1.4.4) Co-Infections of HIV and Mycobacterial Species.....	30
<b>1.5) Antimicrobial Resistance as a Global Threat Using the Example of MRSA .....</b>	<b>31</b>
<b>1.6) The 10/90 Gap.....</b>	<b>32</b>
<b>1.7) Objectives of This Work .....</b>	<b>33</b>
<b>2) Publications.....</b>	<b>35</b>
<b>2.1) Research Article I .....</b>	<b>35</b>
<b>2.2) Research Article II.....</b>	<b>47</b>
<b>2.3) Research Article III.....</b>	<b>58</b>
<b>2.4) Research Article IV .....</b>	<b>76</b>

<b>3) Results and Discussion.....</b>	<b>101</b>
3.1) General Aspects .....	101
3.2) Synthesis and Chemical Characterization of Phytochemical Analogs....	101
3.3) Isolation and Characterization of Secondary Metabolites from Plants.	102
3.4) Characterization and Standardization of Plant Extracts.....	103
3.5) Stability Studies on Phytochemicals.....	103
3.6) Biological Activity Studies.....	104
3.6.1) Antiplasmodial Activity .....	104
3.6.2) Antimycobacterial Activity of Natural Products .....	105
3.6.3) Latency Reversal Activity .....	106
3.6.4) Anti-HIV Activity .....	107
3.6.5) Activity Against <i>S. aureus</i> .....	107
3.6.6) Cytotoxicity Studies .....	108
3.6.7) Further Antimicrobial Activities.....	109
3.7) Discussion of Biological Activity of KA Analogs .....	110
3.8) Microbiological Method Development .....	112
3.8.1) Oxygen Levels of Hypoxic Assays .....	113
3.8.2) Evidence of LOPs Belonging to NRPs.....	114
3.8.2.1) Growth Behaviour.....	114
3.8.2.2) Morphology.....	114
3.8.2.3) Phenotypical Drug Resistance and Sensitivity.....	115
3.8.3) Possible Applications of the LOPs Assay .....	115
3.9) Experiments to Extend the LOP Assay by Using a 3-Hydroxy-Chromone Dye Trehalose Conjugate .....	116
3.9.1) Combination of Hypoxia and Starvation .....	116
3.10) Contribution of the LOPs Assay to the Drug Development Process in our Working Group .....	118
3.10.1) Activity of RNA Polymerase Inhibitors.....	118
3.10.2) Activity of Squaramides against <i>M. abscessus</i> LOPs.....	120
<b>4) Summary.....</b>	<b>121</b>
<b>4) Zusammenfassung .....</b>	<b>122</b>
<b>5) References .....</b>	<b>123</b>
<b>6) Appendices .....</b>	<b>XII</b>
6.1) Experimental part of unpublished results.....	XII
6.1.1) Synthesis and chemical characterization of compounds.....	XII
6.1.2) Agar Diffusion Test as a First Determination of Anti-Infective Activities on Different Microorganisms .....	XVIII

---

6.1.3) Experiments on Starvation Models .....	XVIII
<b>6.2) Supplementary Information Publication I.....</b>	<b>XIX</b>
<b>6.3) Supplementary Information Publication II .....</b>	<b>XXI</b>
<b>6.4) Supplementary Information Publication III.....</b>	<b>XXV</b>
<b>6.5) Supplementary Information Publication IV .....</b>	<b>XXVIII</b>
<b>Publication List.....</b>	<b>XXXII</b>
<b>Curriculum Vitae.....</b>	<b>XXXIV</b>
<b>Eidesstattliche Erklärung .....</b>	<b>XXXV</b>

## List of Tables

Table 1: Cytotoxicity values of <b>KP</b> and <b>KA</b> in different cell lines, evaluated in literature studies.	6
Table 2: Treatment regimens for pulmonary disease caused by mycobacterial infections....	21
Table 3: Comparative data on epidemiology of NTM-PD in SSA and countries of the Western world.....	23
Table 4: Selection of hypoxic models to study NRPs of mycobacteria.....	28
Table 5: Biological activity of 1,8-dihydroxyanthrones and anthraquinones.....	111

## List of Figures

Figure 1: <i>Kniphofia foliosa</i> and selected phytochemicals thereof. ....	4
Figure 2: Chemical structures of the most prominent catechins of <i>camellia sinensis</i> and flavan-3-ol, the base scaffold of catechins.....	7
Figure 3: Map of SSA Region and overview of cases and deaths of the three major communicable diseases in the WHO African Region in comparison to the numbers worldwide.....	9
Figure 4: Different approaches to an HIV cure that are currently investigated. ....	13
Figure 5: Illustration of the principal idea of the shock and kill approach. ....	14
Figure 6: Chemical structures of quinine and artemisinin, antiplasmodial components of <i>Cinchona pubescens</i> and <i>Artemisia annua</i> . ....	16
Figure 7: Life cycle of the plasmodium parasite.....	17
Figure 8: Estimated TB incidence rates in 2022. ....	19
Figure 9: Microscopic pictures of two different non-tuberculous mycobacterial species. ....	20
Figure 10: Regional estimates of TB incidence [absolute numbers] disaggregated by age and sex, compared with case notifications 2022. ....	22
Figure 11: Formation of granulomas in lung lesions of TB patients.....	24
Figure 12: Models to study non-replicating persisters of <i>M. tuberculosis</i> . ....	26
Figure 13: Methylene blue as an indicator for oxygen concentration in hypoxic setups. ....	27
Figure 14: Global trends in the estimated number of deaths caused by TB and HIV.....	30
Figure 15: Retrosynthetic idea to access 1,8 dihydroxyanthrones.....	101
Figure 16: Synthesized anthrones and anthraquinones. ....	102
Figure 17: Effects of 1,8 dihydroxyanthrones and analogs on J-lat 9.2 cells. ....	106
Figure 18: Development of object numbers in previously non-starved (orange) and starved (green) cultures upon nutrition availability.....	117
Figure 19: Regrowth of differently pre-treated <i>M. abscessus</i> cultures in ADS containing 7H9 medium under aerobic (5 % CO <sub>2</sub> ) conditions. ....	117

---

Figure 20: Chemical structure of the initial hit (MMV688845) and the lead compound 2 of the compound class of AAPs.....	119
Figure 21: Dose dependent activity of RNA polymerase inhibitors. ....	119
Figure 22: General structure of squaramides and dose dependent activity of one squaramide in aerobic (red) and hypoxic (blue) conditions on <i>M. abscessus</i> .....	120

## List of Abbreviations

3HCT .....	3-hydroxy-chromone-dye trehalose conjugate
AAP .....	<i>N</i> α-aroyl- <i>N</i> -aryl-Phenylalanine Amides
AC .....	anthracenone
ADS .....	albumin dextrose saline
AIDS .....	Acquired Immune Deficiency Syndrome
AMR .....	antimicrobial resistance
AN .....	anthrone
APCI .....	atmospheric pressure chemical ionization
AQ .....	anthraquinone
ART .....	anti-retroviral therapy
ARV .....	anti-retrovirals
bNAB .....	broadly neutralizing antibody
CAR-T .....	chimeric antigen receptor T cell
CD .....	cluster of differentiation
CDC .....	Centers for Disease Control and Prevention
CF .....	cystic fibrosis
COPD .....	chronic obstructive pulmonary disease
CPT .....	conventional pharmacotherapy
CRISPR .....	clustered regularly interspaced short palindromic repeats
DiaMOND .....	Diagonal measurement of n-way drug interactions
DMF .....	dimethylformamide
DMSO .....	dimethylsulfoxide
DMT .....	DNA methyltransferase
DNA .....	desoxy-ribonucleic acid
DosR .....	Dormancy survival regulator
DS .....	drug susceptible
DSM .....	Deutsche Sammlung für Mikroorganismen
EGCG .....	epigallocatechin gallate
GFP .....	green fluorescent protein
HDAC .....	Histone deacetylase
HIV .....	Human Immunodeficiency virus
HMT .....	Histone methyltransferase
HPLC .....	high performance liquid chromatography
HTS .....	high-throughput screening
IC .....	inhibitory concentration
ICD .....	International Statistical Classification of Diseases and Related Health Problems
LOP .....	low-oxygen persister
LORA .....	low-oxygen-recovery-assay
LR .....	latency reversing
LTR .....	long terminal repeat
MAB .....	<i>Mycobacterium abscessus</i>
MAC .....	<i>Mycobacterium avium</i> complex
MB .....	methylene blue
MDR .....	multidrug resistant
MIC .....	minimum inhibitory concentration
mRNA .....	mitochondrial ribonucleic acid
MRSA .....	methicillin resistant <i>S. aureus</i>
MS .....	mass spectrometry

---

MSSA .....	methicillin susceptible <i>S. aureus</i>
NMR .....	nuclear magnetic resonance spectroscopy
NR .....	nitrate reductase
NRP .....	non-replicating persister
NTM.....	Non-tuberculous mycobacteria
p-ANAPL.....	pan-African natural products library
PBS .....	phosphate buffered saline
PD.....	pulmonary disease
PFA .....	para formaldehyde
PKC.....	protein kinase C
PLWHIV .....	people living with HIV
RGM.....	rapidly growing mycobacteria
RNA .....	ribonucleic acid
RT .....	reverse transcriptase
SFU.....	Simon Fraser University
SSA.....	sub-Saharan Africa
ssRNA.....	single-stranded RNA
TB.....	tuberculosis
TLC.....	thin layer chromatography
TW .....	tween 80/polysorbate 80
UV .....	ultra violet
WHO.....	World Health Organisation
XDR .....	extensively drug resistant

#### Notes on Formatting

Scientific names of plants, bacteria, fungi and parasites as well as all Latin expressions are written in *italics*, names of plant families and person's names are printed in SMALL CAPITALS. Compound names and publications are given in **bold**.





# 1) Introduction

This thesis deals with anti-infective constituents from African (medicinal) plants in the context of the most important communicable diseases in this part of the world: HIV, Malaria and mycobacterial infections. Two approaches are therefore combined: The first approach focuses on the constituents itself and presents information on synthetical, analytical and microbiological investigations to evaluate their anti-infective potential. Three publications resulted that contribute to the cumulative character of this thesis. The second approach is a methodological one and describes the development of a novel microbiological tool that can be used to study plant constituents and other compounds on an important yet neglected part of mycobacterial populations – the persister cells. This tool was designed to be applicable for laboratories that do not have access to extensive instrumentation with especially sub-Saharan laboratories in mind. By developing this method, I hope to contribute to research on medicinal plants close to their natural habitats. The fourth publication of this cumulative thesis resulted from this part of the project.

The introductory section of this thesis provides information on phytopharmaceuticals in the context of sub-Saharan countries, on the investigated plant metabolites and on the major communicable diseases in this region. As antimicrobial resistance is a global threat, the last section in this introductory chapter is dedicated exemplarily to the background of methicillin resistant *S. aureus* infections. Because of drug scarcity, resistance is less problematic in sub-Saharan Africa (SSA) compared to industrialized countries. For example, prevalence of multidrug resistant tuberculosis (MDR-TB) is generally low in SSA with the Republic of South Africa showing the highest prevalence among those countries [1].

## 1.1) Plants and Their Secondary Metabolites as Medicines

Plants play an important role in human life. They were essential for food production but were also early recognized for effects other than serving as an energy source. There is archaeological evidence of plants being used as medicines already in early times of mankind of which only two are named for illustrative purpose: Chamazulene present on dental calculus from a Neanderthal individual from Spain [2] and medicinal plants recovered from Ötzi's body [3]. The latter example dates back to 3400-3100 BC. Throughout history every culture developed their own "traditional medicine" depending on the availability of plants and animals found in their habitat [2]. As the mentioned examples show, all over the world, mankind relied on plants to treat sickness and disease. In the early 19<sup>th</sup> century, several discoveries, e.g. the extraction of morphine from opium in 1804 by Sertürner, led to the understanding that certain ingredients of plants are responsible for the therapeutic effect of the plant as a whole. These ingredients were later understood as secondary plant metabolites. In contrast to primary metabolism that produces compounds which are essential for growth and development of a plant, secondary metabolism leads to molecules that are not directly relevant for physiological processes as growth and reproduction.

Secondary metabolites help the plant to survive in its special environment. Those include for example flowering dyes to attract insects or molecules that protect them from herbivores. The extraction and purification of isolated secondary plant metabolites and their use instead of the plant or its crude extracts was the starting point of **conventional pharmacotherapy** (CPT) that is widespread in industrialized countries nowadays. CPT mostly uses well characterized compounds instead of plants and is often referred to as ‘modern’ medicine in contrast to ‘traditional’ medicine. These terms can imply a devaluation of certain treatment approaches. Within this thesis, I will therefore use the expression CPT instead to describe the approach to diagnose an ailment according to the international classification of diseases (ICD) and treat it according to official guidelines. These official guidelines are based on the evidence of clinical studies. The expression ‘**traditional**’ **medicine** is used to emphasize the wealth of knowledge that has been collected and passed on over many centuries and thus highlights the richness of the respective culture. However, this thesis focuses on plant metabolites although traditional medicine often includes the use of animal derived products and different inorganic substances. Therefore, and to avoid the association with ‘old-fashioned’, the terms **phytomedicine**, **phytochemicals** and **medicinal plants** are used instead unless direct or indirect citations hinder it.

## 1.2) The Prominent Role of Phytopharmaceuticals in Sub-Saharan-Africa

The World Health Organization (WHO) aimed to strengthen the role of the above mentioned traditional medicine within their member states by publishing a traditional medicine strategy in 2013 [4]<sup>1</sup>. A large majority of people living in the WHO African region heavily rely on medicinal plants for their health. Three documented examples among many are the population of Ethiopia [5, 6], Tanzania [7] and Uganda [8] where a majority relies on phytomedicines. Until today, phytomedicine is far from being supplanted by CPT in Ethiopia, not even in urban centers of the country where it is most available compared to the rural areas [9]. HILL explains this by the history “by which biomedicine [equivalent to CPT] became deeply imbricated with local therapeutic tools and techniques” [9], page 75. The African’s “belief in traditional and herbal medicine” was especially visible during the COVID-19 pandemic and “resulted in the local production of medicine in Africa against COVID-19” [10]. COVID organics® was produced in Madagascar from *Artemisia*, a plant that is highly effective against Malaria. However, the clinical efficacy of this product remains unclear at the time of writing, but serves as example of the importance of phytomedicine in SSA until today.

It would be reductionistic to explain the importance of phytomedicine within the ‘therapeutic landscape’ [9] in SSA countries with economic reasons or the availability thereof only. It also roots in the different understanding of health and illness in industrialized and

---

<sup>1</sup> There is an updated draft of this strategy currently under consultation that will probably soon be published: The draft is available online at [https://cdn.who.int/media/docs/default-source/tci/draft-traditional-medicine-strategy-2025-2034.pdf?sfvrsn=dd350962\\_1](https://cdn.who.int/media/docs/default-source/tci/draft-traditional-medicine-strategy-2025-2034.pdf?sfvrsn=dd350962_1) (last visited October 2024).

African countries. HILL for example describes the understanding of health by Highland Ethiopians “as a state of equilibrium” where the “equilibrium between organs in the body is equally important as a state of equilibrium between the individual body and the larger social body” and highlights the crucial role of emotional and spiritual well-being in physical health [9]. The overall goal of [also spiritual] “rituals is the relief from illness and misfortune” [9]. Similarly, healing in Botswana is embedded in a philosophy of relationship between individuals, nature and ancestors. This philosophy is termed “botho” (Setswana: “ubuntu”) and also understands diseases as an imbalance in these relationships [11]. Traditional healers therefore pay attention to several aspects of illness which often also have religious connotations using herbal medicine. Innocent *et al.* also highlight the discrepancies between “traditional African and modern Western medicine” in “the description of symptoms and concepts of underlying diseases” in their review on Tanzanian medicinal plants for the treatment of respiratory bacterial infections [7]. At the moment of writing, several countries are in a process of balancing the preservation of traditional knowledge and at the same time of their culture and the regulation of herbal medicine distribution. A study on the complex area of herbal medicine regulation in Nigeria could serve as an example [12].

### 1.3) Investigated Plants and Secondary Plant Metabolites

The following chapter describes two plants and their constituents that were the main focus of the first part of this thesis.

#### 1.3.1) *Kniphofia foliosa* Hochst

*Kniphofia foliosa* L. (ASPHODELACEAE) is a plant within the genus *Kniphofia* [13]. The most prominent member of this plant family is *Aloe vera*. *Kniphofia* species are endemic mostly to Africa and their ethnomedicinal uses have been reviewed [14, 15]. *K. foliosa* is found in the mountainous regions of Ethiopia [13]. A picture of its inflorescence is shown in Figure 1. The plant is used in traditional Ethiopian medicine to treat wounds, abdominal cramps, cervical and breast cancer, gonorrhea and hepatitis B [16]. A variety of secondary plant metabolites have been isolated from different parts of this plant [15, 17] of which some are presented in Figure 1. The main chemical classes of these phytochemicals are monomeric and dimeric anthraquinones as well as different phenyl anthraquinones and phenyl anthrones. They are structurally related to crysophanol. In addition to these, two naphthalene derivatives and another compound were isolated [16].

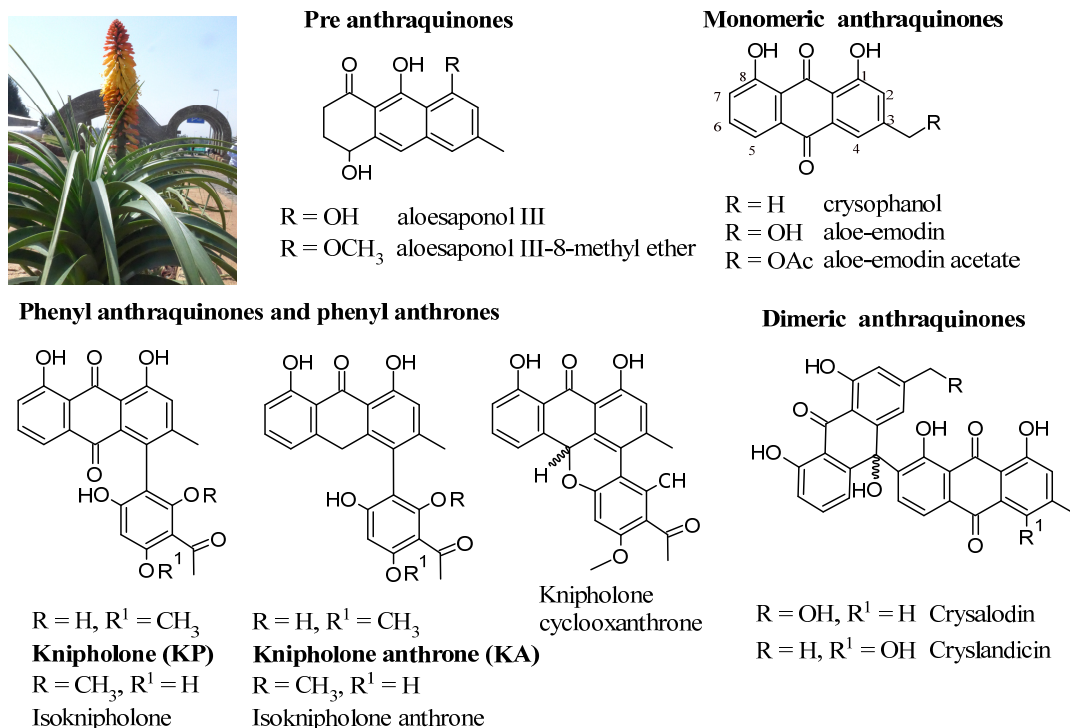


Figure 1: *Kniphofia foliosa*<sup>2</sup> and selected phytochemicals thereof.

<sup>2</sup> The picture was taken in Gullele Botanical Garden, Ethiopia (© TriSusTain: <https://trisustain.uni-halle.de/>).

The main characteristic of anthraquinones and related phytochemicals of the genus *Kniphofia* are the 1,8-dihydroxylation and the methylation in position 3 of the anthraquinone nucleus. DAGNE AND STEGLICH were the first to characterize constituents of the genus *Kniphofia* and isolated the anthraquinone knipholone (**KP**) in 1984 from the roots of *K. foliosa* [18]. The respective anthrone, knipholone anthrone (**KA**), was described ten years later and isolated from the stem of the plant [19]. Investigations on **KP** and **KA** were central to one of the projects in this thesis and are therefore described in some detail in the following section.

**Axial chirality of phenyl derivatives.** The methyl group in position 3 of the anthraquinone scaffold hinders rotation along the phenyl axis. This leads to axial chirality. BRINGMANN and his group presented the first and atropo enantioselective total synthesis of knipholone in 2001 [20]. Both molecules were proven to be *P*-configured by circular dichroism [21].

Applications in traditional medicine led to several *in vitro* studies to confirm pharmacological activity. Some studies were performed on crude extracts or fractionated extracts but several provided information on isolated compounds of the plant as well. Those revealed **KP** and **KA** to possess several biological activities.

**Antiplasmodial activity.** Among the various biological activities of this compound class, this is probably the best studied. Several groups have provided evidence on the activity against *Plasmodium* species either of extracts or fractionated extracts of the plant's roots and rhizomes, or of isolated compounds [22-24]. The crude extract of *K. foliosa* rhizomes showed antiplasmodial activity also *in vivo* [25]. One suggestion on the mechanism of action is the introduction of free radicals leading to oxidative stress or the intervention in heme detoxification [26]. Recently a molecular docking study suggested glutathione S-transferase as the potential target of knipholone in *P. falciparum* [27]. In contrast, ALEBACHEW *et al.* suggested *P. falciparum* I-lactate dehydrogenase as the potential target [25]. Thus, the mechanism of action still needs to be verified. However, all studies provide evidence that phytochemicals of this plant have antiplasmodial potential. When **KP** was investigated in comparison to **KA**, the anthrone was slightly more active [22, 23] but the most active antiplasmodial component of *K. foliosa* was joziknipholone A [23, 28].

**Leukotriene metabolism inhibition.** WUBE *et al.* reported **KP** to inhibit the leukotriene metabolism and suggested the compound as a potential anti-inflammatory agent [29]. **KA** was not included in this study; thus, its leukotriene metabolism inhibition potential is unclear at the time of writing.

**Anti-oxidant and pro-oxidant activity.** HABTEMARIAM reported the antioxidant potential of **KA** to be twice as high as epicatechin (the structure of this catechin is found on page 7 in section 1.3.2). **KA** scavenged radicals and complexed free iron ions [30]. In contrast, **KP** failed in another study to scavenge free radicals [29]. In the presence of  $\text{Cu}^{2+}$ , the antioxidant activity of **KA** was reversed to pro-oxidant. **KA** generated reactive oxygen species by reducing  $\text{Cu}^{2+}$  to  $\text{Cu}^{+}$  what led to DNA damage in a concentration dependent manner [31].

**Cytotoxicity.** HABTEMARIAM showed **KA** to be cytotoxic against different cancer cell lines and observed a necrotic cell death by loss of membrane integrity instead of signs for

apoptosis [32]. In contrast, no cytotoxic activity could be observed for **KP** up to 240  $\mu\text{M}$ . The difference in cytotoxicity between both compounds was in line with BRINGMANN'S result on other mammalian cell lines [22]. Table 1 lists available data on cytotoxicity studies for both compounds.

*Table 1: Cytotoxicity values of **KP** and **KA** in different cell lines, evaluated in literature studies.*

	<b>KP</b>		<b>KA</b>		Ref
Human cell lines	THP-1 <sup>a</sup>	IC <sub>50</sub> >240 $\mu\text{M}$	THP-1 <sup>a</sup>	IC <sub>50</sub> 0.9 $\mu\text{M}$	[32]
	U937 <sup>b</sup>	IC <sub>50</sub> >240 $\mu\text{M}$	U937 <sup>b</sup>	IC <sub>50</sub> 0.5 $\mu\text{M}$	[32]
Other mammalian cells	L6 <sup>c</sup>	MIC <sup>y</sup> 76 $\mu\text{M}$	L6 <sup>c</sup>	MIC <sup>1</sup> 8.8 $\mu\text{M}$	[22]
	Macroph <sup>d</sup>	MIC <sup>1</sup> >69 $\mu\text{M}$	Macroph <sup>d</sup>	MIC <sup>1</sup> <24 $\mu\text{M}$	[22]
	B16 <sup>e</sup>	IC <sub>50</sub> >240 $\mu\text{M}$	B16 <sup>e</sup>	IC <sub>50</sub> 3.3 $\mu\text{M}$	[32]
	RAW264.7 <sup>f</sup>	IC <sub>50</sub> >240 $\mu\text{M}$	RAW264.7 <sup>f</sup>	IC <sub>50</sub> 1.6 $\mu\text{M}$	[32]
Brine shrimp assay		ED <sub>50</sub> 580 $\mu\text{M}$	n.d.		[29]
Acute oral toxicity in mice	evaluated for fractionated hydroalcoholic extract instead of isolated compounds; save at 2000 mg/kg				[25]

<sup>a</sup> human acute monocytic leukaemia cells; <sup>b</sup> promonocytic U937 leukaemic cells; <sup>c</sup> rat skeletal muscle myoblast; <sup>d</sup> mouse peritoneal macrophages; <sup>e</sup> mouse melanoma cells; <sup>f</sup> mouse monocyte tumor; <sup>1</sup> the authors did not further specify what minimal inhibitory meant.

### 1.3.2) *Camellia sinensis*

*Camellia sinensis* (THEACEAE) is a shrub in the genus *Camellia*. Today, two varieties of this species (*C. sinensis* var. *sinensis* and *C. sinensis* var. *assamica*) are mainly grown to harvest the leaves for the production of tea. Tea is an aqueous extract of the leaves which is consumed in different cultures globally. The huge variety of tea originates from different handling after harvesting. Green tea is prepared from dried leaves and black tea is prepared from crushed leaves that are subjected to an oxidation process at approximately 40°C. In 2017, countries of the African continent produced about 20 % of the world's black tea production - 656 000 tons - and accounted for about 5 % of the world's black tea consumption [33]. Even though produced compared to consumed amounts of black tea were higher in many of these countries, it is a common beverage and easily accessible throughout sub-Saharan Africa.

Tea is a rich source of catechins. Those polyphenolic plant metabolites belong to the large group of flavonoids. Catechins are analogues of flavan-3-ol whose chemical structure is displayed in Figure 2 together with the main catechins of tea. Due to the oxidation process, the composition of catechins is different for black and green tea. In green tea epigallocatechin gallate (**EGCG**) is the main catechin while in black tea oligomeric oxidation products of catechins dominate [34]. In plants they are mostly found as glycosides.

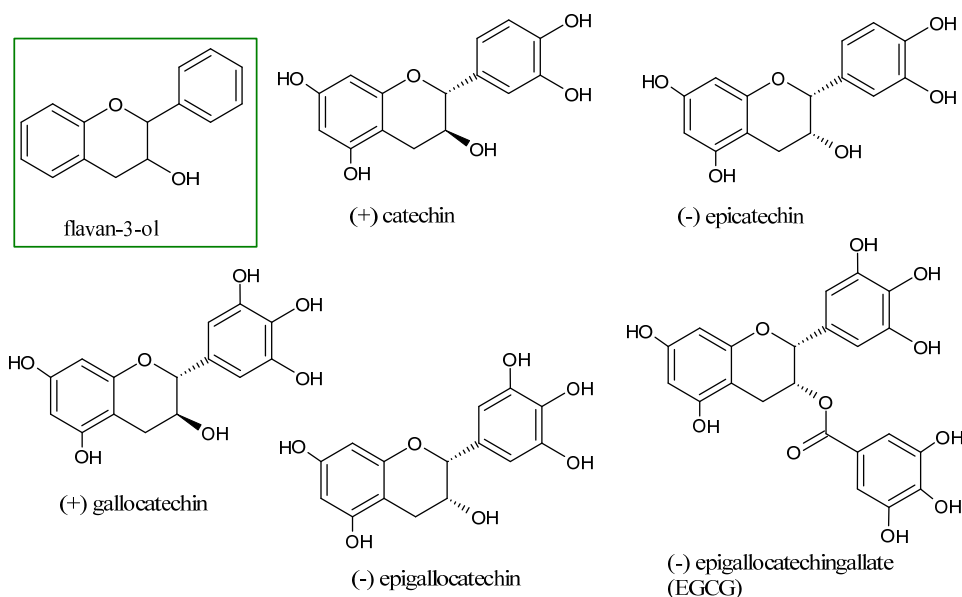


Figure 2: Chemical structures of the most prominent catechins of *camellia sinensis* and flavan-3-ol, the base scaffold of catechins.

Catechins have antioxidant and radical scavenging activities. The main catechin in green tea, EGCG, was reported to be antibacterial (reviewed in [35, 36]), but the first report of the **anti-infective activity** of tea is almost 120 years old [37]. Catechins and other natural phenolic compounds were also reported to act **antiplasmodial** (as reviewed in [38]). However, investigations in mice proved the opposite to be true *in vivo* [38].

Among the antibacterial activity of tea extracts and tea catechins, the activity against methicillin resistant *Staphylococcus aureus* (MRSA) [39] is especially interesting due to the

importance of this pathogen (as explained from page 31 on (Antimicrobial Resistance, section, 1.5)). The efficacy of tea catechins on MRSA was investigated in some **clinical studies**<sup>3</sup>. Catechins, when inhaled, were able to reduce MRSA in sputum in 47 % of the cases compared to 15 % of the control group [40] and MRSA disappeared in half of the decubitus patients when debridement was performed with green tea compared to no change in the control group where debridement was performed with saline.

In addition, catechins are reported to act **synergistically** with different antibacterial drugs offering the opportunity to support the treatment of infections with CPT [36]. Together with its excellent safety profile, as proven by the long history of tea consumption and its widespread accessibility and low costs, this could be an interesting herb in prevention of infections or in supporting the treatment of the same.

The poor **bioavailability** of even the monomeric catechins (as reviewed in [44]) hampers their use in the treatment of systematic infections. In most cases, even very high doses of 800 mg EGCG only resulted in less than 5 µmol/L EGCG in the plasma (see Table 4 publication [44]).

---

<sup>3</sup> There are only a few clinical studies that investigated the effect of catechins on MRSA [40-43] which could be due to the high cost of these investigations in contrast to low reimbursement companies expect due to patent issues with natural compounds.



## 1.4) Common Infectious Diseases in Sub-Saharan-Africa

The WHO classifies HIV, malaria and tuberculosis (TB) as the three major communicable diseases in the WHO African Region [45]. In addition, this region represents the highest percentage of cases worldwide for two of the diseases: Two thirds of all people living with HIV globally live in the African region and this region carries 95 % of the global malaria burden. Additionally, 23 % of all TB cases and 35 % of TB related deaths were found here in 2021 [45]. The top 10 countries facing the highest combined burden of malaria, TB and HIV in the African Region all belong to SSA and are highlighted in Figure 3 within countries belonging to SSA. The importance of these infectious diseases is also reflected by the fact that monographs of the International Pharmacopoeia [46] focus on active pharmaceutical ingredients of these indications<sup>4</sup>.

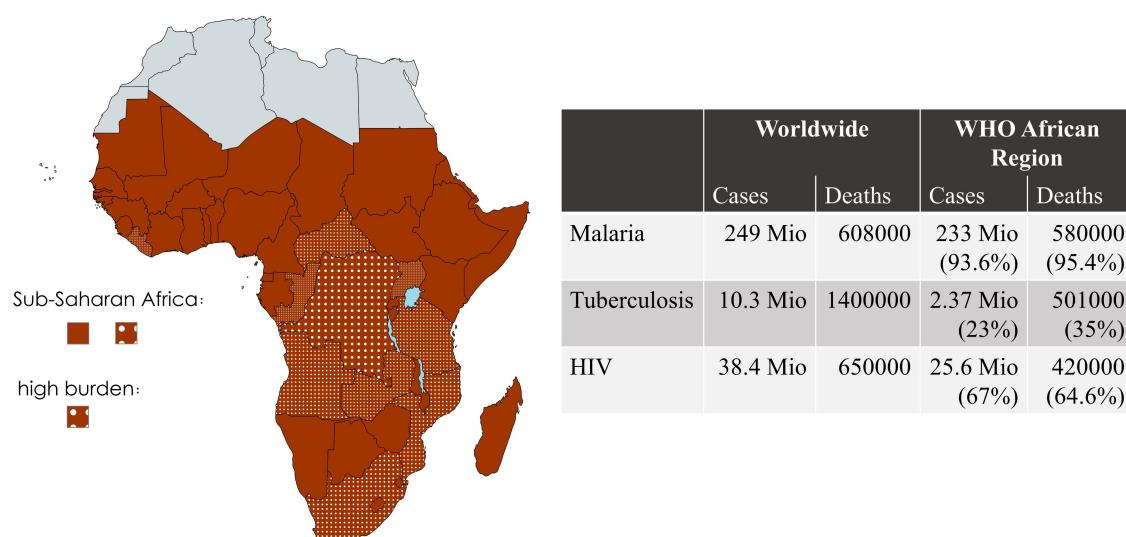


*Figure 3: Map of SSA Region and overview of cases and deaths of the three major communicable diseases in the WHO African Region in comparison to the numbers worldwide.*

*Countries belonging to SSA are highlighted in red within the continent of Africa. The ten countries with the highest combined burden of malaria, HIV and TB in 2021 are highlighted with white dots<sup>5</sup>. Relative numbers were calculated compared to numbers worldwide.*

The following section gives a short introduction into each of these infectious diseases and presents aspects that are relevant for the objective and results of this thesis. Although malaria is the main communicable disease within SSA, it played a minor role in this thesis. This is why the relevant chapter is kept short compared to HIV and mycobacterial infections.

<sup>4</sup> "The role of pharmacopeias in sustainable quality control – an African perspective" talk by Prof. Dr. Eliangiringa Kaale from Muhimbili University of Health and Applied Sciences, Dar-es-Salaam, Tanzania given in Halle (Saale) on 16<sup>th</sup> October 2024.

Access to the Ph. Int. via: <https://digicollections.net/phint/2022/index.html#p/home>

<sup>5</sup> This map was generated with mapchart.net using data from [45].

### **1.4.1) HIV Infections**

#### **1.4.1.1) General Information on Epidemiology, Disease and Therapy**

The HIV epidemic was first recognized in the 1980s. In 2023, 39.9 million people globally lived with HIV (PLWHIV, people living with HIV) with 630 000 HIV related deaths worldwide (1.6 % of PLWHIV) [47]. As already stated, the WHO African Region is disproportionally affected by this epidemic, carrying 65 % of the cases worldwide with HIV still remaining the leading cause of death in southern Africa [48]. There was tremendous effort to reduce HIV in the last years being successful in many sub-Saharan countries [45]. However, children in this region are still accounting for 81 % of all new HIV infections among children worldwide [47].

An infection with the human immunodeficiency virus 1 (HIV) affects CD4<sup>+</sup> cells thereby causing a destruction of the immune system of the host that becomes visible by decreasing numbers of CD4<sup>+</sup> T cells. When CD4<sup>+</sup> T cells fall below 200 cells/ $\mu$ L, the most advanced stage of infection is reached with the immune system weakened to an extent that opportunistic infections by various pathogens are acquired and/or cancer is developed. The symptomatic presentation of an HIV related illness (a list of more than 20 diseases) together with a verified HIV infection is called Acquired Immune Deficiency Syndrome (AIDS). These secondary diseases are the leading causes of death for PLWHIV. Untreated, HIV infections progress to AIDS with typically only three years to survive this diagnosis as stated by the Center for Disease Control and Prevention (CDC)<sup>6</sup>. With anti-retroviral therapy (ART), the infection can be turned into a manageable disease with life-long medications.

Over 40 years of research have led to a great understanding of the HIV-1 virus, its components and their role in the life cycle of the virus and the infection of human cells as reviewed in e.g. [49]. This introductory section on HIV instead focuses on the virus's ability to integrate into the host's genome and how this leads to the formation of a viral reservoir. Furthermore, the limitations of current treatment options are explained to understand the necessity of a new treatment approach that aims for a cure of the infection instead of only suppressing viral replication.

HIV-1 is a retrovirus within the genus *Lentivirus*. Its single stranded RNA (ssRNA) together with different proteins is encapsulated and protected by different membranes. In contrast to RNA-viruses which carry their genome as mRNA that can directly be translated into proteins by the host's RNA-polymerase, retroviruses need to transcribe their RNA genome 'back' into DNA in order to make it available for protein biosynthesis. Two viral proteins play a major role in this process: The viral reverse transcriptase (RT) and the viral integrase. As mentioned above, HIV targets CD4<sup>+</sup> cells, because it needs their distinct membrane proteins to enter cells. The viral life cycle contains a step in which the viral genome is integrated by the integrase into the host cells' DNA.

---

<sup>6</sup> Available from <https://www.cdc.gov/hiv/about/index.html>; accessed 20<sup>th</sup> September 2024.

Current antiretrovirals (ARV) target various steps of the viral life cycle. Today, ART is a combination therapy, introduced in 1996. It is also referred to as highly active antiretroviral therapy as it inhibits many different targets. Current regimes are able to suppress viremia to undetectable levels. The overall goals of HIV therapy are to restore CD4<sup>+</sup> cells, to keep the immune system working, prevent acquiring of opportunistic infections and the progression to AIDS in order to expand life expectancy and ensure a normal life of PLWHIV. ART is also used for prevention<sup>7</sup> and as a pre- and post-exposure prophylaxis of uninfected people living at high risk of HIV infections. Guidelines are provided to treat patients according to their situation (adult and pediatric ART, perinatal therapy, therapy of co-infections).

#### *1.4.1.2) The Latent Reservoir: A Major Hurdle to an HIV-Cure*

Upon ART interruption, a viral rebound is observed within two to eight weeks [50]. This viral rebound arises from a latent reservoir and life-long ART is necessary to prevent reseeding from this reservoir. This chapter will explain why only a small portion of infected cells make up this reservoir and describe the molecular mechanisms that are the basis of this phenomenon.

Viral DNA only contributes to the reservoir if it is integrated in the hosts genome (pro-viral DNA), because extrachromosomal genetic information persists only for a few days [51]. In addition, the integrated DNA needs to encode for replication competent viruses. This is not the case for about 90-95 % of pro-viral cells sampled from individuals because they are genetically defect [52]. However, these defective pro-viruses can still activate the host's immune surveillance after partly expression of viral antigens and play a role in HIV-associated inflammation [53]. Only a small portion of pro-viral cells (about 5-10 %) harbor an intact pro-virus and built up the 'latent reservoir' with the majority found in **CD4<sup>+</sup> memory T cells**<sup>8</sup>. This latent reservoir is already established in early stages of the infection [55] and immediate initiation of ART after HIV infection can only lead to a reduced reservoir size but is not able to prevent the formation of it [50]. Latently infected cells evade the immune surveillance due to either very low or no level of viral transcription. This leads to a very long half-life of the CD4<sup>+</sup> memory T cell reservoir which is persistent even on long-term ART and estimated at 44 months [56, 57].

The current scientific consensus understands latency in HIV infections as "a byproduct of the achievement of immunological memory" [50, 58]: activation of naïve T cells results in activated effector T cells. These are more susceptible to HIV infection due to higher expression of CCR5 than newly activated CD4<sup>+</sup> T cells. CCR5 is a coreceptor that is important during entry of HIV into host cells. Consequently, effector T cells are more likely to get

---

<sup>7</sup> Treatment as prevention is based on the fact that suppression of viral load in PLWHIV to undetectable limits prevents transmission of HIV to uninfected people (U=U meaning undetectable = untransmittable).

<sup>8</sup> A recent study highlighted the role of microglia as cells of the latent reservoir due to their long lifespan and their resistance to viral cytopathy. In addition these cells are hard to penetrate by ARVs [54].

infected. At the same time, some of these effector T cells will enter a quiescent state to preserve immunological memory (a physiological process). Because this process involves gene silencing to establish the quiescent state of resting memory cells it results in resting infected cells that do not express HIV proteins and are therefore invisible to the immune system. Most other CD4<sup>+</sup> cells (monocytes, macrophages, dendritic cells and various subtypes of T cells) that were infected are actively proliferating CD4<sup>+</sup> cells and will be eliminated either by host immune surveillance or cytolytic effects.

The molecular mechanisms involved in latency mostly belong to epigenetic regulation mechanisms who remodel the chromatin structure to enhance or prevent transcription initiation and or elongation [50, 59]. This is mostly done by regulation of the position of the respective nucleosomes. Those mechanisms include DNA methylation, histone deacetylation and histone methylation that regulate the pro-viral promoter long terminal repeat (LTR). The HIV-1 LTR belongs to the group of bivalent promoters that contain activating as well as transcription repressing histones leading to a “reversible epigenetically repressed state poised for rapid transcription” [50]. Another molecular mechanism of latency is the sequestration of important signaling factors for transcription within the cytosol together with very low concentrations of the host’s transcription elongation factor that also plays a critical role in viral transcription initiation [50].

#### *1.4.1.3) Limitations of Current Treatment and Strategies Towards a Cure*

Current treatment options are markedly effective and life expectancy has been substantially prolonged by ART. Nevertheless, some limitations remain. Although new antiretroviral drugs significantly reduced side effects compared to the first generation of ARV, a life-long medication still includes the risk of toxic side effects cumulated over a long therapeutic period [48]. PLWHIV also still have a higher risk of several comorbidities compared to HIV negative people such as HIV associated neurocognitive disorder [54]. In addition, resistance towards ART is still an issue [60], although it has become fewer since the replacement of the single by a combination therapy [48]. This is the case especially in countries with “restricted access to multiple classes of ARV” [59]. One reason for a high resistance rate is the nature of the viral reverse gene transcription because the RT lacks a proofreading mechanism. Eventually, ART is no cure of the infection even though it suppresses viremia to undetectable levels in the blood of PLWHIV. There is always the possibility of viral rebound from infected cells after ART discontinuation [48].

Research is undertaken to tackle this problem and several approaches are investigated in order to cure HIV. An overview is given in Figure 4.

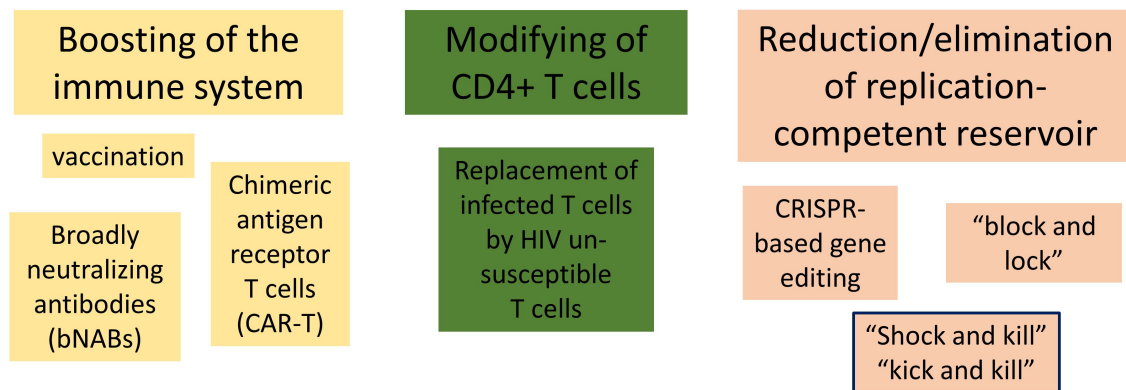


Figure 4: Different approaches to an HIV cure that are currently investigated.

The first area of research aims to boost the immune system by vaccination, the use of broadly neutralizing antibodies (bNABs) [61, 62] or chimeric antigen receptor T cells (CAR-T, a genetically modified CD8<sup>+</sup> T cell) to eradicate infected cells [63]. Another research field was inspired by the few examples of HIV patients that have been cured after undergoing a chemotherapy with subsequent haematopoietic stem cell transplantation. Those transplanted cells carried a mutation that made them HIV unsusceptible [64]. Therefore, this approach aims to modify CD4<sup>+</sup> T cells to imitate the described scenario [65]. The third field deals with the elimination or silencing of the latent reservoir. One strategy in this field uses CRISPR-based gene editing as a snipping tool to eliminate integrated HIV genes from the host's genome [66]. Another approach is to increase the latency of the virus by epigenetic changes to make a transcription of integrated HIV genes impossible. This approach is referred to as "block and lock" [67]. The third approach aims for the opposite by reactivating viral expression in order to make infected cells visible to the immune system which then either eliminates these cells precisely or cells will be eliminated due to viral damage [68-70].

As part of this thesis, plant constituents were investigated for their latency reversal (LR) activity. Therefore, the next chapter will explain this approach to an HIV cure in more detail.

#### 1.4.1.4) Latency Reversal and the Method of Shock and Kill

The basic idea of the 'shock and kill' also known as 'kick and kill' approach is shown in Figure 5. The first part represents the latent reservoir which is 'invisible' to the immune system due to missing expression of viral genes. This reservoir was discussed earlier (see 1.4.1.2) and is a major hurdle to a sterilizing cure of HIV infections. Infected cells can be made 'visible' by using LR agents that promote transcription of integrated viral genes. The killing of these infected cells then occurs either by cytolytic viral effects or due to cells of the immune system recognizing and eliminating those infected cells. A simultaneous ART is essential to avoid reseeding of viral particles in uninfected cells thereby preventing the enlargement of the reservoir. Whereas the first approaches in this field relied on the cytolytic effect of the virus to kill its reservoir or the unboosted immune system only (referred to as

“non-specific latency reversal or LRA 1.0”) later approaches focused on a more immune system-based approach (“immune-based latency reversal or LRA 2.0”) [69].

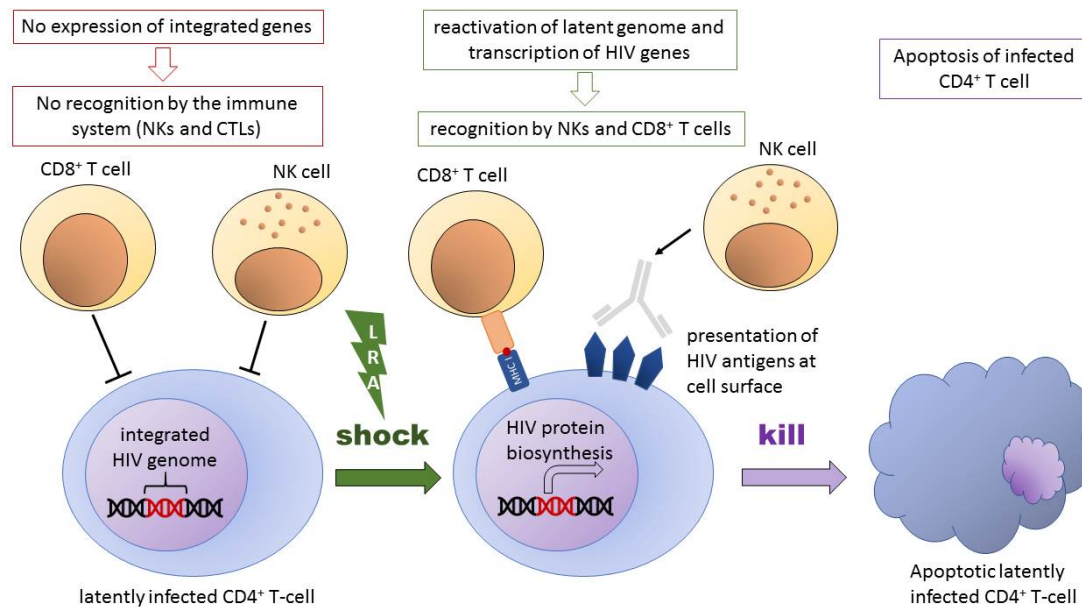


Figure 5: Illustration of the principal idea of the shock and kill approach.

NK: natural killer cells, CD8<sup>+</sup> T cell: cytotoxic T lymphocyte, LRA: latency reversal agent, MHC I: major histocompatibility complex I, TCR: T cell receptor; adopted from [68].

LR agents target different molecular mechanism of latency (as discussed above; see 1.4.1.2) and include “Protein kinase C (PKC) activators, DNA methyltransferase (DMT) inhibitors, Histone methyltransferase (HMT) inhibitors and Histone deacetylase (HDAC) inhibitors” [59]. Several hurdles in the search for LRAs are the inefficiency to reactivate the whole reservoir or toxicity issues. However, it is still a subject of current research. Only recently, results from a clinical phase II study were presented in September 2024 [71]. In this study, the *in vivo* effect of a combination therapy with an HDAC inhibitor (chidamide<sup>9</sup>) and an immune system checkpoint inhibitor (ASC22, targeting the PD-L1 membrane protein<sup>10</sup> in immune cells) were investigated in 15 HIV positive individuals under ART. By combining two molecules that are able to reverse latency with one of them potentially restoring T cell function in addition, the authors hoped for a LR activity with subsequently decrease in HIV reservoir. Despite being safe in ART suppressed individuals<sup>11</sup> and effective in reversing

<sup>9</sup> Chidamide (Tucidinostat) is approved for the treatment of peripheral T cell lymphoma in China.

<sup>10</sup> Programmed death – ligand 1 (PD-L1) is located on the membrane of immune cells and the ligand of the programmed death 1 receptor (PD-1 receptor) which is a transmembrane receptor of the CD28 family. This receptor is a crucial negative regulator of T cell function. Biologicals targeting either PD-1 or PD-L1 inhibit their interaction thereby partially restoring T cell dysfunction. In addition, they were suggested to enhance HIV expression in latently infected CD4<sup>+</sup> cells. ASC22 is the active pharmaceutical ingredient of Envafoimab® which is approved for treatment of different kinds of cancer in China and the USA. For detailed information on the study approach and design see [71].

<sup>11</sup> Over 12 weeks with an additional 12 weeks of follow up.

latency, ASC22 and chidamide in combination fell “short in effectively eradicating the HIV reservoir” [71].

### 1.4.2) Malaria

Malaria is caused by parasites of the genus *Plasmodium* that are transmitted to humans by female *Anopheles* mosquitoes. The WHO reported an estimated 249 million cases in 2022 worldwide, while Sub-Saharan Africa is again affected disproportionately [72]. 93 % of the estimated cases occurred in the WHO African Region, although it only covers roughly half of the 85 malaria endemic countries [72]. Children under the age of five accounted for 78 % of all deaths in this region, similar to the proportion worldwide (76 %) [72]. The species *falciparum* causes the majority of cases within the WHO African Region. Only 0.5 % of the cases were caused by *P. vivax* in 2022 [72]. This species is predominant in South East Asian countries where it is responsible for roughly half the cases. However, in contrast to *P. falciparum*, *P. vivax* can hide in the liver in a dormant state and cause rebounding malaria.

Phytopharmaceuticals played a major role in the therapeutical history of malaria and compounds derived from secondary plant metabolites are still the main therapeutics up to date. From mid-17<sup>th</sup> century on, extracts of *Cinchona pubescens* (RUBIACEAE) bark were the main therapeutic option for malaria. Quinine (see Figure 6), its active constituent, was isolated in 1820 which led to cultivation in plantations and subsequent industrial extraction of quinine for medical use until World War II. Thereafter, the synthetic analogue chloroquine dominated the market. Today high resistance levels of *P. falciparum* hinder its use in many malaria endemic areas. In 2015, the WHO recommended another plant constituent instead as the standard therapy of malaria. Artemisinin-based combination therapy includes analogs of the secondary plant metabolite artemisinin, a constituent of *Artemisia annua* L. (ASTERACEAE). Artesunate, artemether and dihydroartemisinin are implemented in today's standard therapeutic regimens against malaria. Figure 6 shows the chemical structure of artemisinin, whose antiplasmodial activity and structure was discovered by TU YOUYOU and colleagues [73]. For his discovery, To YOUYOU was awarded the Nobel Prize in 2015.

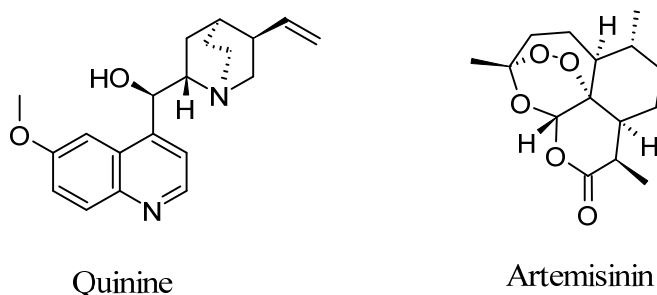


Figure 6: Chemical structures of quinine and artemisinin, antiplasmodial components of *Cinchona pubescens* and *Artemisia annua*.

A minor part of this thesis is dedicated to research in the field of natural products active against malaria. Therefore, this chapter only briefly introduces the life cycle of the parasite to contextualize the anti-plasmodial assay performed on asexual blood stages of a chloroquine sensitive *P. falciparum* strain.



### 1.4.2.1) The life cycle of the parasite

The parasites of the genus *Plasmodium* have a complex life cycle that involves two hosts: *Anopheles* mosquitos and humans. The parasite develops through various stages that take place in different locations: mosquito stage, human liver stage and human blood stage as depicted in Figure 7.

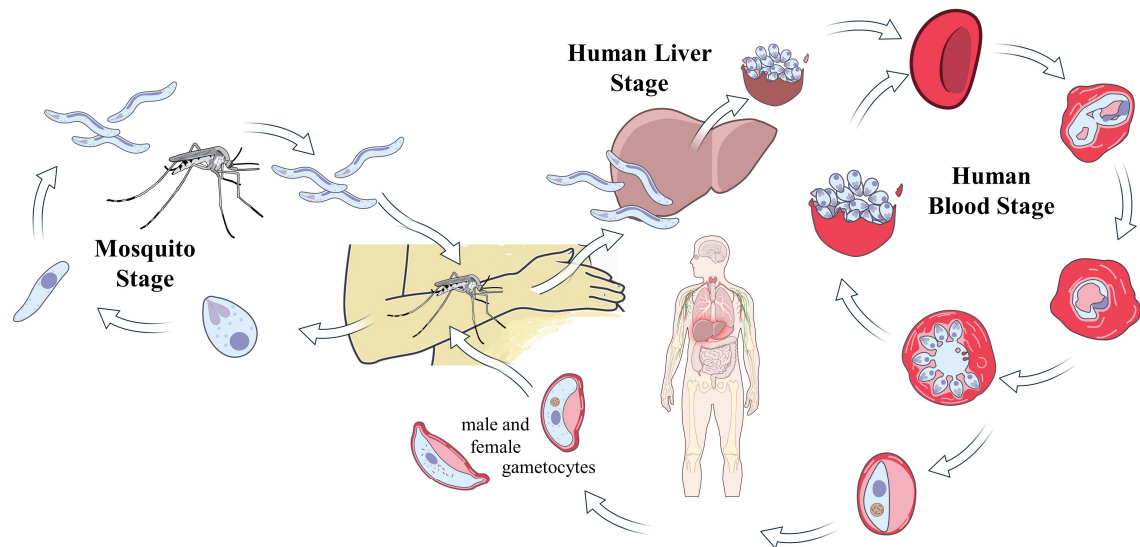


Figure 7: Life cycle of the plasmodium parasite.

Figure was prepared using free illustrations and icons from NIH BIOART<sup>12</sup>.

**Human Liver Stage.** The infection of humans occurs during a blood meal of an infected *Anopheles* mosquito which injects sporozoites into the blood stream. Those migrate to the liver and infect liver cells, where they mature into schizonts. These infected liver cells rupture and release merozoites into the blood stream. The human liver stage is not diagnosable in routine diagnosis. Two species of *Plasmodium* (*P. ovale* and *P. vivax*) are able to survive in a dormant stage in the liver and can cause infections of the blood stream even after years of dormancy.

**Human Blood Stage.** Merozoites, which were released from the liver, infect specifically red blood cells. Within this stage the parasite is partly visible as ring shaped trophozoite under the microscope. This serves as diagnostic tool. Blood samples from patients are screened for erythrocytes that contain trophozoites. Trophozoites mature and again release merozoites. This stage is also referred to as the asexual blood stage. The rupture of erythrocytes with subsequent release of merozoites is a recurring cycle of a certain duration and responsible for the clinical symptoms. The duration is specific for the respective parasite

<sup>12</sup> Source: <https://3d.nih.gov/entries/BIOART-012345>.

species which is aiding the diagnosis. Some of the trophozoites mature into sexual gametocytes. Those are ingested by *Anopheles* mosquitos during another blood meal.

**Mosquito Stage.** Within the mosquito, the sexual gametocytes fuse to build an ookinete that matures into an oocyst. From this cell, infectious sporozoites are released into the mosquito's salivary glands from where they can be injected into the human blood stream during a blood meal.

### 1.4.3) Tuberculosis and Infections with Non-tuberculous Mycobacteria

#### 1.4.3.1) General Information on Origin, Epidemiology and Treatment

*Mycobacterium tuberculosis*, an obligate aerobe, slow growing, acid-fast, rod-shaped bacterium, is the causative agent of TB, the third major communicable disease in the WHO African Region [45]. According to the WHO, tuberculosis remained the world's second leading cause of death from a single infectious agent in 2022 [74]. Nigeria and the Democratic Republic of the Congo, two countries from Sub-Saharan Africa, are found among the eight countries covering two-third of the global tuberculosis burden [74]. Although India and other Asian countries are the leading countries regarding infections with tuberculosis, the African region accounted for 23 % of the incidence cases in 2022 [74], second only to the leading Asian region with an incidence of 208/100.000 people [45]. In contrast, the incidence in Germany was 4.9/100.000 people in 2022 [75]. The difference in incidence rates between countries can also be seen in Figure 8. While the WHO European and American regions mostly present with incidences less than 10 cases/100.000 people per year, many countries belonging to sub-Saharan Africa have incidences of 100 cases with some countries exceeding 500/100.000 people per year.

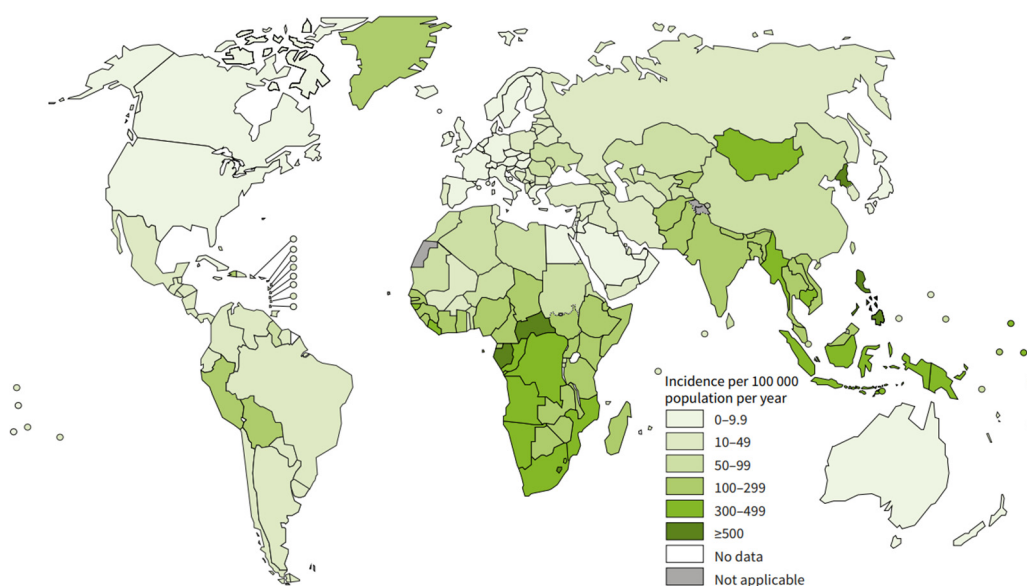
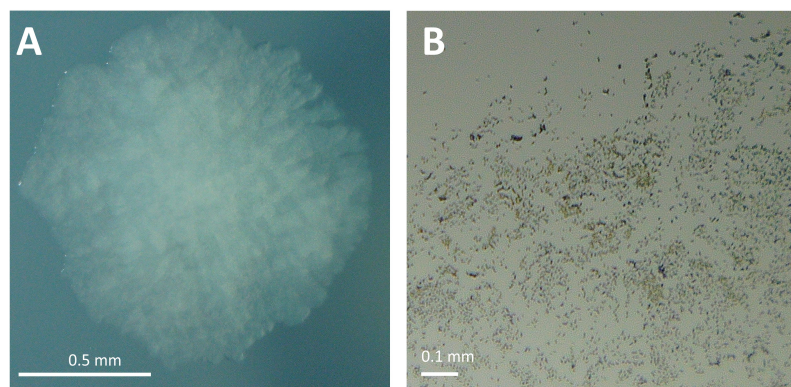


Figure 8: Estimated TB incidence rates in 2022<sup>13</sup>.

Beside *M. tuberculosis* and *M. leprae* (the etiologic agent of lepra, an infectious skin disease) that are both obligate pathogens, the genus *Mycobacterium* contains about 200 species that are collectively termed non-tuberculous mycobacteria (NTM) [76]. Most of them

<sup>13</sup> Reprinted from [74], published under the Creative Commons Attribution-NonCommercial-ShareAlike 3.0 Intergovernmental Organization licence CC BY-NC-SA 3.0 IGO.

are environmental bacteria, with a small percentage being opportunistic pathogens that can cause severe infections of the lung (non-tuberculous mycobacterial pulmonary disease (NTM-PD)) or of other organs [76], comparable to *M. tuberculosis* that can cause extrapulmonary infections too. Among NTM, *M. abscessus* and members of the *M. avium* complex are responsible for about 80-89 % of NTM-PD [76]. NTM infections can present clinically similar to tuberculosis and NTM also share diagnostic laboratory parameters with *M. tuberculosis*. This complicates their differentiation and can lead to misinterpretation of the infection as extensively drug resistant TB (XDR-TB). Since NTM are environmental bacteria, colonization by these bacteria is not necessarily resulting in NTM disease. To distinguish between the two, criteria of the American Thoracic Society/Infectious Disease Society of America are applied. Modern molecular tools (e.g. GenoType mycobacteria direct line probe assay) help in differentiating *M. tuberculosis* from NTM as well as determining the species and even subspecies of the found NTM [77]. In SSA countries these tools are used in reference laboratories, but are mostly not available for routine health care [78].



**Figure 9:** Microscopic pictures of two different non-tuberculous mycobacterial species.  
**A:** Colony of *M. abscessus* subsp. *abscessus*, rough morphotype, grown on solid medium.  
**B:** Smear, showing *M. aurum* DSM cells, stained with Ziehl-Neelsen. Pictures were taken with TOMLOV DM602 Pro.

As most NTM are opportunistic pathogens, infections are mostly relevant for patients with pre-existing lung damage (such as cystic fibrosis (CF), chronic obstructive lung disease (COPD) or previous TB infection and smoking) and/or suboptimal conditions of the immune system (due to HIV infections, drug treatment or aging) [76]. Regarding patients from SSA, ABBEW *et al.* identified additional risk factors for NTM infections such as silicosis, occupational exposure (such as working in the mining industry or agricultural sector) and malnutrition [78] that are not relevant to the same extent in industrialized countries. While relatively high cure rates for TB are reported (85 % for drug susceptible TB (DS-TB), 60 % for multidrug resistant TB (MDR-TB) and 30-50 % for XDR-TB), the positive treatment outcome for NTM-PD is in the range of XDR TB (33-54 %) [79]. Table 2 gives an overview of the current treatment regimens of mycobacterial lung diseases. Due to a clinical trial published in 2020 [80], the treatment of patients with drug resistant TB was successfully shortened from 18-24 to a six-month regimen from 2022 on.

Table 2: Treatment regimens for pulmonary disease caused by mycobacterial infections according to [74, 81, 82].

DS-TB	MDR TB and XDR TB	MAC-PD	MAB-PD
4 months:	6 months:	until sputum cultures remain negative for 12 months	
rifapentine	bedaquiline	macrolide	3-6 antibiotics
isoniazid	pretomanid	(azithromycin/ clarithromycin)	selected on basis of drug susceptibility profile;
pyrazinamide	linezolid	rifamycin	<u>in general:</u>
moxifloxacin	with/without moxifloxacin	(rifampicin/ rifabutin) ethambutol	macrolide as backbone plus amikacin and/or cefoxitin both i.v.)
		adding amikacin (i.v.) for cavitary disease	

DS: drug susceptible; MAB-PD: *M. abscessus* pulmonary disease; MAC-PD: *M. avium* complex pulmonary disease; MDR: multidrug resistant; TB: tuberculosis; XDR: extensively drug resistant

For the treatment of tuberculosis, there are official guidelines of the American Thoracic Society of the CDC depending on the susceptibility status of *M. tuberculosis*. As can be seen from Table 2, treatment of infections with *M. abscessus* are less clearly guided, which is due to limited information on which recommendations are based. This highlights the urgent need for clinical trials to approve *in vitro* results of drugs within clinical application.

**Epidemiology:** There are differences in patient groups of mycobacterial pulmonary lung disease. While male and female children are affected by *M. tuberculosis* equally, male patients increasingly account for the majority of tuberculosis cases among adults [83] (adult men 55 %, adult women 33 % and children under 15 years of age 12 % of the estimated cases in 2022 [74]). This is true for the WHO African Region (Figure 10) as well as for regions of the Western world (Europe and regions of the Americas). Differences between the two are found in the total number of cases as discussed above and regarding the distribution by age, due to different demography of the population in Africa. Its population is younger and people have a lower life expectancy (42 % of the population in the WHO African region are under 15 years [45]; life expectancy 64.5 years [84]) compared to the Western world (15 % of the population of Europe in 2019 was under 15 years old; life expectancy 80.6 years in 2022 [85]).

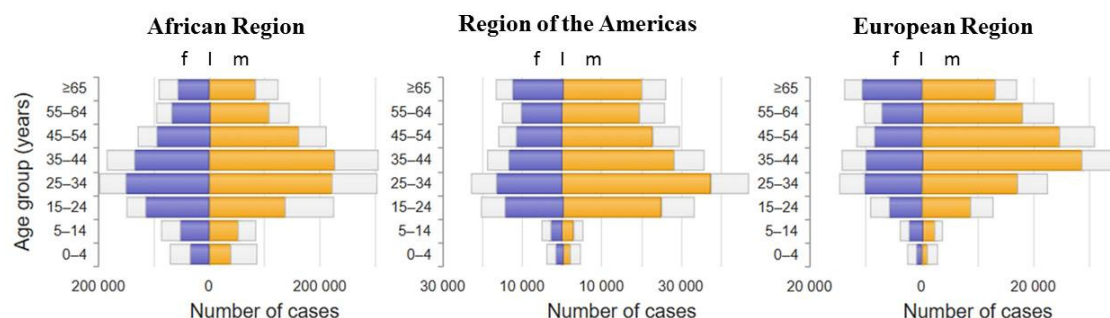


Figure 10: Regional estimates of TB incidence [absolute numbers] disaggregated by age and sex, compared with case notifications 2022<sup>14</sup>.

Female (f) in purple; male (m) in orange, note the different scales of the x-axis.

Data on the epidemiology of NTM infections is sparse since it is not a reportable disease in most countries. However, in western countries a higher prevalence in elderly female patients with lower body mass index [87, 88] is reported than in men. In contrast, 75 % of NTM-PD patients in sub-Saharan Africa are male. However, this finding could be biased by several factors (e.g. access to health care facilities or cultural aspects). In view of the sparse data available, this is an indication of a different situation only. The following Table 3 lists data on epidemiology of NTM infections to compare patient groups and species of mycobacteria responsible for pulmonary infections between SSA and the Western world.

<sup>14</sup> Adjusted from [86], published under the Creative Commons Attribution-NonCommercial-ShareAlike 3.0 Intergovernmental Organization license: CC BY-NC-SA 3.0 IGO.

Table 3: Comparative data on epidemiology of NTM-PD in SSA and countries of the Western world.

	Sub-Saharan Africa Data retrieved from [89]	Western World Data retrieved from [76, 90, 91] <sup>1</sup>
Prevalence	7.5 % (in pulmonary samples)	In CF patients 5-10 %
Patient group	male 75 % female 25 % children <sup>2</sup> age 33-44 years median 35	prevalence [per 100.000] in men 6.45 women 16.78 > 50 years
Predominantly isolated species	27.7 % <i>M. avium</i> complex 7.0 % <i>M. scrofulaceum</i> 4.7 % <i>M. kansasii</i> 1.2 % RGM <sup>3</sup>	77.6 % <i>M. avium</i> complex 17.3 % <i>M. simiae</i> 10.5 % <i>M. gordonae</i> 7.8 % <i>M. abscessus</i>
Species responsible for PD	69.2 % <i>M. kansasii</i> 13.9 % <i>M. scrofulaceum</i> 13.5 % <i>M. avium</i> complex 1.9 % <i>M. lentiflavum</i> 0.8 % <i>M. simiae</i> 0.4 % <i>M. palustre</i> 0.4 % <i>M. abscessus</i>	80-89 % <i>M. avium</i> complex and <i>M. abscessus</i>

<sup>1</sup> Reference [91] presents data from a global review, however no study was included from sub-Saharan Africa and more than half of the studies were performed in western countries. Due to limited data in general regarding epidemiology of NTM infections, this was accounted acceptable to give an idea on patient data and therefore included in this table. <sup>2</sup> Three studies included in the review exclusively studied NTM infections in children, however the authors did not calculate the overall rate of infections in children throughout SSA. <sup>3</sup> Rapidly growing mycobacteria (RGM) within this study include *M. fortuitum*, *M. chelonae* and *M. abscessus* and were mainly reported from eastern African countries.

From the little data available, it can be concluded that there are several differences between patients from SSA and patients in the Western world. While in the Western world mostly female elderly women suffer from NTM-PD and these infections are mostly caused by members of the *M. avium* complex and *M. abscessus*, in SSA mostly men in their middle ages suffer from pulmonary disease caused by *M. kansasii* with *M. avium* complex causing 13.5 % of NTM-PD only. The younger age of patients in SSA could however also refer to a younger population in general as mentioned before.



### 1.4.3.2) The Role of Granulomas in Mycobacterial Infections

Pulmonary infections with *M. tuberculosis* and NTM can lead to the formation of characteristic lung lesions, called granulomas<sup>15</sup> [94, 95]. These granulomas are visible in radiographic pictures and serve as a diagnostic indicator next to clinical symptoms in the diagnosis of PD [96]. Granulomas are studied extensively *ex vivo* in animal models as well as in patient samples. They are well structured complexes with a typical architecture, consisting of a variety of immune cells in different states [95].

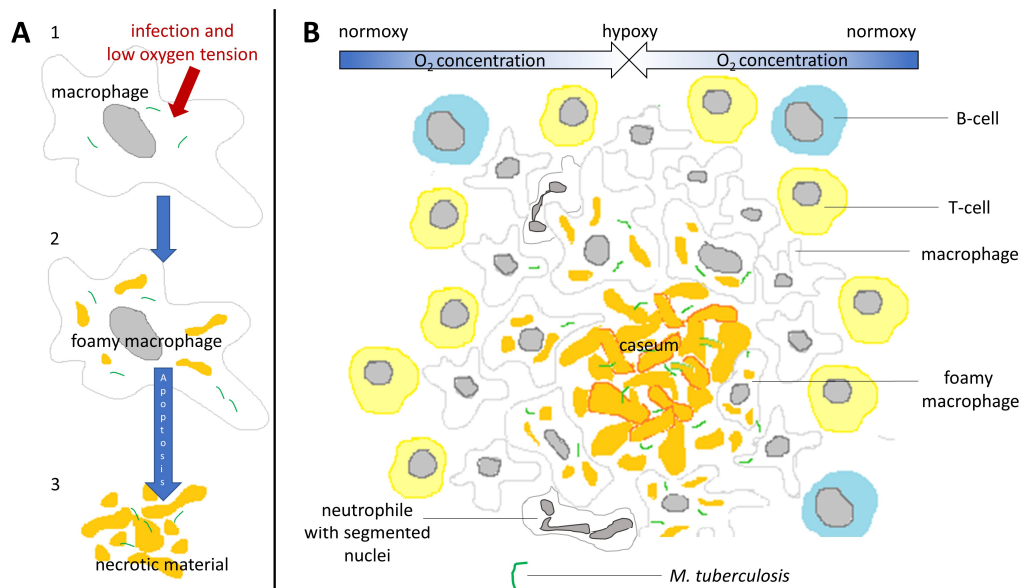


Figure 11: Formation of granulomas in lung lesions of TB patients.

**A: Changes that a macrophage undergoes** in the course of granuloma formation. (1) Decreased vascular efficiency leads to low oxygen tension in lung lesions. In combination with the reaction upon an infection, this leads to agglomeration of lipid droplets within infected macrophages (2). These cells are called foamy macrophages due to their microscopic appearance. (3) They necrotize and thereby release bacterial and cellular content into inner caseum. **B: Architecture of a typical granuloma**, where oxygen gradually decreases from the outside to the center of the granuloma. The inner necrotic center (caseum) consists of cellular compartments of dead immune cells, lipid rich agglomerates from foamy macrophages and bacteria that survive in this hypoxic and greasy environment by several mechanisms. The caseum is surrounded by infected foamy macrophages, infected macrophages and neutrophils which try to control the infection by phagocytizing bacteria. The outer rim is built up by B- and T- cells, which contribute to the control of infection by recruiting additional immune cells and activate macrophages through the release of cytokines [97].

Figure 11 describes the complex process of granuloma formation using the example of infection with *M. tuberculosis*. Due to inefficient vascularization, the necrotic centres of

<sup>15</sup> The formation of granulomas is a typical attribute of pulmonary TB infections. However, infections with NTM in immunocompromised patients poorly lead to formation of granulomas, instead diffuse disease manifestation is seen [92], whereas in immunocompetent patients, granuloma formation is frequently seen, similar to TB [93]. This fact highlights the role of the immune system in the formation of granulomas.



granulomas are hypoxic [98]. The mechanisms of mycobacteria to survive this environment despite several strategies of the immune system to control the infection and kill the bacteria are described in the following section.

#### 1.4.3.3) *Non-replicating Persisters of Mycobacteria*

Compared to pulmonary infections caused by other bacteria than mycobacteria, tuberculosis and NTM-PD require an exceptional long drug treatment of at least four months [96] (see also Table 2 in section 1.4.3.1). Often, this treatment takes longer, even up to years, especially in the case of NTM. Several reasons contribute to this problem such as a significantly longer doubling time compared to other bacteria [99, 100], the formation of biofilms [101, 102] (which is however not unique to mycobacteria), the ability to survive in barely druggable reservoirs (like macrophages [103, 104], granulomas [97, 105] and mucus in CF patient's airways [106]) and *M. tuberculosis* modulating the immune system of the host [107] to prevent effective intervention by the immune system.

Upon external stimuli (like hypoxia, high concentrations of nitric oxide (e.g. in macrophages), elevated carbon monoxide levels), *M. tuberculosis* induces the expression of dormancy regulator genes (DosR) [108] that induce transition to a non-replicating state in which bacteria can survive. DosR genes are essential for survival of *M. tuberculosis* in hypoxia [109] as well as of *M. abscessus* [110, 111]. The subpopulation of mycobacteria in a dormant state is called non-replicating persisters (NRPs) and is an important inductor for persistent infection in patients [112]. Following WOOD's definition, **persisters** are "bacteria that evade the effects of antibiotics without undergoing genetic variation" [113] in contrast to **resistant** bacteria, where mutations are the reason for the ineffectiveness of drugs.

#### 1.4.3.4) *Models to Mimic NRPs in Vitro*

Several environmental factors induce transition to NRPs, besides expression of DosR, and many of them are used in models to study and understand mechanisms in these bacteria. This section will touch on the variety of models and explain the ones using hypoxia as external trigger of transition to the NRP state in more detail.

Literature regarding models of NRP for *M. tuberculosis* has been reviewed [114, 115] and models mimicking environmental stressors that induce transition to a NRP state are displayed in Figure 12.

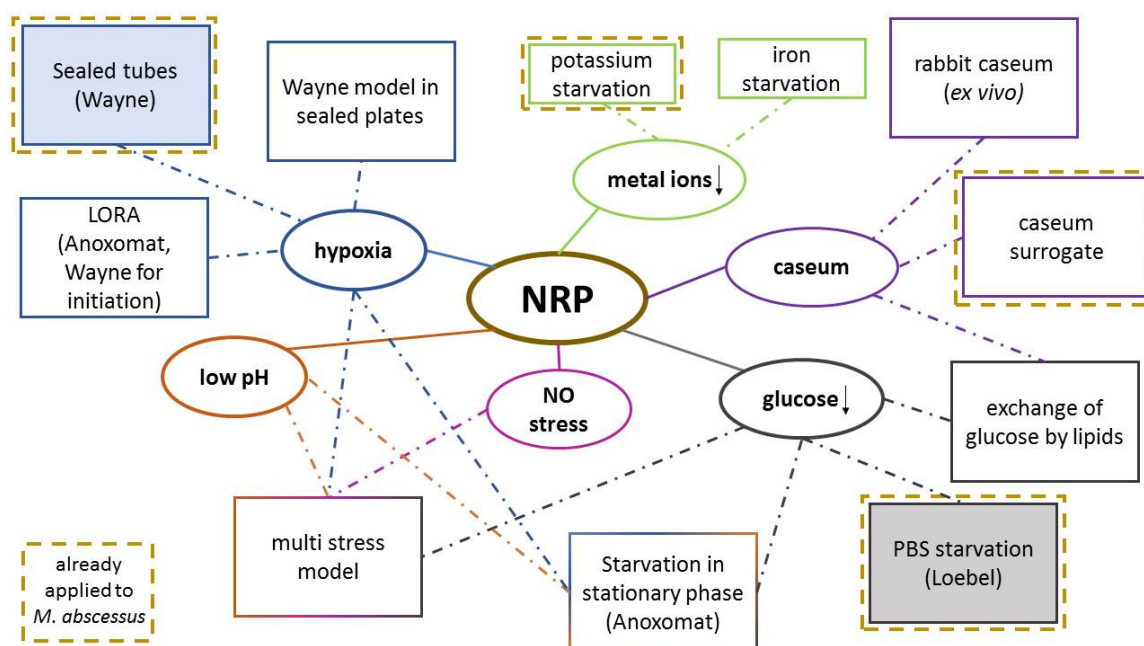


Figure 12: Models to study non-replicating persisters of *M. tuberculosis*.

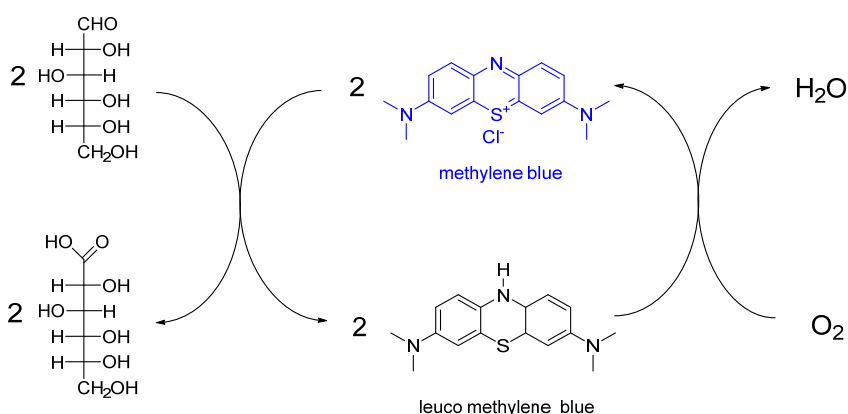
Note that this map aims to give an overview and does not include every single model that was applied to force *M. tuberculosis* into the non-replicating state.

The diversity of models is due to the complex nature of persistence. While some authors focus on understanding a specific part of persistence by simplifying the model as much as possible to clearly connect cause and effect, others try to build up models that are more physiologically relevant when mimicking conditions that are found in granulomas by combining several stressors within one model. NRPs obtained by different models show a variety of common properties, but are not congruent. They, for example, differ in their drug susceptibility profile as metronidazole is inactive in replicating and nutrient starved non-replicating *M. tuberculosis* [116], but bactericidal to hypoxic non-replicating *M. tuberculosis* [117].

Two simple but important approaches to obtain and study NRPs are highlighted in Figure 12 among the other models. In 1933, LOEBEL was the first to describe culturing *M. tuberculosis* in simple PBS [118] (Figure 12, grey model, bottom right). This simple approach is used until today to study *M. tuberculosis* and was applied successfully to *M. abscessus* as well [119, 120]. The model highlighted in blue is the most important access to hypoxic NRPs of *M. tuberculosis* and was described in 1996 by WAYNE *et al.* [121]. This model was applied to *M. abscessus* by several groups [111, 119, 122]. Due to slightly different phenotypes obtained upon the type of model, authors use to add the information on how the cells were obtained when describing the population (e.g. nutrient starved *mycobacteria* as in [123-125]). This part of the project focuses on hypoxic models to widen the scope of drug activity determination for compounds synthesized in the research group of PROF. PETER IMMING. We therefore use the term of **low-oxygen persisters (LOPs)** of *M. abscessus* to describe the subpopulation of cells that are obtained in our setup. This new model was developed as part of this thesis and is described in detail in publication IV as well as in the

summary and discussion part of this thesis (see page 111, section 3.8). Although, hypoxic models for the generation of NRPs are among those which focus on one environmental factor only, they are hard to set up since mycobacteria are aerobic bacteria and usually need to be cultured in aerobic conditions. Sudden onset of hypoxia was described as lethal for *M. tuberculosis* [126] as well as for *M. abscessus* [110].

**Definition of Hypoxic Conditions in NRP Models for Mycobacteria.** A solution of methylene blue (MB) is an accepted tool to indicate the oxygen concentration in hypoxic setups for mycobacteria [119, 121, 122, 127, 128]. This phenothiazine dye gets reduced by dissolved glucose resulting in the colorless leuco methylene blue. This leuco-form is then subsequently re-oxygenated by dissolved oxygen (Figure 13). When the available oxygen concentration is too low to drive the equilibrium to the oxidized form, the solution will stay colorless. This concentration is defined as hypoxic and used as a marker by many groups without further determination of dissolved oxygen concentration.



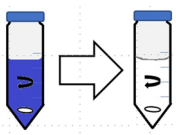
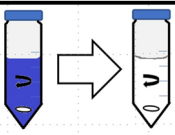
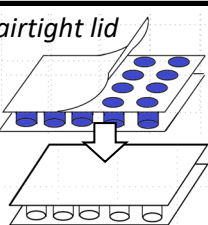
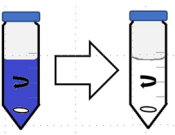




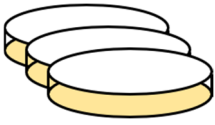
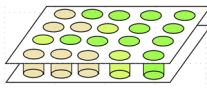
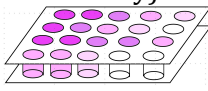
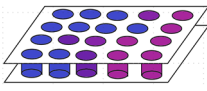
*Figure 13: Methylene blue as an indicator for oxygen concentration in hypoxic setups. Reduction of methylene blue to its leuco-form by glucose. The reoxygenation is dependent on the availability of oxygen dissolved in the culture medium. If the concentration is too low to drive the equilibrium to the oxidized form, the solution will stay colorless.*

Since the solubility of oxygen in aqueous medium is dependent on various factors such as temperature, pH and composition of the medium, the absolute concentration of oxygen in the head space upon decolorization may therefore vary in different setups. WAYNE defines fading of the indicator as “microaerophilic” (1 % dissolved oxygen of the original saturation level in his setup) and decolorization as “anaerobic” (0.06 % saturation of oxygen) [121]. The term “hypoxic” in this work refers to a setup that leads to decolorized methylene blue.

**Hypoxic Models for Mycobacteria.** Table 4 presents a selection of hypoxic models developed to study *M. tuberculosis* under hypoxic conditions that are explained in the following.

Table 4: Selection of hypoxic models to study NRPs of mycobacteria.

The table summarizes the method of oxygen reduction, compound addition, read out and equipment, positioning the methods by their dis- and advantages; GFP: green fluorescent protein, HTS high-throughput screening, resp. NR: respiratory nitrate reductase.

	WAYNE	LORA	KHAN	Hypoxic resazurin assay
$O_2 \downarrow$  NRP- generation		 Hypoxic parent culture transf. to plates	 airtight lid	
Compound addition by			Before hypoxia 	
Incubator	Any	Anoxomat	Any	Any
Read out	CFU count 	GFP – after recovery phase 	GRIESS reaction (resp. NR activity) 	Transfer to plates - Resazurin 
Advantage	<ul style="list-style-type: none"> <li>- simple</li> <li>- no plasmids</li> <li>- cheap</li> </ul>	<ul style="list-style-type: none"> <li>- HTS compatible</li> </ul>	<ul style="list-style-type: none"> <li>- HTS compatible</li> </ul>	<ul style="list-style-type: none"> <li>- enables easier read out of the Wayne model</li> </ul>
Disadvan- tages	<ul style="list-style-type: none"> <li>- labour intensive</li> <li>- risk of injury</li> <li>- not HTS compatible</li> </ul>	<ul style="list-style-type: none"> <li>- preparation of hyp. parent cult. in WAYNE'S model</li> <li>- expensive (anoxomat)</li> <li>- only for GFP expressing strains</li> </ul>	<ul style="list-style-type: none"> <li>- studies another phenotype</li> <li>- possible compound interference with reagents for GRIESS reaction</li> </ul>	<ul style="list-style-type: none"> <li>- risk of injury</li> <li>- risk of confusion (refill)</li> <li>- possible compound interference with resazurin</li> </ul>

**WAYNE'S model** uses the replication and the respiration of mycobacteria that are stirred in sealed tubes with 0.5 head space ratio to self-generate hypoxic conditions [121]. Compounds are added by syringe after onset of hypoxia to minimize re-entry of oxygen. The activity of compounds is determined by CFU count.

The Low-oxygen-recovery-assay (**LORA**) was developed by CHO *et al.* as an high-throughput screening (HTS) compatible model for hypoxic NRPs of *M. tuberculosis* [129]. It uses the WAYNE model to prepare a hypoxic parent culture that is transferred to microtiter plates after transition to the NRP stage. To prevent resuscitation, the culture is handled quickly and solvents are kept cold. The assay itself is performed in a special incubator (anoxomat) that can be operated with fixed gas concentrations and also operated at 0 % oxygen. Thereafter, the culture is given a short outgrowth phase in aerobic conditions to allow onset of metabolism. The metabolic activity is determined by measurement of luciferase activity.

**KHAN *et al.*** transferred WAYNE'S approach to microtiter plates and used the NRP dependent induction of a nitrite reductase for an indirect readout [128]. However, in this approach, compounds are added before the onset of hypoxia, which consequently determines their activity on a culture that is about to transition into the non-replicating state only and thereby address another phenotype of mycobacteria, different from the one in the WAYNE model.

The **hypoxic resazurin assay** [130] is basically a WAYNE model that uses a resazurin readout after refilling the content of the tubes into microtiter plates.

As can be seen from the table, there is a lack of a model that combines simplicity and safety, while relying on a direct read out method to prevent possible interference of reagents with investigated compounds.

#### 1.4.4) Co-Infections of HIV and Mycobacterial Species

Among TB cases worldwide in 2022, 6.3 % accounted for patients, co-infected with HIV [74]. Considering patients from the WHO African Region, this proportion is particularly higher, with regions in the southern parts exceeding 50 % of all TB cases being co-infected with HIV [74]. Figure 14 visualizes the impact of those co-infections. Approximately a third of all HIV-related deaths is due to TB infections, which makes TB the leading cause of death among PLWHIV. According to ICD, death caused by TB within the group of HIV positive patients is attributed as death by HIV.

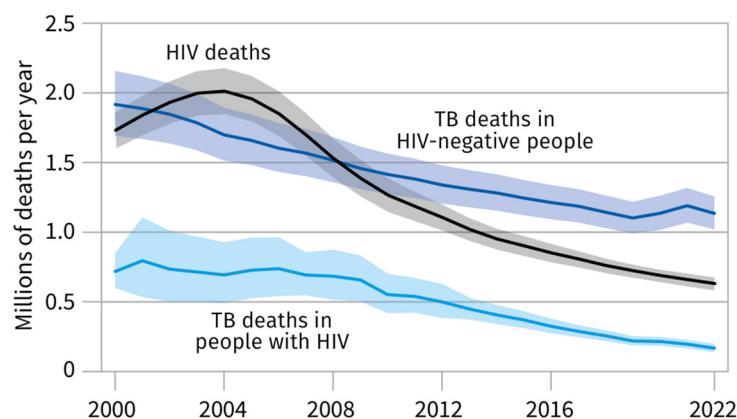


Figure 14: Global trends in the estimated number of deaths caused by TB and HIV. Shaded areas represent 95 % uncertainty intervals. Reprinted from [131]<sup>16</sup>.

NTM infections also contribute to mycobacterial co-infections with HIV. This was shown by a meta-analysis on autopsied HIV patients in SSA in 2021. They determined the prevalence of NTM PD and TB during the autopsy to range from 1.3 % to 27.3 % and 11.8 % to 48.7 % respectively. The authors calculated the NTM PD vs TB prevalence ratio and found “for every seven HIV patients died with mycobacterial infections, there was one died with NTM infection” [132]. HIV is a known risk factor for TB and NTM infections [76]. However, in the light of less diagnostic tools available for routine health care, it is hard to distinguish between mycobacterial species and adequately choose the correct antibacterial therapy that is also challenging in countries of the Western world [89].

<sup>16</sup> Distributed under the terms of Creative Commons Attribution-NonCommercial-ShareAlike 3.0 IGO licence (CC-BY-NC-SA 3.0 IGO).

## 1.5) Antimicrobial Resistance as a Global Threat Using the Example of MRSA

Antimicrobial resistance (AMR) was already mentioned as an issue in the different introductory chapters. A meta-study from 2022 stated bacterial AMR to be “a leading cause of death around the world with the highest burden in low-resource settings” [133]. An estimated 1.27 million deaths worldwide were directly attributable to bacterial AMR out of the estimated 4.95 million deaths that were associated with<sup>17</sup> bacterial AMR. Of both, sub-Saharan countries had the highest death rates, although the fraction of deaths involving infections that are associated with resistance were lowest [133]. This is probably due to the higher fraction of deaths that involve infection compared to other parts of the world (45.6-53.5 % vs 11.5 % in Central Europe [133]). These data may also reflect the availability of second- and third-line therapeutic options in different parts of the world.

MRSA was the leading pathogen in high-income countries, while it was the fourth leading pathogen in SSA countries [133]. *S. aureus* is a spherically shaped Gram-positive bacterium and a normal participant of the human microbiota. It is frequently isolated from the skin, the nose and from the upper respiratory tract. *S. aureus* colonizes most people without any harm, but can cause severe infections as pneumonia, blood stream or surgical-site infections or infections of wounds [134]. Those are often acquired in health-care facilities, especially in intensive-care units and are difficult to treat due to high levels of resistance. A worldwide surveillance system was launched in 2015 by the WHO to standardize AMR surveillance. Categories for antibiotic as “access”, “watch” and “reserve” should help to reduce AMR development. Many hospitals have action plans on how to reduce the transmission of MRSA.

Active phytopharmaceuticals could contribute to the treatment of infections with resistant bacteria, especially in settings where other options are less available. At the same time these could reduce the amount of antibacterials used.

---

<sup>17</sup> Deaths attributable to AMR are “based on an alternative scenario in which all drug-resistant infections were replaced by drug-susceptible infections” and deaths associated with AMR are “based on an alternative scenario in which all drug-resistant infections were replaced by no infection” [133].

## 1.6) The 10/90 Gap

As mentioned before, the SSA countries are highly affected by the described diseases in terms of cases as well as in terms of deaths (as can be seen from the table in Figure 3 on page 9). Yet, according to the Global Forum of Health, only 10 % of research funding is put towards countries where 90 % of preventable deaths occur. This is referred to as the 10/90 gap [135]. Activists use this claim to support their goal of achieving global equality. But it needs to be interpreted with caution. STEVENS, for example, calls the 10/90 gap a “red herring” that misinterprets the reason for diseases in many low-income countries and states that most diseases in these countries are caused by poverty instead of unavailability of drugs [136]. However, the imbalance in research possibility between researchers from the global north and the global south still is an issue in 2024 [137, 138]. In her thesis, HILL also touched on “the question of power and knowledge” within the context of scientific verification of traditional medicine [9]. This question is also important in finding a balance between phytomedicine and CPT in African countries as mentioned at the beginning of the introduction. This thesis understands the 10/90 gap as the evidenced inequality between global north and south and aims to work towards closing it.



## 1.7) Objectives of This Work

This work contributes to the field of anti-infective research of phytochemicals from African medicinal plants in two aspects: Firstly, by a **variety of investigations on phytochemicals** and secondly by the **development of a microbiological tool** that will be applicable in even sparsely equipped laboratories enabling investigations on antimycobacterial activity of plant metabolites in close proximity to their natural habitat.

**Investigations** were carried out on constituents of *Kniphofia foliosa* and *Camellia sinensis* and contain the following aspects:

### *K. foliosa*:

- 1) **Extract, purify and characterize** known constituents from medicinal plants to provide enough material in sufficient quality for subsequent investigations.
- 2) **Synthesize analogs** of 1,8 dihydroxyanthrone using a direct synthesis route.
- 3) **Provide data on stability** of two phytochemicals, namely knipholone and knipholone anthrone to understand assay-assay variation in a collaborator's laboratory.
- 4) **Evaluate the antimicrobial potential and the cytotoxicity** of isolated and synthesized compounds. The traditional use of the plant, the existing literature and the accessibility to assay systems through cooperation partners should guide the selection of the respective models. The obtained knowledge about compound stability should be considered during those assays.

### *C. sinensis*:

- 1) **Analyze data** on catechin content of different tea extracts that were standardized for their EGCG content for further microbiological studies.
- 2) **Analyze obtained data on the disinfecting ability of tea extracts** on resistant clinical isolates of *S. aureus* in order to determine the potential of tea as an easy-accessible tool in the fight against antimicrobial resistance.

The **development of a microbiological tool** includes the following aspects:

- 1) Find an easy approach to study compound activity on non-replicating persisters of mycobacteria under hypoxic conditions.
- 2) Provide evidence for the transition from a replicating to a non-replicating culture.
- 3) Proof the concept with known antimycobacterial compounds.
- 4) Apply the method to phytochemicals.



## 2) Publications

This section presents the results of my thesis in form of articles published in peer-reviewed journals. Each research article is preceded by a short summary and a description of my own contribution to this article.

### 2.1) Research Article I

#### **Antibacterial and Disinfecting Effects of Standardised Tea Extracts on More than 100 Clinical Isolates of Methicillin-Resistant *Staphylococcus aureus***

**Ruth Feilcke**, Volker Bär, Constanze Wendt, Peter Imming

**MDPI, Plants**

*Plants*. **2023**, 12(19):3440

Publication Date: September 29, 2023

Doi: 10.3390/plants12193440

##### Summary

This publication presents data on the bactericidal effect of tea extracts on *Staphylococcus aureus* confirming the known effect of *camellia sinensis* extracts based on a large collection of clinical isolates. Particular attention was paid to the use of a standardized extract in order to facilitate comparability with other studies. This study was initiated by a request from clinicians and our results encouraged the recommendation of tea extracts as a valuable addition to standard treatment of MRSA infections. Tea is consumed throughout Sub-Saharan countries and therefore easily accessible. This can contribute to lower costs in the health care sector not only in countries with lower resources, but also help in the fight against raising antibacterial resistance throughout the world.

##### Own contribution

Data curation and visualization, Writing – original draft; rewriting and editing; Experiments were carried out by the second author during the time of his diploma thesis.



## Article

# Antibacterial and Disinfecting Effects of Standardised Tea Extracts on More than 100 Clinical Isolates of Methicillin-Resistant *Staphylococcus aureus*

Ruth Feilcke <sup>1</sup>, Volker Bär <sup>1</sup>, Constanze Wendt <sup>2,3</sup> and Peter Imming <sup>1,\*</sup>

<sup>1</sup> Institut für Pharmazie, Martin-Luther-Universität Halle-Wittenberg, Kurt-Mothes-Str. 3, 06120 Halle, Germany

<sup>2</sup> Zentrum für Infektiologie, Universität Heidelberg, Im Neuenheimer Feld 324, 69120 Heidelberg, Germany

<sup>3</sup> Labor Dr. Limbach & Kollegen GbR, Medizinisches Versorgungszentrum, Im Breitspiel 15, 69126 Heidelberg, Germany

\* Correspondence: peter.imming@pharmazie.uni-halle.de; Tel.: +49-345-5525175; Fax: +49-345-5527237



**Citation:** Feilcke, R.; Bär, V.; Wendt, C.; Imming, P. Antibacterial and Disinfecting Effects of Standardised Tea Extracts on More than 100 Clinical Isolates of Methicillin-Resistant *Staphylococcus aureus*. *Plants* **2023**, *12*, 3440. <https://doi.org/10.3390/plants12193440>

Academic Editors: Laura Grañiela Vicaş and Mariana Eugenia Mureşan

Received: 9 August 2023

Revised: 25 September 2023

Accepted: 26 September 2023

Published: 29 September 2023



**Copyright:** © 2023 by the authors. Licensee MDPI, Basel, Switzerland. This article is an open access article distributed under the terms and conditions of the Creative Commons Attribution (CC BY) license (<https://creativecommons.org/licenses/by/4.0/>).

**Abstract:** Methicillin-resistant *Staphylococcus aureus* (MRSA) infections are still a major problem in hospitals. The excellent safety profile, accessibility and anti-infective activity of tea extracts make them promising agents for the treatment of infected wounds. To investigate the possibility of sterilising MRSA-infected surfaces, including skin with tea extracts, we determined the MICs for different extracts from green and black tea (*Camellia sinensis*), including epigallocatechin gallate (EGCG), on a large number of clinical isolates of MRSA, selected to represent a high genetic diversity. The extracts were prepared to achieve the maximal extraction of EGCG from tea and were used as stable lyophilisate with a defined EGCG content. All extracts showed a complete inhibition of cell growth at a concentration of approx. 80 µg/mL of EGCG after a contact time of 24 h. Time–kill plots were recorded for the extract with the highest amount of EGCG. The reduction factor (RF) was 5 after a contact time of 240 min. EGCG and tea extracts showed an RF of 2 in methicillin-sensitive *S. aureus*. Extracts from green and black tea showed lower MICs than an aqueous solution with the same concentration of pure EGCG. To the best of our knowledge, we are the first to show a reduction of 99.999% of clinically isolated MRSA by green tea extract within 4 h.

**Keywords:** multi-resistance; *Staphylococcus*; tea extracts; *Camellia sinensis*; time–kill plot

## 1. Introduction

Infections with methicillin-resistant *Staphylococcus aureus* (MRSA) have become a large problem for hospitals in most countries since 1990. Together with cephalosporin-resistant *Escherichia coli*, MRSA still causes the highest portion of disability-adjusted life years by infections with antibiotic-resistant bacteria in Europe [1] and is the second of six leading pathogens for deaths associated with resistance worldwide [2]. Within Europe, the portion of MRSA in invasive isolates shows a high variability between different countries, ranging from 0.9% in Norway to 42.9% in Cyprus in the years 2020–2022 [3,4]. Although the EU/EEA population-weighted MRSA percentage has been decreasing for more than 5 years now, the treatment of MRSA infections is still a major issue as they appear to cause a higher mortality rate than those caused by methicillin-susceptible *S. aureus* [5].

The antimicrobial activity of green and black tea extracts (leaves of *Camellia sinensis*) and their isolated constituents has been known since 1906 [6]. In vitro data indicated that tea extracts of ordinary brewing strength also inhibited the growth of MRSA [7]. Of the tea extract constituents, epigallocatechin gallate (EGCG) was especially investigated and was reported to have an MIC against *S. aureus* below 100 µg/mL [8]. In vivo studies on the activity of tea extracts against MRSA are rare but provide reason for hope [9–11]. Although the antibacterial and antiviral effects, excellent safety profile and easy accessibility

of tea extracts are well-known, their routine and controlled application in medicine is still uncommon. To guide clinicians on how to apply tea extracts, we set out to investigate their practicality as disinfectants. In contrast to published reports, we set on preparing extracts with high amounts of EGCG along with low amounts of caffeine, and standardised the extracts for EGCG.

The purpose of this study was to investigate the activity of different *Camellia sinensis* extracts with defined EGCG content against a large number of genetically diverse MRSA strains that were isolated in hospitals in Germany [12] compared with pure EGCG as the lead compound and positive control, by determining minimum inhibitory concentrations, and—very important for sterilisation and disinfection—by determining the contact time that led to a significant reduction in colony-forming units. All steps were optimised as for practical handling to serve as a guideline for the facile preparation of solutions for the topical treatment of MRSA infections.

## 2. Results

### 2.1. EGCG Content of the Tea Extracts

While Wang et al. (2008) [13] wrote that EGCG epimerised rapidly but was only slowly hydrolysed by high temperatures and boiling water, we found that EGCG easily hydrolyses and underlies oxidative processes in solution. For the purpose of this study, we therefore prepared a storage-stable lyophilizate, which would also be suitable for antibacterial treatment after dissolving in water. A lyophilised green tea extract (GTE) and black tea extract (BTE) were examined for EGCG content using the method described in Section 4.2. The EGCG content of GTE (20%) was twice the amount of BTE (11%). Consequently, the green tea extract was diluted to obtain standardised solutions of equal EGCG content (see Sections 4.3.1 and 4.3.2).

### 2.2. Comparison of Inhibition by Pure EGCG, Black and Green Tea Extracts in Selected MRSA Strains

The effect of different tea extracts and EGCG on the bacterial growth of 23 different strains is shown in Figure 1. At 40 µg/mL EGCG content, BTE inhibited more than 60% of the tested strains, whereas pure EGCG and GTE inhibited approx. 10% only. Table 1, “Average”, shows that there is no statistically significant difference in MIC between BTE, GTE and EGCG. However, this satisfies the fact that there are differences in sensitivity between individual strains. Since in medical practice, strain identification are usually not performed, mixtures of BTE and GTE should be used.

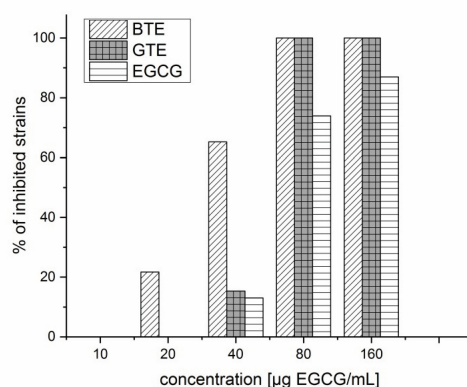


**Figure 1.** Comparison of the inhibition effectivity of different tea extracts in comparison with pure EGCG on MRSA. GTE was tested on 111 strains, while BTE and EGCG on 23 different strains (clinical isolates and type cultures, see Section 4.3.3). BTE, black tea extract; GTE, green tea extract; MRSA, methicillin-resistant *Staphylococcus aureus*.

**Table 1.** Comparison of activity of GTE, BTE and pure EGCG on the growth of MRSA strains. MIC expressed in  $\mu\text{g/mL}$  of EGCG content on 23 different strains. BTE, black tea extract; EGCG, epigallocatechin gallate; GTE, green tea extract; MIC, minimal inhibitory concentration; MRSA, methicillin-resistant *Staphylococcus aureus*; MSSA, methicillin-sensitive *Staphylococcus aureus*.

Strain	BTE	GTE	Pure EGCG
BL12357-98	20	40	40
BL14179-99	20	40	80
BL3341-99	80	80	80
BL5024-99	80	80	160
BL5808-02	40	40	80
BL9783-98	80	40	80
CH18203-97	20	40	80
HY138-00	20	40	40
HY1971-02	40	80	80
HY1975-02	40	80	160
HY2075-03	80	40	160
HY684-01	80	40	80
KL11072-00	20	40	40
KL14292-00	40	80	80
KL1486-00	40	80	80
KL15760-02	40	80	80
KL2495-99	80	80	80
LB2301-99	80	80	80
LB5375-02	40	80	>160
LB5714-03	40	40	80
Average	$49 \pm 25$	$60 \pm 21$	$88 \pm 39$
MIC 50	40	80	80
MIC 90	80	80	160
MRSA ATCC 43300	40	80	80
MSSA ATCC 29213	80	80	160
MSSA ATCC 6538	40	80	>160

### 2.3. MIC50 and MIC90

MIC50 as well as MIC90 were determined for the different solutions. The MIC50 and MIC90 of the GTE were determined to be 80  $\mu\text{g EGCG/mL}$  each. However, inhibitory effects became visible at lower concentrations (Figure 2 and Table 1).

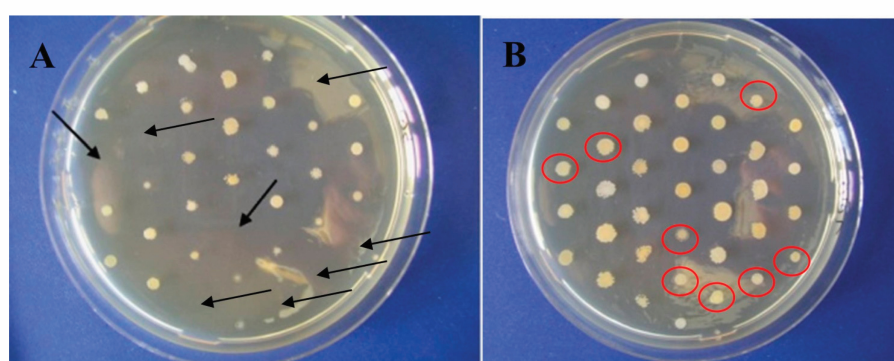


**Figure 2.** Comparison of the inhibitory effect of GTE on a selection of 36 different MRSA strains. (A) Colonies at 40  $\mu\text{g/mL}$  EGCG in GTE. (B) Colonies at 20  $\mu\text{g/mL}$  EGCG in GTE. The arrows highlight the absence of growth, the red circles show the same strains growing at the lower concentrations of EGCG. EGCG, epigallocatechin gallate; GTE, green tea extract; MRSA, methicillin-resistant *Staphylococcus aureus*.

The average MIC for GTE out of all 111 tested strains was  $74 \pm 14$   $\mu\text{g}$  EGCG/mL. The MIC<sub>50</sub> and MIC<sub>90</sub> of the BTE, expressed as EGCG content, were determined to be 40 and 80  $\mu\text{g}$  EGCG/mL, respectively. Pure EGCG had a weaker antibacterial activity compared to both tea extracts with MIC<sub>50</sub> and MIC<sub>90</sub> at 80 and 160  $\mu\text{g}$  EGCG/mL, respectively. Table 1 lists MICs for a number of tested strains. The average MIC (49  $\mu\text{g}$  EGCG/mL) of BTE out of 23 strains tested on both extracts was lower than that of GTE (60  $\mu\text{g}$  EGCG/mL). Only three strains were less sensitive for BTE than for GTE. In more than half of the strains (13/23), BTE was more active than GTE.

#### 2.4. Effect of Contact Time on Reduction Factor

Figure 3 shows the dependency of the reduction factor of GTE at 80  $\mu\text{g}$  EGCG/mL on contact time for selected bacterial strains. All strains showed a higher reduction with time elapsing. The contact time required to kill 99.999% of the bacteria depended on the tested strains. We found a higher sensitivity for the GTE of clinical isolates than of the strains from culture collections.

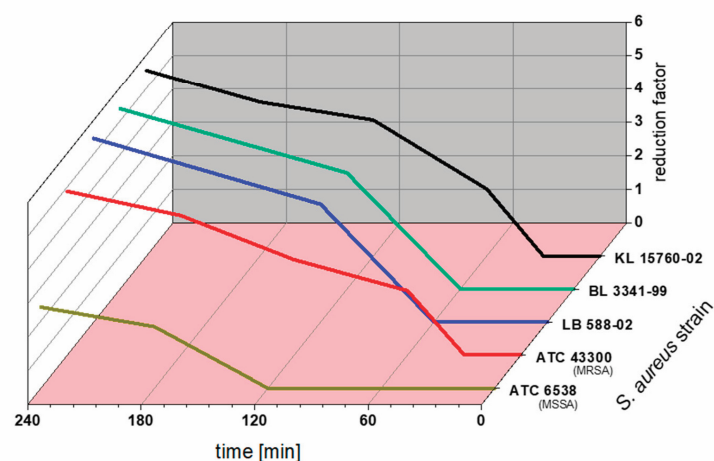


**Figure 3.** Three-dimensional plot of contact time, reduction factor and *S. aureus* strain for GTE at 80  $\mu\text{g}$  EGCG/mL. EGCG, epigallocatechin gallate; GTE, green tea extract.

Although ATCC 43300 showed the first effects after 60 min, ATCC 43300 and ATCC 6538 did not reach the intended reduction factor of 5, which all clinical isolates reached within 4 h. However, we did not see a concentration-dependant fashion as the tested concentrations of 40, 80 and 160  $\mu\text{g}$  EGCG/mL of the GTE showed similar results (see Figure S1).

### 3. Discussion

Usual brewing techniques normally yield concentrations of 10–45  $\mu\text{g}$  EGCG /mL for black tea and 78–130  $\mu\text{g}$  EGCG/mL for green tea [14]. By preparing a lyophilizate, we achieved a higher EGCG content that allowed us to maintain this concentration range even after dilution with agar. At the same time, this lyophilisate is chemically much more stable and can easily be dissolved in water.

EGCG was chosen as the lead and standard because: (1) it is present in all kinds of tea (fermented, semi fermented and non-fermented) in low to high amounts [14–17] and (2) of all antibacterial constituents, EGCG was found to have the lowest MIC [18]. EGCG uniquely enables a direct activity comparison of black and green tea extracts.

The tested solutions were all active against clinically isolated MRSA as well as against strains from culture collections of MSSA and MRSA. There were differences in susceptibility of the different strains, as expected, because of genetic diversity. Clinical isolates showed a higher susceptibility than type cultures. While the precise reason for this was not



investigated, it lends support to the suggested use of tea extracts against MRSA infections. Solutions containing only pure EGCG showed the lowest activity, necessitating higher concentrations for growth inhibition. This corroborates that antibacterial activity in tea extracts is not only based on EGCG, even though this compound is the one with the highest activity among the constituents investigated in the past [19]. BTE was more active than GTE, confirming the finding of Yam et al. [20], who reported that out of 17 teas (black, green and semi-fermented), a black tea infusion showed the highest antimicrobial potency. The different antimicrobial activities of different preparations of *Camellia sinensis* leaf extracts most likely are due to the additional presence of mono-, oligo- and polyphenols (e.g., EGC, ECG, EG). Theaflavin and epicatechin gallate (EG), for instance, were shown to exhibit antimicrobial properties [18]. They occur at comparatively high concentrations in BTE and GTE [18]. However, it needs to be underscored that the solution of BTE needed to be about twice as concentrated as the solution of the GTE in order to adjust the content of EGCG. This consequently led to higher concentrations of additional polyphenols in BTE and is most probably the reason for the higher antibacterial activity of BTE in our study.

Yam et al. [20] presented killing plots over time for a type of Japanese green tea. They only used the strain *S. aureus* USA 12 in 1997, unlike our study, which used a large number of strains selected from clinical isolates and laboratory strains. Yam et al. [20] used a 2% solution, while we used 3.75%. On this basis, the MIC of 0.28 mg extract/mL which they reported is comparable to the 30 µg EGCG/mL in this work, although the average MIC of our extract was 60 µg EGCG/mL. Therefore, while their green tea extract had half the MIC as that which was reported by us, their extract needed three times longer [20] to reduce the number of bacteria than our extract. The first effects were only seen after 8 h at a concentration of 1.5 mg/mL of a 2% tea extract. This concentration is comparable to 160 µg EGCG/mL of the green tea extract in our study that showed a reduction of 99.9% in bacteria after 4 h in four out of five strains (strains from collections and clinical isolates; see Figure S2). Zihadi et al. found a minimum bactericidal concentration (MBC) for green tea extract of 31 mg/mL [21]. In our study, the GTE of 0.4 mg/mL (containing 80 µg EGCG/mL) already led to bactericidal effects, determined as reduction in CFUs. The differences very likely resulted from differences of the tested strain(s). Differences in the amount of constituents in the green tea may also have caused a lower effect of their extract. We could not confirm the concentration dependence reported by Yam et al. as all three tested concentrations in this work showed similar results (see Figures S1 and S3). But our study clearly shows that it is possible to reduce the number of bacteria by a factor of log 5 with an extract from green tea within 4 hrs, since all clinical isolates tested showed a reduction factor of 5. This establishes that extracts from tea not only have bacteriostatic capabilities, but also bactericidal effects. However, even though these results are promising, the time needed for eradication is too long for its usage as a proper disinfectant.

Based on our results and the literature data, some applications for tea extracts in MRSA infections include: (1) the topical treatment of MRSA infections (skin, oral mucosa); and (2) the decolonisation treatment of MRSA-positive patients before surgery. This presently relies on mupirocin, chlorhexanide, octenidine or triclosan [22,23], which have considerably lower MICs [24] than tea extracts. However, in contrast to chlorhexidine and other standard disinfectants, *Camellia sinensis* extracts do not inhibit cell proliferation and there are also no known microbial resistances to this class of substances; whereas in the last years, concerns about resistance of MRSA against several common disinfectants arose [25–27]. Systemic MRSA infections cannot be treated with tea extracts and catechins because the concentrations of EGCG approaching the growth inhibitory concentrations found in this study will not be reached after an oral application of up to 800 mg of EGCG [28–30]. Thus, taken together, for the treatment of large wounds, e.g., after massive burns, and for long-term treatment, a well-tolerated antibacterial with no resistance such as BTE and GTE would be an asset. Treatment should employ mixtures of BTE and GTE as we found different sensitivities of *S. aureus* strains towards either BTE or GTE.



Another possible application consists of the inhalation of aqueous solutions of tea extracts—the same way isotonic sodium chloride solutions are widely used for common colds and dry airways, especially in ventilator bound patients, which requires moisture in the air. The first clinical data in this field provide reason for hope [9], and the extraction process in this work by using 90 °C water instead of boiling water leads to a lower caffeine content [17].

To the best of our knowledge, we are the first to show a reduction of 99.999% of clinically isolated MRSA by green tea extract within 4 h. Additionally, our results suggest that MRSA is more susceptible to BTE and EGCG than MSSA. Although statistical significance cannot be proven, Si et al. (2006) [19] showed comparable results, while Cho et al. reported similar MICs for green tea extract against MSSA and MRSA [31].

#### 4. Materials and Methods

##### 4.1. Preparation of Lyophilisates

The plant material was obtained from the local-state food inspection authority, where its identity had been ascertained beforehand. The plant name was checked with <http://www.theplantlist.org>. Different tea samples were subjected to HPLC to determine the content of EGCG, and teas with high content were chosen for the preparation of lyophilisates. A total of 1.5 g of dry tea samples was crushed and extracted for 10 min in 40 mL of water at 90 °C. Following filtration and cooling to room temperature, the extract was cleared from solids by centrifuging at 5000 rpm. The clear extract was frozen and freeze-dried. We obtained 0.8 g of lyophilisate that was stored in a desiccator at room temperature.

##### 4.2. Determination of EGCG Content in Lyophilisates by Quantitative Thin-Layer Chromatography

The lyophilisate (10 mg) was suspended in 5 mL of methanol, centrifuged, and the supernatant subjected to quantitative HPTLC. The procedure followed a published method [32] with changes in mobile phase and detection as described: mobile phase—chloroform, ethyl acetate, methanol, toluene and formic acid (12:8:4:4:2); detection—scanning with a dual wavelength TLC-scanner type CS-930 from Shimadzu (Kyoto, Japan) at a wavelength of 284 nm directly after drying for 10 min. The reference was 99.36% pure EGCG (PhytoLab, Vestenbergsgreuth, Germany).

##### 4.3. Antibacterial Assays

###### 4.3.1. Lyophilisates and Solutions Tested

###### Green Tea Extract

An amount of 800 mg of GTE lyophilisate (containing 160 mg of EGCG) was dissolved in 50 mL purified water and 355 mg of ascorbic acid was added for stabilisation as suggested by Hatano et al. [33]. We chose a molar ratio of EGCG to ascorbic acid of 5.76 because tea extracts contain a mixture of catechins that are all stabilised by ascorbic acid. This parent solution was diluted by adding purified water to yield solutions of GTE with 1.6 mg EGCG/mL, 0.8 mg EGCG/mL, 0.4 mg EGCG/mL, 0.2 mg EGCG/mL and 0.1 mg EGCG/mL.

###### Black Tea Extract

An amount of 160 mg of BTE lyophilisate (containing 16 mg of EGCG) and 35.5 mg of ascorbic acid (molar ratio of EGCG to ascorbic acid: 5.76) were dissolved in 10 mL of purified water and further diluted by adding purified water to yield solutions of BTE with the same EGCG concentrations as the GTE.

###### Pure EGCG

An amount of 16.26 mg of EGCG (purity 98.4%) and 17 mg of ascorbic acid (molar ratio of EGCG to ascorbic acid of 2.8 due to absence of additionally catechins) were dis-

solved in 10 mL purified water and diluted by adding purified water to obtain the same concentrations of EGCG as in the tea extracts.

#### 4.3.2. Preparation of Agar Plates

The preparation followed the standard protocol in [34] for the “agar dilution method for antimicrobial testing” with the following specific procedure. An aliquot of 2 mL of the appropriate dilution of extract was filled up to 20 mL with standard Mueller–Hinton agar at 55 °C, yielding test concentrations from 20 to 160 µg/mL EGCG equal to 0.002–0.016% EGCG (see Table 2). The plates were carefully tilted to ensure mixing. Four plates with GTE and one plate of BTE and pure EGCG were prepared. Additionally, one plate was poured for each dilution only containing the corresponding amount of ascorbic acid as negative control. The plates were stored at 6 °C until use.

**Table 2.** EGCG solutions and extracts used in this study. Column 1 and 2 show the percentage concentration of the whole extracts. Column 3 and 4 list the EGCG content in µg/mL% in the extracts. EGCG: Epigallocatechin gallate; GTE: Green tea extract; BTE: Black tea extract.

Concentration	GTE Extract (%)	BTE Extract (%)	EGCG in Extract (µg/mL)	EGCG in Extract (%)
Dilution 1	0.08	0.16	160	0.016
Dilution 2	0.04	0.08	80	0.008
Dilution 3	0.02	0.04	40	0.004
Dilution 4	0.01	0.02	20	0.002

#### 4.3.3. Selection of Strains for Determining the MIC of Tea Extracts and Pure EGCG

The strains used in this study were collected during a longitudinal study in the university hospital of Heidelberg, Germany [12]. In summary, the strains listed in Table 3 were used for MIC determination. As clinical isolates of MRSA are often clones of strains isolated previously, we purposefully looked for high genetic diversity.

**Table 3.** Number of *Staphylococcus aureus* strains used for MIC determination. BTE, black tea extract; GTE, green tea extract; MRSA, methicillin-resistant *Staphylococcus aureus*; MSSA, methicillin-sensitive *Staphylococcus aureus*.

Strain	GTE	BTE
Clinical MRSA isolates	108	20
ATCC-MRSA strains	1	1
ATCC-MSSA strains	2	2

GTE showed similar results for the 111 strains tested. Considering time and economy factors, we reduced the number of strains tested with BTE and pure EGCG to a limited amount of strains (10 strains with MIC<sub>GTE</sub> 40 µg EGCG/mL, 10 strains with MIC<sub>GTE</sub> 80 µg EGCG/mL and 3 reference strains). Table 1 lists these strains.

#### 4.3.4. Cultivation of Inocula and Inoculation of Agar Plates

The procedure followed the protocol “growth method” described in [34]. The exact steps were as follows. All 111 MRSA-strains were cultivated on blood agar plates (blood agar Columbia, 5% sheep blood, obtained from Oxoid Ltd., Hampshire, United Kingdom). The cultures were individually transferred, using an inoculating loop, and inoculated on plates consisting of the same agar and incubated at 36 °C for 48 h. After visually checking for pure cultures, a culture was taken with a one-time inoculating loop and put into a test tube filled with 10 mL of Mueller–Hinton–Bouillon. The tube was then blanked off and incubated for another 24 h at 36 °C. For each tube, 1 mL of incubated bacteria suspension was taken and mixed with 10 mL of 0.9% NaCl solution. This suspension was checked photometrically and inoculum was prepared to be  $1 \times 10^8$  CFU/mL. Inoculation

of prepared agar plates (Section 4.3.2) was carried out using a multipoint inoculator with 750 µL of bacteria suspended in 0.9% NaCl solution. A maximum of 36 MRSA strains was cultivated per agar plate at 36 °C for 24 h.

#### 4.3.5. Logging of Bacterial Growth; MIC Determination

The agar plates were visually checked for growth. Distinct growth was noted as “+” and less than 10 colonies was noted as “−”. MIC was determined as the lowest concentration where “−” was noted. MIC50 and MIC90 were set as the concentrations at which a growth of 50% or 90%, respectively, of all tested strains were inhibited.

#### 4.3.6. Determination of Reduction Factor of Different Green Tea Extracts

The tests were conducted using the European Standard Method for bactericidal activity in the medical area [35]. The method includes ‘organic stress’, which is intended to simulate biological conditions. Since GTE was examined using this method for the first time, with no data for comparison available, we abstained from applying ‘organic stress’. The test solution was prepared freshly by dissolving 800 mg of GTE with an EGCG content of 20% in 50 mL of water for injection (Ph.Eur.) and adding 35.5 mg of ascorbic acid. This parent solution had an EGCG content of 3.2 mg/mL. The required test solutions were prepared by diluting the parent solution with water for injection to 200, 100 and 50 µg EGCG/mL, respectively. A total volume of 8 mL of the testing solution was mixed with 1 mL purified water and 1 mL of inoculum to result in a starting an inoculation concentration of  $10^9$  CFU/mL because we tested the extracts as disinfectants, not as antibiotics. The mixture was incubated at 36 °C and 500 µL samples were taken after 30, 60, 120, 180 and 240 min. They were neutralised by dilution with 4.5 mL of a neutralising solution (polysorbate 80 30 g/L, lecithin 3 g/L, L-cystein 1 g/L, aqua bidest. ad 1000 mL) and well mixed. After 5 min, dilutions of this mixture were prepared 10 and 100 times and plated on agar to be incubated at 36 °C for 42 h for the counting of CFUs. Two control samples were measured to exclude an influence using the neutralisation method, and two control samples without tea extract were measured to determine the CFU without inhibitory effect (CFUx).

The efficacy of growth inhibition was assessed by plotting the contact time of the three GTE concentrations against the reduction factor. The reduction factor was calculated using this formula:  $\lg(\text{RF}) = \lg(\text{CFUx}) - \lg(\text{CFUy})$ , where CFUx is the number of CFU without the addition of GTE and CFUy is the number of CFU after exposure to a certain concentration of GTE for a specified time.

## 5. Conclusions

Our study proves that it is easy to prepare aqueous solutions of tea extracts that reach the MICs we found. For a tea that contains 10% of EGCG, 160 g will yield a concentration of 80 µg/mL EGCG in 200 L of water (a bathtub). This is the concentration that inhibits the growth of all MRSA strains tested. In order to reach the satisfactory reduction factor of at least 5, according to our data, the bacteria need to be in contact with the solution for at least four hours (see Section 2.4, Figure 3). Consequently, the potential application of black or green tea extracts and EGCG may aid in the long-term treatment of chronic lesions, including the prevention of MRSA (re-)colonisation. We suggest a solution or hydrocolloid dressing, for example, on the basis of carboxymethyl cellulose, containing tea extract that would easily achieve the exposure time necessary for a log 5 reduction. It combines easy preparation with good tolerability.

Prospectively, tea extracts might help to fight the increasing resistance rate by reducing the amount of applied reserve antibiotics. Because of the necessary contact time of 4 h and more, an exclusive tea extract treatment is not very promising, but as an addition to standard therapy, it could prove to be a cost-efficient way of ensuring complete eradication. In some instances, the slightly astringent side-effect may indeed help with treatment, e.g., soft-tissue healing.

**Supplementary Materials:** The following supporting information can be downloaded at: <https://www.mdpi.com/article/10.3390/plants12193440/s1>, Figure S1. Effect of GTE on reduction factor of MSSA ATCC 43300 at tested concentrations. Figure S2. Time-kill-plot for GTE with 160 µg/mL EGCG content for the tested strains. Figure S3. Overview of results for the time-kill-plot experiment.

**Author Contributions:** R.F.: Formal analysis, visualisation, writing—original draft preparation. V.B.: Investigation, performance of experiments, formal analysis. C.W.: Methodology, supervision of antibacterial assays, writing—reviewing and editing. P.I.: Conceptualisation, project administration, supervision of extract preparation and analytical part of experiments, writing—reviewing and editing. All authors have read and agreed to the published version of the manuscript.

**Funding:** This research received no external funding.

**Data Availability Statement:** The data presented in this study are available on request from the corresponding author.

**Conflicts of Interest:** The authors declare no conflict of interest.

### Abbreviations

BTE: black tea extract; EG: epicatechin gallate; EGC: epigallocatechin; EGCG: epigallocatechin gallate; GTE: green tea extract; Ph.Eur.: European Pharmacopoeia; RF: reduction factor; MIC: minimal inhibitory concentration; MRSA: methicillin-resistant *Staphylococcus aureus*; MSSA: methicillin-sensitive *Staphylococcus aureus*.

### References

- Cassini, A.; Högberg, L.D.; Plachouras, D.; Quattrocchi, A.; Hoxha, A.; Simonsen, G.S.; Colomb-Cotinat, M.; Kretzschmar, M.E.; Devleeschauwer, B.; Cecchini, M. Attributable deaths and disability-adjusted life-years caused by infections with antibiotic-resistant bacteria in the EU and the European Economic Area in 2015: A population-level modelling analysis. *Lancet Infect Dis* **2019**, *19*, 56–66. [\[CrossRef\]](#)
- Murray, C.J.; Sharara, F.; Swetschinski, L.; Aguilar, G.R.; Gray, A.; Han, C.; Bisignano, C.; Rao, R.; Wool, E.; Johnson, S.C.; et al. Global burden of bacterial antimicrobial resistance in 2019: A systematic analysis. *Lancet* **2022**, *399*, 629–655. [\[CrossRef\]](#) [\[PubMed\]](#)
- WHO Regional Office for Europe. European Centre for Disease Prevention and Control. In *Antimicrobial Resistance Surveillance in Europe 2022–2020 Data*; WHO Regional Office for Europe: Copenhagen, Denmark, 2022.
- European Centre for Disease Prevention and Control. Surveillance Atlas of Infectious Diseases. Available online: <https://atlas.ecdc.europa.eu/public/index.aspx> (accessed on 8 June 2022).
- Steinmann, J.; Buer, J.; Pietschmann, T.; Steinmann, E. Anti-infective properties of epigallocatechin-3-gallate (EGCG), a component of green tea. *Br. J. Pharmacol.* **2013**, *168*, 1059–1073. [\[CrossRef\]](#)
- McNaught, J.G. On the action of cold or lukewarm tea on *Bacillus typhosus*. *J. R. Army Med. Corps* **1906**, *7*, 372–373.
- Toda, M.; Okubo, S.; Hiyoshi, R.; Shimamura, T. The bactericidal activity of tea and coffee. *Lett. Appl. Microbiol.* **1989**, *8*, 123–125. [\[CrossRef\]](#)
- Ikigai, H.; Nakae, T.; Hara, Y.; Shimamura, T. Bactericidal catechins damage the lipid bilayer. *Biochim. Et Biophys. Acta (BBA) Biomembr.* **1993**, *1147*, 132–136. [\[CrossRef\]](#)
- Yamada, H.; Tateishi, M.; Harada, K.; Ohashi, T.; Shimizu, T.; Atsumi, T.; Komagata, Y.; Iijima, H.; Komiyama, K.; Watanabe, H. A randomized clinical study of tea catechin inhalation effects on methicillin-resistant *Staphylococcus aureus* in disabled elderly patients. *J. Am. Med. Dir. Assoc.* **2006**, *7*, 79–83. [\[CrossRef\]](#)
- Fujii, M.; Ohrui, T.; Sato, T.; Sato, T.; Sato, N.; Sasaki, H. Green tea for decubitus ulcer in bedridden patients. *Geriatr. Gerontol. Int.* **2003**, *3*, 208–211. [\[CrossRef\]](#)
- Fujii, M.; Sato, T.; Sato, T.; Sasaki, H. Green tea for tinea manuum in bedridden patients. *Geriatr. Gerontol. Int.* **2004**, *4*, 64–65. [\[CrossRef\]](#)
- Petersdorf, S.; Oberdorfer, K.; Wendt, C. Longitudinal study of the molecular epidemiology of methicillin-resistant *Staphylococcus aureus* at a university hospital. *J. Clin. Microbiol.* **2006**, *44*, 4297–4302. [\[CrossRef\]](#)
- Wang, R.; Zhou, W.; Jiang, X. Reaction kinetics of degradation and epimerization of epigallocatechin gallate (EGCG) in aqueous system over a wide temperature range. *J. Agric. Food Chem.* **2008**, *56*, 2694–2701. [\[CrossRef\]](#) [\[PubMed\]](#)
- Wu, J.; Xie, W.; Pawliszyn, J. Automated in-tube solid phase microextraction coupled with HPLC-ES-MS for the determination of catechins and caffeine in tea. *Analyst* **2000**, *125*, 2216–2222. [\[CrossRef\]](#) [\[PubMed\]](#)
- Wang, K.; Liu, F.; Liu, Z.; Huang, J.; Xu, Z.; Li, Y.; Chen, J.; Gong, Y.; Yang, X. Comparison of catechins and volatile compounds among different types of tea using high performance liquid chromatograph and gas chromatograph mass spectrometer. *Int. J. Food Sci. Technol.* **2011**, *46*, 1406–1412. [\[CrossRef\]](#)
- Lin, Y.-S.; Tsai, Y.-J.; Tsay, J.-S.; Lin, J.-K. Factors affecting the levels of tea polyphenols and caffeine in tea leaves. *J. Agric. Food Chem.* **2003**, *51*, 1864–1873. [\[CrossRef\]](#) [\[PubMed\]](#)

17. Wang, H.; Provan, G.J.; Helliwell, K. HPLC determination of catechins in tea leaves and tea extracts using relative response factors. *Food Chem.* **2003**, *81*, 307–312. [\[CrossRef\]](#)
18. Taguri, T.; Tanaka, T.; Kouno, I. Antimicrobial activity of 10 different plant polyphenols against bacteria causing food-borne disease. *Biol. Pharm. Bull.* **2004**, *27*, 1965–1969. [\[CrossRef\]](#)
19. Si, W.; Gong, J.; Tsao, R.; Kalab, M.; Yang, R.; Yin, Y. Bioassay-guided purification and identification of antimicrobial components in Chinese green tea extract. *J. Chromatogr. A* **2006**, *1125*, 204–210. [\[CrossRef\]](#)
20. Yam, T.; Shah, S.; Hamilton-Miller, J. Microbiological activity of whole and fractionated crude extracts of tea (*Camellia sinensis*), and of tea components. *FEMS Microbiol. Lett.* **1997**, *152*, 169–174. [\[CrossRef\]](#)
21. Zihadi, M.A.H.; Rahman, M.; Talukder, S.; Hasan, M.M.; Nahar, S.; Sikder, M.H. Antibacterial efficacy of ethanolic extract of *Camellia sinensis* and *Azadirachta indica* leaves on methicillin-resistant *Staphylococcus aureus* and shiga-toxigenic *Escherichia coli*. *J. Adv. Vet. Anim. Res.* **2019**, *6*, 247. [\[CrossRef\]](#)
22. MRSA-Decolonisation-Treatment-Healthcare-Providers, Government of Western Australia Departement of Health. Available online: [https://www2.health.wa.gov.au/Articles/A\\_E/Decolonisation-treatment-for-MRSA](https://www2.health.wa.gov.au/Articles/A_E/Decolonisation-treatment-for-MRSA) (accessed on 21 December 2022).
23. MRSA-Decolonisation-Treatment-Regime, National Health Service. Available online: <https://www.esht.nhs.uk/leaflet/mrsa-decolonisation-treatment-regime/> (accessed on 21 December 2022).
24. Aftab, R.; Dodhia, V.H.; Jeanes, C.; Wade, R.G. Bacterial sensitivity to chlorhexidine and povidone-iodine antiseptics over time: A systematic review and meta-analysis of human-derived data. *Sci. Rep.* **2023**, *13*, 347. [\[CrossRef\]](#)
25. Labrecque, S.; Shah, S.; Fergus, D.; Parry, M.F. Mupirocin susceptibility of staphylococci 2022: Is It time for a change in MRSA decolonization protocols? *Am. J. Infect. Control* **2023**, *51*, 725–728. [\[CrossRef\]](#) [\[PubMed\]](#)
26. Sritharadol, R.; Hamada, M.; Kimura, S.; Ishii, Y.; Srichana, T.; Tateda, K. Mupirocin at subinhibitory concentrations induces biofilm formation in *Staphylococcus aureus*. *Microb. Drug Resist.* **2018**, *24*, 1249–1258. [\[CrossRef\]](#) [\[PubMed\]](#)
27. Van den Poel, B.; Saegeman, V.; Schuermans, A. Increasing usage of chlorhexidine in health care settings: Blessing or curse? A narrative review of the risk of chlorhexidine resistance and the implications for infection prevention and control. *Eur. J. Clin. Microbiol. Infect. Dis.* **2022**, *41*, 349–362. [\[CrossRef\]](#) [\[PubMed\]](#)
28. Chow, H.S.; Cai, Y.; Alberts, D.S.; Hakim, I.; Dorr, R.; Shahi, F.; Crowell, J.A.; Yang, C.S.; Hara, Y. Phase I pharmacokinetic study of tea polyphenols following single-dose administration of epigallocatechin gallate and polyphenon E. *Cancer Epidem Biomark.* **2001**, *10*, 53–58.
29. Lee, M.-J.; Maliakal, P.; Chen, L.; Meng, X.; Bondoc, F.Y.; Prabhu, S.; Lambert, G.; Mohr, S.; Yang, C.S. Pharmacokinetics of tea catechins after ingestion of green tea and (-)-epigallocatechin-3-gallate by humans: Formation of different metabolites and individual variability. *Cancer Epidem Biomark.* **2002**, *11*, 1025–1032.
30. Yang, C.S.; Chen, L.; Lee, M.-J.; Balentine, D.; Kuo, M.C.; Schantz, S.P. Blood and urine levels of tea catechins after ingestion of different amounts of green tea by human volunteers. *Cancer Epidem Biomark.* **1998**, *7*, 351–354.
31. Cho, Y.-S.; Schiller, N.L.; Oh, K.-H. Antibacterial effects of green tea polyphenols on clinical isolates of methicillin-resistant *Staphylococcus aureus*. *Cur Microbiol.* **2008**, *57*, 542–546. [\[CrossRef\]](#)
32. Min, Z.; Peigen, X. Quantitative analysis of the active constituents in green tea. *Phytother. Res.* **1991**, *5*, 239–240. [\[CrossRef\]](#)
33. Hatano, T.; Tsugawa, M.; Kusuda, M.; Taniguchi, S.; Yoshida, T.; Shiota, S.; Tsuchiya, T. Enhancement of antibacterial effects of epigallocatechin gallate, using ascorbic acid. *Phytochemistry* **2008**, *69*, 3111–3116. [\[CrossRef\]](#)
34. Wiegand, I.; Hilpert, K.; Hancock, R. Agar and broth dilution methods to determine the minimal inhibitory concentration (MIC) of antimicrobial substances. *Nat. Protoc.* **2007**, *3*, 163–175. [\[CrossRef\]](#)
35. Gebel, J.; Werner, H.; Kirsch-Altena, A.; Bansemir, K. Chemical disinfectants and antiseptics-Quantitative suspension test for the evaluation of bactericidal activity of chemical disinfectants for instruments used in the medical area—Test method and requirements (phase 2, step 1); German version EN 13727. In *Standardmethoden der DGHM zur Prüfung chemischer Desinfektionsverfahren*; mhp-Verlag: Wiesbaden, Germany, 2003; pp. 18–23.

**Disclaimer/Publisher’s Note:** The statements, opinions and data contained in all publications are solely those of the individual author(s) and contributor(s) and not of MDPI and/or the editor(s). MDPI and/or the editor(s) disclaim responsibility for any injury to people or property resulting from any ideas, methods, instructions or products referred to in the content.



## 2.2) Research Article II

### **Biological activity and stability analyses of knipholone anthrone, a phenyl anthraquinone derivative isolated from *Kniphofia foliosa* Hochst.**

**Ruth Feilcke**, Georgette Arnouk, Boingotlo Raphane, Khumoekae Richard, Ian Tietjen, Kerstin Andrae-Marobela, Frank Erdmann, Susanne Schipper, Katja Becker, Norbert Arnold, Andrej Frolov, Norbert Reiling, Peter Imming, Serge A.T. Fobofou

**Elsevier, Journal of Pharmaceutical and Biomedical Analysis**

*J Pharm Biomed Anal*, **2019**, 174:277

Publication Date: September 10, 2019

Doi: 10.1016/j.jpba.2019.05.065

#### Summary

In this article we present the results on several biological activity studies on knipholone anthrone that was extracted during my thesis such as antiplasmodial, antimycobacterial and anthelmintic assays that were performed by our cooperation partners. The variety of assays were chosen according to reported activity in literature and on the basis of the originating plant to be used to treat different ailments in sub-Saharan African countries. Next to a cytotoxicity study we present a detailed study on the stability in different media to explain assay to assay variations observed by some cooperation partners from Simon Fraser University.

#### Own contribution

Extraction, purification and chemical characterization of Knipholone and Knipholone anthrone, stability study in two culture media, design and supervision of the stability study in PBS/acetonitrile and water undertaken by the Master student GEORGETTE ARNOUK and evaluation of data obtained by her, coordination of results from different cooperation partners, data curation and visualization, rewriting and editing.





Contents lists available at ScienceDirect

## Journal of Pharmaceutical and Biomedical Analysis

journal homepage: [www.elsevier.com/locate/jpba](http://www.elsevier.com/locate/jpba)

## Biological activity and stability analyses of knipholone anthrone, a phenyl anthraquinone derivative isolated from *Kniphofia foliosa* Hochst.



Ruth Feilcke<sup>a</sup>, Georgette Arnouk<sup>a</sup>, Boingotlo Raphane<sup>b</sup>, Khumoeke Richard<sup>c</sup>, Ian Tietjen<sup>c</sup>, Kerstin Andrae-Marobela<sup>b</sup>, Frank Erdmann<sup>a</sup>, Susanne Schipper<sup>d</sup>, Katja Becker<sup>d</sup>, Norbert Arnold<sup>e</sup>, Andrej Frolov<sup>e,f</sup>, Norbert Reiling<sup>g,h</sup>, Peter Imming<sup>a</sup>, Serge A.T. Fobofou<sup>a,e,\*</sup>

<sup>a</sup> Institute of Pharmacy, Martin Luther University Halle-Wittenberg, Wolfgang-Langenbeck-Str. 4, 06120 Halle (Saale), Germany

<sup>b</sup> Department of Biological Sciences, Faculty of Science, University of Botswana, Block 235, Private Bag, 0022 Gaborone, Botswana

<sup>c</sup> Faculty of Health Sciences, Simon Fraser University, Burnaby, Canada

<sup>d</sup> Biochemistry and Molecular Biology, Interdisciplinary Research Center, Justus Liebig University Giessen, Heinrich-Buff-Ring 26-32, 35392 Giessen, Germany

<sup>e</sup> Department of Bioorganic Chemistry, Leibniz Institute of Plant Biochemistry, Weinberg 3, 06120 Halle (Saale), Germany

<sup>f</sup> Department of Biochemistry, St. Petersburg State University, 199904 St. Petersburg, Russia

<sup>g</sup> Research Center Borstel, Leibniz Lung Center, 23845 Borstel, Germany

<sup>h</sup> German Center for Infection Research (DZIF), Partner Site Hamburg-Lübeck-Borstel, 23845 Borstel, Germany

## ARTICLE INFO

## Article history:

Received 21 January 2019

Received in revised form 13 May 2019

Accepted 29 May 2019

Available online 31 May 2019

## Keywords:

Knipholone anthrone  
anti-HIV activity  
Stability analysis  
Natural products  
Medicinal plants

## ABSTRACT

Knipholone (**1**) and knipholone anthrone (**2**), isolated from the Ethiopian medicinal plant *Kniphofia foliosa* Hochst. are two phenyl anthraquinone derivatives, a compound class known for biological activity. In the present study, we describe the activity of both **1** and **2** in several biological assays including cytotoxicity against four human cell lines (Jurkat, HEK293, SH-SY5Y and HT-29), antiparasmodial activity against *Plasmodium falciparum* 3D7 strain, anthelmintic activity against the model organism *Caenorhabditis elegans*, antibacterial activity against *Aliivibrio fischeri* and *Mycobacterium tuberculosis* and anti-HIV-1 activity in peripheral blood mononuclear cells (PBMCs) infected with HIV-1<sub>c</sub>. In parallel, we investigated the stability of knipholone (**2**) in solution and in culture media. Compound **1** displays strong cytotoxicity against Jurkat, HEK293 and SH-SY5Y cells with growth inhibition ranging from approximately 62–95% when added to cells at 50  $\mu$ M, whereas KA (**2**) exhibits weak to strong activity with 26, 48 and 70% inhibition of cell growth, respectively. Both **1** and **2** possess significant antiparasmodial activity against *Plasmodium falciparum* 3D7 strain with IC<sub>50</sub> values of 1.9 and 0.7  $\mu$ M, respectively. These results complement previously reported data on the cytotoxicity and antiparasmodial activity of **1** and **2**. Furthermore, compound **2** showed HIV-1<sub>c</sub> replication inhibition (growth inhibition higher than 60% at tested concentrations 0.5, 5, 15 and 50  $\mu$ g/ml and an EC<sub>50</sub> value of 4.3  $\mu$ M) associated with cytotoxicity against uninfected PBMCs. The stability study based on preincubation, HPLC and APCI-MS (atmospheric-pressure chemical ionization mass spectrometry) analysis indicates that compound **2** is unstable in culture media and readily oxidizes to form compound **1**. Therefore, the biological activity attributed to **2** might be influenced by its degradation products in media including **1** and other possible dimers. Hence, bioactivity results previously reported from this compound should be taken with caution and checked if they differ from those of its degradation products. To the best of our knowledge, this is the first report on the anti-HIV activity and stability analysis of compound **2**.

© 2019 Elsevier B.V. All rights reserved.

## 1. Introduction

Phenyl anthraquinones (PAQs) are a biosynthetically distinct class of biaryl-like natural products composed of an anthraquinone skeleton and an acylphloroglucinol moiety [1,2]. The natural chem-

\* Corresponding author at: Institute of Pharmacy, Martin Luther University Halle-Wittenberg, Wolfgang-Langenbeck-Str. 4, 06120 Halle (Saale), Germany.  
E-mail address: [sfobofou@ipb-halle.de](mailto:sfobofou@ipb-halle.de) (S.A.T. Fobofou).

<https://doi.org/10.1016/j.jpba.2019.05.065>

0731-7085/© 2019 Elsevier B.V. All rights reserved.



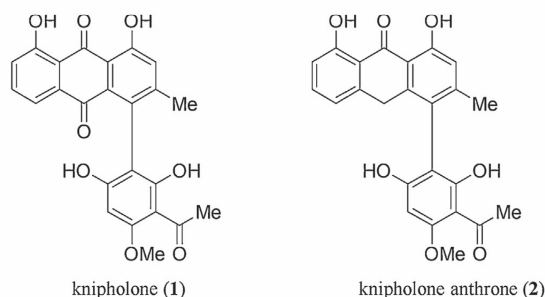


**Fig. 1.** Chemical structures of knipholone (1) and knipholone (2) isolated from *K. foliosa*.

ical diversity of this class of compounds is mainly based on the *O*-methylation pattern of the acylphloroglucinol nucleus, the occurrence of chrysophanol anthrone as the anthraquinone skeleton, the degree of oxidation of the anthraquinone moiety, or dimerization [1,2]. Since the initial isolation of knipholone (KP, 1) and knipholone anthrone (KA, 2) in 1984 and 1993, respectively (Fig. 1), from the roots of *Kniphofia foliosa* Hochst., (Asphodelaceae) [1–4], PAQs have subsequently been found in plants of the genera *Kniphofia*, *Bulbine*, *Bulbinella* (Asphodelaceae) and *Senna* (Leguminosae) [2]. While some PAQs are reported to exhibit remarkable antiparasitic, cytotoxic and antioxidant activity [1,2], the biological activities of most PAQs remain unexplored.

*K. foliosa* is an Ethiopian medicinal plant traditionally used for the treatment of abdominal cramps and wound healing [4]. As part of our continuing investigation of bioactive compounds from African medicinal flora [5,6], here we tested the stability of compounds 1 and 2 in solutions and different media. We further assessed these compounds for a broad range of biological activities including anti-HIV-1<sub>c</sub>, antiparasitic, antibacterial, anthelmintic and cytotoxic effects in several human cell lines and primary cells.

## 2. Material and methods

### 2.1. Materials and chemicals

Authentic samples of knipholone (1) and knipholone anthrone (2) were obtained from the Pan African Natural Product Library (pANAPL) and used as references. Additionally, we isolated compound 2 from *K. foliosa* as previously described [3,4]. Distilled water was used for HPLC and acetonitrile was HPLC grade and commercially available. The buffer solution PBS (pH = 7.4) was prepared by dissolving Na<sub>2</sub>HPO<sub>4</sub> · 2H<sub>2</sub>O (3.1807 g), KH<sub>2</sub>PO<sub>4</sub> (0.6 g) and NaCl (5.85 g) in distilled water (1 L).

### 2.2. Instrumentation and analytical studies

HPLC-chromatograms were done on a WATERS HPLC-system (WATERS 600 controller, Waters 717 plus auto-sampler, Waters 2996 photodiode array detector) using a LiChroCART® 125-4, LiChrospher® 100 RP-18e (5 μm) column, eluent: ACN:H<sub>2</sub>O (60:40 v/v), flow rate: 1 mL/min, injection volume: 20 μL, injection per vial: 3, run time: 20 min. Specificity of the system was validated by injecting a reference sample of knipholone (1) and the closely related compound knipholone anthrone (2), which resulted in two separated peaks with matching DAD-UV-spectra. Linearity was proven by analyzing 6 concentrations ranging from 2.3 to 23 μM: correlation coefficient: 0.99923 (pearson's corr. coefficient), y-intercept: -78.631, slope of the regression line: 380.39 and residual sum of squares 0.9985 (R<sup>2</sup>).

APCI-MS stability assays in buffer systems were performed on an Advion Expression S mass spectrometer with atmospheric solids analysis probe (ASAP) measuring unit. MS experiments were performed in positive mode (mass scan ranges: *m/z* 50–1000 and 250–700). 500 μL of knipholone anthrone (2) in cell media was prepared and kept in a temperature-controlled heating oven at 37 °C over 400 min. At defined points, 45 μL of the mixture was transferred to a new vessel, mixed with 45 μL of 1 N HCl, shaken and thoroughly mixed after addition of 150 μL of ethyl acetate. After phase separation, 90 μL of the upper layer was transferred to a new tube and directly analyzed by APCI-MS. The ratio of intensity *I*(*m/z* 421.2)/*I*(*m/z* 435.2) was determined for all samples, where *m/z* 421.2 and 435.2 belong to 2 and 1, respectively. The correlation between the ratio of intensity in APCI-MS and the ratio of concentration was verified by four quality control samples (300 μM 2, 200 μM 2/100 μM 1, 150 μM 2/150 μM 1 and 100 μM 2/200 μM 1 in PBS, each 100 μL), which lead to an exponential correlation with residual sum of squares of 0.9968 (R<sup>2</sup>). <sup>1</sup>H NMR spectra were recorded on Agilent 400 MHz VNMRs and Agilent 500 MHz DD2 NMR spectrometers at 400 and 500 MHz for 1 and 2, respectively. The <sup>1</sup>H NMR chemical shifts (δ) are reported relative to tetramethylsilane (TMS).

### 2.3. Plant material and extraction of knipholone anthrone (2)

The plant material *Kniphofia foliosa* Hochst. used in this study for the extraction of 2 was kindly provided by Prof. Ermias Dagne from the Addis Ababa University, Ethiopia. It was identified by Prof. Sebebe Demissew, botanist and keeper of the Ethiopian National Herbarium where a voucher specimen (Sebebe D. and Ermias D. 2396) is deposited.

359 g of air-dried and powdered roots of *K. foliosa* were macerated in petroleum ether (445 mL) and filtered. The residue was extracted with ethyl acetate at room temperature for 30–45 min (percolation) and a brownish extract was obtained after solvent removal. Compound 2, a yellow substance, was obtained by recrystallization of the ethyl acetate extract in acetone. The above procedures were repeated five times to give five batches of extraction in a row, each resulting to the respective following amounts of 2 in different purities: (amount, HPLC purity: 1504 mg, 89.9%; 576.9 mg, 70.5%; 115 mg, 91%; 90 mg, 86.6%; 61.5 mg; 80.3%). The overall amount of 2 collected from the five batches was 2.35 g. The NMR data of 2 (1504 mg, 89.9% HPLC purity) matched those of the authentic knipholone anthrone (2) obtained from the pANAPL and available in our group [3]. However, two major peaks could be observed in the HPLC chromatogram of the most successful extraction of 2 (1504 mg, 89.9% HPLC purity, see Figs. S1 and S2 in the Supporting Information). Comparing with authentic knipholone (1) and freshly dissolved knipholone anthrone (2) batch, the peaks at 4.5 and 6 min (*R<sub>t</sub>*) could be assigned to 1 and 2, respectively. Hence, the major impurity in compound 2 could be attributed to knipholone (1). Details about the stability of 2 in solutions and media are described in Section 3.6.

### 2.4. Cytotoxicity

Compounds 1 and 2 were initially incubated for 24 h in RPMI-1640 cell culture medium supplemented with 5 mM L-glutamine and 10% (v/v) FCS (Biocrom, Berlin) with alamarBlue reagent (Invitrogen, CA) without cells and then spectroscopically analyzed to exclude any interference between the test compounds and the redox-sensitive assay reagent resazurin in alamarBlue (R). Fluorescence at 590 nm was the readout. None of the compounds had an influence on the signal (data not shown).

HEK293 cells (DSMZ Braunschweig, ACC305) and SH-SY5Y cells (DSMZ Braunschweig, ACC209) were incubated in Dulbecco's Mod-

ified Eagle Medium (DMEM) supplemented with 10% (v/v) FCS and 5 mM L-glutamine (Biochrom, Berlin) at 37 °C in a humidified incubator with 5% CO<sub>2</sub>. The Jurkat (DSMZ Braunschweig, ACC282) and HT-29 (DSMZ Braunschweig, ACC299) cells were cultured in the same manner as HEK293 and SH-SY5Y cells but with RPMI-1640 medium in place of DMEM. Cells were seeded at  $1\text{--}2.5 \times 10^3$  cells per well in a 96-well cell culture plate (TPP, Switzerland). Compounds were added immediately to the medium at stated concentrations. After 24 h, cell viability was measured by adding alamarBlue reagent according to the manufacturer instructions and incubating cells for a further 6 h. Detection of viable cells was performed using a FLUOstar OPTIMA microplate reader (BMG Labtec). All measurements were performed in triplicate, and data are presented as mean  $\pm$  SD.

## 2.5. *M. tuberculosis* activity tests

Bacteria: Stably green fluorescent protein (GFP)-expressing *M. tuberculosis* bacteria (H37Rv strain) were generated as previously described [7] and cultured in 7H9 complete medium (cat# 271310; BD Difco; Becton Dickinson) supplemented with oleic acid-albumin-dextrose-catalase (OADC, 10%; BD, # 212351), 0.2% glycerol, and 0.05% Tween 80. At mid-log phase (OD<sub>600</sub> = 0.4) cultures were harvested and frozen in aliquots at  $-80^\circ\text{C}$ .

**Compound preparation and assay procedure:** 45 ml 7H9 (without glycerol and without Tween 80) was supplemented with 5 ml OADC. Starting from compound stock solutions in DMSO of 10 mg/ml, 1  $\mu\text{L}$  of each compound was diluted with 800  $\mu\text{L}$  7H9 test medium. 80  $\mu\text{L}$  of each concentration was added in triplicate to a black 96 well plate with a clear bottom (Corning). The amount of aliquots of *Mtb* bacteria needed were thawed in a heating block at 37 °C and centrifuged for 10 min at 3700 x g (Heraeus, Swingout rotor). The supernatant was discarded and the bacteria were re-suspended in 7H9 test medium to reach a concentration of  $2 \times 10^6/20 \mu\text{L}$ . 20  $\mu\text{L}$  of the bacterial suspension was added to the wells containing 80  $\mu\text{L}$  well in the absence (control) or presence of the compounds. Each plate was prepared with rifampicin (National Reference Center, Borstel) as a reference compound (dilutions in water) which has a known inhibitory activity against *M. tuberculosis* at 0.1 and 1  $\mu\text{g}/\text{ml}$ . Plates were sealed with an air-permeable membrane (Porvair Sciences) and cultured under mild agitation (Rotamax 120, Heidolph), not stacked, at 37 °C in an incubator. Bacterial growth was determined at day 7 by measuring the relative fluorescence intensity using a microplate reader (Synergy 2, Biotek).

## 2.6. *P. falciparum* cell culture and determination of EC<sub>50</sub> values

The *P. falciparum* 3D7 strain was cultured as described [8] with slight modifications. Parasites were propagated in RBCs (A+) in RPMI 1640 medium (Gibco, Paisley, UK) supplemented with 0.5% Albumax, 9 mM glucose, 0.2 mM hypoxanthine, 2.1 mM L-glutamine, and 22  $\mu\text{g}/\text{ml}$  gentamycin at 3.3% hematocrit and 37 °C in a gaseous mixture consisting of 3% O<sub>2</sub>, 3% CO<sub>2</sub> and 94% N<sub>2</sub>. Synchronization of *P. falciparum* parasites was carried out with 5% (w/v) sorbitol [9]. *P. falciparum* trophozoites were enriched by magnet separation [10]. The half maximal effective concentration (EC<sub>50</sub>) of antimalarial drugs on *P. falciparum* 3D7 asexual blood stages was determined by the [<sup>3</sup>H] hypoxanthine incorporation assay as described elsewhere [11].

## 2.7. Anthelmintic activity

This assay was performed on the model organism *Caenorhabditis elegans* as described by Thomsen et al. 2012 [12]. The Bristol N2 wild type strain of *C. elegans* was used in the anthelmintic assay.

The nematodes were cultured on NGM (Nematode Growth Media) petri plates using the uracil auxotroph *E. coli* strain OP50 as food source [12]. After 4 days of cultivation the nematodes were transferred from the petri plate to a 15 mL falcon tube by rinsing each plate twice with 2 mL M9 buffer. The worm suspension was centrifuged for 1 min at 800 G. After removal of the supernatant the nematodes were washed again with 2 mL M9 buffer under the same conditions and, depending on the number of animals, resuspended in 2 to 8 mL M9 buffer. To this suspension 10  $\mu\text{L}$  penicillin-streptomycin-solution (10 mg/mL) was added. After triply counting the nematodes in 10  $\mu\text{L}$  solution droplets under a stereo microscope (Olympus SZX12) the worm number was adjusted to 20–30 animals per 20  $\mu\text{L}$ . The assay was performed in 384 well plates. The outer wells were filled with water to minimize evaporation. To the test wells 20  $\mu\text{L}$  worm suspension was added and the number of living and dead animals in each well were counted using the cell culture microscope Olympus CKX41. The number of living nematodes is consistent with 100%. At staggered intervals 20  $\mu\text{L}$  test solution (test compound in 4% DMSO in M9 buffer) was added followed by microscopic enumeration of living and dead test organism after 30 min incubation. In all the assays, the solvent DMSO (2%) and the standard anthelmintic drug ivermectin (10  $\mu\text{g}/\text{mL}$ ) were used as negative and positive controls, respectively. All the assays were done in triplicate.

## 2.8. *Aliivibrio fischeri* bioassay

Isolated compounds were tested against the Gram negative bacterium *Aliivibrio fischeri* at two different concentrations 1 and 100  $\mu\text{M}$ . *A. fischeri* is a model and non-pathogenic bacterium, which grows easily and can be used in bioluminescence assay. The assay was performed using *A. fischeri* test strain DSM507 (batch no. 1209) [13]. Briefly, for each assay, a fresh glycerol stock was incubated in 25 mL Boss medium at 100 rpm and 23 °C for 16–18 h and was afterwards diluted with fresh BOSS medium to an appropriate cell number (luminescence value between 30,000 and 50,000 RLU). The assay was conducted on black flat bottom 96 well plates (Brand cellGrade™ premium, STERILE R) in a final volume of 200  $\mu\text{L}$  of Boss medium containing 1% DMSO in each well (100  $\mu\text{L}$  diluted bacterial solution and 100  $\mu\text{L}$  test solution). The plates were incubated in the dark at 23 °C and 100% humidity without lid and without shaking for 24 h. The bioluminescence (obtained in relative luminescence units, RLU) is dependent on the cell density and was determined after 24 h using the microplate reader Tecan Genios Pro. The whole wavelength range was detected for 1000 ms without preliminary shaking to avoid secondary oxygen effects. The results (mean value  $\pm$  standard deviation, n=6) are given as relative values (% inhibition) in comparison to the negative control (bacterial growth, 1% DMSO, without test compound). Negative values indicate an elevation of luminescence /increase of bacterial growth. Chloramphenicol (100  $\mu\text{M}$ ) was used as positive control and induced the complete inhibition of bacterial growth.

## 2.9. Anti-HIV activity

Inhibition of HIV-1c replication by compounds **1** and **2** was measured as previously described [14] using the HIV-1c molecular clone MJ4 [15] for the infection of peripheral blood mononuclear cells (PBMCs) obtained from HIV-1 seronegative donors (a kind gift of the Botswana National Blood Bank). HIV-1c (MJ4) p24 antigen production was quantified by enzyme-linked immunosorbent assay (ELISA, XpressBio, Frederick, MD, USA) according to manufacturer's instructions after exposure of infected PBMCs to compounds at different concentrations. In this assay azidothymidine (AZT, Zidovudine, Retrovir®, GlaxoSmithKline) was included as the positive control. Viability of PBMCs exposed to compounds

were determined as previously described [14] using the viability indicator MTT (Sigma). Best-fit dose–response curves were generated from triplicate assays and the half-maximal effective concentrations ( $EC_{50}$ , drug concentration that caused a 50% reduction in p24 antigen levels as compared to controls), as well as the half-maximal cytotoxic concentration ( $CC_{50}$ , drug concentration that caused 50% of cell death compared to controls) were calculated from the dose–response data using GraphPad Prism 4.0 software (GraphPad Software, La Jolla, CA, USA). Data are presented as mean  $\pm$  S.D. from triplicate determination.

### 3. Results and discussions

#### 3.1. Tested compounds

Compounds studied (Fig. 1) were two phenyl anthraquinone derivatives including knipholone (KP, **1**) and knipholone anthrone (KA, **2**) isolated from *K. foliosa*. The isolation and identification of compounds **1** and **2** from *K. foliosa* were previously reported [3,4].

#### 3.2. Cytotoxicity

**1** and **2** were first tested for cytotoxic activity against four human cell lines: T cell leukemia (Jurkat), embryonic kidney (HEK293), neuroblastoma (SH-SY5Y) and colon cancer (HT-29) (Fig. 2). These cell lines represent different types of tissues or somatogenetic origins. Treatment with either compound at 50  $\mu$ M caused cytotoxic effects (Fig. 2A). The cytotoxicity against Jurkat, HEK293 and SH-SY5Y cell lines was more pronounced in the presence of **1**, which caused cell growth inhibition ranging from approximately 62–95% at 50  $\mu$ M. **1** also exhibited strong cytotoxicity against Jurkat and SH-SY5Y cell lines with percentages of reduction of cell viability of approximately 88 and 95%. 50  $\mu$ M of **2** resulted in 26, 48 and 70% reduction of viability in cultures of Jurkat, HEK293 and SH-SY5Y cells, respectively. In contrast, 50  $\mu$ M of either **1** or **2** resulted in little to no cytotoxicity against HT-29 cancer cells (Fig. 2A). Dose-response curves with **1** and **2** at higher concentrations (50, 100, 250 and 500  $\mu$ M) after 24 h incubation with the less sensitive cell line HT-29 revealed concentration dependent cytotoxicity with  $EC_{50}$  values of  $350.6 \pm 57.5$   $\mu$ M and  $162.4 \pm 16.9$   $\mu$ M, respectively. Notably, some knipholone derivatives were described to exhibit tumor-specific cytotoxicity ( $IC_{50}$  24–25  $\mu$ M) against HSC-2 oral squamous cell carcinoma cells comparable to or slightly weaker than positive-control etoposide ( $IC_{50}$  24  $\mu$ M) [16]. Furthermore, other studies reported the comparative cytotoxicity of **1** and **2** in leukaemic and melanocyte cancer cell lines [17]. It was found that **2** induced a rapid onset of cytotoxicity with  $IC_{50}$  values ranging from 0.5 to 3.3  $\mu$ M. In comparison to **2**, **1** was 70–480-times less toxic to cancer cells. The cytotoxicity of **2** was coupled with a quick loss of membrane integrity leading to necrotic cell death as revealed by morphological and biochemical studies [17]. Our results for **1** and **2** further support that PAQs are potential leads for future cancer drug development, as these compounds exhibit potent cytotoxicity against only a subset of cancer cell lines. The mode of action of PAQs has not been established yet. However, phenolic compounds from plants constitutionally related to PAQs, like anthraquinones, triggered both apoptosis and necrosis or induced DNA damage in cancer cells [18–21]. The extent and the timing of apoptosis were strongly dependent on the cell line, the type of the anthraquinone and its dose, and were mediated by caspase-3 activation, a cysteine-aspartic protease essential for programming cell death and inflammation [18–21]. Further studies will show if this mechanism also operates with **1** and **2**.

To investigate the stability of **1** and **2** in our assay media, the tested compounds and medium were preincubated for 4 h in

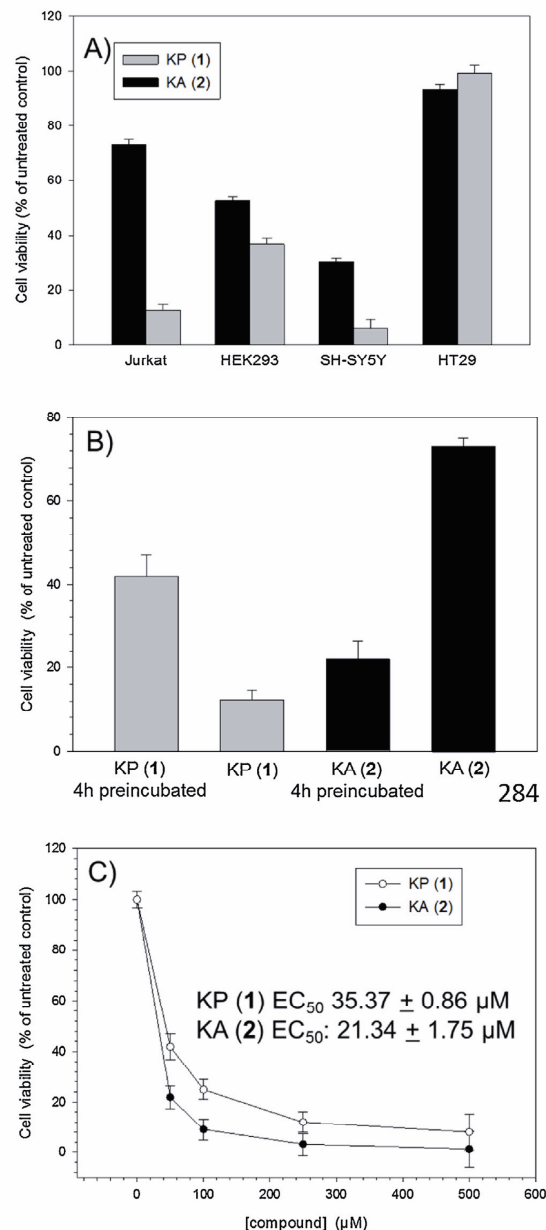


Fig. 2. A) Cytotoxicity of **1** and **2** at 50  $\mu$ M in Jurkat, HEK293, SH-SY5Y and HT-29 cells, 24 h incubation. B) Comparison of cytotoxic activity of **1** and **2** at 50  $\mu$ M in Jurkat cells with and without 4 h preincubation in medium and 24 h incubation with cells. C) Dose-response curves of **1** and **2** following a 4 h preincubation in medium before administration to Jurkat cells and 24 h incubation with cells. DMSO was used as control.

cell culture conditions before evaluating the cytotoxicity (dose-response curves) after 24 h incubation with Jurkat cells. The results are summarized in Fig. 2C. Fig. 2B depicts the cytotoxic activity of both **1** and **2** without preincubation (Fig. 2A) and with 4 h compound preincubation in medium (Fig. 2C) and at 50  $\mu$ M. Importantly, the comparison (Fig. 2B) reveals that the results of the



**Table 1**  
Antiplasmodial activities of **1** and **2** against *P. falciparum* 3D7 strain.

Compound	IC <sub>50</sub> (μM)
KP ( <b>1</b> )	1.930
KA ( <b>2</b> )	0.729
KA ( <b>2</b> ) after 24 h in solution	0.443
Chloroquine	0.005

cytotoxicity with and without 4 h preincubation of the tested compounds in the assay medium are dramatically different, indicating that both **1** and **2** are unstable or degrade in the assay medium. The instability of **2** implies that the biological activity attributed to **2** might be influenced by or derived from its degradation reaction or degradation products in media.

### 3.3. Antiplasmodial activity

Malaria remains a major public health threat, and the development of drug-resistant *Plasmodium* strains poses serious challenges [22,23]. Current antiparasmodial drugs stem from six major drug classes: aminoquinolines, arylaminoalcohols, artemisinins, antifolates, antibiotics and inhibitors of the respiratory chain [23]. The problem of resistance urges the search for new drug candidates active against a broad range strains to all *Plasmodium* strains.

The relatively strong antiparasmodial activity previously reported for **1** and **2** against two strains of *P. falciparum*, K1 (chloroquine-resistant strain) and NF54 (chloroquine sensitive strain) [1], prompted us to evaluate the activity of both compounds against *P. falciparum* 3D7, a chloroquine-sensitive strain. The results are presented in Table 1. Both **1** and **2** exhibited substantial antiparasmodial activity against *P. falciparum* 3D7 strain with IC<sub>50</sub> values of 1.9 and 0.7 μM. This activity is similar to that reported for both **1** and **2** against *P. falciparum* K1 and NF54 strains [1].

While we thus corroborated the literature activity, the issue of stability was addressed by keeping **2** in DMSO solution for 24 h at room temperature under darkness before addition to *P. falciparum*. Surprisingly, **2** after 24 h preincubation was more active than the same sample without preincubation (Table 1). So, in this case, the degradation products of **2** were more active than the parent compound. This suggests that there are some other degradation products that might be more active than either of **1** and **2**, but have not yet been identified in the degradation media. Alternately, compounds **1** and **2** might act synergistically, leading to increased activity. The ratio of **1** and **2** after 24 h incubation of **2** in DMSO was determined by APCI-MS. Both **1** and **2** were still present as a 54:46 mixture. No other degradation products could be detected by using this method (see Fig. S3a, Supporting Information). This substantiates the suspicion of a synergism between **1** and **2**. For further testing both hypotheses future studies should comprise synergy tests in cell culture evaluating mixtures of compounds **1** and **2** in different ratios as determined by APCI-MS. Furthermore, it would be of interest to systematically study whether **2** is degraded to only **1** or there are more degradation products.

### 3.4. Anti-HIV-1 activity

Despite the development of highly active anti-retroviral therapy (HAART) regimens, the discovery of additional anti-HIV drugs with lower cost and side-effects, improved accessibility, and/or improved effectiveness against drug-resistant virus strains remains a priority [24,25]. We therefore tested the anti-HIV-1<sub>c</sub> activity of **1** and **2** using primary PBMCs infected with HIV-1<sub>c</sub> (MJ<sub>4</sub>). While **1** was not active, **2** demonstrated antiviral and cytotoxic effects

against mock-infected PBMCs at concentrations in the range of 0.01–50 μg/mL. Results are summarized in Fig. 3.

Compound **2** displayed an inhibition of HIV-1<sub>c</sub> (MJ<sub>4</sub>) replication as measured by the inhibition of HIV-1 p24 antigen production of more than 60% over a concentration range of 0.5 to 50 μg/mL (Fig. 3A). The maximum of inhibition was observed at 15 μg/mL with 79.0 ± 1.0% and slightly less at 50 μg/mL (70.6 ± 4.2%). However, viability of PBMCs decreased substantially after exposure to **2** over the same concentration range (Fig. 3B) with a viability of 51.3 ± 3.1% at 15 μg/mL and only 28.0 ± 2.0% at 50 μg/mL. In order to determine the dose-response relation of **2**, we chose a lower concentration range from 0.01 to 15 μg/mL. Compound **2** inhibited HIV-1<sub>c</sub> (MJ<sub>4</sub>) p24 antigen production in a concentration-dependent manner (Fig. 3C) with a maximum of 58.2 ± 0.4% which corresponded to a relative EC<sub>50</sub> value of 1.8 μg/mL (4.3 μM). The EC<sub>50</sub> value of **2** was substantially higher than the positive control AZT displaying an EC<sub>50</sub> value of 0.49 μM (data not shown). The maximum of inhibitory activity of **2** varied between batches and was found to be sensitive to freeze-thaw procedures suggesting stability issues with this compound. We note that some anthraquinones were reported to possess anti-HIV-1 activity by inhibiting HIV-1 reverse transcriptase [26], and anthraquinone derivatives have been shown to exert their anti-HIV activity particularly through inhibition of reverse transcriptase-associated ribonuclease H function [27]. Although further studies are required to elucidate the antiviral mechanisms of **2** our results support the use of PAQs as a new chemical lead for future HIV antiretroviral therapies.

### 3.5. Anthelmintic and antibacterial activity

Compounds **1** and **2** were further tested for anthelmintic activity against the model organism *Caenorhabditis elegans*, where less than 20% growth inhibition was observed for both compounds at concentrations up to 500 μg/mL. **1** and **2** were further assessed for their ability to inhibit the bacteria *Aliivibrio fischeri* and *Mycobacterium tuberculosis*, where no more than 30% growth inhibition was observed at concentrations up to 100 μM and 10 μg/mL, respectively. These results suggest that both **1** and **2** have minimal anthelmintic and antibacterial activities, at least in these *in vitro* models, supporting that PAQs have selective anti-infective properties.

### 3.6. Stability studies of **2**

The difference of biological activity observed for **2** with or without preincubation in media or solvents and its chemical features (potential reductant; oligophenol) caused us to investigate the stability of this natural product in different media and solvents.

#### 3.6.1. Stability of compound **2** in media

To determine the stability of **2**, the compound was incubated in three different cell media MEM, DMEM, RPMI1640 (containing salts, glucose, amino acids and proteins) under physiological conditions at 37 °C. The degradation products and remaining **2** were monitored over time by APCI-MS. After extracting **2** and its degradation product **1** from the aqueous media using ethyl acetate, the relative ratios of **2** and **1** over time were expressed from the peak intensities of ionized compounds as detected by APCI-MS. The results are shown in Fig. 4A. Incubation of **2** in the three aqueous media at 37 °C led to total degradation of the compound after 400 min (Fig. 4A). The APCI-MS data (Fig. 4C and D) at different times (after 0, 30 and 60 min.) show a decrease in the intensity of **2** (*m/z* 421) and an increase of the peak intensity of **1** (*m/z* 435) in the tested media. The instability observed for **2** is not unique for this compound since other anthrone derivatives are also reported to readily oxidize to anthraquinones or dimerize

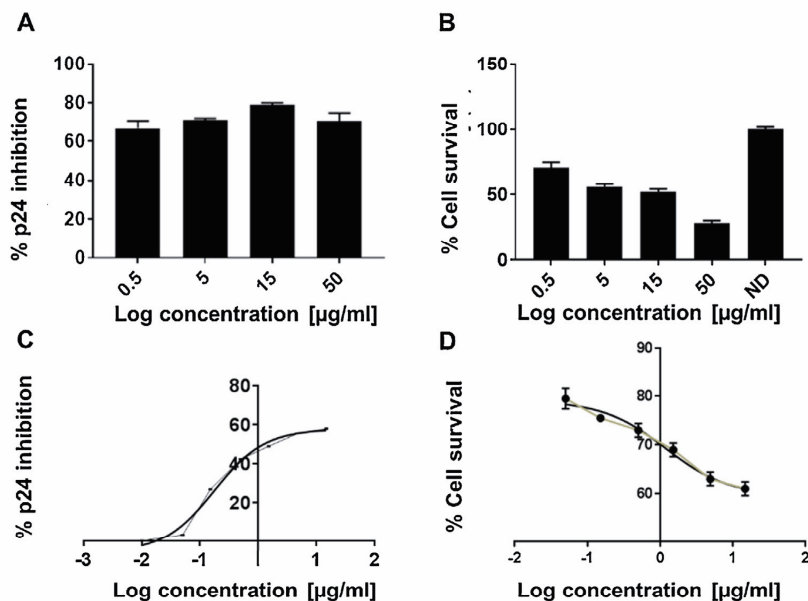


**Fig. 3.** Anti-HIV-1<sub>c</sub> (MJ<sub>4</sub>) activity of **2** in PBMCs. (A) PBMCs were infected for 2 h at 37 °C with HIV-1<sub>c</sub> (MJ<sub>4</sub>) clone in the presence of different concentrations of **2**. P24 core protein levels from supernatants relative to no drug control were determined seven days after infection. Note maximum percentage of p24 inhibition of  $79.0 \pm 1.0\%$  at 15 μg/mL. (B) Viability of mock-infected PBMCs measured using MTT after exposure to **2** at indicated concentrations. ND, no drug. (C) Dose response curve measuring HIV-1<sub>c</sub> (MJ<sub>4</sub>) p24 antigen inhibition relative to no drug control. Note calculated relative EC<sub>50</sub> value of 4.3 μM. (D) Concentration-dependent cytotoxicity of mock-transfected PBMCs exposed to indicated concentration of **2**. Note calculated relative CC<sub>50</sub> value of 2.8 μM. (C, D) Grey: actual measurements; black: best fit curve. Data are presented as means and S.D. from triplicate determinations.

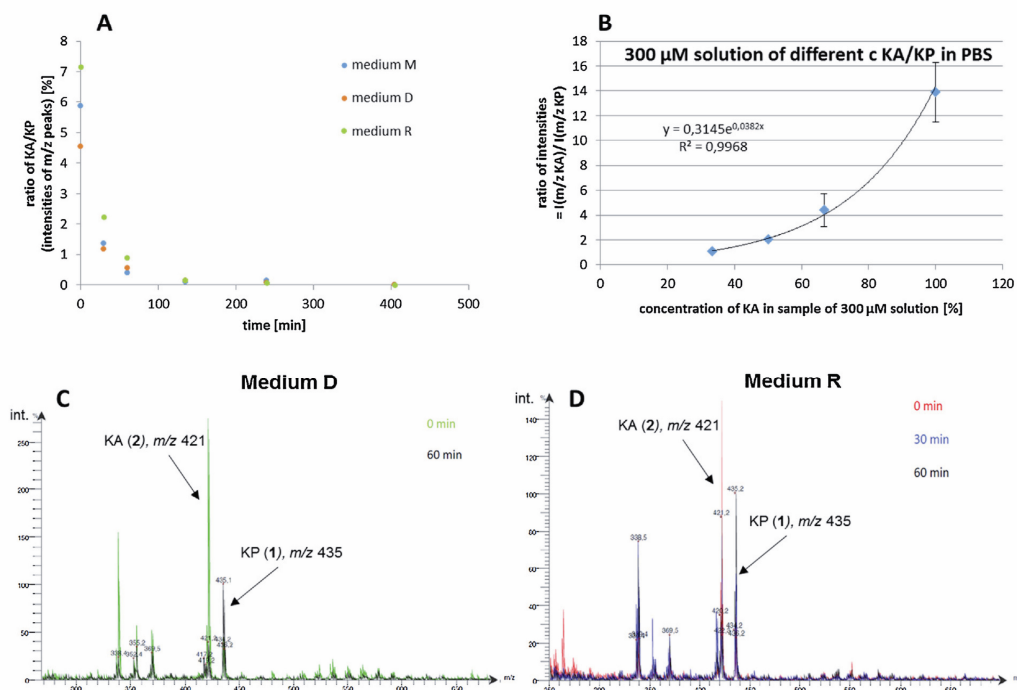


**Fig. 4.** A) Degradation of KA (**2**) in different media over time (APCI-MS detection). B) Relationship between concentrations of KA (**2**) in a sample and ratio of KA/KP intensities (APCI-MS detection). C) and D) Comparison of MS spectra of the EtOAc extract from media showing a clear increase of KP (**1**) and decrease of KA (**2**) over time. The other peaks (at  $m/z$  338, 352, 355, 369, etc.) observed in C) and D) along with the targeted ion signals at  $m/z$  421 and 435 are most likely impurities originating from media and APCI-MS background ions.

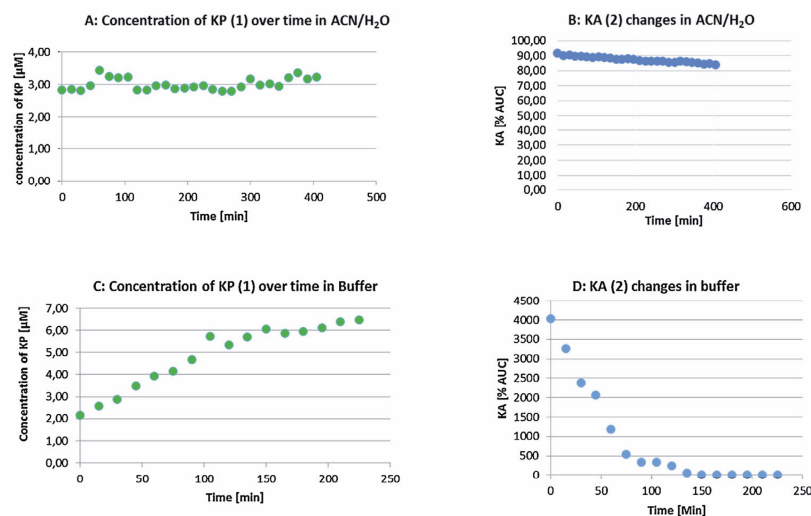


**Fig. 5.** HPLC stability study of **2** in ACN/H<sub>2</sub>O (60:40) and buffer. The concentration of **1** was calculated from the calibration curve in ACN/H<sub>2</sub>O (60:40, v/v). Direct detection of degradation of **2** is not possible due to the instability and the lack of possibility to obtain a calibration curve. Therefore the % remaining compared to the amount at  $t_0$  is displayed instead of the absolute amount in  $\mu\text{M}$ . However, detecting the change in **1** concentration (formed from the degradation of **2**) is possible. AUC = Area under curve.

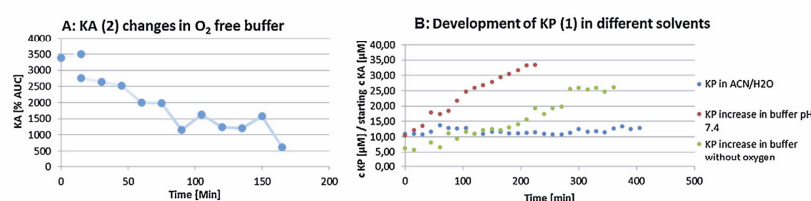


**Fig. 6.** A) HPLC stability study of **2** in O<sub>2</sub> free buffer. AUC = Area under curve. B) Comparison of rates of **1** formation in different solutions. The direct detection of KA degradation is not possible due to the instability and the lack of possibility to obtain a calibration curve. However, detecting the change in **1** concentration (formed from the degradation of **2**) is possible and the concentrations could be calculated.

[28]. For example, rhein-9-anthrone easily degrades in contact with oxygen or solutions to form the relatively stable products rhein (anthraquinone derivative) and the dimeric sennidin A and B [28]. Dithranol (1,8-dihydroxy-9-anthrone), an effective drug for the treatment of chronic stable plaque psoriasis is highly sensitive to light and elevated temperatures [29]. This drug readily undergoes oxidation to a range of degradation products including danthron and dithranol dimer, which are thought to contribute to the undesired effects and are inactive or less active in terms of anti-psoriatic potency [29]. In our study, we could not detect any dimer of **2**. This might be because the compound poorly ionizes in APCI-MS.

The validity of our approach was ensured by examining four different ratios of **2**/**1** of known concentrations in PBS. The corresponding ratios of **1**(**2**)/**1**(**1**), as detected by APCI-MS peak intensities (**1** represents the peak intensity, see Fig. 4B), were determined and plotted as depicted in Fig. 4B. As expected, the ratio **1**(**2**)/**1**(**1**) increased as concentrations KA/KP increased.

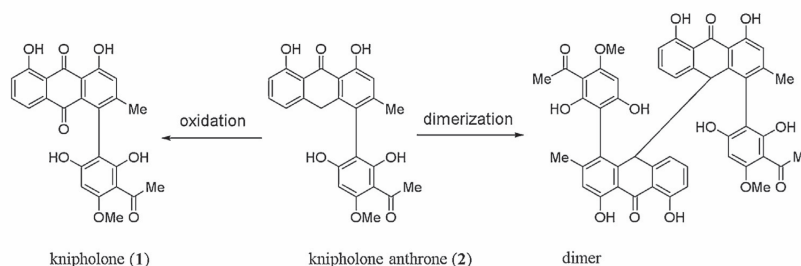
### 3.6.2. Stability of **2** in solution

Compound **2** could be isolated by extracting the dried and powdered *K. foliosa* roots with ethyl acetate followed by the recrystallization of the resulting ethyl acetate extract in acetone [3]. An attempt to use other separation techniques like column chromatography caused problems and revealed that **2** easily oxidized to form **1**. Previous authors easily performed the oxidation of **2** in methanol and KOH to form **1** [3]. Therefore, we investigated the stability of **2**

in different solutions and conditions. Investigation of the stability of **2** in ACN:H<sub>2</sub>O (60:40, v/v) for 7 h reveals that the compound is relatively stable in this solvent mixture (Fig. 5A and B). The concentration of **1** changed from 2.83  $\mu\text{M}$  ( $t = 0$  min) to 3.24  $\mu\text{M}$  after 7 h, which indicated a slow rate of compound **2** oxidation. However, **2** degraded rapidly in buffer (PBS, pH = 7.4) (Fig. 5C and D).

Fig. 5C shows the change in the concentrations of **1** over time in a buffer solution, calculated depending on the calibration curve performed in the buffer (see Experimental Section). The figure displays an increase from 2.17 to 6.46  $\mu\text{M}$  (198%) within the first 225 min, indicating a much higher rate of **2** oxidation occurring in buffer than in ACN/H<sub>2</sub>O (60:40). In fact, after 135 min, **2** was no longer visible in the HPLC chromatogram ( $R_t = 6$  min).

In addition, the stability of **2** was investigated in buffer solution under oxygen free conditions to understand any effect of atmospheric oxygen on the degradation rate of **2**, which was indeed slower when the preparation was held under argon with a minimum presence of oxygen. This was accomplished by oxygen free preparation of all the solutions as well as filling the vials under the least oxygen contact possible. In contrast to the degradation of KA (**2**) in buffer where the compound is totally decomposed after 135 min, a short delay in decomposition can be observed under oxygen free conditions (Fig. 6A). Comparison of KA (**2**) decomposition (respectively **1** formation) in different solutions (Fig. 6B) reveals that the highest and fastest rate of decomposition occurred in buffer solution with normal oxygen conditions compared to the samples



**Scheme 1.** Oxidation and proposed dimerization products from knipholone anthrone (2) degradation.

prepared and filled under reduced oxygen content which showed a lower rate of degradation. The highest stability of **2** was observed in ACN/H<sub>2</sub>O; however, after 10 days, no trace of **2** could be detected in this solution by TLC analysis (results not shown) (Scheme 1).

#### 4. Conclusion

Here we perform a series of *in vitro* biological and stability studies which indicate that PAQs, exemplified by **1** and **2**, are a potential source of novel cytotoxic, antiparasmodial and anti-HIV compounds. However, the instability of **2** in media and other solutions indicates that caution should be taken about pharmacological data available for this compound in the literature and it should be carefully evaluated if (1) preincubation increases or decreases activity, and/or (2) the assay data differ from those of the PAQ degradation products or mixtures thereof.

#### Declarations of conflicts of interest

None.

#### Acknowledgement

The authors wish to thank Siegrid Franke for her excellent support in cell culture. Prof. Ermias Dagne (Addis Ababa University, Ethiopia) is acknowledged for kindly collecting and providing *K. foliosa*. This study was supported by the DAAD/BMBF Trisustain project (<https://trisustain.uni-halle.de/>) and the LOEWE Center DRUID (project B3 to KB). BR, KAM and IT were also supported by Sub-Saharan African Network for TB/HIV Research Excellence (SANTHE), a DELTAS Africa Initiative [grant # DEL-15-006]. SATF is grateful to the Alexander von Humboldt Foundation for financial support.

#### Appendix A. Supplementary data

Supplementary material related to this article can be found, in the online version, at doi:<https://doi.org/10.1016/j.jpba.2019.05.065>.

#### References

- [1] G. Bringmann, D. Menche, M. Bezabih, B.M. Abegaz, R. Kaminsky, Antiplasmodial activity of knipholone and related natural phenylanthraquinones, *Planta Med.* 65 (1999) 757–758.
- [2] G. Bringmann, J. Mutanyatta-Comar, M. Knauer, B.M. Abegaz, Knipholone and related 4-phenylanthraquinones: structurally, pharmacologically, and biosynthetically remarkable natural products, *Nat. Prod. Rep.* 25 (2008) 696–718.
- [3] E. Dagne, A. Yenesew, Knipholone anthrone from *Kniphofia foliosa*, *Phytochemistry* 34 (1993) 1440–1441.
- [4] E. Dagne, W. Steglich, Knipholone: a unique anthraquinone derivative from *Kniphofia foliosa*, *Phytochemistry* 23 (1984) 1729–1731.
- [5] S.A. Fobofou, K. Franke, G. Sanna, A. Porzel, E. Bullita, P. La Colla, L.A. Wessjohann, Isolation and anticancer, anthelmintic, and antiviral (HIV) activity of acylphloroglucinols, and regioselective synthesis of empetrifranzinans from *Hypericum roeperianum*, *Bioorg. Med. Chem.* 23 (2015) 6327–6334.
- [6] S.A. Fobofou, K. Franke, A. Porzel, W. Brandt, L.A. Wessjohann, Tricyclic acylphloroglucinols from *Hypericum lanceolatum* and regioselective synthesis of selancins A and B, *J. Nat. Prod.* 79 (2016) 743–753.
- [7] K. Kolbe, L. Möckl, V. Sohst, J. Brandenburg, R. Engel, S. Malm, C. Bräuchle, O. Holst, T.K. Lindhorst, N. Reiling, Azido pentoses: a new tool to efficiently label *Mycobacterium tuberculosis* clinical isolates, *Chembiochem* 18 (2017) 1172–1176.
- [8] W. Trager, J.B. Jensen, Human malaria parasites in continuous culture, *Science* 193 (1976) 673–675.
- [9] C. Lambros, J.P. Vanderberg, Synchronization of *Plasmodium falciparum* erythrocytic stages in culture, *J. Parasitol.* 65 (1979) 418–420.
- [10] F. Paul, S. Roath, D. Melville, D.C. Warhurst, J.O. Osisanya, Separation of malaria-infected erythrocytes from whole blood: use of a selective high-gradient magnetic separation technique, *Lancet* 2 (1981) 70–71.
- [11] D. Kasozi, F. Mohring, S. Rahlfs, A.J. Meyer, K. Becker, Real-time imaging of the intracellular glutathione redox potential in the malaria parasite *Plasmodium falciparum*, *PLoS Pathog.* 9 (2013), e1003782.
- [12] H. Thomsen, H. Reider, K. Franke, L.A. Wessjohann, J. Keiser, E. Dagne, N. Arnold, Characterization of constituents and anthelmintic properties of *Hagenia abyssinica*, *Sci. Pharm.* 80 (2012) 433–446.
- [13] T. Backhaus, K. Froehner, R. Altenburger, L.H. Grimme, Toxicity testing with *Vibrio fischeri*: a comparison between the long term (24 h) and the short term (30 min) bioassay, *Chemosphere* 35 (1997) 2925–2938.
- [14] M.M. Leteane, B.N. Ngwenya, M. Muzila, A. Namushe, J. Mwinga, R. Musonda, S. Moyo, Y.B. Mengestu, B.M. Abegaz, K. Andrae-Marobela, Old plants newly discovered: *Cassia sieberiana* D.C. and *Cassia abbreviata* Oliv.Oliv. Root extracts inhibit in vitro HIV-1c replication in peripheral blood mononuclear cells (PBMCs) by different modes of action, *J. Ethnopharmacol.* 141 (2012) 48–57.
- [15] T. Ndung'u, B. Renjifo, V. Novitsky, M.F. McLane, S. Gaolekwe, M. Essex, Molecular cloning and biological characterisation of full length HIV-1 subtype C from Botswana, *Virology* 278 (2000) 390–399.
- [16] M. Kuroda, Y. Mimaki, H. Sakagami, Y. Sashida, Bulbinolonesides A–E, phenylanthraquinone glycosides from the roots of *Bulbinella floribunda*, *J. Nat. Prod.* 66 (2003) 894–897.
- [17] S. Habtemariam, Knipholone anthrone from *Kniphofia foliosa* induces a rapid onset of necrotic cell death in cancer cells, *Fitoterapia* 81 (2010) 1013–1019.
- [18] A. Kocova-Chyla, J.J. Skierski, K. Kania, Z. Józwiak, Mechanisms of induction of apoptosis by anthraquinone anticancer drugs aclarubicin and mitoxantrone in comparison with doxorubicin: relation to drug cytotoxicity and caspase-3 activation, *Apoptosis* 10 (2005) 1497–1514.
- [19] K. Kagedal, D. Bironaitė, K. Ollinger, Anthraquinone cytotoxicity and apoptosis in primary cultures of rat hepatocytes, *Free Radic. Res.* 31 (1999) 419–428.
- [20] L. Huang, T. Zhang, S. Li, J. Duan, F. Ye, H. Li, Z. She, G. Gao, X. Yang, Anthraquinone G503 induces apoptosis in gastric cancer cells through the mitochondrial pathway, *PLoS One* 9 (2014) 1–13.
- [21] J. Chiang, J. Yang, C. Ma, M. Yang, H. Huang, T. Hsia, H. Kuo, P. Wu, T. Lee, J. Chung, Danthron, an anthraquinone derivative, induces DNA damage and caspase cascades-mediated apoptosis in SNU-1 human gastric cancer cells through mitochondrial permeability transition pores and bax-triggered pathways, *Chem. Res. Toxicol.* 24 (2011) 20–29.
- [22] World Health Organization (WHO), World Malaria Report, 2017 <http://www.who.int/malaria/publications/world-malaria-report-2017/en/>.
- [23] A. Sharma, I.O. Santos, P. Gaur, V.F. Ferreira, C.R. Garcia, D.R. da Rocha, Addition of thiols to o-quinone methide: new 2-hydroxy-3-phenylsulfanylmethyl[1,4]naphthoquinones and their activity against the human malaria parasite *Plasmodium falciparum* (3D7), *Eur. J. Med. Chem.* 59 (2013) 48–53.
- [24] W. Li, X. Li, E. De Clercq, P. Zhan, X. Liu, Discovery of potent HIV-1 non-nucleoside reverse transcriptase inhibitors from arylthioacetanilide structural motif, *Eur. J. Med. Chem.* 102 (2015) 167–179.
- [25] V. Asensi, J. Collazos, E. Valle-Garay, Can antiretroviral therapy be tailored to each human immunodeficiency virus-infected individual? role of pharmacogenomics, *World J. Virol.* 4 (2015) 169–177.
- [26] R.F. Schinazi, C.K. Chu, R. Babu, B.J. Oswald, V. Saalman, D.L. Cannon, B.F.H. Eriksson, M. Nars, Anthraquinones as a new class of antiviral agents against human immunodeficiency virus, *Antiviral Res.* 13 (1990) 265–272.

- [27] F. Esposito, A. Corona, L. Zinzula, T. Kharlamova, E. Tramontano, New anthraquinone derivatives as inhibitors of the HIV-1 reverse transcriptase-associated ribonuclease H function, *Chemotherapy* 58 (2012) 299–307.
- [28] W. Grimminger, E. Leng-Peschlow, Instability of rhein-9-anthrone as a problem in pharmacological and analytical use, *Pharmacol.* 36 (1988) 129–137.
- [29] M. Estanqueiro, J. Conceição, M.H. Amaral, J.M.S. Lobo, Use of solid dispersions to increase stability of dithranol in topical formulations, *Braz. J. Pharm. Sci.* 50 (2014) 583–590.





## 2.3) Research Article III

# The African natural product knipholone anthrone and its analogue anthralin (dithranol) enhance HIV-1 latency reversal

Khumoekae Richard, Cole Schonhofer, Leila B. Giron, Jocelyn Rivera-Ortiz, Silven Read, Toshitha Kannan, Natalie N. Kinloch, Anika Shahid, **Ruth Feilcke**, Simone Wappler, Peter Imming, Marianne Harris, Zabrina L. Brumme, Mark A. Brockman, Karam Mounzer, Andrew V. Kossenkov, Mohamed Abdel-Mohsen, Kerstin Andrae-Marobela, Luis J. Montaner, and Ian Tietjen

**American Society for Biochemistry and Molecular Biology,  
Journal of Biological Chemistry**

*J Biol Chem*, **2020**, 295(41):14084

Publication Date: October 9, 2020

Doi: 10.1074/jbc.RA120.013031

### Summary

In this article we present the results of the latency reversal activity of a secondary plant metabolite that was extracted and characterized during my thesis, as well as of a related building block thereof, synthesized in our labs, acting as LR agent. The cytotoxicity of investigated compounds was determined in various cell lines and first attempts could be made to clarify their molecular mechanism. The paper also includes synergy studies showing that the extracted metabolite not only induces LR but also synergizes with known LR agents.

### Own contribution

Extraction, purification and chemical characterization of knipholone anthrone to enable comparison with the authentic sample from pan-African natural products library (pANABL) library, where a high assay to assay variability in activity was observed by our collaborators at SFU<sup>18</sup>; Supervision of the diploma student SIMONE WAPPLER and her work to explore synthetic approaches to dithranol; Rewriting and Editing

This paper was chosen to be part of the thesis although the own contribution was minor compared to the first author because the extraction of the pure compounds was essential for the whole project. Furthermore, it was our idea to investigate the core structure of **KA** (dithranol) for its LR activity. This led to the discovery of a new pharmacological activity of the approved drug dithranol/anthralin, acting as LR agent. Several synthesized compounds

---

<sup>18</sup> Personal communication by our cooperation partners.

were tested alongside but found to be inactive (as discussed in the summary and discussion section 3.6.3) and were therefore not included in the publication.

This publication is furthermore very important to understand the whole idea of the part of the thesis that deals with 1,8 dihydroxyanthrones because the discovery of **KA**'s LR activity was the main start of us being interested in this project.



# The African natural product knipholone anthrone and its analogue anthralin (dithranol) enhance HIV-1 latency reversal

Received for publication, February 12, 2020, and in revised form, August 6, 2020. Published, Papers in Press, August 11, 2020, DOI 10.1074/jbc.RA120.013031

Khumoekae Richard<sup>1</sup>, Cole Schonhofer<sup>1</sup>, Leila B. Giron<sup>2</sup>, Jocelyn Rivera-Ortiz<sup>2</sup>, Silven Read<sup>1</sup>, Toshitha Kannan<sup>2</sup>, Natalie N. Kinloch<sup>1,3</sup>, Anika Shahid<sup>1,3</sup>, Ruth Feilcke<sup>4</sup>, Simone Wappler<sup>4</sup>, Peter Imming<sup>4</sup>, Marianne Harris<sup>3</sup>, Zabrina L. Brumme<sup>1,3</sup>, Mark A. Brockman<sup>1,3,5</sup>, Karam Mounzer<sup>6</sup>, Andrew V. Kossenkov<sup>2</sup>, Mohamed Abdel-Mohsen<sup>2</sup>, Kerstin Andrae-Marobela<sup>7</sup>, Luis J. Montaner<sup>2</sup>, and Ian Tietjen<sup>1,2,\*</sup>

From the <sup>1</sup>Faculty of Health Sciences, Simon Fraser University, Burnaby, British Columbia, Canada, the <sup>2</sup>Wistar Institute, Philadelphia, Pennsylvania, USA, the <sup>3</sup>British Columbia Centre for Excellence in HIV/AIDS, Vancouver, British Columbia, Canada, the <sup>4</sup>Institut für Pharmazie, Martin-Luther-Universität Halle-Wittenberg, Halle, Germany, the <sup>5</sup>Department of Molecular Biology and Biochemistry, Simon Fraser University, Burnaby, British Columbia, Canada, the <sup>6</sup>Jonathan Lax Immune Disorders Treatment Center, Philadelphia Field Initiating Group for HIV-1 Trials, Philadelphia, Pennsylvania, USA, and the <sup>7</sup>Department of Biological Sciences, University of Botswana, Gaborone, Botswana

Edited by Craig E. Cameron

A sterilizing or functional cure for HIV is currently precluded by resting CD4<sup>+</sup> T cells that harbor latent but replication-competent provirus. The “shock-and-kill” pharmacological approach aims to reactivate provirus expression in the presence of antiretroviral therapy and target virus-expressing cells for elimination. However, no latency reversal agent (LRA) to date effectively clears viral reservoirs in humans, suggesting a need for new LRAs and LRA combinations. Here, we screened 216 compounds from the pan-African Natural Product Library and identified knipholone anthrone (KA) and its basic building block anthralin (dithranol) as novel LRAs that reverse viral latency at low micromolar concentrations in multiple cell lines. Neither agent’s activity depends on protein kinase C; nor do they inhibit class I/II histone deacetylases. However, they are differentially modulated by oxidative stress and metal ions and induce distinct patterns of global gene expression from established LRAs. When applied in combination, both KA and anthralin synergize with LRAs representing multiple functional classes. Finally, KA induces both HIV RNA and protein in primary cells from HIV-infected donors. Taken together, we describe two novel LRAs that enhance the activities of multiple “shock-and-kill” agents, which in turn may inform ongoing LRA combination therapy efforts.

The use of combination antiretroviral therapy (cART) has been a resounding success in terms of reducing HIV/AIDS-related morbidity and mortality as well as HIV transmission (1). As of 2018, 23.3 million people living with HIV, or 62% of the global HIV/AIDS burden, were reliably accessing cART (UNAIDS (2019) Global HIV & AIDS statistics—2019 fact sheet; <https://www.unaids.org/en/resources/fact-sheet>; accessed September 11, 2019). However, cART does not cure HIV due to resting CD4<sup>+</sup> T cells that persistently bear integrated and immunologically invisible provirus. As these

persistent proviral reservoirs can reactivate at any time to produce infectious virus, cART must be taken for life (2–5).

One method toward developing a sterilizing or functional HIV cure involves use of latency reversal agents (LRAs) that induce HIV-1 provirus expression. HIV reactivation, coupled with immunotherapy support (6), could render infected cells “visible” to the host immune system, whereas co-administration of cART would prevent further seeding of viral reservoirs (7, 8). This approach, frequently termed “shock-and-kill,” could theoretically eliminate an individual’s viral reservoir and/or reduce the viral reservoir to a point that cART-free remission is achievable, provided that sufficiently effective LRAs and immune enhancers can be identified. Numerous LRAs have been described, representing different functional classes. The majority represents protein kinase C (PKC) activators and histone deacetylase (HDAC) inhibitors, although agents that act by other mechanisms, such as BET bromodomain and DNA methyltransferase inhibition, have also been intensively studied (9, 10). However, LRAs tested to date in humans have shown limited clinical success due to extensive toxicity, poor efficacy, inconsistent viral reactivation, and/or insufficient engagement of cellular “kill” mechanisms (9, 11). New LRA-based strategies are likely to be needed to circumvent these issues.

Toward this goal, several groups report that combinations of LRAs from different functional classes can synergistically enhance latency reversal (12–14). For example, Jiang *et al.* (14) described that the PKC activator ingenol-3-angelate (PEP005) and the BET bromodomain inhibitor JQ1, which each alone stimulated an ~25-fold increase in HIV transcription *in vitro*, could induce a 250-fold increase when applied in combination. Similar results are also reported using primary CD4<sup>+</sup> T cells from HIV-infected donors (12–14). These observations suggest that optimized LRA combinations may promote broader latency reversal at lower concentrations, thereby maximizing virus reactivation while limiting drug toxicities and other off-target effects. Thus, discovery of LRAs that enhance the activities of existing LRA clinical candidates would support efforts to identify optimized LRA combinations.

This article contains supporting information.

\*For correspondence: Ian Tietjen, [itietjen@wistar.org](mailto:itietjen@wistar.org).

14084 J. Biol. Chem. (2020) 295(41) 14084–14099

© 2020 Richard et al. Published under exclusive license by The American Society for Biochemistry and Molecular Biology, Inc.

This is an Open Access article under the CC BY license.

## Anthrones as HIV latency reversal agents

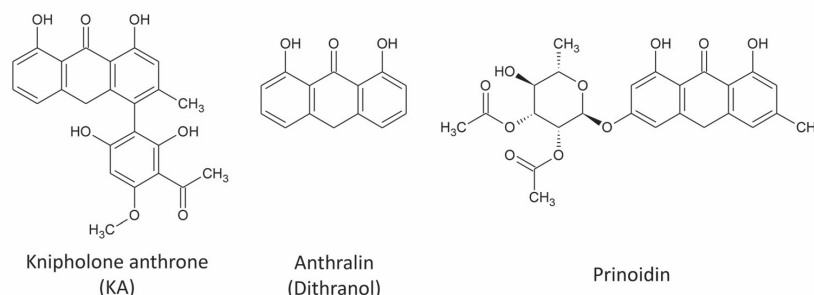


**Figure 1.** Structures of identified LRAs.

Pure compounds isolated from natural products are a rich source of unique chemical diversity and new LRAs. For example, we previously screened a library of 257 compounds originating from marine natural products and identified four (1.6%) that reversed HIV latency in both cell line and primary cell models (15). LRA “hit” rates of 1.0% or more have also been reported by others (16, 17). Based on these observations, we hypothesized that new LRAs that can enhance the activities of existing agents could be isolated from additional natural product-based compound libraries. Here, we describe the results of a screen of the pan-African Natural Product Library (pAN-APL), which contains compounds originating from African medicinal plants (18, 19). From this screen, we identified and characterized knipholone anthrone (KA), in addition to its synthetic analog anthralin (dithranol), as novel LRAs that synergize with established HIV latency reversal agents.

## Results

### Discovery of novel LRAs from pure natural products

To identify new LRAs from natural product sources, we used the Jurkat-derived J-Lat 9.2 cell line, which contains a noninfectious HIV provirus where premature stop codons are engineered into *env* and where *nef* is replaced with a GFP reporter (20). Detection of GFP in these cells, as measured by flow cytometry, thus indicates HIV provirus expression. Using this assay, we screened 216 pure compounds from the pANAPL at 5  $\mu\text{g}/\text{ml}$  for 24 h and identified one compound, KA (Fig. 1), which at 5  $\mu\text{g}/\text{ml}$  ( $\sim 12 \mu\text{M}$ ) induced GFP expression in  $6.1 \pm 5.2\%$  of cells (mean  $\pm$  S.D.). Based on this observation, we then screened 16 additional anthrones from pANAPL and commercially available sources at 10  $\mu\text{M}$  (Fig. S1) and observed that anthralin (dithranol; Fig. 1) also induced  $6.9 \pm 2.4\%$  GFP-positive cells. A third anthrone, prinoidin (Fig. 1), was also observed to induce  $2.8 \pm 0.7\%$  GFP-positive cells; however, it was not explored further due to its limited availability. No other assessed anthrones induced latency reversal. KA and anthralin were therefore selected for further study.

### KA and anthralin reverse HIV latency in multiple *in vitro* cell models

To investigate the *in vitro* latency reversal properties of these anthrones in detail, we next measured the dose-response profiles of KA and anthralin in live J-Lat 9.2 cells. In parallel, we

also assessed the activities of control LRAs, including the PKC activator prostratin and the HDAC inhibitor panobinostat. Examples of latency reversal in J-Lat 9.2 cells, as measured by GFP expression, are shown in Fig. 2A. In these studies, treatment of J-Lat 9.2 cells with 10  $\mu\text{M}$  prostratin induced  $15.8 \pm 2.7\%$  GFP-positive cells, whereas stimulation with 0.3  $\mu\text{M}$  panobinostat resulted in  $40.5 \pm 3.8\%$  GFP-positive cells (Fig. 2B). In contrast, 10  $\mu\text{M}$  KA resulted in  $7.1 \pm 1.6\%$  GFP-positive cells, whereas 10  $\mu\text{M}$  anthralin induced  $7.2 \pm 0.5\%$  positive cells. Using the approach of Hashemi *et al.* (21) and normalizing to the average GFP response for 10  $\mu\text{M}$  prostratin as described previously (15), the relative  $\text{EC}_{50}$  values for prostratin, panobinostat, KA, and anthralin were calculated to be  $5.4 \pm 1.4$ ,  $0.14 \pm 0.02$ ,  $10.4 \pm 1.0$ , and  $12.1 \pm 1.7 \mu\text{M}$ , respectively (Table 1).

To investigate whether latency reversal due to KA and anthralin was independent of the proviral integration site in J-Lat cells, we next assessed their dose-response profiles in the related cell lines J-Lat 8.4 and J-Lat 10.6 (Fig. 2, C and D). Whereas results were broadly consistent with those from J-Lat 9.2 cells, a few differences were observed. For example, whereas 10  $\mu\text{M}$  prostratin induced  $5.0 \pm 1.1\%$  GFP-positive, live J-Lat 8.4 cells, 0.3  $\mu\text{M}$  panobinostat induced GFP in only  $1.4 \pm 0.9\%$  of J-Lat 8.4 cells, indicating that this cell line is less responsive to this HDAC inhibitor. In contrast, KA and anthralin induced  $5.0 \pm 2.5$  and  $1.8 \pm 0.8\%$  GFP-positive live cells, respectively (Fig. 2C). When normalized to 10  $\mu\text{M}$  prostratin, the relative  $\text{EC}_{50}$  values of prostratin, panobinostat, KA, and anthralin were  $5.0 \pm 0.9$ ,  $0.46 \pm 0.12$ ,  $7.4 \pm 2.6$ , and  $12.6 \pm 1.9 \mu\text{M}$ , respectively (Table 1). Similarly, in live J-Lat 10.6 cells, which in our hands (and as described previously (23, 24)) induced spontaneous GFP expression in  $7.6 \pm 0.2\%$  of cells and as described previously (22, 23), 10  $\mu\text{M}$  prostratin induced  $76.0 \pm 0.8\%$  GFP-positive cells, whereas 0.3  $\mu\text{M}$  panobinostat induced GFP in  $23.7 \pm 1.8\%$  of cells. Comparatively,  $36.2 \pm 13.7$  and  $30.8 \pm 2.4\%$  of cells were induced by 10  $\mu\text{M}$  KA and anthralin, respectively (Fig. 2D). When normalized to 10  $\mu\text{M}$  prostratin, we recorded relative  $\text{EC}_{50}$  values of  $1.9 \pm 0.9$ ,  $0.64 \pm 0.09$ ,  $16.0 \pm 5.5$ , and  $16.2 \pm 1.2 \mu\text{M}$  for prostratin, panobinostat, KA, and anthralin (Table 1). The observation that the latency reversal properties of KA and anthralin are broadly consistent across multiple cell lines suggests that their activities are not dependent on specific proviral integration sites, at least in Jurkat-derived T cell lines.

To determine whether KA and anthralin's latency reversal was independent of cell type, we next treated OM-10.1 cells,

Anthrones as HIV latency reversal agents

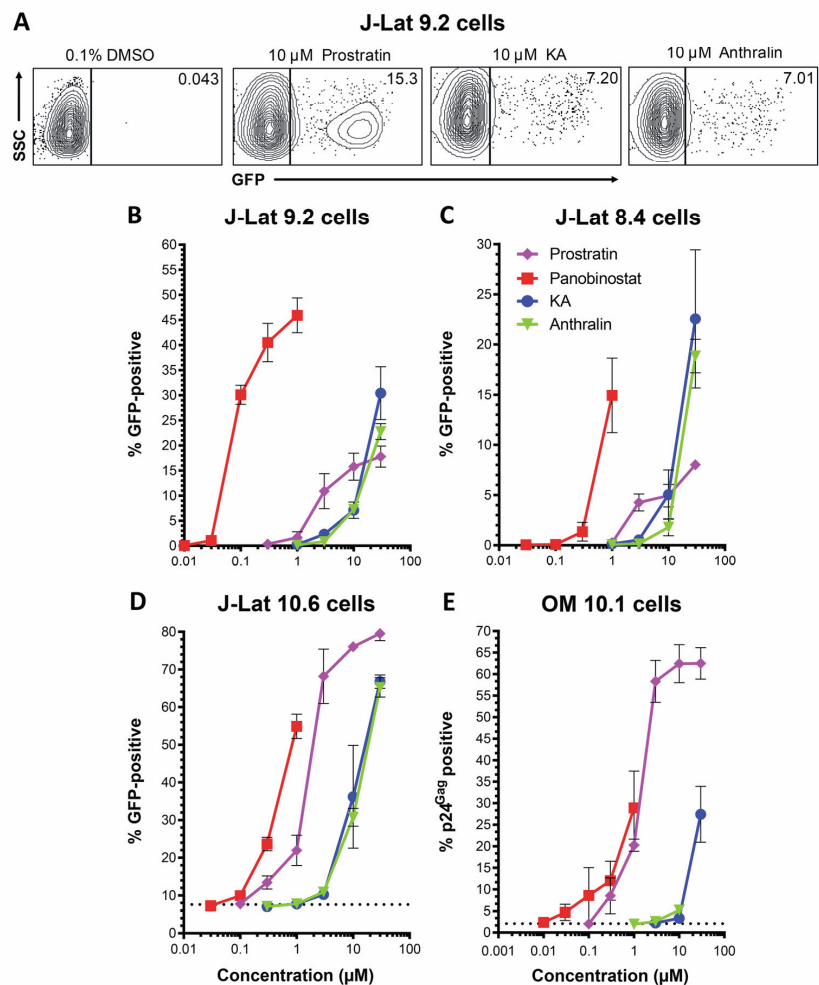


**Figure 2.** KA and anthralin reverse HIV latency *in vitro*. **A**, representative flow cytometry data showing latency reversal, as measured by GFP expression, in J-Lat 9.2 cells. Values indicate percentage GFP-positive cells for each condition. **B–D**, dose-response profiles of control LRAs panobinostat and prostratin, in addition to KA and anthralin, are shown in J-Lat 9.2 (**B**), J-Lat 8.4 (**C**), and J-Lat 10.6 (**D**) T cells. **E**, dose-response profiles of LRAs in OM10.1 promyeloid cells, as measured by cellular expression of viral p24<sup>Gag</sup> protein. Dotted lines in **C** and **D** indicate baseline levels of spontaneous latency reversal. Error bars, S.D.

**Table 1**  
Relative activities of LRAs *in vitro*. Data are presented as relative EC<sub>50</sub> values (in  $\mu$ M) normalized to the average GFP response for 10  $\mu$ M prostratin (i.e. the concentration required to induce 50% of the signal observed by 10  $\mu$ M prostratin) (21)

Cell line	Prostratin	Panobinostat	KA	Anthralin
	$\mu$ M	$\mu$ M	$\mu$ M	$\mu$ M
J-Lat 9.2	5.4 $\pm$ 1.4	0.14 $\pm$ 0.02	10.4 $\pm$ 1.0	12.1 $\pm$ 1.7
J-Lat 8.4	5.0 $\pm$ 0.9	0.46 $\pm$ 0.12	7.4 $\pm$ 2.6	12.6 $\pm$ 1.9
J-Lat 10.6	1.9 $\pm$ 0.9	0.64 $\pm$ 0.09	16.0 $\pm$ 5.5	16.2 $\pm$ 1.2
OM10.1	2.7 $\pm$ 1.0	1.6 $\pm$ 0.5	>30	>30

which are derived from HL-60 promyelocyte cells and contain an integrated, replication-competent provirus. Similar to J-Lat 10.6 cells, we observed that OM10.1 cells spontaneously expressed p24<sup>Gag</sup> protein in 2.1  $\pm$  0.2% of cells. Treatment of OM-10.1 cells with 10  $\mu$ M prostratin for 24 h stimulated virus

expression in 62.4  $\pm$  4.4% of live cells, whereas 0.3  $\mu$ M panobinostat induced provirus expression in only 12.0  $\pm$  4.5% of cells. Notably, 10  $\mu$ M KA elicited only 3.3  $\pm$  0.7% p24<sup>Gag</sup>-positive live cells, whereas 10  $\mu$ M anthralin induced 5.2  $\pm$  1.2% p24<sup>Gag</sup>-positive live cells (Fig. 2E). Whereas improved responses were observed with 30  $\mu$ M KA (27.4  $\pm$  6.5% p24<sup>Gag</sup>-positive live cells), extensive toxicity precluded measurements of 30  $\mu$ M anthralin. When normalized to 10  $\mu$ M prostratin, the relative EC<sub>50</sub> values for prostratin, panobinostat, KA, and anthralin were 2.7  $\pm$  1.0, 1.6  $\pm$  0.5, >30, and >30  $\mu$ M, respectively (Table 1). Thus, KA and anthralin may more effectively reverse latency in T cell–derived lines. Taken together, these results suggest that both KA and anthralin induce provirus expression across multiple cell lines and proviral integration sites, although KA and anthralin’s activities varied, depending on the cell line.

## Anthrones as HIV latency reversal agents

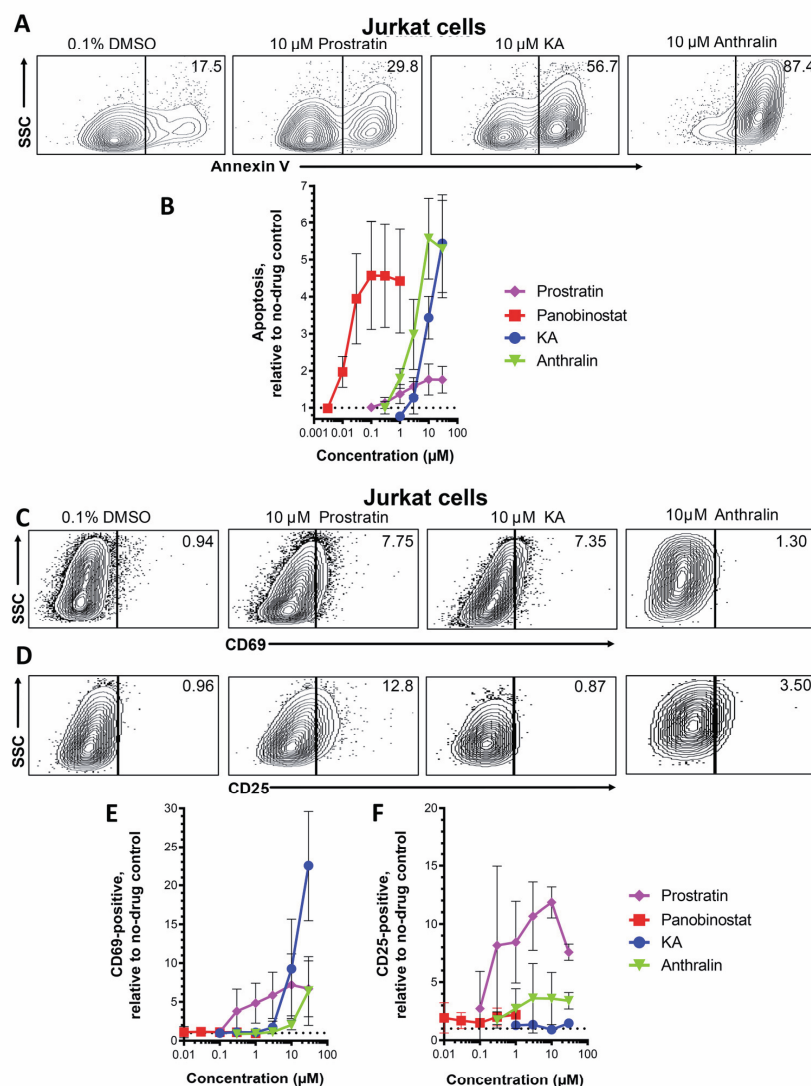


**Figure 3.** Effects of LRAs on *in vitro* cell viability and expression of cell activation markers. *A*, representative flow cytometry data showing Jurkat cell apoptosis, as measured by annexin V detection. Values indicate percentage of annexin-positive cells. *B*, dose-response profiles of panobinostat, prostratin, KA, and anthralin on apoptosis in Jurkat cells. Data are presented as -fold increase in annexin V-positive cells relative to cells treated with 0.1% DMSO (dotted line). *C* and *D*, representative flow cytometry data showing Jurkat cells stained for CD69 (*C*) or CD25 expression (*D*). Values indicate percentage of CD69- or CD25-positive cells, respectively. *E* and *F*, dose-response profiles of LRAs on CD69 (*E*) and CD25 (*F*) expression in Jurkat cells. Data are presented as -fold increases in each marker relative to cells treated with 0.1% DMSO (dotted lines). Error bars, S.D.

#### Effects of KA and anthralin on apoptosis and cell activation markers

To directly assess the impact of KA and anthralin on cell viability, we next treated Jurkat cells (the parental cell line of J-Lat cells) with LRAs as described above. Following treatment, cells were then assessed for surface expression of the early apoptotic marker annexin V by flow cytometry. Fig. 3*A* shows representative results of apoptotic cells in the presence of LRAs, where control data are consistent with previous results (15), whereas Fig. 3*B* shows dose-response profiles where data were normalized to the percentage of

apoptotic cells in control cell cultures treated with 0.1% DMSO. In this assay, 10  $\mu$ M prostratin induced only a  $1.8 \pm 0.4$ -fold increase in apoptosis, whereas 0.3  $\mu$ M panobinostat induced a  $4.6 \pm 1.4$ -fold increase, consistent with our previous results (15). Like panobinostat, both KA and anthralin also induced apoptosis: for example, 10  $\mu$ M KA resulted in a  $3.4 \pm 0.6$ -fold increase in apoptotic cells, whereas 10  $\mu$ M anthralin caused a  $5.6 \pm 1.1$ -fold increase (Fig. 3*B*). These results suggest that, like the HDAC inhibitor panobinostat, both KA and anthralin induce apoptosis *in vitro* at concentrations that also induce latency reversal.



## Anthrones as HIV latency reversal agents

To assess whether KA and anthralin may also affect T cell activation, Jurkat cells were treated with LRAs for 24 h and stained for the T cell activation markers CD69 and CD25. Fig. 3 (C and D) shows representative results of CD69 and CD25 expression in live-gated Jurkat cells in the presence of LRAs, respectively, whereas Fig. 3 (E and F) shows dose-response profiles normalized to marker expression in control cells treated with 0.1% DMSO. As expected, based on previous observations (24, 25), 10  $\mu\text{M}$  prostratin induced a  $7.2 \pm 4.0$ -fold increase in CD69 expression, relative to cells treated with 0.1% DMSO, whereas no detectable increase in CD69 expression was observed with any concentration of panobinostat (Fig. 3E). Notably, 10  $\mu\text{M}$  KA induced a  $9.3 \pm 6.4$ -fold increase in CD69 expression, whereas 30  $\mu\text{M}$  induced an up to  $22.5 \pm 7.1$ -fold increase. In contrast, 10  $\mu\text{M}$  anthralin induced only a  $2.0 \pm 0.6$ -fold increase in CD69-positive cells, whereas 30  $\mu\text{M}$  induced a  $6.4 \pm 4.4$ -fold increase. Also consistent with previous observations (24, 25), 10  $\mu\text{M}$  prostratin induced an  $11.8 \pm 1.3$ -fold increase in CD25 expression, whereas no more than a  $2.0 \pm 0.8$ -fold increase in CD25 expression was observed with 0.3  $\mu\text{M}$  panobinostat (Fig. 3F). However, neither KA nor anthralin induced CD25 expression to levels approximating those of prostratin: no increase was observed for KA at any concentration, whereas 10  $\mu\text{M}$  anthralin induced only a maximal  $3.6 \pm 2.2$ -fold increase. These observations indicate that KA is a particularly potent inducer of at least a subset of T cell activation markers *in vitro*, whereas anthralin can also induce T cell activation markers at high concentrations.

### KA and anthralin do not function as PKC activators or HDAC inhibitors

To date, numerous LRAs have been reported to act through two major cellular pathways: PKC activation and HDAC inhibition (9, 10). To determine whether KA and anthralin function as PKC activators, we asked whether their activities in live J-Lat 9.2 cells were antagonized by the pan-PKC inhibitor GÖ-6983 (26). Following a 24-h treatment with LRAs, additional co-treatment with 1  $\mu\text{M}$  GÖ-6983 resulted in complete suppression of GFP expression induced by a 10  $\mu\text{M}$  concentration of the PKC activator prostratin (0.4% GFP-positive cells relative to cells treated with only prostratin), but not by a 0.3  $\mu\text{M}$  concentration of the HDAC inhibitor panobinostat (Fig. 4A). Furthermore, no loss of GFP expression was observed when 1  $\mu\text{M}$  GÖ-6983 was added to J-Lat cultures treated with either 10  $\mu\text{M}$  KA or anthralin (in both cases, >95% of cells treated without GÖ-6983 maintained GFP). This indicates that KA and anthralin do not function as PKC activators *in vitro*.

To assess whether KA and anthralin function as HDAC inhibitors, we used a commercially available HDAC-Glo I/II assay kit, which quantifies class I and II HDAC activity in live Jurkat cells via a cell-permeable, acetylated, luminogenic peptide substrate. With this approach, HDAC inhibitors should antagonize cellular deacetylation of the fluorogenic substrate and reduce luminescence readout. As expected, panobinostat was a potent cellular HDAC inhibitor in this assay: 0.1  $\mu\text{M}$  inhibited  $96.4 \pm 1.2\%$  of luminescence, whereas 0.3 nM inhibited  $52.5 \pm 1.2\%$  (Fig. 4B). In contrast, up to 30  $\mu\text{M}$  prostratin

did not affect cellular HDAC activity. Similarly, neither KA nor anthralin had any activity at up to 30  $\mu\text{M}$ , indicating that these LRAs also do not function as HDAC inhibitors *in vitro*.

### Latency reversal by KA and anthralin are regulated by reactive oxygen species and/or metal ions

Both KA and anthralin are reported to promote oxidative stress in cells (27–29). KA is also reported to chelate metal ions (27). If one or more of these properties are required by KA or anthralin for latency reversal, then blocking these pathways should antagonize these LRAs. To test this hypothesis, we first treated J-Lat 9.2 cells with 10  $\mu\text{M}$  prostratin, 0.1  $\mu\text{M}$  panobinostat, 10  $\mu\text{M}$  KA, or 10  $\mu\text{M}$  anthralin for 24 h in the presence or absence of modulators of oxidative stress or free metal ions (Fig. 5). Modulators included GSH (a scavenger of reactive oxygen species), deferoxamine (an iron chelator), and bathocuproine (a Cu(I) chelator).

In the presence of increasing concentrations of GSH, we observed that anthralin-induced GFP, but not GFP induced by KA, prostratin, or panobinostat, was inhibited (Fig. 5A). Whereas complete inhibition of anthralin's activity was not observed, treatment of J-Lat 9.2 cells with 100  $\mu\text{M}$  GSH reduced anthralin-dependent latency reversal to  $45.0 \pm 6.5\%$  of cells treated with anthralin in the absence of GSH. In contrast, no inhibition of KA was observed with GSH concentrations as high as 3 mM. GSH in the absence of LRAs had no effect on GFP expression (data not shown). These observations suggest that the latency reversal properties of anthralin, but not KA or control LRAs, are dependent on cellular oxidative stress.

In contrast, treatment of J-Lat 9.2 cells with increasing concentrations of deferoxamine resulted in enhanced latency reversal when co-incubated with KA, where 300  $\mu\text{M}$  boosted the activity of 10  $\mu\text{M}$  KA to  $130.7 \pm 10.6\%$  of cells expressing GFP in the absence of deferoxamine (Fig. 5B). In the presence of 10  $\mu\text{M}$  anthralin, 300  $\mu\text{M}$  deferoxamine caused a  $2.6 \pm 0.4$ -fold increase in GFP expression relative to cells treated with anthralin alone. In contrast, both prostratin and panobinostat were slightly inhibited by 300  $\mu\text{M}$  deferoxamine ( $69.5 \pm 3.9$  and  $77.1 \pm 17.1\%$  GFP-positive cells, respectively). These results suggest that the activities of both KA and anthralin are either inhibited by iron ions or otherwise stimulated by deferoxamine *in vitro*.

Finally, treatment of cells with 100  $\mu\text{M}$  bathocuproine inhibited GFP expression induced by 10  $\mu\text{M}$  KA, where only  $39.6 \pm 11.8\%$  of GFP-positive cells were observed relative to KA-treated cells without bathocuproine. This suggests that KA's activity depends on the presence of copper ions. GFP expression induced by anthralin and panobinostat was also affected by 100  $\mu\text{M}$  bathocuproine ( $50.2 \pm 24.6$  and  $21.9 \pm 17.1\%$  of GFP expression, respectively; Fig. 5C), suggesting that their activity is also dependent on copper. In contrast, prostratin's activity was enhanced in the presence of bathocuproine, where, for example, 100  $\mu\text{M}$  boosted GFP expression to  $159.1 \pm 44.4\%$  of cells treated with prostratin alone. Taken together, these results suggest that the latency reversal properties of anthralin are dependent on both oxidative stress and metal ions, whereas KA's properties are dependent only on metal ions.



## Anthrones as HIV latency reversal agents

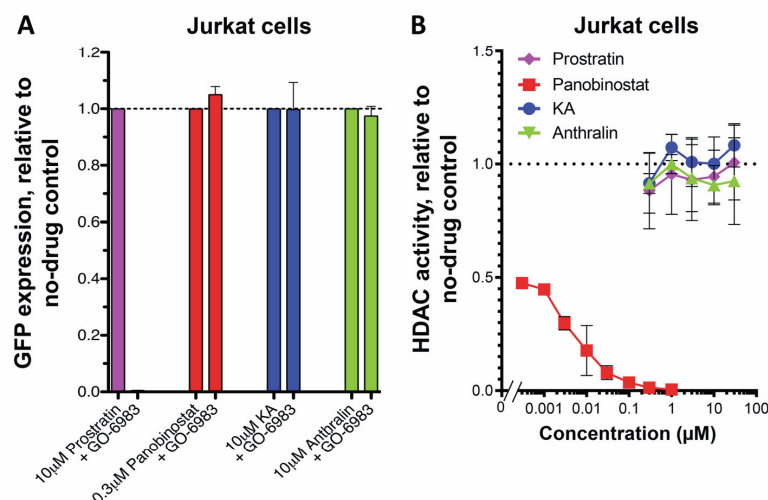


**Figure 4.** KA and anthralin are not PKC activators or HDAC inhibitors. A, effects of panobinostat, prostratin, KA, and anthralin on latency reversal in J-Lat 9.2 cells in the presence of pan-PKC inhibitor GO-6983. B, effects of LRAs on cellular HDAC activity, as measured by HDAC-Glo assay. Error bars, S.D.

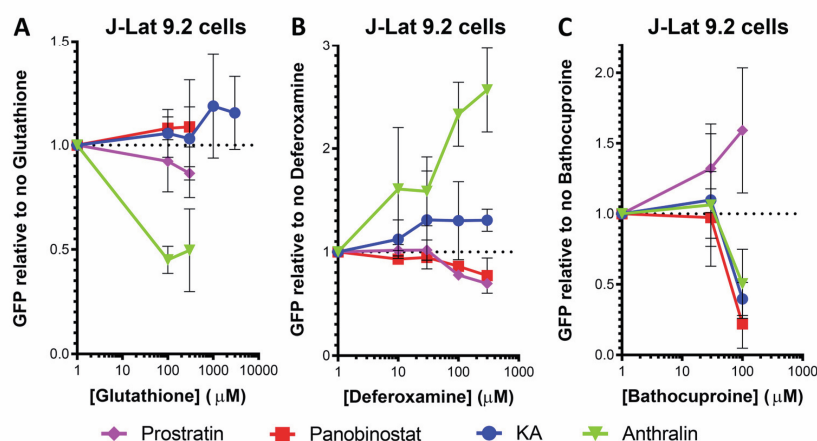


**Figure 5.** Effects of LRAs on HIV latency reversal in J-Lat 9.2 cells in the presence of the anti-oxidant GSH (A), iron chelator deferoxamine (B), and copper chelator bathocuproine (C). Error bars, S.D.

#### KA and anthralin induce distinct gene expression profiles *in vitro*

To identify potential mechanisms by which KA and anthralin may induce HIV transcription *in vitro*, we next treated three independent preparations of J-Lat 10.6 cells for 24 h with 0.1% DMSO vehicle control, prostratin (10 μM), panobinostat (0.1 μM), or KA or anthralin (10 μM). Cells were then harvested for RNA extraction, and global transcriptional profiles were assessed by RNA-Seq. High-quality sequence data were obtained for all samples with the potential exception of cells treated with anthralin, which contained ~21.5% of total transcriptome reads observed in other samples, which was suggestive of cellular toxicity. From these data, we identified a total of 8707 unique differentially expressed genes (false discovery rate (FDR) < 5%) affected by at least one treatment when compared with DMSO-treated samples. Anthralin and panobinostat had

the largest effects on overall transcription with overlap of over 2000 genes (Fig. 6A).

The four sets of genes affected by each individual treatment were then analyzed for enrichment of canonical pathways using Ingenuity Pathway Analysis (Fig. 6B). Consistent with the established role of prostratin as a PKC agonist, we identified distinct up-regulation of genes involved in PKCθ signaling (Z-score = 4.1; see "Experimental procedures") and NF-κB activation by viruses (Z-score = 2.7; Fig. 6B). Additionally, we found activation of CD28 signaling and cytokine signaling and production, whereas PD-1/PD-L1 pathways were inhibited, consistent with T cell activation (Fig. 6B). In contrast, cells treated with panobinostat activated cellular senescence, unfolded protein response, and the antiproliferative role of TOB (transducer of ErbB2) in T cell signaling, suggestive of reduced cellular activation and mild to moderate cytotoxicity. Also, consistent with

# Anthrones as HIV latency reversal agents

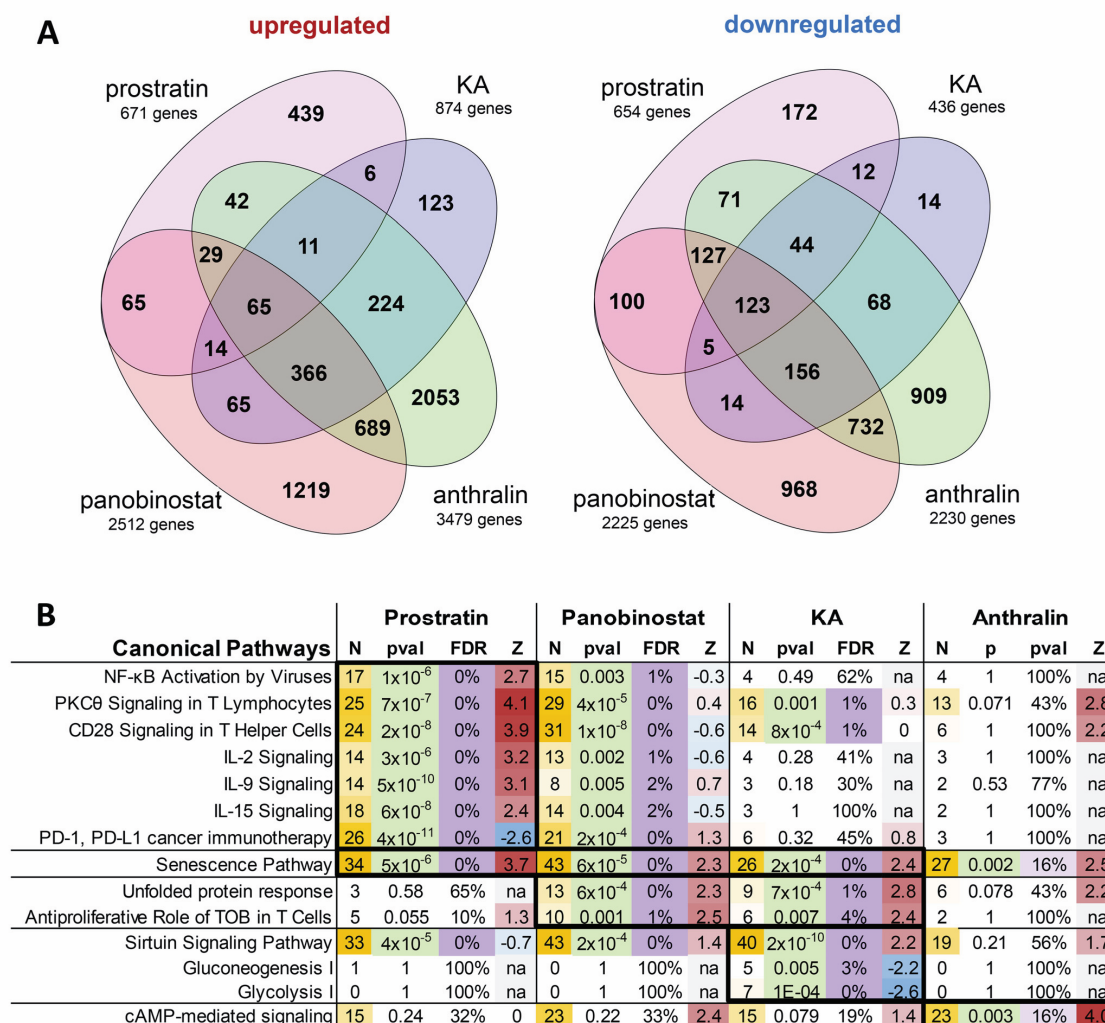


**Figure 6. Effects of LRAs on *in vitro* global gene expression as measured by RNA-Seq.** A, Venn diagrams showing number of significantly up-regulated or down-regulated genes (FDR < 5%) in J-Lat 10.6 cells treated with prostratin, panobinostat, KA, or anthralin, when compared with cells treated with 0.1% DMSO. B, Ingenuity Pathway Analysis results of genes identified in A that passed FDR < 5% and |Z-score| > 2 thresholds. For each pathway, data listed include Z-scores (Z) for predicted pathway state (where positive and negative values indicate activation or inhibition by treatment, respectively), number of affected genes (N), p value (pval), and FDR. p values < 0.05, FDR < 5% (or <20% for anthralin) thresholds are highlighted. Number of genes and Z-scores are highlighted as scales.

induction of T cell quiescence in cells treated with panobinostat, genes affected by prostratin were frequently induced in the opposite direction of T cell activation and cytokine signaling (Fig. 6B).

Cells treated with KA also had several affected gene pathways that were also observed in panobinostat-treated cells. However, KA-treated cells also had particularly strong and unique activation of the sirtuin signaling pathway (Z-score = 2.2). This result suggests that KA might disproportionately support latency reversal via sirtuin-mediated enhancement of Tat deacetylation and priming to initiate new cycles of viral transcription (30). Additional pathways unique to KA treatment included inhibition of gluconeogenesis and glycolysis (Z-scores = -2.2 and -2.6, respectively; Fig. 6B).

Finally, although cells treated with anthralin resulted in the largest number of significantly affected genes ( $n = 5709$ ; Fig. 6A), no signaling pathways were identified at FDR < 5% significance. However, among the most strongly affected pathways unique to anthralin treatment was cAMP-mediated signaling, which exhibited borderline significance ( $p = 0.003$ ; FDR = 0.16; Z-score = 4.0), which is suggestive of anthralin uniquely acting in part by driving cAMP or protein kinase A-mediated viral transcription (31, 32). Taken together, these results suggest that KA and anthralin affect gene expression and induction of pathways distinct from those of control LRAs and further suggest that they induce latency reversal by distinct mechanisms.

## Anthrones as HIV latency reversal agents

### KA and anthralin synergize with multiple LRAs

When applied in combination, LRAs with similar mechanisms of action tend to exhibit additive effects, whereas LRAs representing different functional classes frequently result in synergistic (*i.e.* greater than additive) effects (12–15). To examine whether KA and anthralin can enhance the activities of established LRAs, we treated J-Lat 9.2 cells with KA or anthralin in combination with control LRAs at concentrations that induce submaximal GFP expression. We first assessed whether 3  $\mu\text{M}$  KA and 10  $\mu\text{M}$  anthralin could synergize with control LRAs tested at a single concentration. Control LRAs included prostratin (10  $\mu\text{M}$ ), panobinostat (0.1  $\mu\text{M}$ ), TNF $\alpha$  (10 ng/ml), the BET bromodomain inhibitor JQ1 (0.7  $\mu\text{M}$ ) (12–14), and the DNA methyltransferase inhibitor 5-aza-2'-deoxycytidine (Aza-CdR; 1  $\mu\text{M}$ ) (33). For each combination, synergism was assessed using the Bliss independence model (12, 14), where a calculated  $\Delta f_{\text{axy}}$  value  $> 0$  indicates evidence of synergistic effects (see “Experimental procedures”). In this study, we conservatively defined evidence of synergism as a  $\Delta f_{\text{axy}}$  value  $> 1$ .

In all cases, KA enhanced the activities of control LRAs (Fig. 7, A and B). For example, when administered alone, 3  $\mu\text{M}$  KA induced GFP in  $5.5 \pm 1.7\%$  of live cells, whereas 10  $\mu\text{M}$  prostratin induced GFP in  $12.4 \pm 3.1\%$  of live J-Lat 9.2 cells. However, when cells were co-incubated with 10  $\mu\text{M}$  prostratin and 3  $\mu\text{M}$  KA, we observed  $38.2 \pm 9.4\%$  GFP-positive cells (Fig. 7A). This represented a 2.1-fold increase over what would be expected by additive effects ( $\sim 17.9\%$ ) and significant evidence of synergism as measured by the Bliss independence model ( $\Delta f_{\text{axy}} = 20.3 \pm 5.0$ ;  $p = 7.8 \times 10^{-4}$ ; Fig. 7B). KA also synergized with 0.1  $\mu\text{M}$  panobinostat, which induced  $21.9 \pm 6.2\%$  GFP expression on its own but  $45.0 \pm 4.1\%$  GFP expression in combination with KA ( $\Delta f_{\text{axy}}$  of  $17.6 \pm 7.2$ ;  $p = 0.0055$ ; Fig. 7, A and B). Similarly, whereas 10 ng/ml TNF $\alpha$  induced  $16.8 \pm 3.3\%$  GFP-positive cells on its own, the addition of KA resulted in  $43.2 \pm 5.1\%$  GFP-positive cells ( $\Delta f_{\text{axy}}$  of  $20.8 \pm 1.7$ ;  $p = 9.7 \times 10^{-6}$ ). When 3  $\mu\text{M}$  KA was combined with a 0.7  $\mu\text{M}$  concentration of the BET bromodomain inhibitor JQ1 (which exhibited no LRA activity on its own in J-Lat cells), we observed  $9.8 \pm 5.1\%$  GFP-positive cells and a borderline significant  $\Delta f_{\text{axy}}$  of  $4.2 \pm 3.7$  ( $p = 0.064$ ). Finally, whereas 1  $\mu\text{M}$  Aza-CdR also exhibited no activity on its own in live J-Lat cells, the addition of KA increased GFP-positive cells to  $16.0 \pm 4.5\%$  GFP-positive cells and a  $\Delta f_{\text{axy}}$  of  $10.4 \pm 3.0$  ( $p = 0.0015$ ). These results indicate that 3  $\mu\text{M}$  KA significantly synergizes with four of five control LRAs at these concentrations *in vitro*.

Similar results were observed when control LRAs were co-incubated with anthralin (Fig. 7, C and D). For example, when administered alone, 10  $\mu\text{M}$  anthralin induced  $4.5 \pm 2.3\%$  GFP expression in live J-Lat 9.2 cells, whereas 10  $\mu\text{M}$  prostratin induced  $11.0 \pm 3.1\%$  GFP-positive cells in paired experiments. However, when cells were co-incubated with 10  $\mu\text{M}$  prostratin plus anthralin, we observed  $32.5 \pm 8.4\%$  live GFP-positive cells (Fig. 7C). This represented a 1.8-fold increase over the expected additive effects ( $\sim 16.5\%$ ) and a significant  $\Delta f_{\text{axy}}$  of  $17.0 \pm 9.0$  ( $p = 0.0056$ ; Fig. 7D). In addition, 10  $\mu\text{M}$  anthralin also enhanced the activity of 0.1  $\mu\text{M}$  panobinostat and 10 ng/ml TNF $\alpha$  ( $\Delta f_{\text{axy}}$  =  $4.2 \pm 3.2$  and  $13.2 \pm 3.9$ ;  $p = 0.023$  and  $4.0 \times$

$10^{-4}$ , respectively; Fig. 7, C and D). Co-administration of 10  $\mu\text{M}$  anthralin with 0.7  $\mu\text{M}$  JQ1 also resulted in a  $\Delta f_{\text{axy}}$  value of  $11.1$

$\pm 3.0$  ( $p = 0.0053$ ), whereas anthralin plus 1  $\mu\text{M}$  Aza-CdR resulted in a  $\Delta f_{\text{axy}}$  value of  $5.1 \pm 0.8$ ;  $p = 0.0013$ ). Thus, 10  $\mu\text{M}$  anthralin significantly synergized with all control LRAs at these concentrations *in vitro*. In contrast, no obvious enhancement of GFP expression was observed when KA was combined with anthralin (data not shown), although the poor viability of cells treated with both agents made interpretation of these data difficult.

We next asked what concentrations of KA and anthralin were required to achieve synergy with a control LRA. In this experiment, J-Lat 9.2 cells were treated with 10  $\mu\text{M}$  prostratin in the presence of multiple concentrations of KA or anthralin (Fig. 7, E and F). We observed additionally synergistic provirus expression when 10  $\mu\text{M}$  prostratin was co-incubated with 1 and 10  $\mu\text{M}$  KA (Fig. 7E), with calculated  $\Delta f_{\text{axy}}$  values of  $10.9 \pm 5.1$  and  $19.1 \pm 6.2$ , respectively ( $p = 0.0088$  and  $0.0023$ , respectively; Fig. 7F), in addition to the previously described synergy with 3  $\mu\text{M}$  KA (*i.e.* Fig. 7A). Prostratin also synergized with 1, 3, and 30  $\mu\text{M}$  anthralin (Fig. 7E), where  $\Delta f_{\text{axy}}$  values were calculated as  $4.7 \pm 3.6$ ,  $5.7 \pm 4.0$ , and  $16.1 \pm 11.6$ , respectively ( $p = 0.024$ ,  $0.018$ , and  $0.019$ , respectively; Fig. 7F), in addition to the previously described synergy with 10  $\mu\text{M}$  anthralin (Fig. 7C). In summary, these results indicate that both KA and anthralin synergize with control LRAs representing multiple functional classes and at concentrations as low as 1  $\mu\text{M}$ .

### KA but not anthralin induces HIV-1 expression *ex vivo*

We next sought to investigate whether KA and/or anthralin can reactivate HIV proviruses in primary cells directly isolated from HIV-infected, cART-suppressed individuals. However, we first assessed the extent to which LRAs affected viability of isolated CD4 $^{+}$  cells obtained from three uninfected donors, as determined using ViaCount cell viability dye (34). LRAs assessed in this assay included 10  $\mu\text{M}$  prostratin, KA, or anthralin, whereas 100 ng/ml phorbol myristate acetate (PMA) + 0.1  $\mu\text{g/ml}$  ionomycin was applied as a positive control. For each condition,  $10^6$  cells were cultured in 1 ml of medium in the presence of test agents and 100 units/ml IL-2 for 24 h before assessment of cell viability. Consistent with *in vitro* observations (Fig. 3, A and B), the effects of LRAs on cell viability after 24-h incubation extended to primary CD4 $^{+}$  cells (Fig. 8A). For example, CD4 $^{+}$  cells treated with PMA + ionomycin resulted in  $93.3 \pm 6.8\%$  viability relative to cells treated with 0.1% DMSO, whereas 10  $\mu\text{M}$  prostratin resulted in  $86.2 \pm 11.4\%$  viability. Cells treated with 10  $\mu\text{M}$  KA resulted in  $54.2 \pm 27.9\%$  viability, indicating detectable but moderate cytotoxicity. In contrast, almost complete loss of cell viability was observed with CD4 $^{+}$  cells treated with 10 ( $2.0 \pm 1.6\%$  viability; Fig. 8A) or 3  $\mu\text{M}$  anthralin (data not shown).

We next assessed whether PMA + ionomycin, prostratin, KA, or anthralin at the same concentrations and treatment durations described above could induce viral RNA expression, as measured by quantitative PCR (qPCR), from  $10^6$

# Anthrones as HIV latency reversal agents

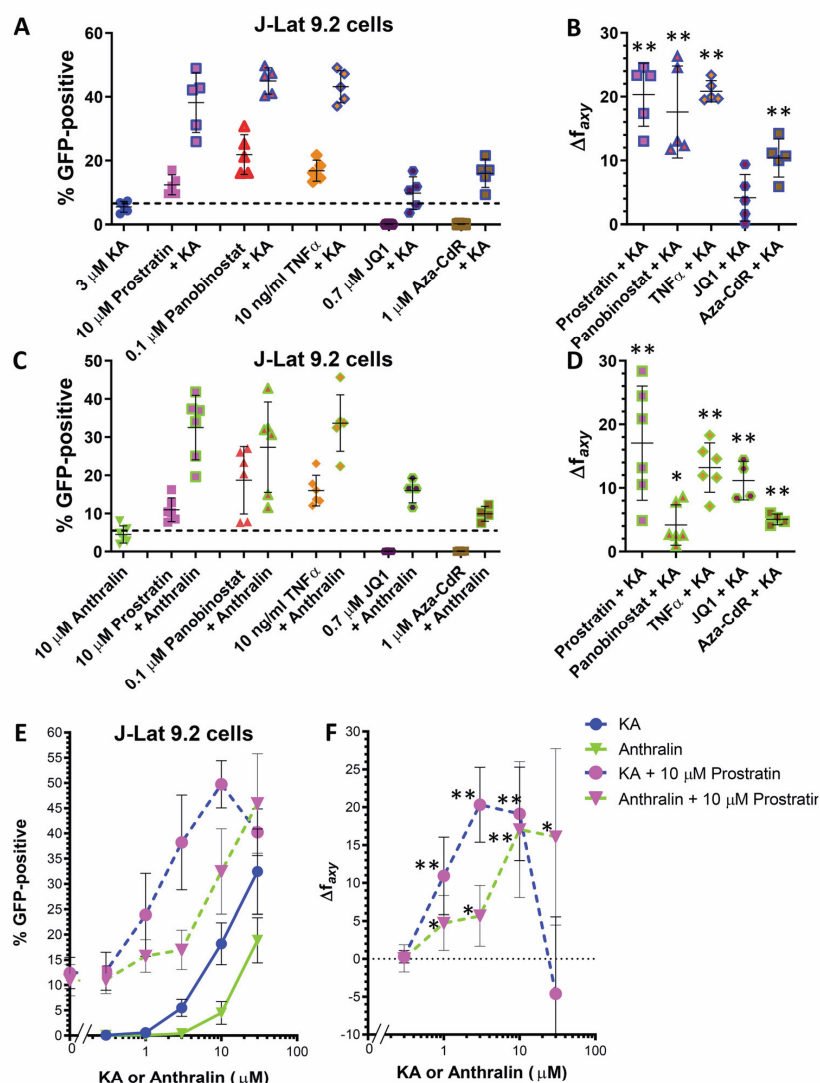


**Figure 7. KA and anthralin synergize with LRAs on multiple functional classes *in vitro*.** A, effects of 3  $\mu\text{M}$  KA on latency reversal in J-Lat 9.2 cells in the presence of 10  $\mu\text{M}$  prostratin, 0.1  $\mu\text{M}$  panobinostat, 10 ng/ml TNF $\alpha$ , 0.7  $\mu\text{M}$  JQ1, and 1  $\mu\text{M}$  Aza-Cdr. B, extent of synergism in J-Lat 9.2 cells treated with KA plus control LRAs in A, as measured by the Bliss independence model. C and D, effects of 10  $\mu\text{M}$  anthralin on latency reversal (C) and synergism (D) in J-Lat 9.2 cells in the presence of control LRAs. Data are arrayed as described in A and B. E and F, effects of KA and anthralin on latency reversal (E) and synergism (F) in the presence of 10  $\mu\text{M}$  prostratin. In E, "0" on the x axis indicates the activity of 10  $\mu\text{M}$  prostratin in the absence of KA or anthralin. Data shown for 10  $\mu\text{M}$  prostratin plus 3  $\mu\text{M}$  KA or 10  $\mu\text{M}$  anthralin are the same data shown in A–D. \*,  $p < 0.05$ ; \*\*,  $p < 0.01$  between the observed and predicted responses assuming strictly additive effects (*i.e.* Bliss independence model-based synergism) from at least four independent experiments. Error bars, S.D.

isolated CD4<sup>+</sup> T cells obtained from three HIV-infected donors (cultured in 1 ml of medium; Fig. 8B). qPCR results were normalized to co-amplified 18S housekeeping gene copy number and respective copy number standards to determine absolute copies of HIV per million CD4<sup>+</sup> cells (Table S1). Following treatment, PMA + ionomycin increased viral RNA expression in two of three donors compared with baseline expression in cells treated with 0.1% DMSO control (average across three donors of 576  $\pm$  486 viral RNA copies per million CD4<sup>+</sup> cells treated with

PMA + ionomycin versus 435  $\pm$  311 copies/million cells in DMSO-treated cells; Table S1). Similar results were also observed in CD4<sup>+</sup> cells treated with prostratin (average across three donors of 916  $\pm$  765 copies/million cells). Notably, increased viral RNA expression was also observed in two of three donors treated with KA (average 3365  $\pm$  4563 copies/million cells; Fig. 8B and Table S1). These results suggest that KA induces total viral RNA expression in primary CD4<sup>+</sup> T cells on par with established LRAs. In contrast, CD4<sup>+</sup> cells treated with anthralin



## Anthrones as HIV latency reversal agents

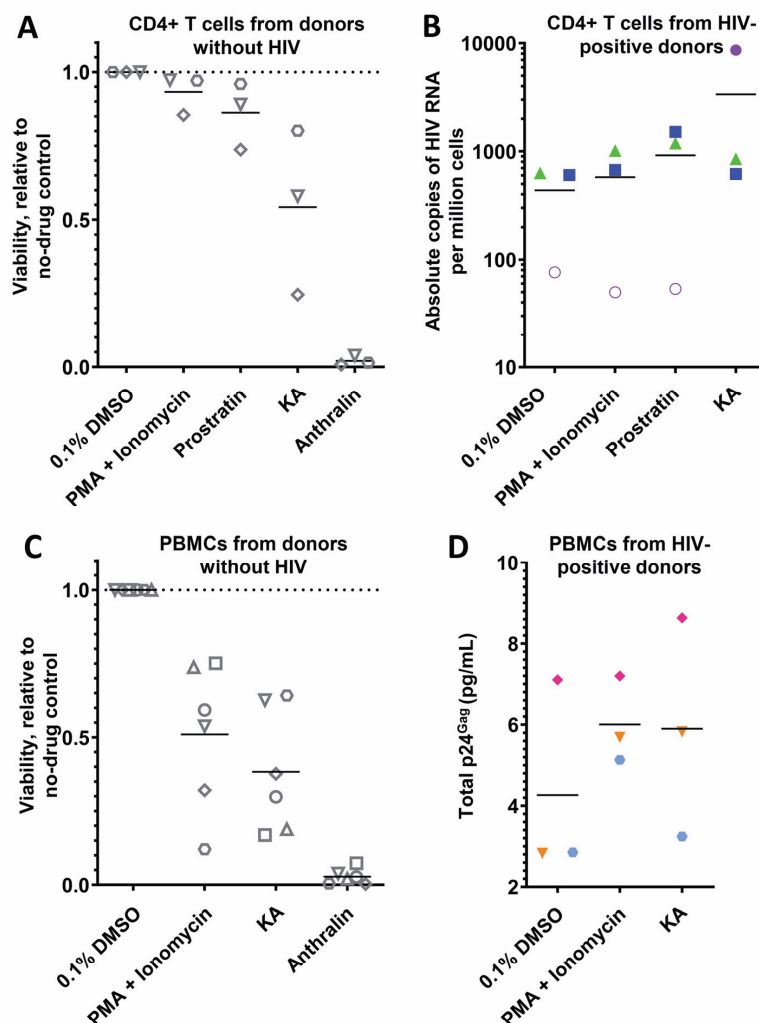


**Figure 8. Effects of LRAs on primary cells.** A, effects of LRA treatments (100 ng/ml PMA + 1  $\mu$ M ionomycin, or 10  $\mu$ M prostratin, KA, or anthralin) on viability of CD4<sup>+</sup> T cells from three uninfected donors after 24 h, as measured by ViaCount viability stain. B, effects of LRAs on total HIV RNA copies per million CD4<sup>+</sup> T cells isolated from three cART-suppressed, HIV-infected donors. Empty circles indicate the limit of detection, where no viral RNA was observed. C, effects of LRA treatments on viability of PBMCs from six uninfected donors after 24 h, as measured by ViaCount viability stain. D, effects of LRAs on p24<sup>Gag</sup> production in total cell lysate and cell culture supernatants of PBMCs from three additional cART-suppressed, HIV-infected donors. For each panel, shapes and/or colors denote individual donors.

resulted in extensive cell death, as observed by microscopy, and viral RNA was not detected (data not shown). To validate whether KA enhances HIV production *ex vivo*, we also assessed its effects on peripheral blood mononuclear cells (PBMCs). When  $3 \times 10^5$  PBMCs from six uninfected donors were cultured at  $1.5 \times 10^6$  cells/ml and assessed for viability following 24-h incubation with PMA + ionomycin, we observed  $51.0 \pm 24.7\%$  viability relative to PBMCs treated with 0.1% DMSO (Fig. 8C). However, cells treated with 10  $\mu$ M KA resulted in  $38.3 \pm 20.8\%$  viability, indicating elevated but comparable toxicity when compared with control PMA + ionomycin in whole PBMC cultures. In contrast, nearly complete loss of cell viability was again

observed with PBMCs treated with 10  $\mu$ M ( $2.8 \pm 2.6\%$  viability; Fig. 8C) or 3  $\mu$ M anthralin (data not shown).

We next treated  $3 \times 10^5$  PBMCs from three additional HIV-infected donors (separate from those in Fig. 8B) with PMA + ionomycin or KA at  $1.5 \times 10^6$  cell/ml for 24 h, as described above, and quantified combined lysate and supernatant p24<sup>Gag</sup> protein using a commercially available ELISA kit (Fig. 8D) (15). Data were then normalized to internal kit standards to calculate total p24<sup>Gag</sup> protein. Per donor, PMA + ionomycin induced an average  $1.6 \pm 0.5$ -fold increase in p24<sup>Gag</sup> relative to PBMCs treated with 0.1% DMSO, with two of three donors exhibiting at least 1.8-fold increases. Across all donors, this resulted in a combined average of  $6.0 \pm 1.1$  pg/ml p24<sup>Gag</sup> protein in PMA +

## Anthrones as HIV latency reversal agents

ionomycin-treated PBMCs versus  $5.0 \pm 2.5$  pg/ml in DMSO-treated PBMCs (Fig. 8D). In contrast, KA induced an average  $1.5 \pm 0.5$ -fold increase per donor, with 1 donor inducing a 2.1-fold increase in supernatant p24<sup>Gag</sup>, and an average of  $5.9 \pm 2.7$  pg/ml detected in PBMCs across all donors. These results further support KA as having *ex vivo* efficacy. Conversely, extensive cell death, as visualized microscopically, and no p24<sup>Gag</sup> protein were detected from PBMCs treated with 10 or 3  $\mu$ M anthralin (data not shown), further supporting poor *ex vivo* activity of this LRA. Taken together, these results suggest that KA, but not anthralin, enhances the production of both viral RNA and protein from HIV-positive CD4<sup>+</sup> T cells and PBMCs, respectively.

## Discussion

New LRAs and LRA combinations are needed to improve existing “shock-and-kill” HIV therapeutic approaches (9, 35). Here, we screened 216 compounds from pANAPL and 18 chemical analogues to identify KA, anthralin, and prinoindin as novel LRAs, which continues to suggest that chemical libraries of pure compounds from natural products can be rich sources of LRAs (15–17). Although both KA and anthralin, due to their toxicities, are unlikely to be used as LRAs in humans, their distinct activities *in vitro* make them useful probes to further understand the cellular mechanisms of HIV latency and latency reversal. This in turn can aid in the development of future LRAs with reduced toxicities, in addition to LRA combinations with improved efficacies and fewer side effects in clinical studies.

KA is a phenylanthraquinone that was originally isolated from Ethiopian *Kniphofia foliosa* and initially reported to display antiprotozoal activity *in vitro* (36, 37). KA is also reported to possess both pro- and antioxidant activities, depending on the reaction partners and culture or solvent conditions (27, 37). Since its initial discovery, several phenylanthraquinones have been isolated from plants of South Africa, Botswana, Lesotho, Germany, Australia, and Japan (38). In contrast, anthralin (dithranol) is a KA-like molecule and a licensed topical therapy for psoriasis, dermatitis, and eczema, where mechanisms of action include the induction of excessive oxidative stress in targeted cells (28, 29) in addition to induction of antiproliferative and proapoptotic signaling pathways (39). Whereas KA was recently reported by us to inhibit HIV-1 replication in PBMCs infected *in vitro*, with an EC<sub>50</sub> of 4.3  $\mu$ M (40), to our knowledge, this is the first report of anthrones affecting HIV latency.

We observed that both KA and anthralin reversed HIV latency across multiple cell line models with dose dependence, indicating that their activities were independent of the viral integration site, at least in lymphoid-derived cell lines. When assessed *in vitro*, both KA and anthralin also induced cellular apoptosis at levels approximating those of the control HDAC inhibitor panobinostat. Both KA and anthralin, like prostratin, also induced expression of T cell activation markers CD69 and CD25, although KA induced exceptionally strong (*i.e.* up to 22-fold) up-regulation of CD69 but not CD25, whereas anthralin induced weak CD69 and CD25 expression. Thus, despite the observed toxicity and proactivation properties of KA and

anthralin, their distinct profiles, when compared with prostratin and panobinostat, suggested that their effects on T cells may differ from these control PKC activator and HDAC inhibitor functional classes of LRAs. In support of this, our results using both a pharmacological pan-inhibitor of PKC signaling and a cell-based HDAC activity assay indicate that KA and anthralin are neither PKC activators nor HDAC inhibitors.

Based on the known cellular mechanisms of KA and anthralin (27–29), we initially hypothesized that both would reverse HIV latency by promoting “oxidative stress” or enhanced redox traffic, namely the formation of redox-reactive radicals derived from oxygen and from the anthrones themselves. The effects of reactive oxygen species on HIV latency reversal have been described extensively (41), and agents that intensify and uncouple cellular redox processes have been reported as LRAs or inducers of latency reversal *in vitro* and *ex vivo* (16, 42). Redox-reactive species like superoxide induce T cell activation but also promote cell death, whereas factors that mitigate redox-reactive species production tend to favor the maintenance of HIV latency (41). In support of this model, a scavenger of oxidizing species, GSH, inhibited *in vitro* latency reversal induced by anthralin, consistent with the known reactivity of anthralin in promoting oxidative stress. Contrary to our initial hypothesis, however, latency reversal by KA was not inhibited by GSH, indicating that the latency reversal properties of KA cannot solely rest on the anthrone moiety it has in common with anthralin, but that one or more distinct mechanisms of action appear to operate.

The latency reversal effects of both KA and anthralin, in addition to panobinostat, were further inhibited by the copper-sequestering agent bathocuproine. Anthrones are reported to show selectivity toward copper ions and are more easily oxidized in the presence of copper (43). This corroborates that the oxidation reaction could be responsible for driving latency reversal (27, 40). In line with this, latency reversal by KA and anthralin were enhanced by the iron chelator deferoxamine, indicating that KA and anthralin maintain latency reversal following iron sequestration and that iron inhibits them. Superoxide also leads to oxidative dimerization of anthrone derivatives, and physiologically, superoxide is reduced by copper- or iron-containing enzymes (44). Taken together, latency reversal by KA and anthralin appears to require a specific oxidation pathway that is connected to superoxide metabolism and promotes cellular activation, and this pathway is tightly modulated by particular metal ion species.

Despite years of research on both KA and anthralin (27–29, 38), direct molecular targets of these compounds are not yet elucidated. Whereas the exact molecular targets of KA and anthralin in the context of HIV latency reversal also require further investigation, analysis of *in vitro* global gene expression following KA or anthralin treatment indicates distinct expression profiles when compared with control LRAs prostratin or panobinostat. Most notably, KA treatment robustly induced expression of genes related to sirtuin signaling pathways, whereas responses to anthralin treatment were suggestive of up-regulation of cAMP-mediated signaling. To our knowledge, this is the first report linking these agents to these signaling pathways. These leads warrant further validation in cellular

## Anthrones as HIV latency reversal agents

models, although studies would likely require derivatives of anthralin and perhaps KA with reduced cytotoxicities.

We further showed that both KA and anthralin synergize with the activities of LRAs representing PKC activators, HDAC inhibitors, cytokines, BET bromodomain inhibitors, and DNA methyltransferase inhibitors. In most cases, this synergism was statistically significant as measured using the Bliss independence model. These results suggest that future compounds with improved preclinical profiles but similar mechanisms of action to KA or anthralin may be capable of enhancing the activities of existing LRAs which currently exhibit suboptimal efficacies in clinical studies (9, 11).

The ability of KA to promote latency reversal was further confirmed *ex vivo*, as it enhanced production of both viral RNA from CD4<sup>+</sup> T cells and p24<sup>Gag</sup> protein from PBMCs from HIV-infected donors. The moderate toxicity observed with KA also raises the possibility of its use at lower concentrations, where toxicity is less likely, as part of future LRA combination therapies with synergistic effects on latency reversal. The extent to which combination LRA therapies that include KA can be optimized in primary cells also requires further study. In contrast to KA, we were unable to demonstrate *ex vivo* latency reversal by anthralin, where severe oxidative stress is likely driving cell toxicity even at relatively low concentrations. In contrast to our results, a previous study identified 5-hydroxynaphthalene-1,4-dione as a novel LRA in latently infected, Bcl-2-transduced primary CD4<sup>+</sup> cells that also acted through enhanced oxidative stress (16). In this study, 5-hydroxynaphthalene-1,4-dione exhibited an EC<sub>50</sub> of 0.5  $\mu$ M and 50% cytotoxic concentration of 7.7  $\mu$ M in primary cells, indicating an improved therapeutic range relative to anthralin. Like anthralin, this compound also induced weak expression of T cell activation markers, and proviral effects could be mitigated by co-treatment with antioxidant agents. Thus, further support of this latency reversal mechanism in primary cells and in LRA combinations may be better modeled using anthralin analogues with higher therapeutic indices.

Several aspects of our results warrant further study. Most notably, the limited efficacies and toxicities of KA and especially anthralin *in vitro* and *ex vivo* are likely to limit the potential of these agents as future clinical candidates. However, their ability to synergize with numerous LRAs representing different functional classes suggests that chemical derivatives that function like KA or anthralin, but harbor improved preclinical parameters, could eventually contribute to future LRA combination strategies that maximize LRA efficacy while minimizing off-target toxicities in humans.

### Experimental procedures

#### Cells and reagents

Jurkat T cells (clone E6-1) were obtained from the American Tissue Culture Collection (ATCC). J-Lat T cells (clones 8.4, 9.2, and 10.6) and OM-10.1 cells were obtained from the NIH AIDS Reagent Program, Division of AIDS, NIAID, National Institutes of Health (contributed by Drs. Eric Verdin and Salvatore Butera, respectively) (20, 45). Cells were cultured in R10+ medium (RPMI 1640 with HEPES and L-glutamine, 10% fetal bo-

vine serum (FBS), 100 units/ml of penicillin, and 100  $\mu$ g/ml streptomycin (Sigma)).

PBMCs were collected from three uninfected donors in addition to three HIV-infected donors on stably suppressive combination antiretroviral therapy for at least 3 years. Study protocols were approved by the institutional review boards of Simon Fraser University and the University of British Columbia—Providence Health Care Research Institute (REB: H15-03077 (approved March 8, 2016) and H16-02474 (approved November 15, 2016)) and abide by the Declaration of Helsinki principles. CD4<sup>+</sup> T cells were also obtained from an additional three HIV-infected donors on stably suppressive combination antiretroviral therapy (<50 copies/ml of plasma viral load) for 3 years. These study participants were recruited in accordance with the human subject research guidelines of the United States Department of Health and Human Services under the supervision of the Wistar and Philadelphia FIGHT institutional review boards. Written informed consent was obtained from all study participants.

KA was obtained from pANAPL chemical stocks and as described previously (40, 46, 47). Anthralin, prostratin, panobinostat, Aza-CdR, GÖ-6983, deferoxamine, GSH, and bathocuproine were commercially obtained from Sigma. (+)-JQ1 was obtained from Cayman Chemical Co. (Ann Arbor, MI). Annexin V-APC and HIV p24<sup>Gag</sup> antibody KC57-RD1 were purchased from BioLegend (San Diego, CA). CD25-FITC and CD69-phycoerythrin were purchased from BD Biosciences (Mississauga, Ontario, Canada).

#### *In vitro* latency reversal assays

J-Lat and OM-10.1 cells were resuspended in fresh R10+ to a concentration of 10<sup>6</sup> cells/ml, and 2 × 10<sup>5</sup> cells were aliquoted into 96-well plates alongside test agents at defined concentrations or 0.1% DMSO vehicle control and incubated for 24 h. For each experiment, all conditions were performed in duplicate. Following incubation, for experiments using OM-10.1 cells and select experiments with J-Lat cells, p24<sup>Gag</sup> viral antigen was detected by staining cells with anti-p24<sup>Gag</sup> antibody and using the Cytofix/Cytoperm fixation/permeabilization kit (BD Biosciences) according to the manufacturer's instructions prior to flow cytometric analysis. 5000 live cells (as estimated from cells displaying the characteristic forward- and side-scatter parameters of cells treated with 0.1% DMSO) (19) from each cell culture were collected for detection of GFP and/or p24<sup>Gag</sup> expression by flow cytometry (Guava EasyCyte 8HT, EMD Millipore).

#### Detection of cell viability and T cell activation markers

To detect *in vitro* cell viability directly, Jurkat cells were treated with test agents at defined concentrations or 0.1% DMSO vehicle control in duplicate for 24 h and stained with annexin V-APC according to the manufacturer's instructions (BioLegend). To detect markers of cell activation, Jurkat T cells were stained with CD25-FITC or CD69-phycoerythrin antibodies using the Cytofix/Cytoperm fixation/permeabilization kit (BD Biosciences) according to the manufacturer's instructions. Flow cytometry was then performed as described above.



## Anthrones as HIV latency reversal agents

Viability in uninfected PBMCs was measured in the presence of test agents for 24 h using Guava ViaCount reagent (Millipore) and flow cytometry as described previously (34).

### *In vitro* HDAC activity

Cellular HDAC activity was measured in the presence of test agents using the HDAC-Glo I/II assay kit (Promega) according to the manufacturer's instructions. Briefly, Jurkat cells were resuspended in phenol red and FBS-free RPMI 1640 at  $3.0 \times 10^5$  cells/ml, and 10- $\mu$ l cell cultures were aliquoted into white 384-well plates in the presence of test agents or 0.1% DMSO diluted in 10  $\mu$ l of HDAC-Glo Buffer. Following incubation at 37 °C for 90 min, 20  $\mu$ l of HDAC-Glo I/II Reagent plus 1% Triton X-100 was added to each well, mixed, and incubated at room temperature for 30 min. Luminescence was detected using an Infinity M200 multimode plate reader (Tecan Life Sciences). Wells containing only medium were processed in parallel to control for signal background. For each experiment, four replicates of each condition were performed.

### RNA-Seq and data analysis

RNA-Seq and data analysis were performed as described previously (48). RNA was extracted from cells using the AllPrep DNA/RNA/miRNA Universal Kit (Qiagen) with on-column DNase treatment (Qiagen RNase-free DNase set). 100 ng of DNase-treated total RNA was then used for library preparation using the Quant-Seq 3' mRNA-Seq Library Preparation Kit (Lexogen, Vienna, Austria). Library quantity was determined by qPCR (KAPA Biosystems, Inc., Wilmington, MA), and library size was determined using the Agilent TapeStation and DNA High Sensitivity D5000 ScreenTape (Agilent, Santa Clara, CA). Libraries were pooled in equimolar amounts and denatured, and high-output, single-read, 75-base pair sequencing was performed using a NextSeq 500 (Illumina, San Diego, CA).

RNA-Seq data were aligned against the human genome (version hg19) using STAR (49). Raw read counts were estimated using RSEM version 1.2.12 software (50) with Ensemble transcriptome information version GRCh37.13. Raw counts were normalized and tested by DESeq2 (51) to estimate significance of differential expression, where genes that passed the FDR < 5% threshold were considered significant. Gene set enrichment analysis of significant genes was performed using Ingenuity Pathway Analysis software (Qiagen) using the "canonical pathways" category. Nominal *p* values were adjusted for multiple testing using the Benjamini–Hochberg procedure to estimate the FDR (52). Pathways enriched at FDR < 5% and with a predicted activation  $|Z\text{-score}| > 2$  in at least one treatment were reported. Predicted activation Z-score was calculated by Ingenuity Pathway Analysis software based on the direction of gene expression changes and known effect on pathway activity.

### Measures of HIV-1 latency reversal and viability in primary CD4<sup>+</sup> T cells

CD4<sup>+</sup> T cells were isolated from the PBMCs of three HIV-infected antiretroviral therapy-suppressed individuals using the EasySep<sup>TM</sup> Human CD4<sup>+</sup> T Cell Enrichment Kit (STEM-CELL) and allowed to recover in RPMI plus 20% FBS at 37 °C

for 24 h. For each donor,  $10^6$  CD4<sup>+</sup> T cells were then cultured in 1 ml of RPMI plus 20% FBS plus test agent and 100 units/ml IL-2 (Sigma–Aldrich) at defined concentrations for an additional 24 h. Total RNA was then extracted using the AllPrep DNA/RNA/miRNA Universal Kit (Qiagen) with on-column DNase treatment. Cell-associated total elongated HIV-1 RNA was then quantified with a qPCR TaqMan assay using long terminal repeat-specific and control PCR primers and conditions described previously (53). Nucleic acid input from 5  $\mu$ l of isolated total RNA was normalized for cell number by comparing the 18S housekeeping gene copy number with co-amplified copy number standards. Viral RNA per million cells was then determined by comparing results with co-amplified HIV copy number standards. Viability of CD4<sup>+</sup> T cells from three donors without HIV was measured using the culture conditions described above and ViaCount dye (Millipore) according to the manufacturer's instructions.

### Measures of HIV-1 latency reversal and viability in PBMCs

$3 \times 10^5$  PBMCs were incubated in 200  $\mu$ l of R10+ plus for 24 h at 37 °C before the addition of test agents at defined concentrations or 0.1% DMSO in duplicate and further incubation for an additional 24 h. Total cell lysates and supernatants were then measured for detection of p24<sup>Gag</sup> protein by ELISA (Xpress Bio, Frederick, MD) according to the manufacturer's instructions. Results were normalized to kit p24<sup>Gag</sup> protein standards to calculate total p24<sup>Gag</sup> per sample (pg/ml). Viability of PBMCs from six donors without HIV was measured using the culture conditions described above and ViaCount dye (Millipore) according to the manufacturer's instructions.

### Cellular data analysis

Flow cytometry data were analyzed using FlowJo version 10.5.3 software (FlowJo LLC, Ashland, OR). For studies using flow cytometry, background GFP signals in J-Lat cells treated with 0.1% DMSO were set to an average of 0.05–0.15% positive cells, whereas background GFP signals in CEM-GXR cells treated with 0.1% DMSO were set to an average of 1.0%. For flow cytometry experiments measuring CD25/CD69 and p24<sup>Gag</sup>, background fluorescence signals were set to an average of 1.0%. Synergism from LRA combinations was calculated using the Bliss independence model as described previously (12, 15). Here, synergy was defined by the equation,

$$f_{xy,P} = f_{ax} + f_{ay} \pm (f_{ax})(f_{ay}) \quad (\text{Eq. 1})$$

where  $f_{xy,P}$  represents the predicted fractional response due to drugs  $x + y$  assuming strictly additive effects, given the observed fractional responses of drug  $x$  ( $f_{ax}$ ) and drug  $y$  ( $f_{ay}$ ). The experimentally observed fractional response due to drugs  $x + y$  ( $f_{xy,O}$ ) was then compared with the predicted fractional response.

$$\Delta f_{xy} = f_{xy,O} \pm f_{xy,P} \quad (\text{Eq. 2})$$

For a given drug combination, a  $\Delta f_{xy} > 0$  indicates a fractional response greater than what is expected for additive effects. The statistical significance of this difference (*i.e.*  $f_{xy,O}$ )



## Anthrones as HIV latency reversal agents

versus  $f_{axy,p}$ ) was determined using Student's paired (for cell lines) or unpaired (for PBMCs)  $t$  test, where a two-sided  $p$  value of 0.05 was considered significant.

All data are reported as mean  $\pm$  S.D. from at least three independent experiments. For *in vitro* drug combination/synergy studies, all data are reported as mean  $\pm$  S.D. from at least four independent experiments.

### Data availability

All data are contained within the article and [supporting material](#) with the exception of RNA-Seq data, which were generated at the Wistar Institute and are available from the corresponding author upon request (I.T.; [itietjen@wistar.org](mailto:itietjen@wistar.org)).

**Acknowledgments**—We are indebted to the study participants for provision of primary cell samples.

**Author contributions**—K. R., C. S., L. B. G., T. K., A. V. K., and I. T. formal analysis; K. R., C. S., L. B. G., J. R.-O., S. R., T. K., N. N. K., A. S., R. F., S. W., M. H., K. M., A. V. K., K. A.-M., and I. T. investigation; K. R., L. B. G., J. R.-O., S. R., T. K., K. M., A. V. K., M. A.-M., and I. T. methodology; K. R., P. I., and I. T. writing—original draft; L. B. G. and J. R.-O. validation; L. B. G., J. R.-O., Z. L. B., M. A. B., A. V. K., M. A.-M., K. A.-M., L. J. M., and I. T. writing—review and editing; P. I., Z. L. B., M. A. B., A. V. K., K. A.-M., and I. T. conceptualization; P. I., Z. L. B., M. A. B., A. V. K., M. A.-M., K. A.-M., L. J. M., and I. T. supervision; P. I., Z. L. B., M. A. B., A. V. K., K. A.-M., and I. T. project administration; Z. L. B., M. A. B., M. A.-M., K. A.-M., L. J. M., and I. T. funding acquisition; K. M. data curation; A. V. K. software.

**Funding and additional information**—This work was supported by Canadian Institutes for Health Research Grants CIHR PJT-153057 (to I. T., M. A. B., and Z. L. B.) and CIHR PJT-159625 (to Z. L. B.), the Canadian Foundation for AIDS Research (CANFAR) (to I. T., M. A. B., and Z. L. B.), New Frontiers in Research Fund – Explorations Grant NRFRE-2018-01386 (to I. T.), the German Federal Ministry for Education and Research (BMBF), and the German Academic Exchange Service (DAAD) through the PhytoSustain/Trisustain project (to R. F., S. W., P. I., and K. A.-M.). This work was also supported through the Sub-Saharan African Network for TB/HIV Research Excellence (SANTHE) DELTAS Africa Initiative Grant DEL-15-006 (to K. R., K. A.-M., and I. T.). The DELTAS Africa Initiative is an independent funding scheme of the African Academy of Sciences (AAS)'s Alliance for Accelerating Excellence in Science in Africa (AESA) and supported by the New Partnership for Africa's Development Planning and Coordinating Agency (NEPAD Agency) with funding from Wellcome Trust Grant 107752/Z/15/Z and the UK government. M. A.-M. is supported by National Institutes of Health Grants R01 DK123733, R01 AG062383, R01 NS117458, R21 AI143385, R21 AI129636, and R21 NS106970 and Penn Center for AIDS Research Grant P30 AI 045008. This work was also supported by the following grants to Luis J. Montaner: Beyond Antiretroviral Treatment (BEAT)-HIV Delaney Collaboratory Grant UM1AI126620, co-funded by NIAID, NIMH, NINDS, and NIDA, National Institutes of Health. This work was also supported by Merck, Inc; the Philadelphia Field Initiating Group for HIV-1 Trials (Philadelphia FIGHT); the CLAWS

Foundation; the Philadelphia Foundation (Robert I. Jacobs Fund); Ken Nimblett and the Summerhill Trust; Penn Center for AIDS Research Grant P30 AI 045008; and the Herbert Kean, M.D., Family Professorship. K. R. was a recipient of a Canadian Queen Elizabeth II Diamond Jubilee Scholarship, a partnership between the Rideau Hall Foundation, Community Foundations of Canada, and Universities Canada, in addition to a SANTHE Ph.D. fellowship. C. S. and N. N. K. were supported by CIHR Frederick Banting and Charles Best M.Sc. Awards, and N. N. K. now holds a Vanier Doctoral award. M. A. B. holds a Tier 2 Canada Research Chair in viral pathogenesis and immunity. Z. L. B. is supported by a Scholar Award from the Michael Smith Foundation for Health Research. The content is solely the responsibility of the authors and does not necessarily represent the official views of the National Institutes of Health.

**Conflict of interest**—The authors declare that they have no conflicts of interest with the contents of this article.

**Abbreviations**—The abbreviations used are: cART, combination antiretroviral therapy; Aza-Cdr, 5-aza-2'-deoxycytidine; FBS, fetal bovine serum; FDR, false discovery rate; HDAC, histone deacetylase; KA, knipholone anthrone; LRA, latency reversal agent pANAPL, pan-African Natural Product Library; PBMC, peripheral blood mononuclear cells; PKC, protein kinase C; PMA, phorbol myristate acetate; qPCR quantitative PCR.

### References

- Ghosn, J., Taiwo, B., Seedat, S., Autran, B., and Katlama, C. (2018) HIV. *Lancet* **392**, 685–697 [CrossRef Medline](#)
- Finzi, D., Hermankova, M., Pierson, T., Carruth, L. M., Buck, C., Chaisson, R. E., Quinn, T. C., Chadwick, K., Margolick, J., Brookmeyer, R., Gallant, J., Markowitz, M., Ho, D. D., Richman, D. D., and Siliciano, R. F. (1997) Identification of a reservoir for HIV-1 in patients on highly active antiretroviral therapy. *Science* **278**, 1295–1300 [CrossRef Medline](#)
- Siliciano, J., Kajdas, J., Finzi, D., Quinn, T. C., Chadwick, K., Margolick, J. B., Kovacs, C., Gange, S. J., and Siliciano, R. F. (2003) Long-term follow-up studies confirm the stability of the latent reservoir for HIV-1 in resting CD4<sup>+</sup> T cells. *Nat. Med.* **9**, 727–728 [CrossRef Medline](#)
- Strain, M. C., Günthard, H. F., Havlir, D. V., Ignacio, C. C., Smith, D. M., Leigh-Brown, A. J., Macaranas, T. R., Lam, R. Y., Daly, O. A., Fischer, M., Opravil, M., Levine, H., Bachelier, L., Spina, C. A., Richman, D. D., *et al.* (2003) Heterogeneous clearance rates of long-lived lymphocytes infected with HIV: intrinsic stability predicts lifelong persistence. *Proc. Natl. Acad. Sci. U.S.A.* **100**, 4819–4824 [CrossRef Medline](#)
- Wong, J. K., Hezareh, M., Günthard, H. F., Havlir, D. V., Ignacio, C. C., Spina, C. A., and Richman, D. D. (1997) Recovery of replication-competent HIV despite prolonged suppression of plasma viremia. *Science* **278**, 1291–1295 [CrossRef Medline](#)
- Sadowski, I., and Hashemi, F. B. (2019) Strategies to eradicate HIV from infected patients: elimination of latent provirus reservoirs. *Cell. Mol. Life Sci.* **76**, 3583–3600 [CrossRef Medline](#)
- Deeks, S. G. (2012) HIV: shock and kill. *Nature* **487**, 439–440 [CrossRef Medline](#)
- Bullen, C. K., Laird, G. M., Durand, C. M., Siliciano, J. D., and Siliciano, R. F. (2014) Novel *ex vivo* approaches distinguish effective and ineffective single agents for reversing HIV-1 latency *in vivo*. *Nat. Med.* **20**, 425–429 [CrossRef Medline](#)
- Abner, E., and Jordan, A. (2019) HIV “shock and kill” therapy: in need of revision. *Antiviral Res.* **166**, 19–34 [CrossRef Medline](#)
- Hashemi, P., and Sadowski, I. (2019) Diversity of small molecule HIV-1 latency reversing agents identified in low- and high-throughput small molecule screens. *Med. Res. Rev.* **40**, 881–908 [CrossRef Medline](#)

## Anthrones as HIV latency reversal agents

11. Zerbato, J. M., Purves, H. V., Lewin, S. R., and Rasmussen, T. A. (2019) Between a shock and a hard place: challenges and developments in HIV latency reversal. *Curr. Opin. Virol.* **38**, 1–9 [CrossRef Medline](#)
12. Laird, G. M., Bullen, C. K., Rosenbloom, D. I. S., Martin, A. R., Hill, A. L., Durand, C. M., Siliciano, J. D., and Siliciano, R. F. (2015) *Ex vivo* analysis identifies effective HIV-1 latency-reversing drug combinations. *J. Clin. Invest.* **125**, 1901–1912 [CrossRef Medline](#)
13. Darcis, G., Kula, A., Bouchat, S., Fujinaga, K., Corazza, F., Ait-Ammar, A., Delacourt, N., Melard, A., Kabeya, K., Vanhulle, C., Van Driessche, B., Gatot, J. S., Cherrier, T., Pianowski, L. F., Gama, L., *et al.* (2015) An in-depth comparison of latency-reversing agent combinations in various *in vitro* and *ex vivo* HIV-1 latency models identified bryostatin-1+JQ1 and ingenol-B+JQ1 to potentially reactivate viral gene expression. *PLoS Pathog.* **11**, e1005063 [CrossRef Medline](#)
14. Jiang, G., Mendes, E. A., Kaiser, P., Wong, D. P., Tang, Y., Cai, L., Fenton, A., Melcher, G. P., Hildreth, J. E., Thompson, G. R., Wong, J. K., and Dandekar, S. (2015) Synergistic reactivation of latent HIV expression by ingenol-3-Angelate, PEP005, targeted NF- $\kappa$ B signaling in combination with JQ1 induced p-TEFb activation. *PLoS Pathog.* **11**, e1005066 [CrossRef Medline](#)
15. Richard, K., Williams, D. E., de Silva, E. D., Brockman, M. A., Brumme, Z. L., Andersen, R. J., and Tietjen, I. (2018) Identification of novel HIV-1 latency-reversing agents from a library of marine natural products. *Viruses* **10**, 348 [CrossRef Medline](#)
16. Yang, H.-C., Xing, S., Shan, L., O'Connell, K., Dinoso, J., Shen, A., Zhou, Y., Shrum, C. K., Han, Y., Liu, J. O., Zhang, H., Margolick, J. B., and Siliciano, R. F. (2009) Small-molecule screening using a human primary cell model of HIV latency identifies compounds that reverse latency without cellular activation. *J. Clin. Invest.* **119**, 3473–3485 [Medline](#) [CrossRef Medline](#)
17. Doyon, G., Sobolewski, M. D., Huber, K., McMahon, D., Mellors, J. W., and Sluis-Cremer, N. (2014) Discovery of a small molecule agonist of phosphatidylinositol 3-kinase p110 that reactivates latent HIV-1. *PLoS ONE* **9**, e84964 [CrossRef Medline](#)
18. Ntie-Kang, F., Amoa Oguéné, P., Fotso, G. W., Andrae-Marobela, K., Bezabih, M., Ndom, J. C., Ngadjui, B. T., Ogundaini, A. O., Abegaz, B. M., and Meva'a, L. M. (2014) Virtualizing the p-ANAPL library: a step towards drug discovery from African medicinal plants. *PLoS ONE* **9**, e90655 [CrossRef Medline](#)
19. Tietjen, I., Ntie-Kang, F., Mwimanz, P., Oguéné, P. A., Scull, M. A., Idowu, T. O., Ogundaini, A. O., Meva'a, L. M., Abegaz, B. M., Rice, C. M., Andrae-Marobela, K., Brockman, M. A., Brumme, Z. L., and Fedida, D. (2015) Screening of the pan-African Natural Product Library identifies ixoratanin A-2 and boldine as novel HIV-1 inhibitors. *PLoS ONE* **10**, e0121099 [CrossRef Medline](#)
20. Jordan, A., Bisgrove, D., and Verdin, E. (2003) HIV reproducibly establishes a latent infection after acute infection of T cells *in vitro*. *EMBO J.* **22**, 1868–1877 [CrossRef Medline](#)
21. Hashemi, P., Barreto, K., Bernhard, W., Lomness, A., Honson, N., Pfeifer, T. A., Harrigan, P. R., and Sadowski, I. (2018) Compounds producing an effective combinatorial regimen for disruption of HIV-1 latency. *EMBO Mol. Med.* **10**, 160–174 [CrossRef Medline](#)
22. Cummins, N. W., Sainski-Nguyen, A. M., Natesampillai, S., Aboulnasr, F., Kaufmann, S., and Badley, A. D. (2017) Maintenance of the HIV reservoir is antagonized by selective BCL2 inhibition. *J. Virol.* **91**, e00012-17 [CrossRef Medline](#)
23. Williams, S. A., Chen, L. F., Kwon, H., Fenard, D., Bisgrove, D., Verdin, E., and Greene, W. C. (2004) Prostratin antagonizes HIV latency by activating NF- $\kappa$ B. *J. Biol. Chem.* **279**, 42008–42017 [CrossRef Medline](#)
24. Korin, Y. D., Brooks, D. G., Brown, S., Korotzer, A., and Zack, J. A. (2002) Effects of prostratin on T-cell activation and human immunodeficiency virus latency. *J. Virol.* **76**, 8118–8123 [CrossRef Medline](#)
25. Gustafson, K. R., Cardellina, J. H., 2nd, McMahon, J. B., Gulakowski, R. J., Ishitoya, J., Szallasi, Z., Lewin, N. E., Blumberg, P. M., Weislow, O. S., Beutler, J. A., Buckheit, R. W., Jr., Cragg, G. M., Cox, P. A., Bader, J. P., and Boyd, M. R. (1992) A nonpromoting phorbol from the samoan medicinal plant *Homalanthus nutans* inhibits cell killing by HIV-1. *J. Med. Chem.* **35**, 1978–1986 [CrossRef Medline](#)
26. Tietjen, I., Ngwenya, B. N., Fotso, G., Williams, D. E., Simonambango, S., Ngadjui, B. T., Andersen, R. J., Brockman, M. A., Brumme, Z. L., and Andrae-Marobela, K. (2018) The Croton megalobotrys Müll Arg. traditional medicine in HIV/AIDS management: documentation of patient use, *in vitro* activation of latent HIV-1 provirus, and isolation of active phorbol esters. *J. Ethnopharmacol.* **211**, 267–277 [CrossRef Medline](#)
27. Habtemariam, S., and Dagne, E. (2009) Prooxidant action of knipholone anthrone: copper dependent reactive oxygen species generation and DNA damage. *Food Chem. Toxicol.* **47**, 1490–1494 [CrossRef Medline](#)
28. Müller, K. (1996) Antipsoriatic anthrones: aspects of oxygen radical formation, challenges and prospects. *Gen. Pharmacol.* **27**, 1325–1335 [CrossRef Medline](#)
29. Kemény, L., Ruzicka, T., and Braun-Falco, O. (1990) Dithranol: a review of the mechanism of action in the treatment of psoriasis vulgaris. *Skin Pharmacol.* **3**, 1–20 [CrossRef Medline](#)
30. Pinzone, M. R., Cacopardo, B., Condorelli, F., Di Rosa, M., and Nunnari, G. (2013) Sirtuin-1 and HIV-1: an overview. *Curr. Drug Targets* **14**, 648–652 [CrossRef Medline](#)
31. Rabbi, M. F., Al-Harathi, L., and Roebuck, K. A. (1997) TNF $\alpha$  cooperates with the protein kinase A pathway to synergistically increase HIV-1 LTR transcription via downstream TRE-like cAMP response elements. *Virology* **237**, 422–429 [CrossRef Medline](#)
32. Banerjee, A., Li, L., Pirrone, V., Krebs, F. C., Wigdahl, B., and Nonnemacher, M. R. (2017) cAMP signaling enhances HIV-1 long terminal repeat (LTR)-directed transcription and viral replication in bone marrow progenitor cells. *Clin. Med. Insights Pathol.* **10**, 1179555717694535 [CrossRef Medline](#)
33. Kauder, S. E., Bosque, A., Lindqvist, A., Planelles, V., and Verdin, E. (2009) Epigenetic regulation of HIV-1 latency by cytosine methylation. *PLoS Pathog.* **5**, e1000495 [CrossRef Medline](#)
34. Mwimanz, P., Tietjen, I., Miller, S. C., Shahid, A., Cobarrubias, K., Kinloch, N. N., Baraki, B., Richard, J., Finzi, A., Fedida, D., Brumme, Z. L., and Brockman, M. A. (2016) Novel acylguanidine-based inhibitor of HIV-1. *J. Virol.* **90**, 9495–9508 [CrossRef Medline](#)
35. Rasmussen, T. A., and Lewin, S. R. (2016) Shocking HIV out of hiding: where are we with clinical trials of latency reversing agents? *Curr. Opin. HIV AIDS* **11**, 394–401 [CrossRef Medline](#)
36. Bringmann, G., Menche, D., Bezabih, M., Abegaz, B. M., and Kaminsky, R. (1999) Antiplasmodial activity of knipholone and related natural phenyl-anthraquinones. *Planta Med.* **65**, 757–758 [CrossRef Medline](#)
37. Habtemariam, S. (2007) Antioxidant activity of Knipholone anthrone. *Food Chem.* **102**, 1042–1047 [CrossRef](#)
38. Bringmann, G., Mutanyatta-Comar, J., Knauer, M., and Abegaz, B. M. (2008) Knipholone and related 4-phenylanthraquinones: structurally, pharmacologically, and biosynthetically remarkable natural products. *Nat. Prod. Rep.* **25**, 696–718 [CrossRef Medline](#)
39. Ronpirin, C., and Tencomnao, T. (2012) Effects of the antipsoriatic drug dithranol on E2A and caspase-9 gene expression *in vitro*. *Genet. Mol. Res.* **11**, 412–420 [CrossRef Medline](#)
40. Feilcke, R., Arnouk, G., Raphane, B., Richard, K., Tietjen, I., Andrae-Marobela, K., Erdmann, F., Schipper, S., Becker, K., Arnold, N., Frolov, A., Reiling, N., Imming, P., and Fobofou, S. A. T. (2019) Biological activity and stability analyses of knipholone anthrone, a phenyl anthraquinone derivative isolated from *Kniphofia foliosa* Hochst. *J. Pharm. Biomed. Anal.* **174**, 277–285 [CrossRef Medline](#)
41. Benhar, M., Shytaj, I. L., Stamler, J. S., and Savarino, A. (2016) Dual targeting of the thioredoxin and glutathione systems in cancer and HIV. *J. Clin. Invest.* **126**, 1630–1639 [CrossRef Medline](#)
42. Savarino, A., Mai, A., Norelli, S., El Daker, S., Valente, S., Rotili, D., Altucci, L., Palamara, A. T., and Garaci, E. (2009) "Shock and kill" effects of class I-selective histone deacetylase inhibitors in combination with the glutathione synthesis inhibitor buthionine sulfoximine in cell line models for HIV-1 quiescence. *Retrovirology* **6**, 52 [CrossRef Medline](#)
43. Mittal, S. K., Kaur, K., Kumar, S. K. A., Kumar, S., and Kumar, A. (2013) Anthrone derivatives as voltammetric sensors for applications in metal ion detection. *Sensor Lett.* **11**, 223–236 [CrossRef](#)

### Anthrones as HIV latency reversal agents

44. D'Ischia, M., and Protà, G. (1985) Generation and role of superoxide ion in the autooxidation of 1,8-dihydroxy-9-anthrone. *Gazzetta Chimica Italiana* **115**, 511–514
45. Butera, S. T., Perez, V. L., Wu, B. Y., Nabel, G. J., and Folks, T. M. (1991) Oscillation of the human immunodeficiency virus surface receptor is regulated by the state of viral activation in a CD4<sup>+</sup> cell model of chronic infection. *J. Virol.* **65**, 4645–4653 [CrossRef Medline](#)
46. Dagne, E., and Steglich, W. (1984) Knipholone: a unique anthraquinone derivative from *Kniphofia foliosa*. *Phytochemistry* **23**, 1729–1731 [CrossRef](#)
47. Dagne, E., and Yeneseu, A. (1993) Knipholone anthrone from *Kniphofia foliosa*. *Phytochemistry* **34**, 1440–1441 [CrossRef](#)
48. Giron, L. B., Tanes, C. E., Schleimann, M. H., Engen, P. A., Mattei, L. M., Anzurez, A., Damra, M., Zhang, H., Bittinger, K., Bushman, F., Kossenkova, A., Denton, P. W., Tateno, H., Keshavarzian, A., Landay, A. L., *et al.* (2020) Sialylation and fucosylation modulate inflammasome-activating eIF2 signaling and microbial translocation during HIV infection. *Mucosal Immunol.* **13**, 753–766 [CrossRef](#)
49. Langmead, B., and Salzberg, S. L. (2012) Fast gapped-read alignment with Bowtie 2. *Nat. Methods* **9**, 357–359 [CrossRef Medline](#)
50. Li, B., and Dewey, C. N. (2011) RSEM: accurate transcript quantification from RNA-Seq data with or without a reference genome. *BMC Bioinform.* **12**, 323 [CrossRef Medline](#)
51. Love, M. I., Huber, W., and Anders, S. (2014) Moderated estimation of fold change and dispersion for RNA-seq data with DESeq2. *Genome Biol.* **15**, 550 [CrossRef Medline](#)
52. Benjamini, Y., Drai, D., Elmer, G., Kafkafi, N., and Golani, I. (2001) Controlling the false discovery rate in behavior genetics research. *Behavioural Brain Res.* **125**, 279–284 [CrossRef](#)
53. Abdel-Mohsen, M., Chavez, L., Tandon, R., Chew, G. M., Deng, X., Danesh, A., Keating, S., Lanteri, M., Samuels, M. L., Hoh, R., Sacha, J. B., Norris, P. J., Niki, T., Shikuma, C. M., Hirashima, M., *et al.* (2016) Human galectin-9 is a potent mediator of HIV transcription and reactivation. *PLoS Pathog.* **12**, e1005677 [CrossRef Medline](#)

## 2.4) Research Article IV

# A simple *In Vitro* Method to Determine Bactericidal Activity Against *Mycobacterium abscessus* Under Hypoxic Conditions

Ruth Feilcke, Robert Eckenstaler, Markus Lang, Peter Imming, Adrian Richter

**MDPI, Antibiotics**

*Antibiotics*, **2025**, 14(3): 299

Publication Date: March 13, 2025

Doi: 10.3390/antibiotics14030299

### Summary

In this article, we present a new method to cultivate aerobic mycobacteria under hypoxic conditions and thereby determine activity of compounds against non-replicating persisters, a subgroup of mycobacteria that are especially hard to eradicate. Among different stress models, assays under hypoxic conditions to study low oxygen persisters (LOPs) are the most challenging ones, often either labor intensive or doable with expensive equipment only. Our method uses a simple and concise approach to reduce oxygen levels in an appropriate speed to convert a replicating culture into a LOP culture. The low costs and availability of components makes it accessible to many laboratories. We sought to close the 10/90 gap by enabling researchers to contribute to progress in the field of drug discovery for mycobacterial infections, independently from their place of research or their financial scope. The article presents results on characteristics of the obtained culture, providing evidence that the cells have transitioned to a non-replicating state. This tool could also be applied to screening of local plant extracts on LOPs of mycobacteria or directly study patient samples, since the method avoids genetic modification of the bacteria.

### Own contribution

Design, methodology, performing of all experiments concerning characterization of obtained culture (except confocal laser scanning microscopy); writing original draft, rewriting and editing.



## Article

# A Simple In Vitro Method to Determine Bactericidal Activity Against *Mycobacterium abscessus* Under Hypoxic Conditions

Ruth Feilcke, Robert Eckenstaler , Markus Lang, Adrian Richter \* and Peter Imming \*

Institut für Pharmazie, Martin-Luther-Universität Halle-Wittenberg, Wolfgang-Langenbeck-Straße 4, 06120 Halle, Germany

\* Correspondence: adrian.richter@pharmazie.uni-halle.de (A.R.); peter.imming@pharmazie.uni-halle.de (P.I.)

**Abstract:** **Background/Objectives:** Non-replicating persisters (NRPs) of *Mycobacterium abscessus* are a bacterial subpopulation that can survive in the host under unfavorable conditions, such as hypoxia or nutrient starvation. The eradication of these bacteria is difficult, which is one reason for the long treatment duration and treatment failure. The drug discovery process should therefore contain methods to screen activity against NRPs. **Methods:** A hypoxic environment is used to generate NRPs of *M. abscessus* that are termed low-oxygen persisters (LOPs). For this, an oxidation process is used to transition a replicating culture of *M. abscessus* distributed in microtiter plates within a sealable box into LOPs. Colony counting, automated object counting, bactericidal activity determination of known agents, and confocal laser scanning microscopy are used to study the obtained culture. **Results:** The obtained culture shows typical attributes of non-replicating cells, such as significantly reduced replication, the reversibility of the LOP state under aerobic conditions, delayed regrowth on solid medium, altered morphological patterns on a single-cell level, and phenotypic resistance against a variety of clinically relevant antimycobacterial compounds. The study reveals metronidazole and niclosamide as bactericidal against *M. abscessus* LOPs. These compounds can be used as LOP verification compounds within the described model. **Conclusions:** Our model is easily implemented and quickly identifies compounds that are inactive under hypoxic conditions. It can therefore accelerate the identification of clinically effective antimycobacterial drug substances, and can be a helpful tool during the drug development process.



Academic Editor: Marc Maresca

Received: 3 February 2025

Revised: 4 March 2025

Accepted: 5 March 2025

Published: 13 March 2025

**Citation:** Feilcke, R.; Eckenstaler, R.; Lang, M.; Richter, A.; Imming, P. A Simple In Vitro Method to Determine Bactericidal Activity Against *Mycobacterium abscessus* Under Hypoxic Conditions. *Antibiotics* **2025**, *14*, 299. <https://doi.org/10.3390/antibiotics14030299>

**Copyright:** © 2025 by the authors. Licensee MDPI, Basel, Switzerland. This article is an open access article distributed under the terms and conditions of the Creative Commons Attribution (CC BY) license (<https://creativecommons.org/licenses/by/4.0/>).

**Keywords:** hypoxia; low-oxygen persister; MBC determination; *Mycobacterium abscessus*; non-replicating persister; phenotypic resistance

## 1. Introduction

Non-tuberculous mycobacteria (NTM) are a group of mycobacteria distinct from *Mycobacterium tuberculosis* and *Mycobacterium leprae*, the causative agents of tuberculosis (TB) and leprosy, respectively. As NTM infection rates are rising globally, they are becoming a concern for many health systems worldwide [1,2]. The reported treatment successes are “similar to those for extensively drug resistant tuberculosis”, in the region of 54% for *M. abscessus* subsp. *massiliense* and 33% for *M. abscessus* subsp. *abscessus* [3]. Among NTM, the fast-growing *M. abscessus* is intrinsically insensitive to many known TB drugs and most classes of antibiotics [4]. In the last 20 years, tremendous effort to develop new TB drugs has led to three newly approved drugs and a robust drug pipeline [2]. In contrast, the drug pipeline for NTM and *M. abscessus* in particular is sparse [2,5], with not a single new compound entering clinical trials while pre-clinical development is gaining momentum [6].



In addition to the lack of effective treatments for *M. abscessus* disease, another key challenge is the existence of a subpopulation of non-replicating persisters (NRPs) during an infection. NRPs are substantially more difficult to eradicate, and contribute to the characteristically long treatment regimens required for infections with *M. abscessus* and other pathogenic mycobacteria. *M. abscessus* is an obligate aerobic bacterium, which easily adapts to microaerophilic conditions through metabolic reprogramming, leading to a larger subpopulation of NRPs that are able to survive even under hypoxia. In hosts, such low-oxygen and hypoxic conditions are found in granulomas in the lung [7,8] and in mucous plaques of cystic fibrosis patients' airways [9]. Once *M. abscessus* has entered a non-replicating state, most of the few effective drugs become inactive [10]. Among the different methods used to screen against NRPs, including acidic stress [11,12], carbon starvation [13–15], nitric oxide stress [16] and potassium starvation [17,18], hypoxic models [19,20] are the most challenging ones. Most of the screening methods have been developed for *M. tuberculosis* NRPs. Only some of them have been transferred to *M. abscessus*. However, existing methods mimicking hypoxic conditions for *M. abscessus* are either laborious and not microtiter plate-compatible [10,19,21,22], or rely on genetically modified strains [20,23] or the availability of technical devices that ensure hypoxic conditions, like an Anoxomat or a chemostat [12,20,23].

To fill this gap, we sought to develop a hypoxic model that enabled the efficient screening of compounds in a simple way. To emphasize the fact that non-replicating persistent cells in our set up result from their survival in an environment with low levels of oxygen, we refer to these *M. abscessus* cells as low-oxygen persisters (LOPs). The assay set up to investigate compound activity against LOPs should convert an aerobic *M. abscessus* culture to an LOP culture by use of readily available components. The LOP culture so obtained is expected to exhibit typical characteristics of non-replicating persisters, such as markedly less replication, the reversibility of the NRP state (known as resuscitation [18]), morphological changes and phenotypical drug resistance [24]. We confirmed these properties by investigating the growth behavior of the culture during and after hypoxic conditions, using single cell microscopy to determine the morphological appearance of the cells and measuring the activity of various clinically relevant antimycobacterial compounds.

## 2. Results and Discussion

### 2.1. Generation of a Hypoxic Environment by Activated Iron Wool

Oxygen depletion in the LOPs assay was achieved by the oxidation of activated iron wool in a sealable box, monitored with a solution of methylene blue (MB) that changed from blue to colorless. All the components were placed next to the bacterial culture in an airtight box, as shown in Figure 1. This approach was first described by Parker [25], and has not been applied to mycobacteria. The fading of the indicator MB began approximately 4 h after the box was closed, and the decolorization took place about one hour later. We measured the concentration of oxygen after the decolorization of MB, and found 4.5 to 7.4 vol % of oxygen in the headspace and 1.29% air saturation of oxygen within the bacterial suspension, corresponding to 0.197 mg/L or 0.27% dissolved oxygen (see Supplementary Materials Figure S3).

Parker's method met the requirements of our project to establish a robust method with easily accessible components in order to simplify the creation of a hypoxic environment. Most authors reporting on mycobacteria under hypoxic conditions did not quantify the amount of oxygen [10,21,22]. Instead, they also relied on MB as an indicator to monitor the oxygen content. The MB turned colorless in our setup, and the levels of oxygen achieved within the media were in the range of those under Wayne's model [19]. Although MB is a common indicator used to control hypoxic conditions, its application to the bacterial

suspension will result in some (unspecific) interference due to the oxidizing potential of the substance. This could include reactions with components of the culture medium or redox active co-enzymes within the respiratory chain of the bacteria, or the direct inhibition of enzymes, as shown for other species. Keeping the indicator in a separate vial within the setup avoids these disadvantages. Parker's method avoids a sudden onset of hypoxia, as has been described as sterilizing for *M. tuberculosis* [26] and *M. abscessus* [23]. The sachets reduce the amount of oxygen to below 1% within 30 min—too fast for mycobacteria to adapt to [23,26]. Oxygen removal by Parker's method is fast enough to largely avoid the resuscitation of non-replicating cultures after oxygen re-entry during compound addition (see section on evidence for *M. abscessus* transitioning to the LOP state). This eliminates the need to use anaerobic tents or glove boxes to add compounds, again simplifying the procedure and making it more cost-effective.

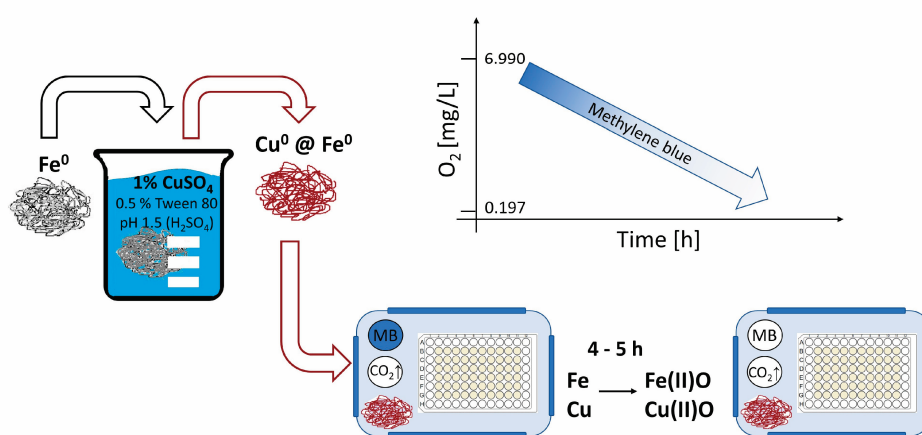


**Figure 1.** Schematic presentation of procedure followed to generate a hypoxic environment (approach adjusted from [25]). Activating of iron wool grade 0 by dipping into an acidic solution of copper sulfate and polysorbate 80 (Tween 80) to spot the iron wool with metallic copper. The activated iron wool is then placed in a sealed box together with a microtiter plate containing a liquid culture of *M. abscessus*. The rapid oxidation of iron and copper leads to the depletion of oxygen concentration to achieve hypoxic conditions within four to five hours. The concentration of oxygen can be monitored with a solution of methylene blue (MB) that changes from blue to colorless upon hypoxia. The reported oxygen levels within the graph correspond to dissolved oxygen within the bacterial suspension under aerobic and hypoxic conditions, respectively.

## 2.2. *M. abscessus* LOP Assay for Determination of Drug Activity In Vitro

The method described above was used to generate *M. abscessus* LOPs directly from a replicating culture of *M. abscessus* via incubation in an airtight box under hypoxic conditions.

Figure 2 depicts the procedure of the assay, which was performed in the same microtiter plate as was used for culture transitioning. The activated iron wool ensured a rapid onset of hypoxic conditions after the re-entry of oxygen due to the addition of test compounds. A robust dilution process in microtiter plates with subsequent spot plating on agar with counting software precluded tedious manual colony counting. Details of the method are given in the Methods section.

Preliminary experiments revealed that the red fluorescence protein (RFP)-harboring strain of the rough morphotype of *M. abscessus* (pTEC27) [27] was unsuitable for culturing under hypoxic conditions due to the extensive loss of the functional plasmid, even though hygromycin selective culturing was employed. We suppose that stressful conditions can

lead to antibiotic resistance being incorporated into the bacterial genome, while extrinsic, useless genetic material is eliminated.

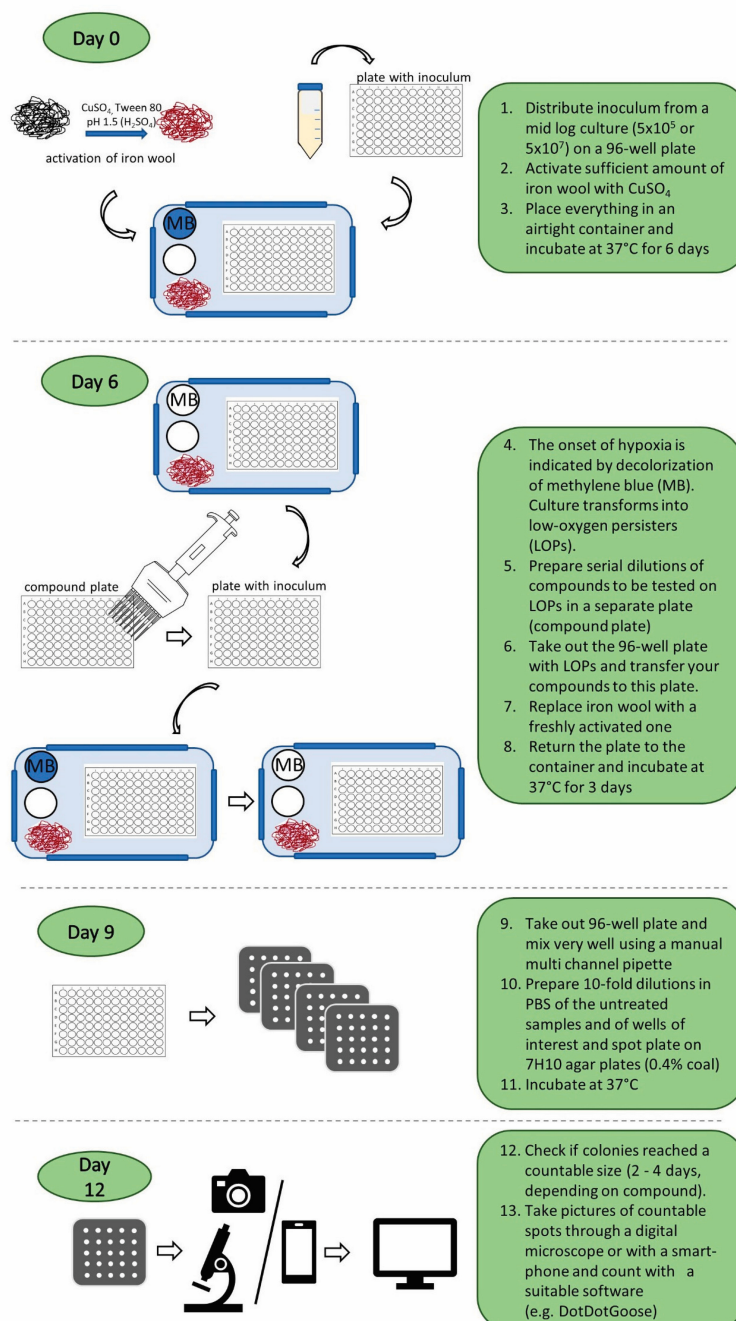


**Figure 2.** Detailed description of the assay procedure to determine bactericidal activity on *M. abscessus* LOPs. MB: methylene blue solution used as an indicator of oxygen concentration. White circle: saturated carbonate solution for the release of  $\text{CO}_2$ .



Wayne's model is normally applied for the determination of in vitro compound activity against hypoxic mycobacteria. It requires one tube for each compound concentration. In contrast, the LOP assay reported here is performed in microtiter plates, enabling higher throughput. Wayne's model relies on the consumption of oxygen by bacteria to deplete oxygen in the set up. In our model, the depletion of oxygen is based on a quick oxidation process that enables the addition of compounds to the hypoxic culture without needles for safer handling (BSL 2). Our approach to a hypoxic model is a less complex method compared to the LORA procedure [20], wherein a hypoxic parent culture needs to be prepared prior to the actual assay with Wayne's model. The maintenance of a hypoxic parent culture to ensure comparable conditions over several experiments is not necessary in the LOPs assay. Our method includes CFU counting, which can be tedious, and this is why we plated spots of several dilutions simultaneously [23] instead of preparing spread plates from bacterial suspensions, where one agar plate is necessary for every single dilution. This approach enabled us to determine the activities of twelve compounds at different concentrations within one day. Spreading out dilutes the remaining antibiotic compound to a greater extent than spot plating. Therefore, the inhibition of bacterial growth on solid medium is possible. To exclude compound carry-over, 0.4% active carbon was added to the solid medium. In doing so, colonies could be detected even in undiluted samples of high concentrations of antimycobacterial compounds. The use of a digital camera in combination with counting software further accelerated the process. This approach is also transferable to smartphone camera systems, precluding additional costs for microscopes, which is in accordance with the goal of making this method available at low costs.

### 2.3. Evidence of *M. abscessus* Transitioning to the LOP State

#### 2.3.1. Activity of Nitroaromatics Against *M. abscessus* LOPs

To ensure the LOP state of the culture in the set-up, an LOPs verification compound for *M. abscessus* was needed. This compound should ideally be inactive against *M. abscessus* under aerobic conditions, but should become bactericidal under hypoxic conditions. The approach of a "switch compound" was inspired by Cho et al., who successfully applied it to *M. tuberculosis* in the LORA [20]. From among the FDA-approved drugs, two substances were chosen, as follows: metronidazole, because of the long ongoing discussion about its activity against NRPs of *M. tuberculosis* (for a summary, see reference [12]), and niclosamide, due to its activity against nutrient-starved *M. abscessus* cells, another type of NRP [15]. To the best of our knowledge, for both compounds, their dose-dependent activities under hypoxic conditions on *M. abscessus* have not been investigated. First, MICs for both compounds were determined under aerobic conditions using the broth dilution method, and we did not find any growth inhibition up to 100  $\mu$ M for metronidazole, or any growth inhibition of at least 90% up to 50  $\mu$ M (due to solubility issues) for niclosamide.

Bactericidal activity under hypoxic conditions was then investigated at two different points in time for drug addition. By following our protocol and adding compounds on day 6, the activity on an LOP culture was determined (Figure 3, orange data points). Additionally, the activities of both compounds were investigated by following a slightly different procedure, adding compounds on day 0 of the experiment, and thereby exploring activity on a culture that transitions into an LOP in the presence of the compound (Figure 3, blue data points). For both compounds, time-dependent activity under hypoxic conditions was found. Metronidazole (Figure 3A) and niclosamide (Figure 3B) reduced CFUs after six days to a greater extent than after three days.

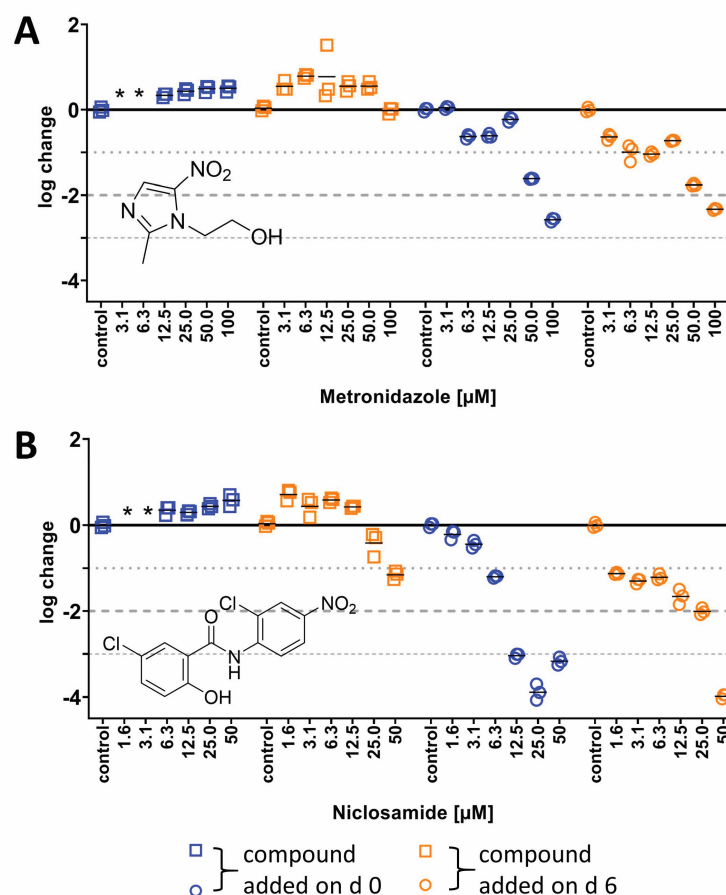


**Figure 3.** Time- and dose-dependent logarithmic changes in the CFU/mL of (A) metronidazole and (B) niclosamide on *M. abscessus* LOPs. **Blue**—drug was added on day 0 of experiment, **orange**—drug was added on day 3, **left, squares**—read out on day 3, **right, circles**—read out on day 6. For the calculation of log change, see the Materials and Methods section. The experiment was carried out in triplicate and is representative of two independent experiments; \* not determined.

For metronidazole, the dose-dependent activity was independent of the time it was added to the bacterial suspension. The activity on an LOP culture (blue data points, Figure 3A) as well as on a culture that transitioned into LOPs in the presence of metronidazole (orange data points, Figure 3A) was similar when comparing data from the same point in time—either no activity after three days, or a reduction in CFUs by >2 log units for 100  $\mu\text{M}$  in both cases. This suggests that the bactericidal quality under hypoxic conditions was only time-dependent at higher concentrations.

The bactericidal activity of niclosamide (Figure 3B) appeared to be influenced by the metabolic state of the culture, since there were differences in colony reduction between LOP cultures (orange data points, Figure 3B) and cultures that transitioned into LOPs in the presence of niclosamide (blue data points, Figure 3B). No reduction was observed after three days when 50  $\mu\text{M}$  niclosamide was added on day 0. In contrast, CFUs were reduced within three days by 1 log unit when compounds were added on day 6. After six days of incubation, niclosamide was more active when added on day 6 (MBC<sub>90</sub> 1.6  $\mu\text{M}$ )

compared to addition on day 3 (6.3  $\mu\text{M}$ ). However, similar values were observed at higher concentrations independent of when it was added.

The MICs for metronidazole and niclosamide were consistent with those in the literature, where no inhibition was found for metronidazole and  $\text{MIC}_{90}$  values for niclosamide were reported to be  $>50 \mu\text{M}$  [28,29]. However, investigations in the literature on hypoxic *M. abscessus* were carried out without verification compounds [21–23]. In most studies, methylene blue served as the sole control. This indicator only allows for monitoring of oxygen concentrations, but does not prove the transition of replicating *M. abscessus* to LOP cells. In contrast, our results reveal two FDA-approved drugs to support the formation of *M. abscessus* LOPs. There is little information on the activity of niclosamide against *M. abscessus* under hypoxic conditions to compare our results with. Lanni et al. included this drug at its maximum serum concentration (1.8  $\mu\text{M}$  [22,30]) in their study. This concentration was in the range of the lowest concentration investigated in this study. They described niclosamide as bacteriostatic under aerobic conditions on *M. abscessus*, but reported only minor differences in CFU/mL when comparing untreated hypoxic *M. abscessus* with treated cultures. Regarding the differences in their set-up (they employed the Wayne model and a clinical isolate instead of the strain ATCC 19977), we consider the observed 1-log reduction at 1.6  $\mu\text{M}$  in our study to be comparable to their results. Nutrient-starved *M. abscessus* was reported to be more susceptible to niclosamide, with a 2-log reduction after 3 days at 25  $\mu\text{M}$  [15]. *M. abscessus* LOPs showed a 0.5-log reduction only after 3 days at 25  $\mu\text{M}$  in our study. The results suggest that instead of niclosamide, metronidazole can be used as a verification compound at 100  $\mu\text{M}$ , leading to a  $>2$ -log reduction in CFUs. In the LORA, the lowest concentration of metronidazole used to verify the non-replicating state was 100  $\mu\text{M}$  [20]. This is still 50 times less than what was used by Khan et al. [31] as a control in a hypoxic *M. tuberculosis* model. While a concentration of 100  $\mu\text{M}$  and higher is too high to consider a compound as active against mycobacteria [32], this is acceptable for the present sole purpose of culture transition verification. To simplify the procedure, either 100  $\mu\text{M}$  metronidazole or 50  $\mu\text{M}$  niclosamide were added on day 0 of the assay. Thereby, at least a 2-log reduction in CFUs was observed and served as proof that the culture transitioned from replicating to *M. abscessus* LOPs.

### 2.3.2. Growth Behaviour of *M. abscessus* LOPs

If the bacterial culture transitions to LOPs, the growth behavior should be seen to differ from a regular bacterial growth curve, as LOPs belonging to NRP should replicate significantly slower [24]. The absence of turbidity was a first indicator that *M. abscessus* did not divide as usual under these conditions within three or even six days. In this time range, *M. abscessus*, when incubated under aerobic conditions, typically reached OD values of about 0.4 and higher, so turbidity would be easily detectable. CFU counting on 7H10 agar developed a comparable number of colonies as were seen for the respective inoculum. This supports our hypothesis of slower replication within our setup.

To further investigate the difference between the starting inoculum and the number of bacteria after being subjected to hypoxia, as well as to ensure viability and cultivability on solid medium, the difference in CFU numbers was investigated over time under aerobic and hypoxic conditions for *M. abscessus*. For this, a culture of *M. abscessus* in the exponential growth phase was distributed across two different 96-well plates. One plate was incubated in the hypoxic box and one plate under aerobic conditions (5%  $\text{CO}_2$ ). At defined points in time, samples were taken, and the CFU/mL was determined by plating on agar. Cultures in both microtiter plates were analyzed over the same period of time. For the hypoxic plate, fewer data points were collected (blue solid line, Figure 4). As the atmosphere in the hypoxic chamber is affected every time it is opened, we sampled every time the box

needed to be opened. After 13 days, the longest period of hypoxia investigated, the plate incubated in the hypoxic box was exposed to aerobic conditions to enable recovery from hypoxic stress. This process was followed by CFU number evaluation (blue dashed line, Figure 4).

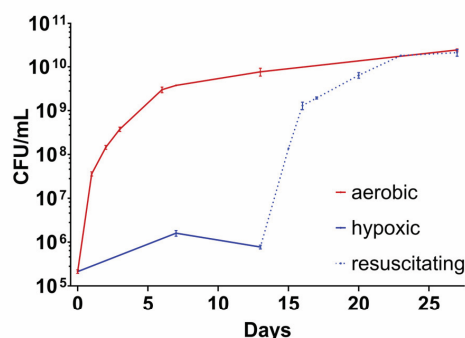


**Figure 4.** Growth of *M. abscessus* culture. **Red:** incubation in a carbon dioxide incubator (5%). **Solid blue:** incubation in the hypoxic box. **Dashed blue:** resuscitating from hypoxia (5% CO<sub>2</sub>). Hypoxia was ended on day 13 of this experiment by opening the hypoxic box and transferring the 96-well plate to the same incubator as the culture denoted by the red curve. Data points are the mean of three replicates, and the experiment shows typical growth curves derived from two independent experiments.

Figure 4 shows the value of CFU/mL over the duration of the experiment. The red curve displays the *M. abscessus* culture that was grown under aerobic (with 5% CO<sub>2</sub>) conditions. The curve shows the expected growth behavior of a culture during an exponential growth phase followed by a stationary phase. The lag phase, which precedes the exponential phase, is skipped due to inoculation from a log phase culture to obtain about  $5 \times 10^5$  CFU/mL. The growth behavior of the hypoxic culture is shown in solid blue. The displayed values represent the amount of CFU/mL that is obtained by the setup in our assay over 13 days. When cultured under hypoxic conditions, there was little change in the number of CFU/mL, which is due to the lower oxygen content that led to a reduced division rate of the bacteria ( $\times 10$  (hypoxic) vs.  $\times 10^4$  (aerobic) within 7 days). An increase in CFU/mL was detectable at day 7, followed by a slight decrease until day 13. The data reflected by the dashed blue line represent the CFU numbers of the culture analyzed during the resuscitation phase in 5% CO<sub>2</sub> after hypoxic incubation for 13 days. Resuscitating cells showed similar growth behaviors as unstressed cultures (compare the red solid and blue dashed lines, Figure 4).

Given the low scatter of values and the typical growth curve as observed under aerobic conditions (see Figure 4), plating from 96-well plates seemed to give reliable results, and plating from cultures grown in tubes appeared to be unnecessary. This enabled the use of microtiter plates in our setup. Manual mixing for at least 20 cycles and the use of polysorbate 80 were useful tools to avoid the clumping of bacteria, and we yielded reasonable results with this approach. We further concluded from the CFU numbers that the cells were still viable and cultivable, which suggests that the depletion of oxygen with activated iron wool was slow enough to not sterilize the culture. The differences in CFU numbers under hypoxic conditions might be explained via the oxygen available at the beginning of the experiment. Because of the slow onset of hypoxia, which is essential to avoid the sterilization of the culture [23,26], the conditions were growth-supporting in the beginning of the assay, and the cells were able to replicate. This led to a slight increase in CFU/mL comparable to the conditions in the Wayne model, whereby cells consumed

the remaining oxygen by multiplying. After the onset of hypoxia (decolorization of MB after about 5 h), *M. abscessus* survived as LOPs, and the cell numbers remained at a similar level. During up to 13 days of hypoxia, the number of CFUs slightly decreased. This could be due to the transition to viable but non-cultivable cells [33], or to some cells entering a non-viable state, as observed by Lanni et al. from day 10 onwards [22]. When comparing growth rates during the first 2 days of growth in aerobic and recovering cultures (Figure 4), no significant differences ( $p = 0.325$ ) between the two conditions were found. This indicates complete resuscitation in liquid medium after two days.

### 2.3.3. Resuscitation of *M. abscessus* LOPs on Solid and in Liquid Medium

Comparing the sizes of colonies on solid medium after the same incubation time, colonies derived from LOP cultures (Figure 5A, blue) were found to be smaller than those from regular *M. abscessus* cultures ( $p < 0.0001$ ; Figure 5A, red).

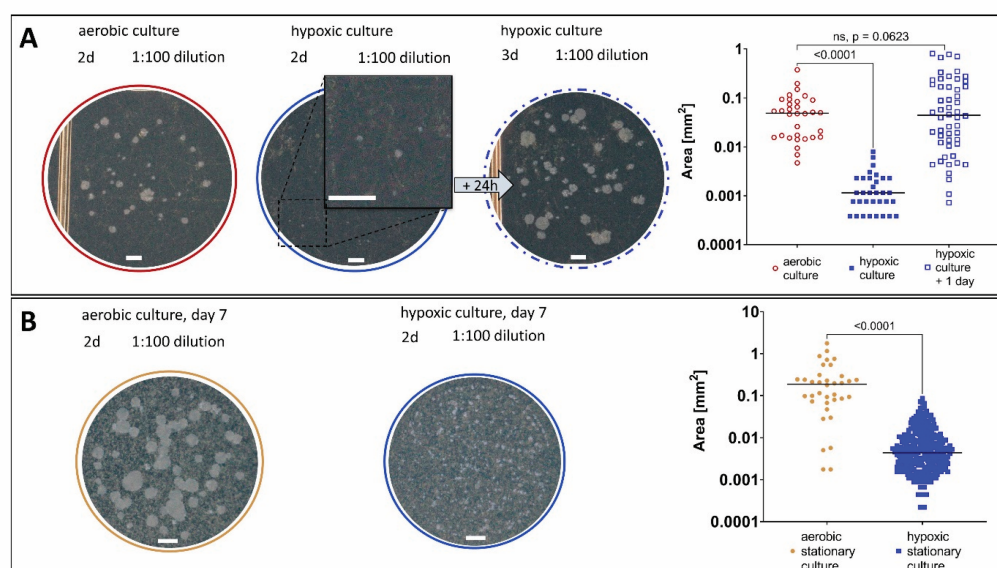


**Figure 5.** Sizes of *M. abscessus* colonies on solid medium (7H10, ADS, Glycerol) under different conditions. The plates were incubated in 5% CO<sub>2</sub> at 37 °C. The areas of detected colonies are displayed with their respective medians, and were compared by t-test within one experiment. (A) Aerobic culture (red) in comparison to a culture after 7 days of hypoxia (blue). After another 24 h, the colonies coming from a hypoxic culture reached a countable size as well (blue dashed). (B) The colonies of *M. abscessus* from an aerobic culture in stationary phase (day 7 of experiment, golden) and colonies from a culture after 7 days of hypoxia (blue), scale bars 1 mm.

This delayed growth was compensated for by an extended incubation time (after an additional 24 h, there was no significant difference in the area of colonies compared to the aerobic culture,  $p = 0.063$ ; Figure 5A; dashed blue). The additional 24 h are a suggested time frame for the resuscitation on solid medium of LOP cells. To exclude the impact of the bacterial metabolism in the stationary phase on the colony size, the size of colonies of an *M. abscessus* culture that had already entered the stationary phase (day 7 of experiment, Figure 5B, red) was compared with that of colonies derived from hypoxic conditions (Figure 5B, blue), and we found the latter to be significantly smaller ( $p < 0.0001$ ). The recovery from stress due to the stationary phase (less nutrition due to many cells) seemed to occur faster than recovery from the LOP state due to hypoxic stress. That stationary



cultures are indeed different from hypoxic cultures was described for *M. tuberculosis* by Voskuil et al., by studying their differential gene expressions [34].

The delayed time to evaluate CFUs is a typical attribute of *M. tuberculosis* NRP, and this property was used as a control by Cho et al. to verify the transition of *M. tuberculosis* into NRPs in their hypoxic model [20]. For *M. abscessus*, it was necessary in our experiment to increase the incubation time of the agar plates by a factor of 1.5 (24 h). Compared to data for *M. tuberculosis*, which is a slow-growing mycobacterium, the delayed growth seems to indicate a reduced metabolism [35,36].

We further proved that the delayed regrowth of *M. abscessus* LOPs also occurred in liquid medium using a method previously published by our group [37] that uses a fluorescent 3-hydroxychromone dye conjugated to trehalose (compound 1, Figure 6) [38] in combination with automated object counting for the detection and evaluation of mycobacteria.

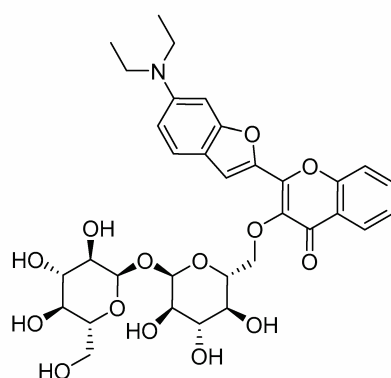


**Figure 6.** Structure of the 3-hydroxychromone dye (compound 1) used to study regrowth in fresh liquid medium of *M. abscessus* cultures derived under different conditions.

As in the growth experiment on solid medium, here, a culture was pre-treated under either hypoxic or aerobic conditions. Then, the cultures were diluted in fresh culture media, sampled, stained with 1 and analyzed by automated object counting (see Section 3.10). A significant difference in the object counts for both cultures at several sampling points was found (see Figure 7), suggesting that the *M. abscessus* LOPs culture indeed showed a delayed re-growth compared to aerated cultures. This result is consistent with the delayed growth rate on solid medium, and indicates a process of resuscitation in which the reduced metabolism of bacterial cells takes time to be reactivated, which slows down the growth rate of the culture.

The absence of an exponential growth rate in liquid medium under hypoxic conditions, the different sizes of colonies between the two cultures on solid medium, as well as the delayed re-growth in liquid medium all strengthen our hypothesis that cells subjected to this setup are in an inactive state. This corroborates that cells in our set up transitioned to LOPs. The ability to recover from hypoxic stress and to transition from LOPs back to actively replicating cells is consistent with the observation made for *M. tuberculosis* in the literature [39], and our results demonstrate that this applies to *M. abscessus* LOPs on solid as well as in liquid medium.

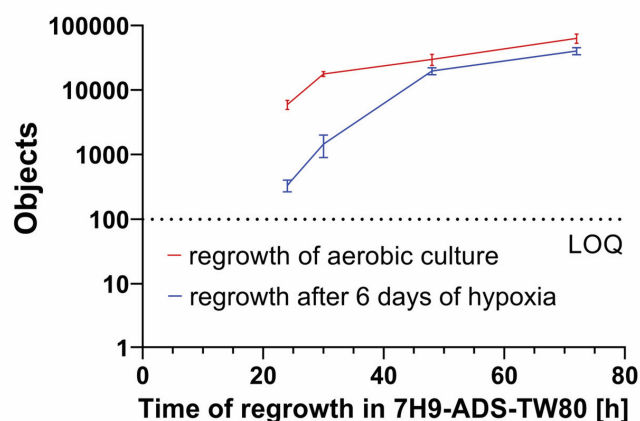


**Figure 7.** Regrowth of *M. abscessus* in liquid medium, starting from the same inoculum for (red) aerobic and (blue) hypoxic conditions (values at  $t = 0$  h were below LOQ, and are therefore not displayed within the graph.) LOQ, limit of quantification.

#### 2.3.4. Morphology of *M. abscessus* Single Cells

Cells were stained with compound **1** to investigate the morphology of *M. abscessus* single cells by confocal laser scanning microscopy. A series of pictures of a representative selection of *M. abscessus* cells was taken for each population. The study was performed as a single blinded investigation, with the person selecting about 40 cells per population while not knowing from which culture the cells were taken. The cells of a culture were sorted by their morphological appearance into three categories before unblinding the study. Figure 8 shows the percentages of different morphological patterns in the total populations of aerobic *M. abscessus* and *M. abscessus* LOPs. All pictures are shown in the Supplementary Materials (Figure S4). Category I includes cells that appear close to one another, category II includes single cells that show brighter staining at the septum and poles compared to other parts of the cell, and category III includes single cells that are homogeneously stained throughout the cell. The aerobe culture was almost evenly distributed over the three categories, with most pictures placed in category II (17/42), followed by category III (15/42) and category I (10/42). In the hypoxic culture, more than half of all pictures were attributed to category III (26/42), followed by category II (14/42), with only two pictures attributable to category I (2/42). The different morphologies, shown by the different distributions of categories, are a further indication that the two cultures differ from each other.

#### 2.3.5. Phenotypical Resistance of LOPs to Antimycobacterial Compounds

The most relevant attribute of mycobacterial NRPs is their robustness against a variety of antimycobacterial compounds. This is well proven for *M. tuberculosis* [40–42] and one of the reasons for the long treatment duration. Yam and colleagues presented a study on a variety of clinically relevant compounds that can be used in the treatment of infections with *M. abscessus* Bamboo, demonstrating that this also applies to *M. abscessus* subsp. *abscessus* [10]. To further ensure the LOP state of a culture subjected to our assay, the differences in the bactericidal activities of several compounds were investigated under aerobic vs. hypoxic conditions. Although there is still no standard therapy regimen for *M. abscessus* pulmonary disease [5,43], some compounds are considered indispensable for the treatment of mycobacterial infections, particularly amikacin, clarithromycin, cefoxitin, rifabutin and moxifloxacin. Additionally, the antimycobacterial cyclodepsipeptide pyridomycin [44] was tested alongside drug candidates from two different antimycobac-

terial classes, viz. two RNA polymerase inhibitors of the *N*- $\alpha$ -aroyl-*N*-aryl-phenylalanine amide (AAP) class of compounds [45] (MMV688845 and compound 2 [46]) and a DNA gyrase inhibitor (compound 3 [47]). All compounds except pyridomycin were reported to show promising in vitro activity against *M. abscessus* under aerobic conditions (Figure 9).

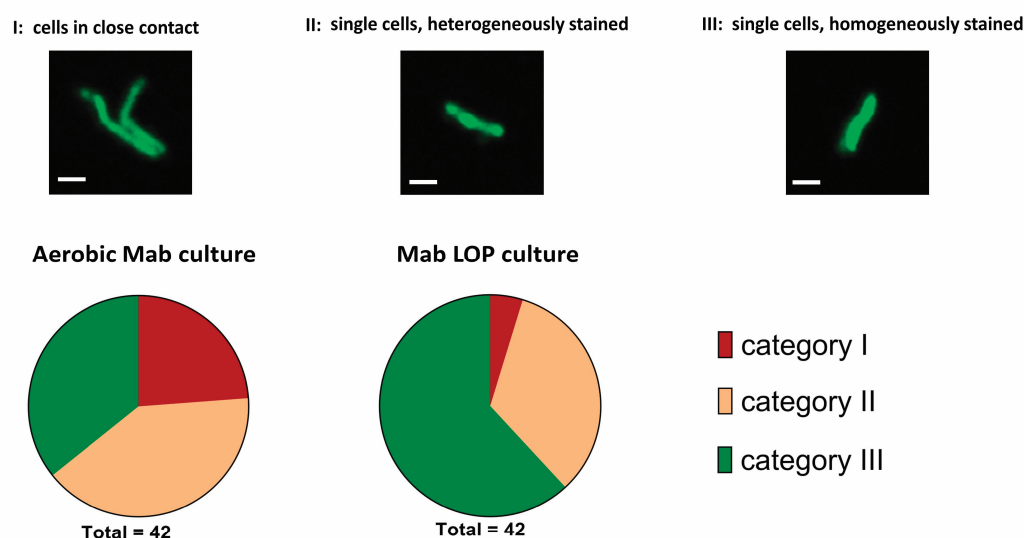


**Figure 8.** Upper part—Exemplary pictures of the three categories; I cells in close contact to each other, II single cells, heterogeneously stained with brighter staining at the septum and poles compared to other parts of the cells, III single cells, homogeneously stained. Scale bar: 1 µm. Lower part—Proportion of cells in the different categories in aerobic and hypoxic bacterial populations; Mab *M. abscessus*.

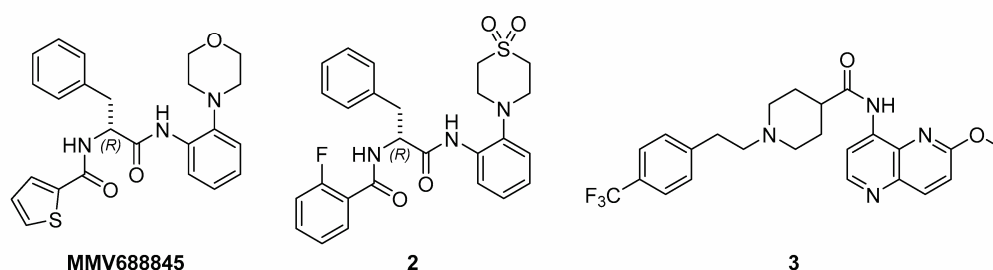


**Figure 9.** Experimental antimycobacterial compounds: MMV688845 and compound 2 belong to the class of AAPs, which are RNA-polymerase inhibitors [45,46], and compound 3 is a new DNA gyrase inhibitor [47].

The dose-dependent activities under both conditions are displayed in Figures 10 and 11. The experimental protocols are reported in the Sections 3.5 and 3.6. The bacterial population was treated for 3 days with the respective compounds, under either aerobic or hypoxic conditions. All compounds were bactericidal to replicating *M. abscessus* (Figures 10 and 11, aerobic conditions, red circles), reducing the CFU values by at least 2 log units, with the exception of pyridomycin, which led to a 1.5-log reduction only at no less than 100 µM. When comparing the activity under aerobic conditions with the activity on LOP cells determined under hypoxic conditions (blue circles, Figures 10 and 11), for most compounds, a loss of bactericidal activity was found. According to their behaviors under hypoxic conditions, the compounds can be categorized into four groups: (I) compounds



that showed no reduction in CFUs at all under hypoxic conditions (cefexitin, pyridomycin, tebipenem (even though the lactamase inhibitor avibactam was added) and compound 3), (II) compounds that reduced CFUs but failed to reach a reduction of 90% (MMV688845 and compound 2), (III) compounds that were able to reduce 90% of CFUs under hypoxic conditions (amikacin and moxifloxacin)) and (IV) those that reduced 99% of CFUs under the investigated concentrations (rifabutin and clarithromycin).

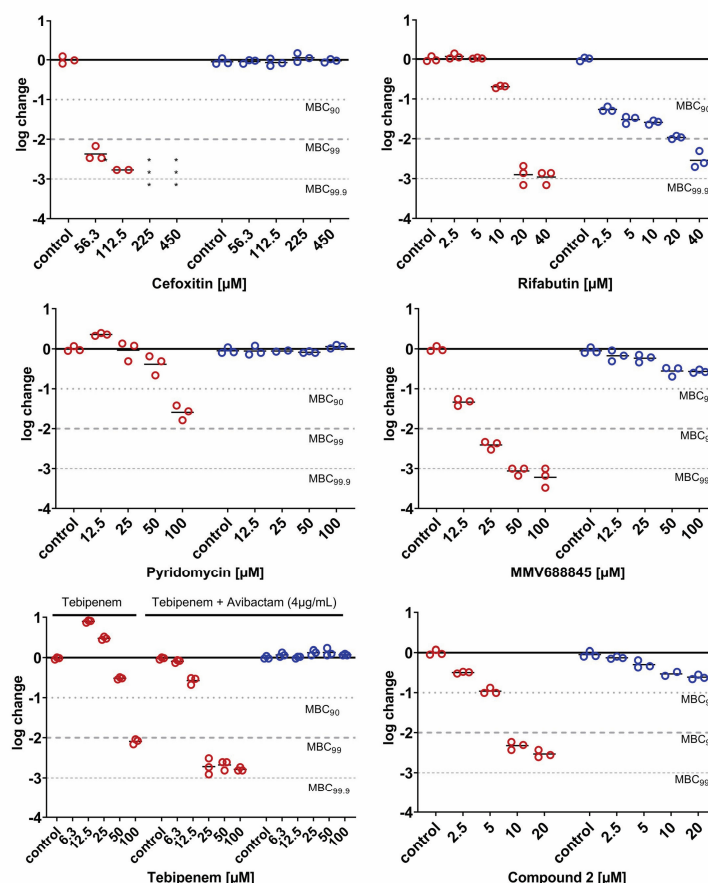


**Figure 10.** Cell wall synthesis inhibitors and RNA-polymerase inhibitors. Dose-dependent logarithmic change in CFU/mL on day 3 under aerobic (red) and hypoxic (blue) conditions. The lines represent the means of a technical triplicate, and individual values are shown as circles. The results are exemplary for at least one of two independent experiments. For the determination of activity under hypoxia, the bacterial culture was incubated under hypoxia for 6 days before treatment start. Number of \* equals number of samples below LOD (100 CFU/mL).

Since all compounds showed lower activity under hypoxia than under aerobic conditions, the results are in line with our expectations. The inactivity of targets due to their silencing as a response to hypoxic stress is a possible reason for the reduced activity. This is supported by the significant changes in the proteome under hypoxic compared to aerobic conditions. For an overview of the literature on *M. tuberculosis*' expression of dormancy genes and metabolic shift, see [24]; for the literature on *M. abscessus*, see [21,23,48]. LOPs replicate markedly less. This should result in their lower sensitivity to compounds that target cell wall synthesis [15]. The complete loss of bactericidal activity against LOPs

seen here in inhibitors of cell wall synthesis (Figure 10) is consistent with findings in the literature [10,15]. Another reason for the loss in activity could be the lower penetration rates under hypoxic conditions due to the altered cell walls of bacteria in response to hypoxic stress. For *M. tuberculosis*, the morphological changes in the membranes of NRPs compared to actively dividing cells were investigated by atomic force microscopy (AFM) and scanning electron microscopy (SEM) by Jakkala et al. in 2019. They described a significantly thicker outer layer, although the peptidoglycan and electron transparent layer were unchanged [49]. This fact impedes the further permeation of drugs through the thick lipophilic cell wall, and is thought to be a reason for the reduced activity of drugs against *M. tuberculosis* NRP.

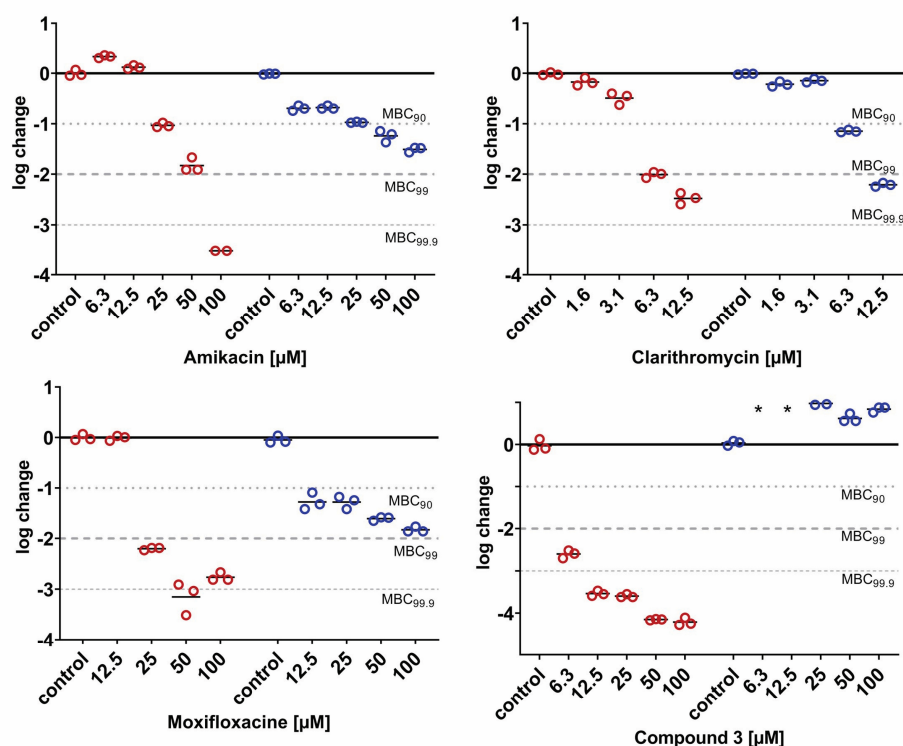


**Figure 11.** Protein synthesis inhibitors amikacin and clarithromycin and gyrase inhibitors moxifloxacin and compound 3. Dose-dependent logarithmic change in CFU/mL on day 3 under aerobic (red) and hypoxic (blue) conditions. Lines represent the mean of a technical triplicate, and individual values are shown as circles. The results are exemplary for at least one of two independent experiments. For the determination of activity under hypoxia, the bacterial culture was incubated under hypoxia for 6 days before treatment start. Number of \* equals number of samples below LOD (100 CFU/mL).

Table 1 summarizes the MIC and MBC values determined in this study, and compares them with reported values. The clinical importance of non-replicating persisters is still underestimated. For instance, there are only two studies [10,22] that have reported their activities on the respective compounds under hypoxic conditions, although some of the compounds are routinely administered in the treatment of *M. abscessus* infections. In contrast to the results in the literature, we provide data covering a range of concentration of the drugs. Therefore, our study can help us to understand the antimicrobial efficacy of clinically relevant compounds.

Table 1 shows that the MICs determined in our study are largely consistent with the results in the literature. Differences in the treatment length, model setup and strains used between the literature and this study complicate the direct comparison of MBC values. Although rifabutin is one of the most important drugs used in the treatment of mycobacterial infections, Lanny et al. are the only ones to have previously reported on its activity under hypoxic conditions. Our results confirm their finding of higher activity under hypoxia compared to aerobic conditions at low concentrations. However, at higher concentrations, slightly lower activities were determined under hypoxia. Nevertheless, in our study, this drug was the most active one under hypoxia among those investigated. This finding suggests the potential importance of rifabutin in the treatment of *M. abscessus* infections.

The two drug candidates of the compound class of AAPs showed different patterns in their activity shifts, acting on the same target as rifabutin but binding to a different target site [50]. MMV688845 and compound 2 showed >2 log reduction at 25  $\mu$ M and 10  $\mu$ M, respectively, but reduced *M. abscessus* LOPs by 0.5 log at 50  $\mu$ M and 10  $\mu$ M only. At a first glance, this result is surprising, because rifabutin's activity in hypoxia proves that the target is still active. At the moment, it can only be assumed that different permeation rates caused this.

Clarithromycin, a very important drug used in the clinic, retained its activity under hypoxia (Figure 11, bottom middle). There are conflicting reports on the bactericidal activity of clarithromycin in replicating *M. abscessus*. Several groups found bactericidal activity [22,51,52] reaching as high as a 3-log reduction within three days at 21  $\mu$ M [51], while others found a bacteriostatic effect only [10]. The differences under aerobic conditions between Yams and our results are consistent with the differences under hypoxia, probably due to the differences in susceptibility to aminoglycosides between the strains. However, our results confirm the shift in activity under hypoxic conditions as observed by Lanni et al. [22].

Our results for amikacin confirm the finding of Kolpen et al., who reported an increase in the killing of oxygenated *M. abscessus* cultures at high concentrations of amikacin compared to anaerobic ones [53]. Our results are again different to Yam's results, as they could not determine any bactericidal activity under hypoxia, further supporting a difference in the susceptibility of the strains. However, our results confirm that this mainstay of therapy has very low activity towards *M. abscessus* LOPs.

Moxifloxacin showed a bimodal shift of activity comparable to that of rifabutin—a higher activity under hypoxia at low concentrations, and a lower activity under hypoxia at higher concentrations. Our results are in the same range as Lanni's, who reported an  $\text{MBC}_{90} > 10 \mu\text{M}$  under hypoxia, but they are again contrary to Yam's results, who did not find any killing at all up to 100  $\mu\text{M}$  [10,22].

The multiple changes in the phenotypical drug susceptibility of *M. abscessus* towards a variety of drugs from different compound classes support the presupposition that culturing *M. abscessus* in the described setup indeed leads to the formation of LOPs from a replicating culture. At the same time, these results confirm alarming reports that there are almost no drugs available in the clinic that are able to eradicate this critical bacterial subpopulation.

**Table 1.** MIC<sub>90</sub> and MBC values determined under aerobic and hypoxic conditions in comparison to results in the literature obtained under the hypoxic Wayne model.

Drug	MIC <sub>90</sub> (μM) Aer	MBC (μM) Aer	MBC (μM) LOPs	Literature Data			Ref.
				MIC <sub>90</sub> (μM) Aer	MBC (μM) Aer	MBC (μM) Wayne	
Pyridomycin	12.5	MBC <sub>90</sub> 100 MBC <sub>99</sub> n.a.	MBC <sub>90</sub> n.a. MBC <sub>99</sub> n.a.	11.6	-	-	[44]
Cefoxitin	28	MBC <sub>90</sub> 56	MBC <sub>90</sub> n.a.	16	MBC <sub>90</sub> 25 <sup>a</sup>	MBC <sub>90</sub> > 100	[10]
Tebipenem (+Avibactam 4 μg/mL)	6.3	MBC <sub>90</sub> 25	MBC <sub>90</sub> n.a.	3–4	MBC <sub>90</sub> 8	-	[52]
		MBC <sub>99</sub> 25	MBC <sub>99</sub> n.a.		MBC <sub>99</sub> 16	-	[52]
					MBC <sub>99,9</sub> 24	-	[52]
Rifabutin	1.3	MBC <sub>90</sub> 20	MBC <sub>90</sub> 2.5	2.3	MBC <sub>90</sub> > 3.5 <sup>b</sup>	MBC <sub>90</sub> 3.5 <sup>b</sup>	[22]
Clarithromycin	0.8	MBC <sub>90</sub> 6	MBC <sub>90</sub> 6.3	0.2	MBC <sub>90</sub> > 100 <sup>a</sup>	MBC <sub>90</sub> > 100 <sup>a</sup>	[10]
		MBC <sub>99</sub> 6	MBC <sub>99</sub> 12.5		MBC <sub>99</sub> 2.7 <sup>b</sup>	MBC <sub>90</sub> 2.7 <sup>b</sup>	[22]
Amikacin	6.3	MBC <sub>90</sub> 25	MBC <sub>90</sub> 25	2	MBC <sub>90</sub> 12.5 <sup>a</sup>	MBC <sub>90</sub> > 100 <sup>a</sup>	[10]
				13.6	MBC <sub>90</sub> > 13.6 <sup>b</sup>	MBC <sub>90</sub> > 13.6 <sup>b</sup>	[22]
Moxifloxacin	6.3	MBC <sub>90</sub> 25	MBC <sub>90</sub> 12.5	2	MBC <sub>90</sub> 3 <sup>a</sup>	MBC <sub>90</sub> > 100 <sup>a</sup>	[10]
		MBC <sub>99</sub> 25	MBC <sub>99</sub> n.a.	10	MBC <sub>99,9</sub> 10 <sup>b</sup>	MBC <sub>90</sub> > 10 <sup>b</sup>	[22]

Aer: aerobic incubation. LOP values were determined via the developed method. n.a.: not achieved. <sup>a</sup> 2 days; <sup>b</sup> 7 days.

### 3. Materials and Methods

#### 3.1. Source of the Materials

The reagents were purchased and used as received. Sigma Aldrich, St. Louis, MO, USA; Middlebrook 7H10 agar, Middlebrook 7H9 broth base, catalase (from bovine liver), polysorbate 80. Pan Reac AppliChem GmbH, Darmstadt, Germany; oleic acid (Ph. Eur. grade). Roche Diagnostics: bovine serum albumin. Grüssing, Filsum, Germany; glucose, glycerol (99%, water free) Na<sub>2</sub>CO<sub>3</sub> (99.5%, anhydrous), NaHCO<sub>3</sub> (99%). ORG Laborchemie, Bunde, Germany; NaCl (99.5% purity). Local hardware store: iron wool (6.5–10 g grade 0). Cell Signaling Technology, Danvers, MA, USA: mounting medium (Signal Stain<sup>®</sup>).

Antibacterial compounds were purchased as follows and dissolved in DMSO (unless otherwise stated): amikacin, 98% (Alfa Aesar, Haverhill, MA, USA dissolved in water and subsequently sterile filtered); avibactam, >98% (BLDpharm (BLD), Shanghai, China); bedaquiline, 99% (AmBeed, Arlington Heights, Illinois, USA); cefoxitin, >98% (Tokyo Chemical Industry Germany (TCI-Germany), Eschborn, Germany); clarithromycin, >98% (TCI Germany); metronidazole, 99% and niclosamide, 97% (VEB Sächsisches Serumwerk, Dresden, Germany); moxifloxacin, >98% (Sigma Aldrich, St. Louis, MO, USA); pyridomycin (kindly provided by Prof. Dr. Shuangjun Lin, State Key Laboratory of Microbial Metabolism, Joint International Laboratory on Metabolic & Developmental Sciences, School of Life Sciences & Biotechnology, Shanghai Jiao, Tong University, Shanghai, China, analyzed by NMR before use), rifabutin, >98% (TCI Germany); tebipenem, 98% (BLD). The 3-hydroxychromone dye trehalose conjugate (compound 1) was synthesized as described in reference [54]. Compound 2, MMV688845 and 3 (dissolved in ethanol) were synthesized as described in the literature [46,47].

Consumables were purchased from the following companies: Saartstedt (Nümbrecht, Germany)—single-use inoculation loop, 50 mL tubes, 2 mL screw cap tubes, 96-well plates (83.3924.500); Eppredia (Portsmouth, NH, USA)—microscope slides (25 × 75 × 1 mm); Brand (Sigma Aldrich, St. Louis, MO, USA)—square glass cover slips.

### 3.2. Bacterial Strain and Culture Medium (Liquid and Solid Medium)

Preparation of working stocks: *M. abscessus* subsp. *abscessus* ATCC 19977 (rough morphotype) was spread on solid medium (a freshly prepared Middlebrook 7H10 agar plate supplemented with 0.2% oleic acid), and 5% bovine serum albumin, 0.2% glucose, 0.0004% catalase, 0.08% NaCl and 0.05% glycerol were added with a sterile single-use inoculation loop and incubated for 3 days at 37 °C, 5% CO<sub>2</sub>. Then, 15 mL of liquid culture medium (Middlebrook 7H9 broth supplemented with 0.08% NaCl, 0.2% glucose, 5% bovine serum albumin and 0.05% polysorbate 80) in a 50 mL tube was inoculated by picking a single colony from a fresh streak plate. After 3 days of incubation at 37 °C (5% CO<sub>2</sub>), the culture was diluted and further incubated until the OD<sub>600</sub> reached 0.6–0.8. The culture was aliquoted by adding 500 µL of the culture into screw cap tubes containing 500 µL of 50% glycerol (in 7H9 broth base, final concentration of glycerine 25%). The screw cap tubes were stored at –80 °C until further use.

### 3.3. Minimum Inhibitory Concentration (MIC) Determination in 7H9 by OD<sub>600</sub> Measurement

Here, 10 mL of liquid medium was inoculated by transferring 1 mL of a working stock into a 50 mL tube and incubating at 37 °C for 24 h. Thereafter, the culture was sub-cultured once and further incubated to reach a mid-log phase with an OD<sub>600</sub> between 0.4 and 0.8, where an OD<sub>600</sub> of 0.5 corresponds to  $5 \times 10^8$  CFU/mL. Then, the required volume of liquid culture medium (see preparation of working stock) was inoculated to reach about  $5 \times 10^5$  CFU/mL, while some experiments were also performed with  $5 \times 10^7$  CFU/mL. MICs were determined by performing a serial dilution broth assay in 96-well plates with a total volume of 200 µL in each well. To reduce evaporation effects, compounds and references were used, starting from column two and row B, respectively, and the wells at the borders of the plate were filled with 200 µL medium. For a schematic depiction of the plate layout, see Figure 12. Column two contained 5 µM bedaquiline as a positive control for antimycobacterial activity, and column three contained 1% DMSO as an untreated control. All compounds were used as a stock solution at 100 times the highest concentration of the intended initial concentration. Then, 4 µL samples of the stock solutions were transferred to the wells of column four, which contained 200 µL of pure medium. Subsequently, the wells were serially diluted using a multichannel pipette (Eppendorf). Thereafter, 100 µL of the prepared inoculum was distributed into each well. The plate was incubated at 37 °C in 5% CO<sub>2</sub> for three days and growth inhibition was determined by OD<sub>600</sub> measurement (FLUOstar OPTIMA, BMG Labtech,  $\lambda = 590$  nm).

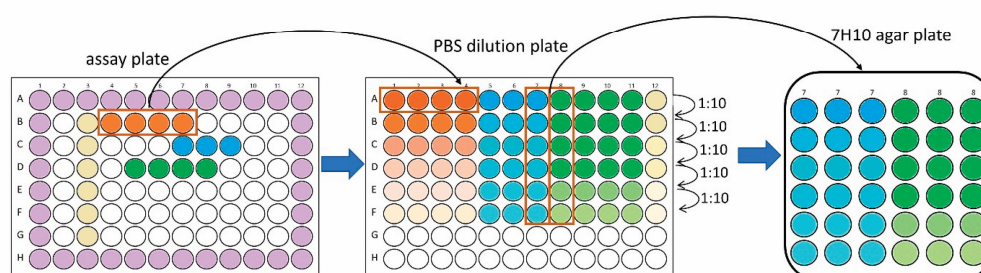


**Figure 12.** Graphical illustration of MBC determination procedure by PBS dilution preparation and spot plating on solid medium. The procedure shows three compounds, selected for MBC determination on solid medium (orange, blue and green wells of assay plate) and the subsequent preparation of a 10-fold serial dilution of these wells in another 96-well plate (PBS dilution plate). Spot plating on square 7H10 agar plates was shown to be exemplarily for two wells only (column 7



and 8 of the PBS dilution plate) in triplicate. Purple wells in the assay plate contain medium only in order to reduce the evaporation of corner wells, while the wells in column 3 (pale yellow) contain the negative control used to determine 100% growth.

### 3.4. Calculation of MIC<sub>90</sub>

MIC<sub>90</sub> was used to determine the activity under aerobic conditions in order to select the right wells for MBC determination. Each assay plate contained six wells of 1% DMSO and six wells of 5 µM bedaquiline as controls. Raw OD values were used to calculate the percentage of growth inhibition compared to DMSO and bedaquiline, according to the following formula:

$$\frac{\text{OD (sample)} - \text{mean OD (bedaquiline)}}{\text{mean OD (bedaquiline)} - \text{mean OD (DMSO control)}} \times (-100) = \% \text{inhibition} \quad (1)$$

The lowest concentration exceeding 90% inhibition is reported as MIC<sub>90</sub>.

### 3.5. LOPs Assay Under Hypoxic Conditions

A box equipped with a tightly sealable lid was used as a hypoxic chamber. Of note, anaerobic pots with a volume of 2.5 L usually used for agar plates were also successfully used as the hypoxic chamber (picture of a setup with an anaerobic pot in Supplementary Materials Figure S1). We used a box with 2.5 L volume. The reduction in oxygen content in a closed system followed a published method, using the conditions described as most effective [25]. In brief, 7 g iron wool was freshly activated as described in [25] with a CuSO<sub>4</sub> solution (1%) containing 0.5% polysorbate 80 as the wetting agent by submerging the iron wool into the solution for 30 s. The pH of the solution was adjusted to 1.5 with concentrated sulfuric acid. Stabilized methylene blue (MB) solution [25] was used as an indicator for the onset of hypoxia and a saturated carbonate solution (Na<sub>2</sub>CO<sub>3</sub>/NaHCO<sub>3</sub>, 1:1) served as the CO<sub>2</sub> source. Both solutions were placed inside the chamber with a 96-well plate filled with the inoculum. Subsequently, the lid was tightly closed (schematic depiction of the setup shown in Figure 3; for a photo of the setup in our laboratory, see Supplementary Materials Figure S2). The box was incubated at 37 °C for six days to ensure transition into LOPs. Thereafter, serial dilutions of compounds were prepared in a new 96 well plate (compound plate) yielding a total volume of 140 µL. After opening the hypoxic chamber, 100 µL of each well of the compound plate was quickly transferred to the hypoxic inoculum plate and the iron wool was replaced with a freshly activated piece. The box was closed again and further incubated at 37 °C for three days. To investigate the activity of metronidazole and niclosamide, incubation was performed for six days in some experiments. Thereafter, the steps described in the section on MBC determination were carried out to determine compound activity.

### 3.6. MBC Determination on Agar

After the incubation of a microtiter plate for the desired time under either aerobic or hypoxic conditions, wells were selected for MBC determination. For a compound that showed activity against *M. abscessus* under aerobic conditions, four to six concentrations were chosen, with the MIC being the lowest of these concentrations. If the assay was performed under hypoxic conditions, the concentrations were selected according to results derived under aerobic conditions to compare results. The selected wells of the assay plate were resuspended using a manual multichannel pipette (~20 cycles) and transferred to row A of a new 96-well plate (PBS dilution plate). Tenfold serial dilutions of each sample were prepared using PBS (Carl Roth) supplemented with 0.025% polysorbate 80. Subsequently, six wells of each column (six dilutions of each sample, 10 µL each) were spot plated in

triplicate on solid medium (see preparation of working stocks) containing 0.4% activated carbon to prevent the possible inhibitory effect of the transferred (active) compound, using a multichannel pipette (Move it®-Eppendorf). The plates were incubated at 37 °C in an atmosphere containing 5% of CO<sub>2</sub>. After the colonies reached a countable size (usually 2–3 days for *M. abscessus*, depending on the impact of hypoxia and the post-antibiotic effects of the investigated compound), pictures of each spot were taken with a digital microscope (Tomlov DM602 Pro 10.1 Inch HDMI, Shenzhen, China). Colonies within one spot were counted using the software DotDotGoose version 1.7.0 [55]. Dilutions with clearly distinguishable colonies closest to 50 were chosen for the calculation of CFU/mL for all samples of interest. The MBC<sub>90</sub> was defined as the lowest compound concentration that exceeded 90% reduction in CFU/mL.

### 3.7. Calculation of Log Change

We calculated the logarithmic change compared to the inoculum according to the following formula:

$$\log \text{ change} = \log_{10} \left( \frac{\text{CFU}}{\text{mL}} (\text{sample}) \right) - \log_{10} \left( \text{mean} \frac{\text{CFU}}{\text{mL}} (\text{drug free control}) \right) \quad (2)$$

The CFU/mL in the drug-free control was determined in aerobic samples on the day when compounds were added to the bacterial culture (inoculum) and in hypoxic samples at the end of hypoxic treatment, to exclude any change in CFU/mL caused by hypoxia alone.

### 3.8. Fluorescent Labeling of *M. abscessus* Cells and Preparation of Samples for Microscopy

The culture of interest (aerobic or hypoxic) was stained in either 96-well plates or in 2 mL screw cap tubes with 100 µM of compound **1** (10 mM in DMSO), manually mixed and subsequently incubated for 2.5 h at 37 °C. When staining was performed in 96-well plates, the stained cultures were afterwards combined in a 2 mL tube. The cultures were pelleted at 6500 rpm for 7 min. The supernatant was replaced with the same volume of a 4% paraformaldehyde (PFA) solution in PBS (Carl Roth) and fixed for 30 min. The sample was washed twice with PBS by pelleting at 6500 rpm for 7 min. After the last washing step, the supernatant was removed as far as possible to reduce background signals of the dye. Then, 50 µL of ethanol (100%) was added and homogenized. Then, 10 µL of the suspension was transferred onto conventional microscope slides drop by drop, allowing the evaporation of ethanol before the next drop was added on the same spot. Then, 10 µL of mounting medium was added on top and covered with square glass coverslips. A negative control was prepared containing unstained aerobic *M. abscessus* cells. The samples were allowed to dry overnight and investigated in a single-blinded study with confocal laser scanning microscopy.

### 3.9. Confocal Laser Scanning Microscopy

Images of *M. abscessus* were acquired using a confocal laser scanning microscope (Nikon A1R) equipped with a 60× oil immersion objective (numerical aperture = 1.4, Plan Apo Lambda, Nikon, Tokyo, Japan). The green fluorescence of compound **1** was excited using the 488 nm laser line of an argon laser (Melles Griot, Rochester, MN, USA) and fluorescence emission was detected in the spectral range of 500–550 nm using a photon multiplier detector unit (Nikon, Tokyo, Japan). Confocal images were acquired at an additional 8× digital zoom. Laser power and detector gain levels were set such that bacterial structures were clearly visible without driving the detector into saturation. The images were processed using NIS-Elements software (Nikon, Tokyo, Japan).

### 3.10. Automated Object Counting Using Fluorescence Microscopy

The procedure was adjusted from a published method [37]. Briefly, bacterial cultures in wells of 96-plates incubated under aerobic or hypoxic conditions were mixed using a manual multichannel pipette, and 2  $\mu$ L of each well was transferred to a plate containing 198  $\mu$ L of fresh liquid medium. These plates were incubated in 37 °C (5% CO<sub>2</sub>) to allow the regrowth of cells. At different points in time, 2  $\mu$ L of compound **1** (10 mM in DMSO) was added to the bacterial suspension to stain the cells and allowed to incubate for another 2.5 h. Thereafter, the wells were homogenized, and 1  $\mu$ L of the suspension was transferred to a black-walled, clear, flat-bottom 96-well plate containing 199  $\mu$ L of filtered 4% PFA solution in PBS for fixation (dilution step due to background noise of the dye). Fluorescence microscopy was then performed using a Thermo Fisher Scientific CellInsight CX5 instrument (Waltham, MA, USA). The samples were analyzed at  $\lambda_{\text{ex}} = 485$  nm and  $\lambda_{\text{em}} = 510\text{--}531$  nm. Then, 21 independent images were acquired per well and analyzed. The valid object count of the GFP filter was matched to the number of bacteria counted. The valid field count was used to check that all fields were in focus under the microscope.

### 3.11. Measuring of CFU Characteristics (Area, Perimeter and Length) on Pictures

Pictures of spots with several colonies were taken with a digital microscope (see Section 3.6) and analyzed using a free copy of Digimizer Version 6.4.3 (MedCalc Software Ltd., Ostend, Belgium). For this, pictures were loaded into the software and processed by binarization. Threshold levels were adjusted to ensure the detection of colonies as objects. The statistical analysis of the obtained values was performed using Graph Pad Prism.

### 3.12. Oxygen Measurement

Oxygen concentration was measured with an optical microsensor (NTH-PSt1 connected to Microx TX3 Presens Precision Sensing GmbH, Regensburg, Germany). The instrument was calibrated immediately before the measurement of the sample following the instructions in the user manual given by the manufacturer. The values are reported as relative percentages of oxygen compared to air-saturated water that has, by definition, an oxygen saturation of 100%. The conversion of values into other units was performed using a calculation software that was provided by the manufacturer of the measurement device, while the recorded temperature was included in the calculation.

## 4. Conclusions

We have here developed a new model to investigate *M. abscessus* under hypoxic conditions in an easy, safe and cost-efficient way. Compound addition in a microtiter plate format after culture transition into LOPs is possible under our model, in contrast to the hypoxic model using microtiter plates, where compounds need to be added before the onset of hypoxia. Our setup includes both a control for reduced oxygen content (MB) and a verification compound (either 100  $\mu$ M metronidazole or 50  $\mu$ M niclosamide) to ensure the transition of the culture into LOPs. The results regarding growth behavior, the morphology of the cells and the phenotypical drug susceptibility of the LOP culture demonstrate that our model leads to the transition of a log-phase culture of *M. abscessus* subsp. *abscessus*, distributed in a 96-well plate, to *M. abscessus* LOPs. Using this model, we have confirmed the well-described phenomenon that hypoxic non-replicating persisters are non-susceptible to a variety of clinically relevant drugs, including important drugs such as amikacin and cefoxitin. Studying drugs in the described LOPs model will help to understand their efficacy in the clinic. Both the Wayne model and ours are not routinely used in the clinic. The Wayne model takes too much time in a therapeutic setting. Our model is characterized



by features that render it amenable to a routine diagnostic setting, such as its easier and faster setup, faster throughput of more samples, and automated evaluation of the assays.

**Supplementary Materials:** The following supporting information can be downloaded at: <https://www.mdpi.com/article/10.3390/antibiotics14030299/s1>, Figure S1: Hypoxic chamber for the investigation on *M. abscessus* LOPs in an anaerobic pot, commonly used in culturing anaerobic bacteria on solid medium; Figure S2: Setup for *M. abscessus* LOP assay in our laboratory, Figure S3: Determined oxygen levels, Figure S4: Representative selection of *M. abscessus* cells pre-treated under two different conditions.

**Author Contributions:** Conceptualization, R.F., A.R. and P.I.; methodology, R.F.; formal analysis, R.F.; investigation, R.F. and R.E.; data curation, R.F. and R.E.; writing—original draft preparation, R.F.; writing—review and editing, A.R., M.L. and P.I.; visualization, R.F.; supervision, A.R. and P.I.; project administration, A.R.; funding acquisition, A.R. All authors have read and agreed to the published version of the manuscript.

**Funding:** This research was funded by Deutsche Forschungsgemeinschaft (DFG, German Research Foundation), grant number 432291016 and by Mukoviszidose gGmbH (Bonn, Germany), the research and development arm of the German Cystic Fibrosis Association Mukoviszidose e. V., project number 2202.

**Institutional Review Board Statement:** Not applicable.

**Informed Consent Statement:** Not applicable.

**Data Availability Statement:** Data will be made available on request.

**Acknowledgments:** We thank Nadine Taudte, Nadine Jänckel and Jens-Ulrich Rahfeld for providing and maintaining the biosafety level 2 facility and Nicole Glaubitz for their helpful suggestions regarding the preparation of the microscopy samples. We thank Shuangjun Lin from Shuanghai Jiao Tong University, Shanghai, China for kindly providing pyridomycin. We thank Courtney Aldrich from the University of Minnesota, Minneapolis, USA for his helpful feedback during manuscript preparation, and Rüdiger W. Seidel for proofreading the manuscript.

**Conflicts of Interest:** The authors declare that they have no conflicts of interest. The funders had no role in the design of the study; in the collection, analyses, or interpretation of data; in the writing of the manuscript; or in the decision to publish the results.

## Abbreviations

The following abbreviations are used in this manuscript:

LOP	Low-oxygen persister
MB	Methylene blue
MBC	Minimum bactericidal concentration
MIC	Minimum inhibitory concentration
NRP	Non-replicating persister
OD	Optical density

## References

1. Johansen, M.D.; Herrmann, J.L.; Kremer, L. Non-tuberculous mycobacteria and the rise of *Mycobacterium abscessus*. *Nat. Rev. Microbiol.* **2020**, *18*, 392–407. [[CrossRef](#)] [[PubMed](#)]
2. Dartois, V.; Dick, T. Therapeutic developments for tuberculosis and nontuberculous mycobacterial lung disease. *Nat. Rev. Drug Discov.* **2024**, *23*, 381–403. [[CrossRef](#)]
3. Pasipanodya, J.G.; Ogbonna, D.; Ferro, B.E.; Magombedze, G.; Srivastava, S.; Deshpande, D.; Gumbo, T. Systematic Review and Meta-analyses of the Effect of Chemotherapy on Pulmonary *Mycobacterium abscessus* Outcomes and Disease Recurrence. *Antimicrob. Agents Chemother.* **2017**, *61*, e01206-17. [[CrossRef](#)] [[PubMed](#)]
4. Boudehen, Y.M.; Kremer, L. *Mycobacterium abscessus*. *Trends Microbiol.* **2021**, *29*, 951–952. [[CrossRef](#)]
5. Griffith, D.E.; Daley, C.L. Treatment of *Mycobacterium abscessus* Pulmonary Disease. *Chest* **2022**, *161*, 64–75. [[CrossRef](#)]

6. Ganapathy, U.S.; Dick, T. Why Matter Matters: Fast-Tracking *Mycobacterium abscessus* Drug Discovery. *Molecules* **2022**, *27*, 6948. [\[CrossRef\]](#) [\[PubMed\]](#)
7. Datta, M.; Via, L.E.; Kamoun, W.S.; Liu, C.; Chen, W.; Seano, G.; Weiner, D.M.; Schimel, D.; England, K.; Martin, J.D.; et al. Anti-vascular endothelial growth factor treatment normalizes tuberculosis granuloma vasculature and improves small molecule delivery. *Proc. Natl. Acad. Sci. USA* **2015**, *112*, 1827–1832. [\[CrossRef\]](#) [\[PubMed\]](#)
8. Via, L.E.; Lin, P.L.; Ray, S.M.; Carrillo, J.; Allen, S.S.; Eum, S.Y.; Taylor, K.; Klein, E.; Manjunatha, U.; Gonzales, J.; et al. Tuberculous granulomas are hypoxic in guinea pigs, rabbits, and nonhuman primates. *Infect. Immun.* **2008**, *76*, 2333–2340. [\[CrossRef\]](#)
9. Worlitzsch, D.; Tarran, R.; Ulrich, M.; Schwab, U.; Cekici, A.; Meyer, K.C.; Birrer, P.; Bellon, G.; Berger, J.; Weiss, T.; et al. Effects of reduced mucus oxygen concentration in airway *Pseudomonas* infections of cystic fibrosis patients. *J. Clin. Investig.* **2002**, *109*, 317–325.
10. Yam, Y.K.; Alvarez, N.; Go, M.L.; Dick, T. Extreme Drug Tolerance of *Mycobacterium abscessus* “Persisters”. *Front. Microbiol.* **2020**, *11*, 359. [\[CrossRef\]](#)
11. Early, J.V.; Mullen, S.; Parish, T. A rapid, low pH, nutrient stress, assay to determine the bactericidal activity of compounds against non-replicating *Mycobacterium tuberculosis*. *PLoS ONE* **2019**, *14*, e0222970. [\[CrossRef\]](#)
12. Gold, B.; Warriar, T.; Nathan, C. A multi-stress model for high throughput screening against non-replicating *Mycobacterium tuberculosis*. *Methods Mol. Biol.* **2015**, *1285*, 293–315.
13. Loebel, R.O.; Shorr, E.; Richardson, H.B. The Influence of Foodstuffs upon the Respiratory Metabolism and Growth of Human Tubercle Bacilli. *J. Bacteriol.* **1933**, *26*, 139–166. [\[CrossRef\]](#)
14. Martins, O.; Lee, J.; Kaushik, A.; Ammerman, N.C.; Dooley, K.E.; Nuermberger, E.L. In Vitro Activity of Bedaquiline and Imipenem against Actively Growing, Nutrient-Starved, and Intracellular *Mycobacterium abscessus*. *Antimicrob. Agents Chemother.* **2021**, *65*, e0154521. [\[CrossRef\]](#)
15. Berube, B.J.; Castro, L.; Russell, D.; Ovechkina, Y.; Parish, T. Novel Screen to Assess Bactericidal Activity of Compounds Against Non-replicating *Mycobacterium abscessus*. *Front. Microbiol.* **2018**, *9*, 2417. [\[CrossRef\]](#)
16. Voskuil, M.I.; Schnappinger, D.; Visconti, K.C.; Harrell, M.I.; Dolganov, G.M.; Sherman, D.R.; Schoolnik, G.K. Inhibition of respiration by nitric oxide induces a *Mycobacterium tuberculosis* dormancy program. *J. Exp. Med.* **2003**, *198*, 705–713. [\[CrossRef\]](#)
17. Mulyukin, A.L.; Recchia, D.; Kostrikina, N.A.; Artyukhina, M.V.; Martini, B.A.; Stamilla, A.; Degiacomi, G.; Salina, E.G. Distinct Effects of Moxifloxacin and Bedaquiline on Growing and ‘Non-Culturable’ *Mycobacterium abscessus*. *Microorganisms* **2023**, *11*, 2690. [\[CrossRef\]](#)
18. Salina, E.G.; Waddell, S.J.; Hoffmann, N.; Rosenkrands, I.; Butcher, P.D.; Kaprelyants, A.S. Potassium availability triggers *Mycobacterium tuberculosis* transition to, and resuscitation from, non-culturable (dormant) states. *Open Biol.* **2014**, *4*, 140106. [\[CrossRef\]](#)
19. Wayne, L.G.; Hayes, L.G. An in vitro model for sequential study of shutdown of *Mycobacterium tuberculosis* through two stages of nonreplicating persistence. *Infect. Immun.* **1996**, *64*, 2062–2069. [\[CrossRef\]](#) [\[PubMed\]](#)
20. Cho, S.H.; Warit, S.; Wan, B.; Hwang, C.H.; Pauli, G.F.; Franzblau, S.G. Low-oxygen-recovery assay for high-throughput screening of compounds against nonreplicating *Mycobacterium tuberculosis*. *Antimicrob. Agents Chemother.* **2007**, *51*, 1380–1385. [\[CrossRef\]](#) [\[PubMed\]](#)
21. Belardinelli, J.M.; Verma, D.; Li, W.; Avanzi, C.; Wiersma, C.J.; Williams, J.T.; Johnson, B.K.; Zimmerman, M.; Whittel, N.; Angala, B.; et al. Therapeutic efficacy of antimalarial drugs targeting DosRS signaling in *Mycobacterium abscessus*. *Sci. Transl. Med.* **2022**, *14*, eabj3860. [\[CrossRef\]](#)
22. Lanni, A.; Borroni, E.; Iacobino, A.; Russo, C.; Gentile, L.; Fattorini, L.; Giannoni, F. Activity of Drug Combinations against *Mycobacterium abscessus* Grown in Aerobic and Hypoxic Conditions. *Microorganisms* **2022**, *10*, 1421. [\[CrossRef\]](#)
23. Simcox, B.S.; Tomlinson, B.R.; Shaw, L.N.; Rohde, K.H. *Mycobacterium abscessus* DosRS two-component system controls a species-specific regulon required for adaptation to hypoxia. *Front. Cell Infect. Microbiol.* **2023**, *13*, 1144210. [\[CrossRef\]](#)
24. Batyrshina, Y.R.; Schwartz, Y.S. Modeling of *Mycobacterium tuberculosis* dormancy in bacterial cultures. *Tuberculosis* **2019**, *117*, 7–17. [\[CrossRef\]](#)
25. Parker, C.A. Anaerobiosis with iron wool. *Aust. J. Exp. Biol. Med. Sci.* **1955**, *33*, 33–37. [\[CrossRef\]](#)
26. Wayne, L.G.; Lin, K.Y. Glyoxylate metabolism and adaptation of *Mycobacterium tuberculosis* to survival under anaerobic conditions. *Infect. Immun.* **1982**, *37*, 1042–1049. [\[CrossRef\]](#)
27. Richter, A.; Strauch, A.; Chao, J.; Ko, M.; Av-Gay, Y. Screening of Preselected Libraries Targeting *Mycobacterium abscessus* for Drug Discovery. *Antimicrob. Agents Chemother.* **2018**, *62*, e00828-18. [\[CrossRef\]](#)
28. Mukherjee, T.; Boshoff, H.; Barry, C.E., 3rd. Comment on: Identification of antimicrobial activity among FDA-approved drugs for combating *Mycobacterium abscessus* and *Mycobacterium chelonae*. *J. Antimicrob. Chemother.* **2012**, *67*, 252–253. [\[CrossRef\]](#)
29. Yang, J.J.; Goff, A.; Wild, D.J.; Ding, Y.; Annis, A.; Kerber, R.; Foote, B.; Passi, A.; Duerksen, J.L.; London, S.; et al. Computational drug repositioning identifies niclosamide and tribromsalan as inhibitors of *Mycobacterium tuberculosis* and *Mycobacterium abscessus*. *Tuberculosis* **2024**, *146*, 102500. [\[CrossRef\]](#)

30. Burock, S.; Daum, S.; Tröger, H.; Kim, T.D.; Krüger, S.; Rieke, D.T.; Ochsenreither, S.; Welter, K.; Herrmann; Slegers, A. Niclosamide a new chemotherapy agent? Pharmacokinetics of the potential anticancer drug in a patient cohort of the NIKOLO trial. *J. Clin. Oncol.* **2018**, *36*, e14536.
31. Khan, A.; Sarkar, D. A simple whole cell based high throughput screening protocol using *Mycobacterium bovis* BCG for inhibitors against dormant and active tubercle bacilli. *J. Microbiol. Methods* **2008**, *73*, 62–68. [\[CrossRef\]](#)
32. Franzblau, S.G.; DeGroot, M.A.; Cho, S.H.; Andries, K.; Nuermberger, E.; Orme, I.M.; Mdluli, K.; Angulo-Barturen, I.; Dick, T.; Dartois, V.; et al. Comprehensive analysis of methods used for the evaluation of compounds against *Mycobacterium tuberculosis*. *Tuberculosis* **2012**, *92*, 453–488. [\[CrossRef\]](#)
33. Ayrapetyan, M.; Williams, T.; Oliver, J.D. Relationship between the Viable but Nonculturable State and Antibiotic Persister Cells. *J. Bacteriol.* **2018**, *200*, e00249–18. [\[CrossRef\]](#)
34. Voskuil, M.I.; Visconti, K.C.; Schoolnik, G.K. *Mycobacterium tuberculosis* gene expression during adaptation to stationary phase and low-oxygen dormancy. *Tuberculosis* **2004**, *84*, 218–227. [\[CrossRef\]](#)
35. Van, N.; Degefu, Y.N.; Leus, P.A.; Larkins-Ford, J.; Klickstein, J.; Maurer, F.P.; Stone, D.; Poonawala, H.; Thorpe, C.M.; Smith, T.C.; et al. Novel Synergies and Isolate Specificities in the Drug Interaction Landscape of *Mycobacterium abscessus*. *Antimicrob. Agents Chemother.* **2023**, *67*, e0009023. [\[CrossRef\]](#)
36. North, R.J.; Izzo, A.A. *Mycobacterial virulence*. Virulent strains of *Mycobacteria tuberculosis* have faster in vivo doubling times and are better equipped to resist growth-inhibiting functions of macrophages in the presence and absence of specific immunity. *J. Exp. Med.* **1993**, *177*, 1723–1733.
37. Mann, L.; Siersleben, F.; Lang, M.; Richter, A. Determination of bactericidal activity against 3HC-2-Tre-labelled *Mycobacterium abscessus* (*Mycobacteroides abscessus*) by automated fluorescence microscopy. *J. Microbiol. Methods* **2024**, *224*, 107002. [\[CrossRef\]](#)
38. Richter, A.; Goddard, R.; Mann, L.; Siersleben, F.; Seidel, R.W. Structural characterization of a 3-hydroxychromone dye trehalose conjugate for fluorescent labelling of mycobacteria. *J. Mol. Struct.* **2024**, *1298*, 137010. [\[CrossRef\]](#)
39. Du, P.; Sohaskey, C.D.; Shi, L. Transcriptional and Physiological Changes during *Mycobacterium tuberculosis* Reactivation from Non-replicating Persistence. *Front. Microbiol.* **2016**, *7*, 1346. [\[CrossRef\]](#)
40. Sarathy, J.P.; Via, L.E.; Weiner, D.; Blanc, L.; Boshoff, H.; Eugenin, E.A.; Barry, C.E., 3rd; Dartois, V.A. Extreme Drug Tolerance of *Mycobacterium tuberculosis* in Caseum. *Antimicrob. Agents Chemother.* **2018**, *62*, e02266–17. [\[PubMed\]](#)
41. Wallis, R.S.; Patil, S.; Cheon, S.H.; Edmonds, K.; Phillips, M.; Perkins, M.D.; Joloba, M.; Namale, A.; Johnson, J.L.; Teixeira, L.; et al. Drug tolerance in *Mycobacterium tuberculosis*. *Antimicrob. Agents Chemother.* **1999**, *43*, 2600–2606. [\[CrossRef\]](#)
42. Xie, Z.; Siddiqi, N.; Rubin, E.J. Differential antibiotic susceptibilities of starved *Mycobacterium tuberculosis* isolates. *Antimicrob. Agents Chemother.* **2005**, *49*, 4778–4780. [\[CrossRef\]](#)
43. Holt, M.R.; Baird, T. Treatment Approaches to *Mycobacterium abscessus* Pulmonary Disease. *Clin. Chest Med.* **2023**, *44*, 785–798. [\[CrossRef\]](#)
44. Hartkoorn, R.C.; Sala, C.; Neres, J.; Pojer, F.; Magnet, S.; Mukherjee, R.; Uplekar, S.; Boy-Rottger, S.; Altmann, K.H.; Cole, S.T. Towards a new tuberculosis drug: Pyridomycin–nature’s isoniazid. *EMBO Mol. Med.* **2012**, *4*, 1032–1042. [\[CrossRef\]](#)
45. Seidel, R.W.; Goddard, R.; Lang, M.; Richter, A. Nalpha-Aroyl-N-Aryl-Phenylalanine Amides: A Promising Class of Antimycobacterial Agents Targeting the RNA Polymerase. *Chem. Biodivers.* **2024**, *21*, e202400267. [\[CrossRef\]](#)
46. Lang, M.; Ganapathy, U.S.; Mann, L.; Abdelaziz, R.; Seidel, R.W.; Goddard, R.; Sequenzia, I.; Hoenke, S.; Schulze, P.; Aragaw, W.W.; et al. Synthesis and Characterization of Phenylalanine Amides Active against *Mycobacterium abscessus* and Other *Mycobacteria*. *J. Med. Chem.* **2023**, *66*, 5079–5098. [\[CrossRef\]](#)
47. Beuchel, A.; Robaa, D.; Negatu, D.A.; Madani, A.; Alvarez, N.; Zimmerman, M.D.; Richter, A.; Mann, L.; Hoenke, S.; Csuk, R.; et al. Structure-Activity Relationship of Anti-*Mycobacterium abscessus* Piperidine-4-carboxamides, a New Class of NBTI DNA Gyrase Inhibitors. *ACS Med. Chem. Lett.* **2022**, *13*, 417–427. [\[CrossRef\]](#)
48. Miranda-CasoLuengo, A.A.; Staunton, P.M.; Dinan, A.M.; Lohan, A.J.; Loftus, B.J. Functional characterization of the *Mycobacterium abscessus* genome coupled with condition specific transcriptomics reveals conserved molecular strategies for host adaptation and persistence. *BMC Genom.* **2016**, *17*, 553. [\[CrossRef\]](#)
49. Jakkala, K.; Ajitkumar, P. Hypoxic Non-replicating Persistent *Mycobacterium tuberculosis* Develops Thickened Outer Layer That Helps in Restricting Rifampicin Entry. *Front. Microbiol.* **2019**, *10*, 2339. [\[CrossRef\]](#)
50. Lin, W.; Mandal, S.; Degen, D.; Liu, Y.; Ebright, Y.W.; Li, S.; Feng, Y.; Zhang, Y.; Mandal, S.; Jiang, Y.; et al. Structural Basis of *Mycobacterium tuberculosis* Transcription and Transcription Inhibition. *Mol. Cell* **2017**, *66*, 169–179.e8. [\[CrossRef\]](#)
51. Greendyke, R.; Byrd, T.F. Differential antibiotic susceptibility of *Mycobacterium abscessus* variants in biofilms and macrophages compared to that of planktonic bacteria. *Antimicrob. Agents Chemother.* **2008**, *52*, 2019–2026. [\[CrossRef\]](#) [\[PubMed\]](#)
52. Xie, M.; Ganapathy, U.S.; Lan, T.; Osiecki, S.; Sarathy, J.P.; Dartois, V.; Aldrich, C.C.; Dick, T. ADP-ribosylation-resistant rifabutin analogs show improved bactericidal activity against drug-tolerant *M. abscessus* in caseum surrogate. *Antimicrob. Agents Chemother.* **2023**, *67*, e0038123. [\[CrossRef\]](#) [\[PubMed\]](#)

53. Kolpen, M.; Jensen, P.Ø.; Qvist, T.; Kragh, K.N.; Ravnholt, C.; Fritz, B.G.; Johansen, U.R.; Bjarnsholt, T.; Høiby, N. Biofilms of *Mycobacterium abscessus* complex can be sensitized to antibiotics by disaggregation and oxygenation. *Antimicrob. Agents Chemother.* **2020**, *64*, e01212-19. [[CrossRef](#)] [[PubMed](#)]
54. Richter, A.; Goddard, R.; Siersleben, F.; Mann, L.; Seidel, R.W. Structural Elucidation of 2-(6-(Diethylamino) benzofuran-2-yl)-3-hydroxy-4 H-chromen-4-one and Labelling of Mycobacterium aurum Cells. *Molbank* **2023**, *2023*, M1647. [[CrossRef](#)]
55. Ersts, P.J. DotDotGoose (1.7.0). American Museum of Natural History, Center for Biodiversity and Conservation. Available online: [https://biodiversityinformatics.amnh.org/open\\_source/dotdotgoose/](https://biodiversityinformatics.amnh.org/open_source/dotdotgoose/) (accessed on 1 September 2023).

**Disclaimer/Publisher’s Note:** The statements, opinions and data contained in all publications are solely those of the individual author(s) and contributor(s) and not of MDPI and/or the editor(s). MDPI and/or the editor(s) disclaim responsibility for any injury to people or property resulting from any ideas, methods, instructions or products referred to in the content.

## 3) Results and Discussion

### 3.1) General Aspects

This section summarizes the key findings of the thesis presented in **publications I-IV** and discusses the results generated across the different publications. Some results of this thesis were not included in **publications I-IV** but are nevertheless reported and discussed within this section. This is to present the results of the respective projects in full detail allowing a conclusion on all facts and make information easily accessible for future work. However, unpublished results are clearly indicated and experimental procedures are found in the appendix of this thesis. This chapter also discusses open questions and presents suggestions and ideas on how to apply the microbiological method that resulted from this thesis.

### 3.2) Synthesis and Chemical Characterization of Phytochemical Analogs

The stereoselective total synthesis of **KP** was described by BRINGMANN *et al.* who reported the successful use of the 'lactone-method' as a synthetical tool to obtain 1,8 dihydroxy-anthraquinones [139]. Within this project, we set out to investigate if a direct phenyl-phenyl coupling using SUZUKI'S method would work instead. The retrosynthetic scheme of the approach is displayed in Figure 15. The commercial availability of a large variety of phenylboronic acids and of danthron (1,8 dihydroxyanthraquinone) were strong arguments for this synthetic approach.

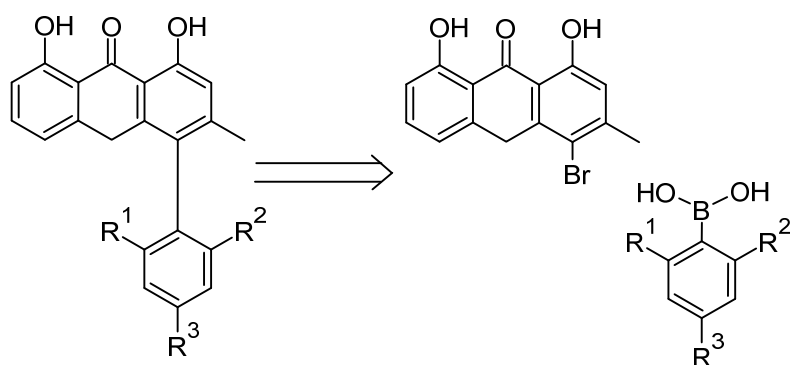


Figure 15: Retrosynthetic idea to access 1,8 dihydroxyanthrones. Derivatives of phenylboronic acid should be coupled with brominated anthrones or anthraquinones by a Pd-catalyzed SUZUKI-MIYAUURA reaction.

The supervision of this synthetic project to elucidate another synthetic route to derivatives of knipholone anthrone was part of this thesis. These synthetic studies were undertaken by diploma student SIMONE WAPPLER. Compound **AC1** was later synthesized by a technical assistant in the lab. The results of this study are only briefly summarized here. Of

the five compounds successfully obtained (chemical structures see Figure 16), anthralin (anthrone **1** (**AN1**)) was found to act as a LR agent and therefore characterized in more detail regarding its biological activity. The results were included in **publication III** and the activity profile will be discussed in section 3.6.3), while this section solely discusses the synthetic aspects.

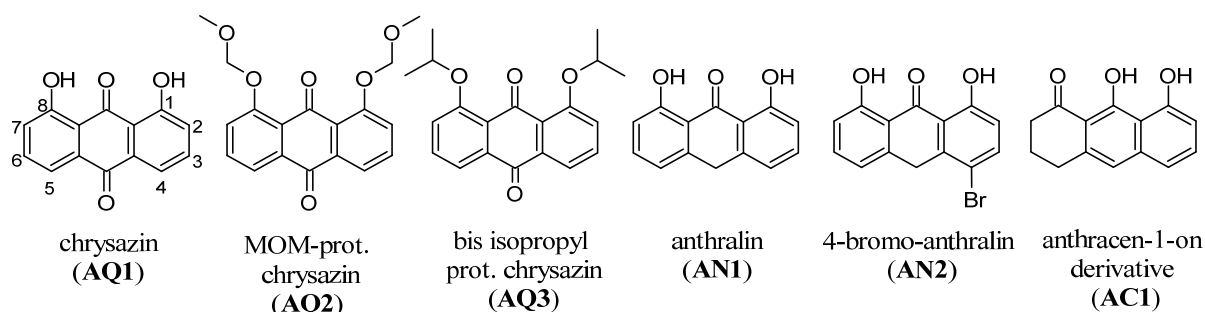


Figure 16: Synthesized anthrones and anthraquinones.

The labeling of carbon atoms according to anthraquinone is exemplarily displayed for compound **AQ1**. The compound labeling refers to their respective core structure: AQ anthraquinone, AN anthrone, AC anthracenone.

Starting from commercially available chrysazin (anthraquinone **1** (**AQ1**)), reduction and subsequent monobromination yielded **AN1** and 4-bromoanthralin (**AN2**) respectively. In a preliminary experiment 4-bromophenol and phenyl boronic acid were successfully coupled using a microwave. However, the coupling of **AN2** with phenylboronic acid using different palladium catalysts was not successful. Instead, debrominated and oxidized products of **AN2**, namely **AN1** and **AQ1**, were detected in the reaction mixture. Literature studies described the ability of **AN1** and **KA** to chelate divalent metal ions [30, 140]. We therefore assumed the failed coupling due to a chelation of the catalyst. In addition, WAPPLER observed the fairly easy oxidation of the C-10 position of **AN2** under basic conditions by APCI MS and by TLC. To circumvent these two problems different protecting groups were introduced at the hydroxyl groups and the sequence of carbonyl reduction at C-10 and coupling with phenyl boronic acid was reversed. However, an analog coupled to a phenyl moiety in position 4 could not be obtained by any of the approaches.

Our synthetical studies thus revealed the direct synthesis route using SUZUKI coupling unfeasible for the synthesis of 1,8 dihydroxy-4-phenyl anthrones. However, the study emerged the compounds displayed in Figure 16 in acceptable purity to be tested with regard to their HIV-LR and/or their antimycobacterial activity. These results will be described and discussed in the section on the biological activity (from page 104 on, section 3.6).

### 3.3) Isolation and Characterization of Secondary Metabolites from Plants

Within this project I extracted a major secondary plant metabolite from the roots of *K. foliosa*. The obtained yield of **KA** from the roots was 0.62 %. **KA** was characterized by NMR,

APCI-MS, circular dichroism-spectra, HPLC and by conversion into **KP** that was compared with a reference sample provided by PROF. ERMIA S DAGNE from Addis Ababa University. The data was in line with existing literature and revealed **KA** to be suitable for biological assessment and stability studies (see **publication II** and **III**). This part of the project was the foundation of various subsequent studies on these compounds because they were not easily accessible by chemical synthesis (as explained in section 3.2).

### 3.4) Characterization and Standardization of Plant Extracts

To investigate anti-infective agents from *C. sinensis* different aqueous extracts were prepared from which various lyophilizates were obtained. The **EGCG** content in all samples was analyzed. The raw data were obtained by VOLKER BÄR, a former diploma student in the working group. As expected, green tea extracts were proven to contain more **EGCG** than black tea extracts (see **publication I**), most probably due to the absence of the oxidation step. For the investigation of antibacterial activity, the lyophilizates were dissolved in water and standardized for **EGCG**, the main active component. In contrast to the use of undefined tea extracts, often found in literature studies, this enabled the direct comparison of disinfecting activity of black and green tea. It also revealed information on the activity of other secondary plant metabolites as a whole against *S. aureus* in addition to the main catechin **EGCG**.

### 3.5) Stability Studies on Phytochemicals

A screen of the p-ANAPL [141] by our cooperation partners at the University of Botswana in Gaborone and the Simon Fraser University in Burnaby, Canada revealed **KA** as a new potential HIV LR agent. But batch to batch variations hampered data analysis. We therefore set out to investigate the stability of freshly isolated compound to understand the source of these high variations. The stability study in culture medium was done by myself with some help of DR. FRANK ERDMANN from our institute. The second stability study in different solvents was undertaken by Master student GEORGETTE ARNOUK under my supervision. Our studies on the isolated compounds and our observations on compounds derived from synthetical approach to this compound class revealed the anthrones as instable molecules that were easily oxidized leading to the respective anthraquinone **KP** and other products. This process was followed over time in different solvents including different cell culture media (see **publication II**). We used this knowledge in subsequent biological studies, although we did not study the detailed metabolic profile of the compounds within the respective culture media. The results highlighted the importance of early stability studies during biological characterization of compounds isolated from plants. Because this effect was not paid attention to by earlier investigations it is unclear to which molecule(s) the observed activity should be attributed. Therefore, the literature results need to be interpreted with caution. The stability data also highlight **KA** and its analogs unsuitable as drug

candidates in their present form. Without more stable analogs it will be hard to go on with even basic research.

### 3.6) Biological Activity Studies

This thesis includes a variety of biological studies that were partly undertaken by cooperation partners, partly by myself. Studies on *M. tuberculosis* were carried out at the Lung Research Center in Borstel in biosafety level 3 facilities. Antimicrobial activity was determined on a variety of several microbes at the Hans-Knöll-Institute in Jena. The data were not included in any publication due to complete absence of activity, but are reported within this thesis for the sake of completeness. Antiplasmodial activity was determined by a PhD student at Justus-Liebig University in Gießen. Anthelmintic activity studies and antibacterial studies on *Aliivibrio fischeri* were undertaken at the Leibniz Institute of Plant Biochemistry. Activity tests on HIV and HIV LR were carried out at Simon-Fraser-University in Burnaby, Canada and at the University of Botswana in Gaborone. The diploma student VOLKER BÄR generated the raw data on MRSA during his stay at the university hospital in Heidelberg. All experiments on *M. abscessus* were carried out by myself in the biosafety level 2 facility at the IZI Fraunhofer Institute, Halle.

#### 3.6.1) Antiplasmodial Activity

As explained in the introductory chapter, the antiplasmodial activity of **phenyl-anthraquinones** has been reported in the literature at the time of this project. Our investigations confirmed the reported activity against the asexual blood stage of the parasite (see **publication II**). The value of our study is the attention that was paid to the stability of the molecules during investigation by comparing pre-incubated **KA** with freshly added **KA**. This investigation suggested degradation products of **KA**, other than the oxidative metabolite **KP**, to be more active than **KA** itself (see **publication II**, table 1). Since dimeric phenyl-anthraquinones, e.g. joziknipholone A, have been reported to have a higher antiplasmodial activity than **KP** and **KA** [23, 28], the formation of such compounds within the assay medium could be an explanation for the higher activity compared to **KA** and **KP**. We did, however, focus on the degradation of the parent compound (**KA**) and the formation of the oxidation product (**KP**) in our stability study and refrained from the identification of other molecules in the mixture (see **publication II** and section 3.5).

Several inhibitory effects of **EGCG and other catechins** against *Plasmodium* strains were reported *in vitro* (as mentioned in the introduction). However, due to the low bioavailability of **EGCG** and other catechins [44] and the opposite *in vivo* activity reported by THIPUBON in 2015 [38], we did not investigate the antiplasmodial activity of the standardized tea extracts.



### 3.6.2) Antimycobacterial Activity of Natural Products

**Catechin EGCG and Tea Extracts.** Lyophilizates of green and black tea extracts standardized for their EGCG content were investigated alongside with **EGCG** for their activity against *M. abscessus* under aerobic and hypoxic conditions using the methods described in **publication IV** and found to be inactive under both conditions. They did not lead to any growth inhibition in aerobic broth dilution assays and also did not reduce the amount of colony forming units under hypoxic conditions in the LOP assay up to a concentration of 430  $\mu\text{M}$  **EGCG**. Due to its inactivity, the data was not included in any of the publications but is mentioned within this thesis for the sake of completeness. This finding is disappointing but it might be explained by the proposed mechanism of action (reviewed in [36]) by which catechins inhibit the growth of *S. aureus*. Those include the direct binding of penicillin-binding protein 2A and membrane disruption. These targets are less easily accessible due to the waxy coating of the mycobacterial membrane, a possible reason for lower susceptibility of mycobacteria to these compounds. Another reason might be potential structural differences in the target between the different bacteria.

**1,8-Dihydroxyanthrones and Respective Anthraquinones. KA and KP** as well as the structurally related compounds **AQ1** and **AN1** were tested for their antitubercular activity against a GFP-bearing H37Rv *M. tuberculosis* strain using the methods described in **publication II**. Due to the restriction of **publication II** to secondary plant metabolites of *K. foliosa*, only results for **KA** and **KP** were included in this publication. Although we observed a slight inhibitory effect (**AQ1** and **AN1** 60 % growth inhibition, **KA** and **KP** 75 % inhibition), none of the four compounds tested achieved a growth inhibition of 90 % at 10  $\mu\text{g/mL}$  (see section “Anthelmintic and Antibacterial Activity” in **publication II**). Consistent with this was the lack of activity against *M. smegmatis* in an agar diffusion test at 10  $\mu\text{g/mL}$  which corresponds to 24  $\mu\text{M}$  (**KA**) and 23  $\mu\text{M}$  (**KP**) (unpublished results, methodology see page XVIII, section 6.1.2). Due to its generally lower susceptibility, we did not additionally investigate **KA** and **KP** for their growth inhibition in *M. abscessus*.

**Pyridomycin.** We included the natural product pyridomycin, a cyclic depsipeptide, in our study because it was reported to be bactericidal to *M. tuberculosis* and to inhibit growth of *M. abscessus* in a broth dilution assay [142]. We confirmed this finding for *M. abscessus* and additionally showed that it is bactericidal against aerobe *M. abscessus* - However, only at a concentration of 100  $\mu\text{M}$  (see **publication IV**, figure 11). This again confirmed the generally lower susceptibility of *M. abscessus* compared to *M. tuberculosis* towards antimycobacterial compounds. Because 100  $\mu\text{M}$  is too high to consider pyridomycin as an interesting bactericidal compound against *M. abscessus* [143], this result may not be clinically important but contributes to the knowledge of the compound in general. As expected, due to its mechanism of action the bactericidal activity was absent under hypoxic conditions, further confirming the existence of the LOP culture in the newly developed model (as discussed in **publication IV** and section 3.8.2.3).

The development of a **new antimycobacterial assay** setup and its validation using a variety of known compounds is described in detail in **publication IV** and will be discussed in section 3.8). This new tool can be used to determine the antimycobacterial activity of plant extracts (as was successfully done for the tea extracts as mentioned above) and isolated compounds under hypoxic conditions in any research setting to help studying plants in close proximity to their habitats.

### 3.6.3) Latency Reversal Activity

**KA** and **KP** were tested together with the synthetic analogs **AQ1**, **AQ2**, **AQ3**, **AN1**, **AN2** and **AC1** (for their chemical structures see Figure 16 in section 3.2) for their LR activity in J-lat 9.2 cells using the method described in **publication III**. Only active compounds were included in the publication. To complete information on this compound class, all results are combined in Figure 17.

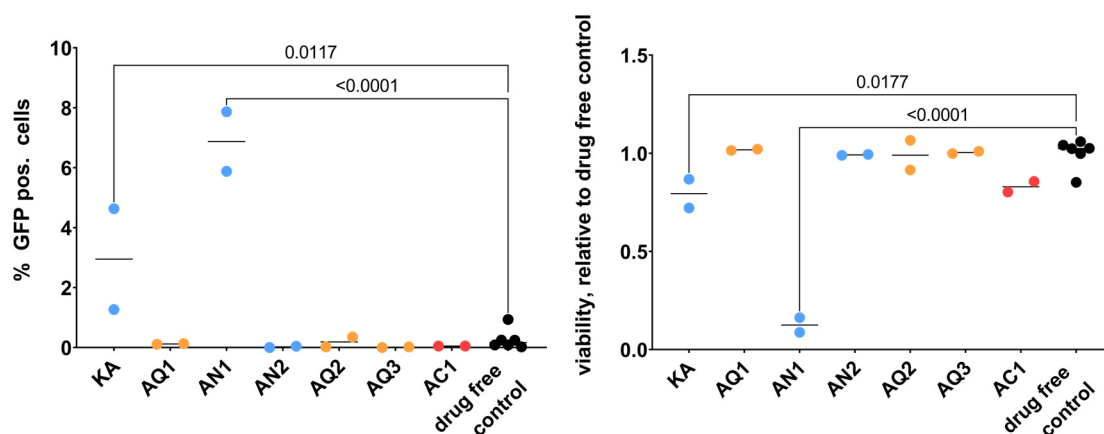


Figure 17: Effects of 1,8 dihydroxyanthrones and analogs on J-lat 9.2 cells.

**Left side:** HIV latency reversal activity, displayed as relative amount of GFP positive J-lat 9.2 cells. **Right side:** viability of J-lat 9.2 cells relative to drug free control. Data reported as mean of two technical replicates and as individual data points. The colors refer to the chemical core structure of the respective molecules: *blue* anthrones, *orange* anthraquinones and *red* anthracenon. The drug free control is shown in black. *p* values obtained by one-way ANOVA test are only reported for data with significant difference ( $p < 0.05$ ) to drug free control.

All anthraquinones (**KP**, **AQ1**, **AQ2**, **AQ3**) in addition to the anthracenone derivative **AC1** were unable to reactivate viral replication. In contrast, two of the three anthrones (**KA** and **AN1**) reversed HIV latency *in vitro* in a dose dependent manner (for details see **publication III**). Interestingly, the anthrone analog **AN2**, which is the 4-brominated analog of **AN1**, did not reverse HIV latency. Too few analogs were available (as explained in section 3.2) to define SAR. Two possible reasons for that observation will be explained, emphasizing the hypothetical character of both. If this compound class should be followed further, these hypotheses should be investigated in future studies to either confirm or reject them. The first hypothesis assumes a target specific LR activity of anthrones. Up to date no target for 1,8 dihydroxyanthrones was identified. However, RICHARD demonstrated in his thesis that **KA**

does not act through common targets of LR agents such as the histone deacetylase or protein kinase C (see **publication III** and [59]). The general activity of the anthrone motif is based on the fact that both, **KA** and **AN1**, showed comparable activity (6-6.9 % reactivated cells) in this assay and a third anthrone, prinoidin, was roughly half as active (2.8 % reactivated cells at a similar concentration) [59]. Then, the absence of **AN2**'s activity could be attributed to a lack of binding to the [still unknown] target. This could be due to steric hinderance by the bulky bromine or the negative inductive effect of this substituent, changing the electron density of the anthrone core and preventing binding. Inactivity due to impermeability is another possible explanation.

The second hypothesis assumes an unspecific mechanism of action for the investigated compounds. The described prooxidant activity of **KA** [144] could for example induce oxidative stress that reverses HIV latency in an unspecific manner. The bromine substituent would reduce this ability.

### 3.6.4) *Anti-HIV Activity*

Anti-HIV activity was determined *ex vivo* in mock infected PBMCs by measuring p24 antigen production as explained in **publication II**. While **KP** was inactive, **KA** inhibited HIV in a concentration dependent manner (see figure 3 in **publication II**). The relative EC<sub>50</sub> value was observed at 4.3 µM. The cytotoxic effect on PBMCs is described in the section on cytotoxicity (see 3.6.6).

### 3.6.5) *Activity Against S. aureus*

Our studies on **tea extracts** were in accordance with the literature: Catechins and tea extracts inhibit MRSA growth and also markedly reduce CFUs within four hours (see **publication I**, figure 1 and 3). Although some of the results were not new, the large collection of clinical isolates that was accessible at the university hospital in Heidelberg enabled the investigation on clinically relevant strains in comparison to the determination on lab strains only. Although **EGCG** was described in the literature as the most active substance of the tea extracts, our results justify the use of the extracts instead of the pure substance due to their higher activity (see figure 1, **publication I**). Using the whole extract instead of a purified constituent further simplifies the procedure and makes this treatment more accessible for the patient himself. This again will help to empower patients to support the approved therapy by applying tea extracts in addition to prescribed medication. However, in the light of the clinical outcome of decubitus, infected with MRSA and topically treated with green tea [41], our study should also encourage clinicians to use tea extracts in the treatment of MRSA infections in addition to antibiotic therapy where appropriate. This is also in line with the well described synergistic effect of catechins with different antibiotics [36], even though we did not include any drug combination assays in our study. The poor bioavailability of catechins, as described in the introduction, restricts their use to applications that ensure high concentrations of catechins at the site of infections. This can be topical treatments (skin or

mucosa) or in case of lung infections the inhalation of tea extracts. Due to the ubiquitous consumption of tea, these extracts are easily accessible and could thus make a valuable contribution against the development of resistance also in SSA countries.

**KA** and **KP** were tested for their activity against *S. aureus* (methicillin susceptible (MSSA) and MRSA strains) in an anti-microbial screen at HKI Jena by agar diffusion test (for the methodology see page XVIII in section 6.1.2). Both compounds did not inhibit the growth at a concentration of 10 µg/mL, which corresponds to 24 and 23 µM respectively.

### 3.6.6) Cytotoxicity Studies

Cytotoxicity studies on **tea extracts** and catechins were not undertaken due to the known safety of tea consumption [36].

Cytotoxicity of **1,8-dihydroxyanthrones** and some analogs was already known for some cell lines as described in the introductory chapters and even led to the suggestion to use these compounds as anticancer therapeutics in the literature [32]. At the time of our study, the *in vivo* acute toxicity of the hydroalcoholic extract of *K. foliosa* was not published [25]. To further complete the toxicity profile, we investigated the effects of **KA** and **KP** on four different human cell lines (see **publication II**). With the stability issues in mind, we dissolved the compounds directly before adding them to the respective cells. While both **KA** and **KP** were not toxic towards HT29 cells, our study revealed **KP** to be more toxic than **KA** for the other three cell lines investigated. This was in contrast to literature studies that reported **KA** to be more toxic than **KP** (see introduction, section 1.3.1). Additionally, we selected the Jurkat cell line for further experiments because it showed the largest difference in cell viability between the two compounds (see **publication II**, figure 2A) and because it is the parental cell line of J-lat cells that were important for LR experiments. We investigated both compounds after preincubation in the respective culture medium to consider their instability in solution. The resulting mixture of molecules could result in a different toxicity compared to the single parent compound. Preincubation of the compounds markedly changed the toxicity (see **publication II**, figure 2B). While the mixture, resulting from preincubation of **KA**, was more toxic than **KA**, the mixture resulting from **KP** was less toxic than **KP**. The large difference in Jurkat cell viability observed between **KA** and **KP** is no longer found after preincubation over the entire concentration range investigated (see **publication II**, figure 2C). These results are in line with the observation that **KA** in solution easily converts into **KP** again highlighting the importance of the stability studies. The reported literature on cytotoxicity needs to be read in the light of these studies. A short time like four hours was enough to change the toxicity of **KA** and **KP** considerably, as shown by our results (see **publication II**). Because this phenomenon has not been described before, investigators may not have paid attention to the time frame between dissolving the compounds and confronting the respective cells. The common usage of stored DMSO stock solutions would further increase this problem. It is therefore unclear which molecule is responsible for the reported toxicity: **KA**, **KP** or a dimer of these molecules. However, if an extract should be administered

as in ALEBACHEW'S *in vivo* study [25], information on the toxicity of the whole extract is more valuable than on the single compounds. Our collaborators also determined the cytotoxicity of **KA** and **anthralin** within the studies on HIV activity on CD4<sup>+</sup> T cells and peripheral blood monocytes from HIV uninfected donors (figure 8, **publication III**). A moderate cytotoxicity of **KA** was detectable in contrast to **anthralin**, where an almost complete loss of cell viability was observed. In addition, the data revealed a strong influence of the donor on cytotoxicity because pronounced differences were found for one compound between different donors. This was true even for well characterized compounds like prostratin and phorbol myristate acetate. However, at the time of writing the reason for this phenomenon remained unclear. Due to the absence of anti-HIV and LR activity, **KP** was not included in studies on CD4<sup>+</sup> T cells and PBMC.

### 3.6.7) Further Antimicrobial Activities

As described in **publication II**, **KA** and **KP** did not show activity against the Gram-negative bacterium *Aliivibrio fischeri* or relevant anthelmintic activity in the model organism *Caenorhabditis elegans*. For the latter, values were comparable if compounds were preincubated or directly added to the microbe (e.g. for **KA**  $14.7 \pm 1.2$  vs.  $12 \pm 2.1$  % inhibition). **KA** and **KP** both did also not inhibit the growth of the following organisms in an agar diffusion test: *Bacillus subtilis*, *Escherichia coli*, *Pseudomonas aeruginosa*, *Enterococcus faecalis*, *Sporobolomyces salmonicolor*, *Penicillium notatum* and *Candida albicans* (unpublished results, methodology see page XVIII in section 6.1.2).

### 3.7) Discussion of Biological Activity of KA Analogs

This section discusses the biological activity of 1,8 dihydroxyanthrones. We were especially interested in answering the question if the diverse activity profile of **KA** (antiplasmodial, latency reversing, cytotoxic to some cells, weak antimycobacterial activity) arose from a general toxicity<sup>19</sup> of those analogs or could be due to a more specific mechanism. Table 5 is a compilation of the biological activity and cytotoxicity data of **KA** and **KP**, with some additional data for **AN1** (anthralin) that was included in the HIV assays due to interesting results.

The highest activity for **KA** and for **KP** was found in the anti-plasmodial assay because concentrations to detect this activity were lowest among all investigated assays. However, in comparison with the activity of chloroquine (see **publication II**) or the activity of analogs of artemisinin [145], which are in the nanomolar range, the antiplasmodial activity of *K. foliosa* metabolites is markedly lower. Nevertheless, the *in vivo* study of the antiplasmodial activity of a *K. foliosa* extract supports further effort in the research on this plant for the treatment of malaria [25]. When going on with antiplasmodial research for this compound class the simultaneous LR activity needs to be kept in mind. This is important because HIV prevalence is high in SSA and antiplasmodial treatment with plant extracts from *K. foliosa* might lead to HIV LR in PLWHIV. However, the low stability of these compounds makes a sufficient bioavailability thereof unlikely. The above might therefore be more of a theoretical problem. It would however be best to proof this hypothesis with experiments.

Considering all biological activities of **KA** and **KP** determined within this thesis, they cannot be addressed as specifically anti-plasmodial compounds. The concentration of **KA** required to obtain synergistic effects with various LR agents is similar to its anti-plasmodial activity although relevant LR activity of **KA** alone was only evident at higher concentrations (see **publication III** and Table 5). Interestingly, the anthraquinone **KP** was not active in this assay in contrast to the anti-plasmodial assay in which both compounds were active. In line with this are the LR activity of anthralin (**AN1**) and the inactivity of chrysazine (**AQ1**) in this assay, both analogs of **KA** and **KP**. This also indicates that the molecular mechanism of LR is more complex than the antiplasmodial mechanism of **KA** and **KP**.

The *ex vivo* anti HIV activity of **KA**, observed in PBMCs, seems to be contradictory to the observed LR activity. However, **KP**'s inactivity in this assay is in line with the LR inactivity of anthraquinones. In the experiment, HIV infection of PBMCs occurred in the presence of **KA**, leading to less antigen p24 production. This can be interpreted as inhibition of antigen p24 production or as less intact HIV integration during cell infection.

---

<sup>19</sup> General toxicity refers to an unspecific mechanism by which molecules are toxic to a wide range of cells from different species and even different domains. This could for example be due to their potential to generate reactive oxygen species (as explained in the introduction) or to their ability to reduce or oxidize cell components.

*Table 5: Biological activity of 1,8-dihydroxyanthrones and anthraquinones. Reported values are displayed as indicated in the respective row. For better comparability, all concentrations are reported in  $\mu\text{M}$ .*

Cell line/ microbe	KP	KA	AN1	Publ
Jurkat	50 $\mu\text{M}$ : $12.3 \pm 2.2$	50 $\mu\text{M}$ : $73.1 \pm 2.0$	n.d.	II
% viability	pre: $41.9 \pm 5.1$	pre: $21.9 \pm 4.5$		
HEK	50 $\mu\text{M}$ : $36.5 \pm 2.5$	50 $\mu\text{M}$ : $52.5 \pm 1.5$	n.d.	II
% viability				
SHSY5Y	50 $\mu\text{M}$ : $5.9 \pm 3.2$	50 $\mu\text{M}$ : $30.3 \pm 1.2$	n.d.	II
% viability				
HT-29	50 $\mu\text{M}$ : $99.1 \pm 3.0$	50 $\mu\text{M}$ : $93.3 \pm 1.8$	n.d.	II
% viability				
CD4 <sup>+</sup> T cells <sup>a</sup>	n.d.	10 $\mu\text{M}$ : $54 \pm 30$	10 $\mu\text{M}$ : $2.0 \pm 1.6$	III
% viability				
PBMC <sup>b</sup>	n.d.	10 $\mu\text{M}$ : $38 \pm 21$	10 $\mu\text{M}$ : $2.8 \pm 2.6$	III
% viability				
mock inf. PBMC	n.d.	36 $\mu\text{M}$ : $51.3 \pm 3.1$	n.d.	II
% viability		120 $\mu\text{M}$ : $28 \pm 2.0$		
LRA <sup>d</sup>	not active	12 $\mu\text{M}$ : $6.1 \pm 5.2$	10 $\mu\text{M}$ : $6.9 \pm 1.4$	III
% reactivated cells		10 $\mu\text{M}$ : $3.0 \pm 2.4$		
LRA synergy	n.d.	1 $\mu\text{M}$	1 $\mu\text{M}$	III
		Lowest conc. where synergy was observed		
Anti-HIV	not active	35.7 $\mu\text{M}$ : $79 \pm 1$	<sup>c</sup>	II
% inhibition				
<i>A. fisheri</i>	not active	not active	n.d.	II
<i>C. elegans</i>	1151 $\mu\text{M}$	1189 $\mu\text{M}$	n.d.	II
% inhibition	$7.1 \pm 0.8$	$12 \pm 2.1$		
	pre: $9.5 \pm 1.9$	$14.7 \pm 1.2$		
<i>M. tuberculosis</i>	23 $\mu\text{M}$ : $76.7 \pm 21.8$	24 $\mu\text{M}$ : $74.3 \pm 1.9$	44 $\mu\text{M}$ : $61.9 \pm 2.8$	II
% growth <sup>e</sup>				
<i>P. falciparum</i>	$1.93 \pm 0.13$	$0.73 \pm 0.29$	$0.36 \pm 0.02$	II
$IC_{50} [\mu\text{M}]$		pre: $0.44 \pm 0.04$	pre: $1.19 \pm 0.01$	

<sup>a</sup> donated by HIV negative individual, <sup>b</sup> donated by HIV positive individual, <sup>c</sup> no viral RNA detected due to extensive cell death; <sup>d</sup> **AQ1** was included in the study, but showed no LRA activity (<0.5 % GFP pos cells); <sup>e</sup> **AQ1** showed comparable values for inhibition of *M. tuberculosis* as **AN1**; pre: preincubated before start of the assay

The complete absence of activity of **KA** and **KP** in several assays on microorganisms across different domains (fungi, bacteria) in contrast to antiplasmodial and LR activity is a strong argument against a general toxic mechanism. This is further supported by the



difference in cytotoxicity between **KA** and **anthralin** in different cell lines, although these molecules share the same core structure and the ability to easily be oxidized at C-10 and thereby reduce other components. A general toxicity of those compounds therefore seems unlikely. The assays on LR performed in J-lat cells also indicate a mechanism of action that is different from a general toxicity of the compounds. LR activity was detected by expression of GFP that was integrated in the viral genome and only detectable upon viral replication and translation of viral genes. Therefore, this signal would not be observed if the mechanism of action was just a general toxicity. In contrast, it suggested a more complex mechanism that remained unclear at the time of writing.

Although a mechanism of action based on general toxicity seems unlikely, **KA** and **KP** as well as anthralin were toxic towards several cell lines (see **publication II** and **III**). *Ex vivo* studies on CD4<sup>+</sup> T cells and PBMC indicated an influence on the toxicity of the molecule by the phenyl substitution in position 4 of the anthrone because anthralin was more toxic than **KA**. The studies on **KA** in comparison to **KP** (see **publication II**) indicated an influence of the oxidation status of C-10 on the toxicity of the molecule. In a study on anthralin analogs, the importance of at least “one phenolic hydroxyl group hydrogen bonded to the C-9 carbonyl oxygen and one benzylic proton at C-10” were highlighted for the tumor promoting activity [140]. This information should be kept in mind when further working on this compound class because this toxic effect is observed over a long period of time only [140].

However, due to the persistent stability issues of **KA** and **KP** it remained unclear at the time of writing if further studies will be undertaken to clarify the open questions regarding the molecular mechanism of action or on the SAR.

### 3.8) Microbiological Method Development

The importance of evaluating the activity of new compounds against the hard-to-eradicate persister population of mycobacteria has been emphasized by the TB scientific community since 2002 [146]. Regarding NTM infections, Wu *et al.* also stated in 2018 that “conventional MIC determination alone is not a good predictor of clinical outcomes” and persister specific assays should therefore be encountered during drug discovery [147]. However, up to date, SAR studies are still mostly done on replicating aerobic cultures due to the greater difficulty of observing inhibition when there is no growth anyway (due to the nature of NRPs). The hurdle is particularly high when it comes to investigations under hypoxic conditions. These assays are often laborious or associated with additional financial investments and costs in order to culture bacteria in anaerobic incubators or handle steps of the process in hypoxic glove boxes.

At the time of this work there was no hypoxic model for *M. abscessus* in microtiter plates to study low-oxygen persisters in a simple and cost-efficient way. As part of this thesis, a low-threshold model was developed to address this research gap. Creating hypoxic conditions is a simple task in itself. The difficulty when working with aerobic mycobacteria under anaerobic conditions is to find a method with the right speed in oxygen deprivation to ensure

a transition into the NRP state rather than sterilizing the culture. Therefore, the first result of this project was to discover that among the methods used for cultivation of anaerobic bacteria, PARKER'S method [148] could be applied to *M. abscessus* to generate low-oxygen persisters. This method is explained and discussed in detail in **publication IV**. PARKER'S method only affords a box with an airtight lid, iron wool and a copper sulphate solution to activate the latter. These components are readily available in most settings and contribute to the goal of the project to keep the method as simple and inexpensive as possible. The reusable box helps to reduce laboratory waste compared to plastic sachets, commonly used in anaerobic culturing setups.

Various preliminary experiments with the rapidly growing non-tuberculous *Mycobacterium aurum* (DSM) were undertaken to find the best conditions for the setup. Those included exploring of different sealing techniques, testing of suitable air tight containers, variations in hypoxic pre-treatment length before compound addition and different methods to determine the activity of the investigated compounds. Subsequent experiments with *M. abscessus* gave first results on how the gathered information could be applied to another mycobacterial species. Finally, all this led to the establishment of a robust assay protocol for the determination of drug activity under hypoxic conditions that should be applicable in most laboratories. The applicability was tested within this work on a variety of compounds including plant extracts. The respective protocol is presented in figure 2 of **publication IV**. The cultures obtained that way are referred to as **low-oxygen persisters (LOPs)**. Various characteristics of this culture were studied in detail to provide evidence of culture transition to the NRP state. Those will briefly be summarized after discussing the oxygen levels that are achieved within this setup and the method to determine compound activity.

### 3.8.1) Oxygen Levels of Hypoxic Assays

Although hypoxic models are applied to various mycobacterial species, there is no clear definition on the term hypoxia within the literature (see 1.4.3.4). Guided by WAYNE'S model [121] we aimed for low oxygen levels in the set up instead of anoxia. Oxygen levels were mainly characterized by two observations: decolorization of MB as explained in the introduction on page 27 and determination of oxygen concentration with an optical oxygen sensor. This was done for a few samples only, while MB was employed in each experiment. The results are found in the Supplementary Information of **publication IV** (included in the appendices of this thesis). The values demonstrated the presence of low levels of oxygen in our setup. An anoxic atmosphere was not necessary to obtain *M. abscessus* cultures which showed typical attributes of NRPs as the results in the section on evidence for this transition (from page 114 on and in **publication IV**) demonstrated.

However, when handling the hypoxic assay, the observation of a slight underpressure while opening the lid served as additional verification of the consumption of air constituents. This phenomenon was already described by PARKER who measured the reduction of pressure. The oxidation process of the activated iron wool reduced the pressure in the hypoxic box

because oxygen was removed from the gas phase and found thereafter as oxidized iron and copper in the solid phase. The reduced pressure was only partly compensated by release of carbon dioxide from the saturated carbonate solution as described by PARKER [148]. This reduced pressure was also recognizable in our setup because it afforded some force to open the lid. It needs to be mentioned that MB was decolorized in one experiment while the reduced pressure was not observed when opening the lid. This indeed influenced the results of this single experiment because they were not reproducible when no reduced pressure was detected (data not shown).

### **3.8.2) Evidence of LOPs Belonging to NRPs**

The applicability of the method to transition a replicating into a non-replicating culture was proven within the scope of this work by characterizing the obtained cultures and comparing their properties with the one expected from literature studies on NRPs. This included investigations on growth behaviour during and after hypoxic conditions and morphological studies on a single cell level. All of this was done in parallel for aerobic cultures for comparison. A study on twelve antimycobacterial compounds was in line with the expectations for NRPs to markedly differ in their activity profile compared to aerobic cultures of the same mycobacterial species. This study included natural products and partially-synthetical natural products, approved antimycobacterial drugs and compounds from early drug development processes. The latter were extensively studied in our research group in the last years and include  $N\alpha$ -aroyl- $N$ -aryl-phenylalanine amides (AAPs) [149, 150] and a DNA-gyrase inhibitor [151, 152] (see figure 9, **publication IV** for the chemical structure of the compounds). The evidence on *M. abscessus* transitioning to the LOP state is presented in **publication IV** and therefore only briefly summarized in the following section.

#### **3.8.2.1) Growth Behaviour**

Our results demonstrated that the obtained cultures showed typical growth attributes of NRPs. *M. abscessus* cultures pre-treated in the hypoxic setup were not able to develop the typical growth curve of aerobic cultures. Instead, as long as cultivated under hypoxic conditions, cell numbers were roughly constant over time, markedly different from aerobic cultures that showed a clear exponential growth phase (figure 4, **publication IV**).

The results also indicated that LOP cells have the ability of NRPs to resuscitate from their state. When the hypoxic stress was discontinued, the cells were able to replicate again which was proved on solid and in liquid medium. Because resuscitation is accompanied by metabolic changes of the cells, we detected delayed growth rates on solid as well as in liquid medium compared to aerobically cultivated *M. abscessus* cells (see figure 4, 5 and 7, **publication IV**).

#### **3.8.2.2) Morphology**

We studied the morphology of LOP cells on a single cell level in collaboration with DR. ROBERT ECKENSTALER from our institute. While culture preparation, pre-treatment and

staining of the cells were part of my work, ECKENSTALER investigated the samples by confocal laser scanning microscopy. To visualize *M. abscessus* cells we used the fluorescent 3-hydroxy-chromone-dye trehalose conjugate (3HCT), (see figure 6 **publication IV** for the structural details; 3HCT = compound 1 in **publication IV**). This dye was designed to be incorporated into the mycobacterial cell wall by KAMARIZA *et al.* [153] for *M. tuberculosis* and *M. smegmatis* and applied to *M. abscessus* in 2024 by my colleague LEA MANN [154]. The synthesis of 3HCT was done by DR. ADRIAN RICHTER. We used this dye to compare the staining pattern of cells in two differently pre-treated cultures. We observed a pronounced difference between aerobically and hypoxically pre-treated cultures (see figure 8 in **publication IV** and figure S4 of **publication IV**). This was a confirmation of the expected different phenotype of the LOP culture.

### 3.8.2.3) Phenotypical Drug Resistance and Sensitivity

Another important evidence for our setup to generate NRPs was the phenotypical resistance we determined for ten antimycobacterial drugs and for compounds from drug discovery processes. Those compounds were highly active against replicating cells of *M. abscessus* except the natural product pyridomycin which showed moderate activity only. In addition to the change from ‘active to non-active’ we found a phenotypic sensitivity of LOPs to two drugs (namely metronidazole and niclosamide) that aerobe cells of *M. abscessus* were not susceptible to. This switch from ‘non-active to active’ enabled us to use them as LOPs verification compounds. The dose dependent activity studies of these compounds are presented in figure 3, 10 and 11, **publication IV**.

### 3.8.3) Possible Applications of the LOPs Assay

We developed the LOPs method to be used without genetic modifications. This makes the method simple as there is no need for maintaining a functional plasmid. It also offers the opportunity to investigate clinical samples with this method. Preliminary experiments during the assay development revealed this setup to be applicable to *Mycobacterium aurum*, a non-pathogenic mycobacterial species. Therefore, it can be assumed that the same approach should be applicable for other mycobacterial species as well. This model could therefore serve as a tool in drug development for different NTM infections.

As the preparation of the assay is done in microtiter plates, a wide application in the field of drug discovery is plausible (e.g. using the DiaMOND assay [155] within this setup).

As shown by the results, this assay offers easy access to LOP cells of *M. abscessus* to further characterize this population of cells by confocal laser scanning microscopy. This approach could be used to study other aspects of LOPs as the question of thickened cell wall compared to replicating cells or to perform drug permeation studies to gain deeper knowledge of LOPs of *M. abscessus* and answer some of the question regarding the inactivity of AAPs in LOPs.

## 3.9) Experiments to Extend the LOP Assay by Using a 3-Hydroxy-Chromone Dye Trehalose Conjugate

### 3.9.1) *Combination of Hypoxia and Starvation*

In the WAYNE model the reduction of oxygen concentration is achieved by the bacteria themselves which consume the oxygen by replication and respiration. Within this model, it is therefore not possible to perform a starvation model (e.g. the LOEBEL model [118]) in combination with hypoxia. The method developed within this work to investigate LOPs mainly reduced the oxygen levels using an oxidation process as explained in **publication IV**. A replication of bacteria to achieve hypoxic conditions is not necessary. We therefore considered a combination of starvation and hypoxia to be possible with this setup. Preliminary experiments were performed to clarify if this question could be answered within the scope of this project. For these experiments the **3HCT**-staining method was used as well.

First, the staining of starved cells that were aerobically cultured was investigated to ensure the usability of the dye for starved cells. The LOEBEL model was already successfully applied to *M. abscessus* by YAM *et al.* [119]. We confirmed the viability and culturability of *M. abscessus* in tubes and in 96-well plates while the culture medium was solely PBS supplemented with 0.05 % tyloxapol for prevention of clumping of the bacteria. Tyloxapol was used instead of TW80 because it cannot be metabolized by mycobacteria, while TW80 was reported to likely serve as a nutrient [119]. Like in previous experiments the starved cells were then diluted into fresh ADS containing 7H9 medium to enable growth by supplying nutrients. At certain points in time samples were taken and stained with **3HCT** to subsequently analyze them by automated object counting with a Thermo Fisher Scientific CellInsight CX5 instrument (Waltham, MA, USA). With this method we followed the regrowth of the starved culture and compared it to the regrowth of a non-starved culture that was diluted from ADS containing 7H9 into fresh 7H9 medium. Conditions were the same for both cultures during the growth phase in fresh medium. Both cultures were diluted to the same inoculum. Figure 18 shows the results of this experiment. Diluted cultures of both conditions showed similar growth behaviour in ADS containing medium. We thereby confirmed findings of others that starved cells of *M. abscessus* are able to replicate if nutrients again become available. We could not observe a delayed growth as found for LOPs cells compared to aerobic cells (see figure 7 in **publication IV**). Therefore, the previously challenged cells seemed to recover faster from starvation than from hypoxia. We further concluded from the results that starved cells can be stained using **3HCT**.

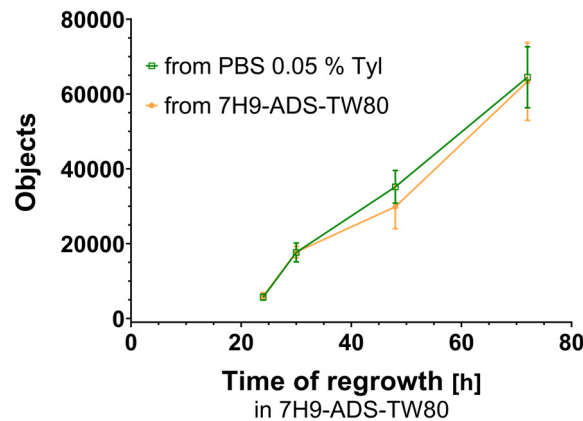


Figure 18: Development of object numbers in previously non-starved (orange) and starved (green) cultures upon nutrition availability. Regrowth was followed in fresh ADS containing 7H9 medium in aerobic conditions (5 % CO<sub>2</sub>).

Next, we investigated if hypoxia and starvation could be combined in the LOPs assay. Figure 19 (B) displays the results of this experiment. To ease comparison, they are placed next to results from non-starved cells that were included in **publication IV** (Figure 19 (A)). The growth behaviour of starved cells after hypoxic pre-treatment is markedly different from cells in nutrient containing medium (compare blue data in B and A).

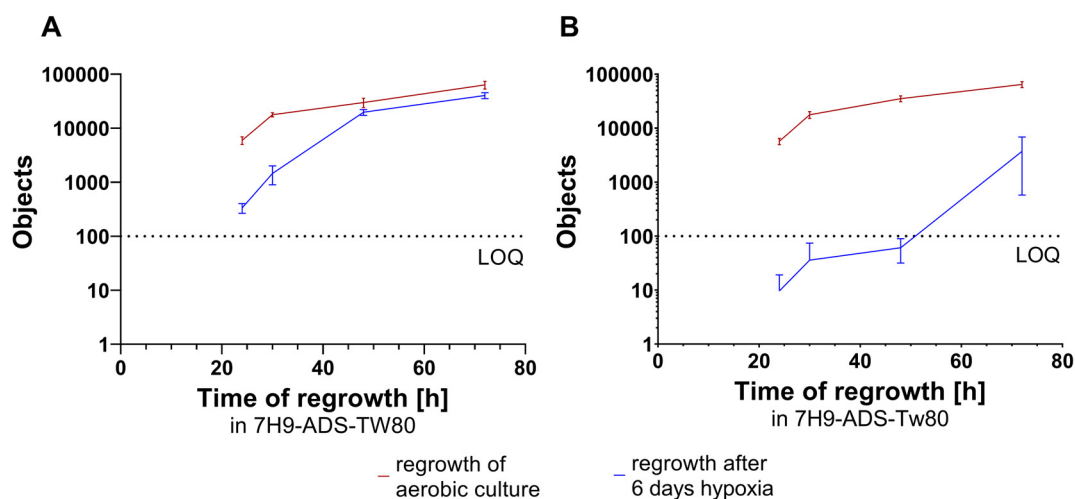


Figure 19: Regrowth of differently pre-treated *M. abscessus* cultures in ADS containing 7H9 medium under aerobic (5 % CO<sub>2</sub>) conditions. (A) Cultures from **nutrient** containing medium after aerobic (red) or hypoxic (blue) pre-treatment and (B) **Starved** cultures after aerobic (red) and hypoxic (blue) pre-treatment. LOQ limit of quantification

Values were below the limit of quantification for three out of four points in time. A combination of starvation and hypoxia therefore seems not possible with this set up. Staining of the cells after hypoxic pre-treatment and after starvation in aerobic conditions was possible (as discussed in **publication IV** and in this section). Therefore, the reason for the low object numbers seems to be attributable to an extensive reduction in cell numbers that

lead to markedly different bacterial concentrations after the dilution step. Even though these results are disappointing, this experiment provides valuable information. The pronounced differences within the first 48 hours of the experiment between starved and non-starved hypoxic *M. abscessus* cultures allow to conclude that starved *M. abscessus* cultures are more sensitive to hypoxia than cultures with sufficient nutrient supply. This could be the starting point for further experiments to understand the mechanisms of the toxicity of hypoxia in combination with starvation.

### **3.10) Contribution of the LOPs Assay to the Drug Development Process in our Working Group**

In addition to the evidence on LOPs existence the study of different compounds under hypoxic conditions yielded information on several new anti-mycobacterial compound classes. Those were developed and investigated in the working group of PROF. PETER IMMING in the last years. The developed assay is a helpful tool to further characterize those compounds. Disappointing but yet interesting results for the AAPs and for the DNA gyrase inhibitor were obtained and included in **publication IV**. Furthermore, six squaramide derivatives that are currently being developed and characterized by PAUL R. PALME in PROF. IMMING'S group have been investigated within this project. Those compounds target the mycobacterial ATPase [156, 157]. To emphasize the importance of this data, some of these results are discussed independently in this chapter.

#### **3.10.1) Activity of RNA Polymerase Inhibitors**

Rifampicin is one of the few drugs with reported retained bactericidal activity against NRPs of *M. tuberculosis* [123]. It still sterilized 90 % of CFUs, although growth inhibiting activity was only observed at considerably higher concentrations than in replicating cultures. *M. abscessus* has an intrinsic resistance to rifampicin [158] but rifabutin, a derivative of rifampicin, is active and bactericidal against *M. abscessus* [159] and was reported to act bactericidal even on NRPs of *M. abscessus* in a caseum surrogate model [160]. It also showed a 1-log reduction at 3.5  $\mu$ M in the hypoxic WAYNE model [122] and is therefore one of the few drugs still active against *M. abscessus* under conditions leading to a non-replicating phenotype. Therefore, we expected compounds targeting the same bacterial target, the bacterial RNA polymerase, to retain their activity within our setup. Figure 20 displays the chemical structure of two AAPs [150]. They were developed by DR. MARKUS LANG and DR. ADRIAN RICHTER over the last years [149].



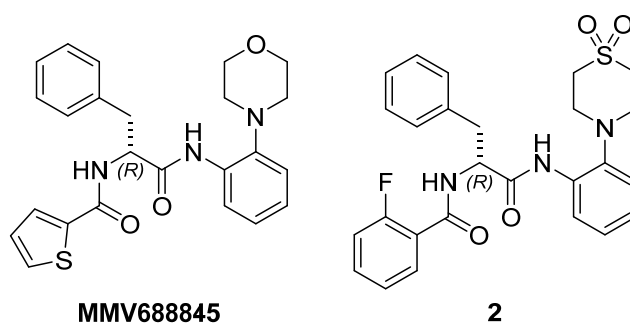


Figure 20: Chemical structure of the initial hit (MMV688845) and the lead compound 2 of the compound class of AAPs.

In line with our expectations and in consistency with the literature [159] we found rifabutin to act bactericidal against replicating *M. abscessus*, as displayed in Figure 21 (A, red data points) (see also **publication IV**). The drug also retained most of its bactericidal activity against *M. abscessus* LOPs even though 3-log reduction was not reached within 40  $\mu\text{M}$  anymore (Figure 21, A, blue data points). Both AAPs were highly active towards replicating *M. abscessus* cells as shown by the results under aerobic conditions (Figure 21, C, red data points), confirming literature data [149]. However, in contrast to rifabutin, both AAPs were inactive against LOPs (Figure 21, B and C blue data points).

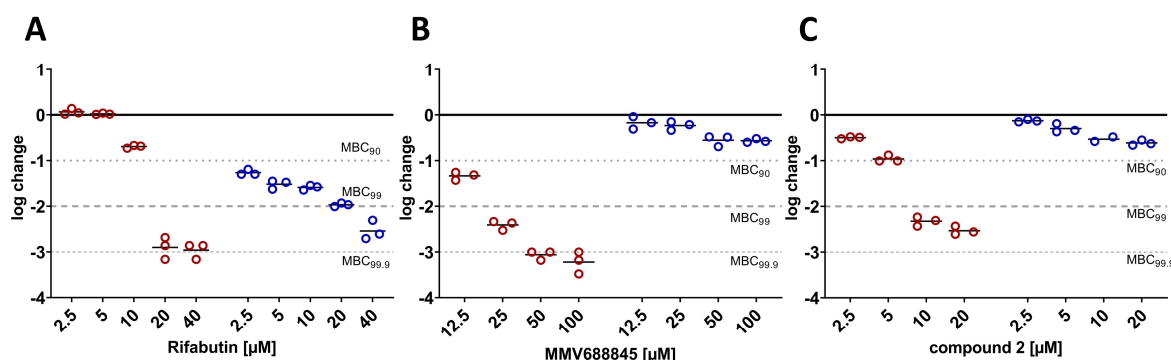


Figure 21: Dose dependent activity of RNA polymerase inhibitors. (A) rifabutin, (B) MMV688845 and (C) compound 2 under aerobic (red) and hypoxic (blue) conditions.

At a first glance these results seem contradictory. As proven by the sensitivity of LOPs against rifabutin, the target is still active under hypoxic conditions. Different hypotheses to clarify this inconsistency were discussed in detail in **publication IV**. One suggestion is a reduced drug permeation [161] due to altered cell wall structure under hypoxic conditions. This alteration was described for *M. tuberculosis* cultured under hypoxia [162] but evidence for *M. abscessus* is less abundant in literature. Information on membrane alteration of *M. abscessus* NRPs under hypoxia are not available but are reported for potassium starved cells [163]. By now, it is not clear how comparable those type of cells are. Another hypothesis is a possible chemical alteration of the compounds by mycobacterial enzymes that were expressed under hypoxia but were absent under aerobic conditions because the influence of

the conditions on altered gene expression was proven for different mycobacteria. It is therefore even plausible that another enzyme might be involved. Within this thesis, the reason for this discrepancy could not be clarified. However, this phenomenon should be addressed in future research. The developed assay will be a helpful tool to generate LOPs and subsequently study the permeation of AAPs under these conditions.

### 3.10.2) Activity of Squaramides against *M. abscessus* LOPs

Within this thesis, six squaramides were characterized regarding their activity on *M. abscessus* LOPs using the method described in **publication IV**. These compounds target the mycobacterial ATPase [156] and are developed by a colleague in the group, PAUL R. PALME. Results on this compound class were not included in **publication IV** but will be incorporated in a manuscript dedicated to squaramides in the near future. Exemplarily, one data set is included in this thesis to highlight the value of the developed assay in the drug discovery process within our working group. Because this data is unpublished, the structure of the discussed compound will not be shown here. However, the general structure of squaramides is displayed in Figure 22.

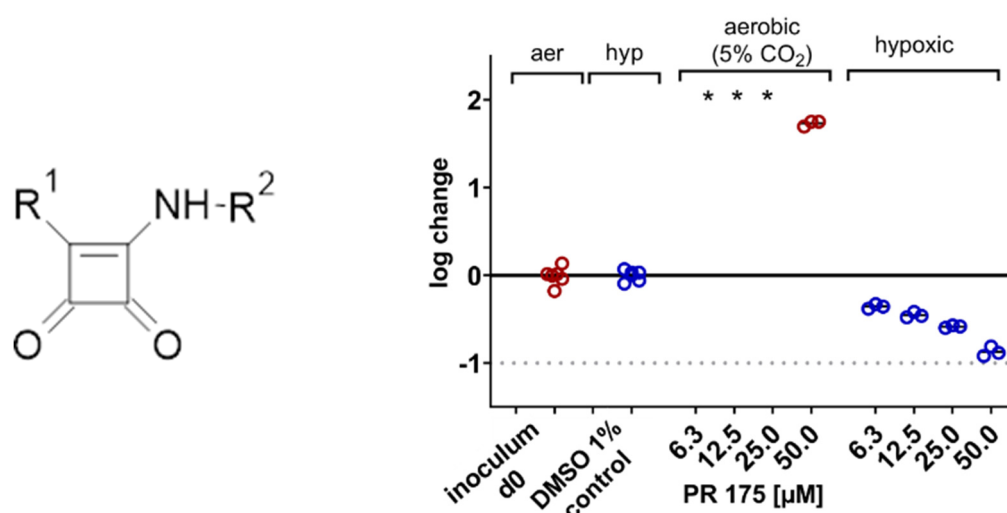


Figure 22: General structure of squaramides and dose dependent activity of one squaramide in aerobic (red) and hypoxic (blue) conditions on *M. abscessus*.

\* indicate enormous bacterial growth, too high to distinguish between single colonies.

At the time of writing, none of the synthesized squaramides performed with MIC<sub>90</sub> < 50 μM under aerobic conditions against *M. abscessus*. This can be seen exemplarily by the data in red in Figure 22. In the presence of PRP175 (50 μM), bacterial growth by almost 10<sup>2</sup> was determined under aerobic conditions. In contrast, under hypoxic conditions, those compounds were slightly bactericidal (blue data, Figure 22). Colonies were reduced by about 90 % under hypoxic conditions.

To further optimize the structures of squaramides, the assays should be performed in the LOPs assay in future instead of relying solely on the aerobic growth inhibition assay to characterize the synthesized compounds.

## 4) Summary

The **first part of this thesis** contributes to the understanding of **secondary plant metabolites** from two plants cultivated in or endemic to sub-Saharan Africa. Firstly, this work demonstrates the efficacy of *Camellia sinensis* extracts on many clinical isolates of methicillin resistant *S. aureus* (MRSA) and therefore supports results from clinical trials to use catechins in the treatment of decubitus, infected with MRSA. Secondly, this thesis has improved the understanding of the activity profile of *Kniphofia foliosa* constituents, namely knipholone and knipholone anthrone. The value of the results presented largely consists in considering the stability properties of the substances during biological activity investigations. The instability even in normal culture medium was assessed for the first time in this work, although various activities were reported in the literature for those constituents. Due to this discrepancy, this thesis also questions biological activity studies reported for knipholone anthrone that paid no attention to the instability of this compound. This thesis furthermore enabled the study of knipholone anthrone as a natural latency-reversal agent by providing knipholone anthrone in sufficient quantity and purity together with some synthetic analogs. Although too few compounds were synthesized for SAR, crucial structural features for anti-infective activity were identified.

The **second part** of this thesis presents a **microbiological assay**. The *in vitro* Low-oxygen-persister (LOP) assay provides a new tool to further characterize new chemical entities under hypoxic conditions. LOPs are especially hard to and at the same time most important to eradicate to successfully treat mycobacterial infections. The assay allows studying bactericidal activity of compounds or plant derived products on LOPs of *M. abscessus*. It is designed in a way that allows it to be used by many microbiological laboratories. Thereby, the assay closes an important gap in the research of new antimycobacterial compounds.

During the course of this work some questions were uncovered that remain to be answered. The molecular mechanism *K. foliosa* constituents is not clear and so is the reason for the reduced activity of some compounds in the LOPs assay. For *N* $\alpha$ -aroyl-*N*-aryl phenylalanine amides (AAPs), the reason for reduced drug activity in the presence of a still active target needs to be clarified. Drug permeation studies under hypoxic conditions would be able to shed light on this. This information will help to guide future decisions in the drug development process.

## 4) Zusammenfassung

Der erste Teil dieser Doktorarbeit trägt zum Verständnis **sekundärer Pflanzeninhaltsstoffe** zweier Pflanzen bei, die in sub-Sahara Afrika heimisch sind oder dort kultiviert werden. Als erstes zeigt diese Arbeit die Wirksamkeit von ***Camellia sinensis***-Extrakten gegen viele klinische Isolate Methicillin resistenter *Staphylococcus aureus* (MRSA). Die *in vitro* Ergebnisse dieser Arbeit stimmen damit mit den klinischen Studien überein, die eine Wirksamkeit von Catechinen in der Behandlung von MRSA infiziertem Dekubitus zeigen konnten. Als zweites erweitert diese Arbeit das Verständnis des Aktivitätsprofils von Inhaltsstoffen von ***Kniphofia foliosa***, namentlich Knipholon und Knipholonanthron. Der Wert der vorgelegten Ergebnisse liegt dabei zu großen Teilen im Berücksichtigen der Stabilitätseigenschaften der Substanzen während der Durchführung biologischer Versuche. Die Instabilität der Moleküle selbst in gewöhnlichen Kulturmedien ist im Rahmen dieser Arbeit erstmalig beschrieben, obwohl verschiedene Aktivitäten für beide Substanzen bereits publiziert wurden. Aufgrund dieser Diskrepanz stellt diese Arbeit biologische Aktivitätsstudien für Knipholonanthron in Frage, die der Instabilität des Moleküls keine Beachtung schenken. Durch das Bereitstellen von Knipholonanthron in ausreichender Menge und Reinheit zusammen mit einigen synthetischen Analoga ermöglichte diese Doktorarbeit darüber hinaus die Untersuchungen an natürlichem Knipholonanthron zur Latenzumkehr von HIV infizierten Zellen. Obwohl zu wenige Substanzen synthetisiert wurden, um Struktur-Wirkungs-Beziehungen aufzuklären, konnten wichtige strukturelle Merkmale für antiinfektive Aktivität identifiziert werden.

Der zweite Teil dieser Doktorarbeit stellt einen **mikrobiologischen Versuchsaufbau** vor. Der *in vitro* Low-oxygen-persister (LOP) Assay ist eine neue Untersuchungsmethode, um Substanzen unter hypoxischen Bedingungen zu charakterisieren. LOPs zu eradizieren ist besonders schwer, gleichzeitig aber besonders wichtig, um mykobakterielle Infektionen erfolgreich zu behandeln. Der Assay erlaubt die Untersuchung von Substanzen oder pflanzenbasierten Produkten auf deren bakterizide Eigenschaften gegenüber LOPs von *Mycobacterium abscessus*. Darüber hinaus wurde bei der Entwicklung des Assay Wert auf eine leichte und kostengünstige Durchführbarkeit gelegt, um die Nutzung in vielen mikrobiologischen Laboren zu ermöglichen. Damit schließt der Assay eine wichtige Forschungslücke.

Im Rahmen dieser Arbeit wurden Fragen aufgeworfen, die unbeantwortet blieben. Der molekulare Mechanismus der *K. foliosa* Inhaltsstoffe ist weiter ungeklärt, wie auch die Wirkungslosigkeit mancher Substanzen im LOP Assay. Der Grund für die geringe Wirksamkeit der  $\alpha$ -aroyl-*N*-aryl Phenylalanin Amide (AAPs) trotz eines aktiven Targets bleibt offen. Permeationsstudien unter hypoxischen Bedingungen könnten wertvolle Informationen hierzu liefern. Diese Informationen werden hilfreich für zukünftige Entscheidungen im Drug-development-Prozess sein.

## 5) References

1. Musa, B.M., Adamu, A.L., Galadanci, N.A., Zubayr, B., Odoh, C.N., and Aliyu, M.H., *Trends in prevalence of multi drug resistant tuberculosis in sub-Saharan Africa: A systematic review and meta-analysis*. PLoS One, **2017**. 12(9): p. e0185105. doi.org/10.1371/journal.pone.0185105
2. Hardy, K., *Paleomedicine and the evolutionary context of medicinal plant use*. Revista Brasileira de Farmacognosia, **2021**. 31: p. 1-15. doi.org/10.1007/s43450-020-00107-4
3. Capasso, L., *5300 years ago, the Ice Man used natural laxatives and antibiotics*. The Lancet, **1998**. 352(9143): p. 1864. doi.org/10.1016/S0140-6736(05)79939-6
4. WHO traditional medicine strategy: 2014-2023
5. Birhanu, T., Abera, D., Ejeta, E., and Nekemte, E., *Ethnobotanical study of medicinal plants in selected Horro Gudurru Woredas, Western Ethiopia*. Journal of Biology, Agriculture and Healthcare, **2015**. 5(1): p. 83-93.
6. Bekele, G. and Reddy, P.R., *Ethnobotanical study of medicinal plants used to treat human ailments by Guji Oromo tribes in Abaya District, Borana, Oromia, Ethiopia*. Universal Journal of Plant Science, **2015**. 3(1): p. 1-8. doi.org/10.13189/ujps.2015.030101
7. Innocent, E., Marealle, A.I., Imming, P., and Moeller, L., *An Annotated Inventory of Tanzanian Medicinal Plants Traditionally Used for the Treatment of Respiratory Bacterial Infections*. Plants, **2022**. 11(7): p. 931. doi.org/10.3390/plants11070931
8. Moyo, M., Aremu, A.O., and van Staden, J., *Ethnopharmacology in sub-Saharan Africa: current trends and future perspectives*. Ethnopharmacology, **2015**: p. 263-278. doi.org/10.1002/9781118930717.ch23
9. Hill, R. *Scientists, Healers and Bioprospectors: The Epistemological Politics of Traditional Medicine in Ethiopia 1930-1998*. Thesis: Stanford University, **2019**
10. Samuel Adu-Gyamfi, *Unrestricted Analysis of the COVID Narrative in Africa: Emphasis on the Ghanaian Medical Context presented at the Conference "The Impact of COVID Restrictions on Low- and Middle-income Countries" at King's College, London April 2023*
11. Prof. Dr. Kerstin Andrae-Marobella from the University of Botswana in her talk on traditional healers in Botswana on 13th of November 2024 in Halle.
12. Eruaga, M.A., Itua, E.O., and Bature, J.T., *Exploring herbal medicine regulation in Nigeria: Balancing traditional practices with modern standards*. GSC Advanced Research and Reviews, **2024**. 18(3): p. 083-090. doi.org/10.30574/gscarr.2024.18.3.0094
13. *Flora of Ethiopia and Eritrea Volume 6 Hydrocharitaceae - Arecaceae* (eds). **1997**, Addis Abeba and Uppsala.
14. Ayalew, H., Tewelde, E., Abebe, B., Alebachew, Y., and Tadesse, S., *Endemic medicinal plants of Ethiopia: Ethnomedicinal uses, biological*

- activities and chemical constituents*. Journal of Ethnopharmacology, **2022**. 293: p. 115307. doi.org/10.1016/j.jep.2022.115307
15. Fayisa Diriba, T. and Mirete Deresa, E., *Botanical description, ethnomedicinal uses, phytochemistry, and pharmacological activities of genus Kniphofia and Aloe: A review*. Arabian Journal of Chemistry, **2022**. 15(9): p. 104111. doi.org/10.1016/j.arabjc.2022.104111
16. Nigussie, G., Tegegn, M., Abeje, D., and Melak, H., *A comprehensive review of the ethnomedicine, phytochemistry, pharmacological activities of the genus Kniphofia*. Pharmaceutical Biology, **2022**. 60(1): p. 1177-1189. doi.org/10.1080/13880209.2022.2085753
17. Aladejana, E.B. and Musara, C., *Kniphofia foliosa Hochst.(Asphodelaceae): Medicinal Uses, Phytochemistry and Pharmacological Properties*. Journal of Pharmacy and Nutrition Sciences, **2021**. 11: p. 13-19. doi.org/10.29169/1927-5951.2021.11.02
18. Dagne, E. and Steglich, W., *Knipholone: a unique anthraquinone derivative from Kniphofia foliosa*. Phytochemistry, **1984**. 23(8): p. 1729-1731. doi.org/10.1016/S0031-9422(00)83479-2
19. Dagne, E. and Yenesew, A., *Knipholone anthrone from Kniphofia foliosa*. Phytochemistry, **1993**. 34(5): p. 1440-1441. doi.org/10.1016/0031-9422(91)80048-6
20. Bringmann, G. and Menche, D., *Stereoselective total synthesis of axially chiral natural products via biaryl lactones*. Accounts of Chemical Research, **2001**. 34(8): p. 615-624. doi.org/10.1021/ar000106z
21. Bringmann, G., Mutanyatta-Comar, J., Knauer, M., and Abegaz, B.M., *Knipholone and related 4-phenylanthraquinones: structurally, pharmacologically, and biosynthetically remarkable natural products*. Natural Product Reports, **2008**. 25(4): p. 696-718. doi.org/10.1039/b803784c
22. Bringmann, G., Menche, D., Bezabih, M., Abegaz, B.M., and Kaminsky, R., *Antiplasmodial activity of knipholone and related natural phenylanthraquinones*. Planta medica, **1999**. 65(08): p. 757-758. doi.org/10.1055/s-2006-960859
23. Induli, M., Gebru, M., Abdissa, N., Akala, H., Wekesa, I., Byamukama, R., Heydenreich, M., Murunga, S., Dagne, E., and Yenesew, A., *Antiplasmodial Quinones from the Rhizomes of Kniphofia Foliosa*. Natural Product Communications, **2013**. 8(9): p. 1261-4. doi.org/10.1177/1934578x1300800920
24. Wube, A.A., Bucar, F., Asres, K., Gibbons, S., Rattray, L., and Croft, S.L., *Antimalarial compounds from Kniphofia foliosa roots*. Phytotherapy Research, **2005**. 19(6): p. 472-476. doi.org/10.1002/ptr.1635.
25. Alebachew, Y., Bisrat, D., Tadesse, S., and Asres, K., *In vivo anti-malarial activity of the hydroalcoholic extract of rhizomes of Kniphofia foliosa and its constituents*. Malaria Journal, **2021**. 20: p. 1-12. doi.org/10.1186/s12936-020-03552-7
26. Osman, C.P. and Ismail, N.H., *Antiplasmodial anthraquinones from medicinal plants: the chemistry and possible mode of actions*. Natural Product Communications, **2018**. 13(12): p. 1591-1597. doi.org/10.1177/1934578X1801301207

27. Sarma, M., Abdalla, M., Zothantluanga, J.H., Abdullah Thagfan, F., Umar, A.K., Chetia, D., Almanaa, T.N., and Al-Shouli, S.T., *Multi-target molecular dynamic simulations reveal glutathione-S-transferase as the most favorable drug target of knipholone in Plasmodium falciparum*. Journal of Biomolecular Structure and Dynamics, **2023**. 41(22): p. 12808-12824. doi.org/10.1080/07391102.2023.2175378
28. Bringmann, G., Mutanyatta-Comar, J., Maksimenka, K., Wanjohi, J.M., Heydenreich, M., Brun, R., Müller, W.E., Peter, M.G., Midiwo, J.O., and Yenesew, A., *Joziknipholones A and B: the first dimeric phenylanthraquinones, from the roots of Bulbine frutescens*. Chemistry–A European Journal, **2008**. 14(5): p. 1420-1429. doi.org/10.1002/chem.200701328.
29. Wube, A., Bucar, F., Asres, K., Gibbons, S., Adams, M., Streit, B., Bodensieck, A., and Bauer, R., *Knipholone, a selective inhibitor of leukotriene metabolism*. Phytomedicine, **2006**. 13(6): p. 452-456. doi.org/10.1016/j.phymed.2005.01.012.
30. Habtemariam, S., *Antioxidant activity of Knipholone anthrone*. Food Chemistry, **2007**. 102(4): p. 1042-1047. doi.org/10.1016/j.foodchem.2006.06.040
31. Habtemariam, S. and Dagne, E., *Prooxidant action of knipholone anthrone: Copper dependent reactive oxygen species generation and DNA damage*. Food and Chemical Toxicology, **2009**. 47(7): p. 1490-1494. doi.org/10.1016/j.fct.2009.03.032
32. Habtemariam, S., *Knipholone anthrone from Kniphofia foliosa induces a rapid onset of necrotic cell death in cancer cells*. Fitoterapia, **2010**. 81(8): p. 1013-1019. doi.org/10.1016/j.fitote.2010.06.021
33. Committee on Commodity Problems, , Current Market Situation and Medium Term Outlook, Twenty-third session of the Intergovernmental Group on Tea, May 2018, Hangzhou, China
34. Wang, K., Liu, F., Liu, Z., Huang, J., Xu, Z., Li, Y., Chen, J., Gong, Y., and Yang, X., *Comparison of catechins and volatile compounds among different types of tea using high performance liquid chromatograph and gas chromatograph mass spectrometer*. International Journal of Food Science & Technology, **2011**. 46(7): p. 1406-1412. doi.org/10.1111/j.1365-2621.2011.02629.x
35. Reygaert, W.C., *Green tea catechins: Their use in treating and preventing infectious diseases*. BioMed research international, **2018**. 2018(1). doi.org/10.1155/2018/9105261.
36. Renzetti, A., Betts, J.W., Fukumoto, K., and Rutherford, R.N., *Antibacterial green tea catechins from a molecular perspective: Mechanisms of action and structure–activity relationships*. Food & function, **2020**. 11(11): p. 9370-9396. doi.org/10.1039/d0fo02054k.
37. McNaught, J., *On the action of cold or lukewarm tea on Bacillus typhosus*. BMJ Military Health, **1906**. 7(4): p. 372-373. doi.org/10.1136/jramc-07-04-08
38. Mamede, L., Ledoux, A., Jansen, O., and Frédérick, M., *Natural Phenolic Compounds and Derivatives as Potential Antimalarial Agents*. Planta Med, **2020**. 86(9): p. 585-618. doi.org/10.1055/a-1148-9000



39. Yam, T., Hamilton-Miller, J., and Shah, S., *The effect of a component of tea (Camellia sinensis) on methicillin resistance, PBP2'synthesis, and beta-lactamase production in Staphylococcus aureus*. The Journal of antimicrobial chemotherapy, **1998**. 42(2): p. 211-216. doi.org/10.1093/jac/42.2.211
40. Yamada, H., Tateishi, M., Harada, K., Ohashi, T., Shimizu, T., Atsumi, T., Komagata, Y., Iijima, H., Komiyama, K., Watanabe, H., Hara, Y., and Ohashi, K., *A Randomized Clinical Study of Tea Catechin Inhalation Effects on Methicillin-Resistant Staphylococcus aureus in Disabled Elderly Patients*. Journal of the American Medical Directors Association, **2006**. 7(2): p. 79-83. doi.org/10.1016/j.jamda.2005.06.002
41. Fujii, M., Ohru, T., Sato, T., Sato, T., Sato, N., and Sasaki, H., *Green tea for decubitus ulcer in bedridden patients*. Geriatrics & Gerontology International, **2003**. 3(4): p. 208-211. doi.org/10.1111/j.1444-1586.2003.00101.x
42. Yamada, H., Ohashi, K., Atsumi, T., Okabe, H., Shimizu, T., Nishio, S., Li, X., Kosuge, K., Watanabe, H., and Hara, Y., *Effects of tea catechin inhalation on methicillin-resistant Staphylococcus aureus in elderly patients in a hospital ward*. Journal of Hospital Infection, **2003**. 53(3): p. 229-231. doi.org/10.1053/jhin.2002.1327
43. Yamashita, S., Yokoyama, K., Matsumiya, N., and Yamaguchi, H., *Successful green tea nebulization therapy for subglottic tracheal stenosis due to MRSA infection*. **2001**. doi.org/10.1053/jinf.2001.0766
44. Manach, C., Williamson, G., Morand, C., Scalbert, A., and Remesy, C., *Bioavailability and bioefficacy of polyphenols in humans. I. Review of 97 bioavailability studies*. Am J Clin Nutr, **2005**. 81(1 Suppl): p. 230S-242S. doi.org/10.1093/ajcn/81.1.230S
45. Trends in communicable and noncommunicable disease burden and control in Africa, WHO Regional Office for Africa; 2023. Licence: CC BY-NA-SA 3.0 IGO.
46. World Health Organization. The International Pharmacopoeia. Geneva: World Health Organization, Dept. of Essential Medicines and Pharmaceutical Policies, 2008.
47. *Global HIV & AIDS Statistics — 2024 Fact Sheet*. Joint United Nations Programme on HIV/AIDS 2024. <https://www.unaids.org/en/resources/fact-sheet>.
48. Mody, A., Sohn, A.H., Iwuji, C., Tan, R.K.J., Venter, F., and Geng, E.H., *HIV epidemiology, prevention, treatment, and implementation strategies for public health*. Lancet, **2024**. 403(10425): p. 471-492. doi.org/10.1016/s0140-6736(23)01381-8
49. German Advisory Committee Blood , S.A.o.P.T.b.B., *Human Immunodeficiency Virus (HIV)*. Transfusion Medicine and Hemotherapy, **2016**. 43(3): p. 203-222. doi.org/10.1159/000445852
50. Mbonye, U. and Karn, J., *The cell biology of HIV-1 latency and rebound*. Retrovirology, **2024**. 21(1): p. 6. doi.org/10.1186/s12977-024-00639-w
51. Surdo, M., Cortese, M.F., Orlandi, C., Di Santo, F., Aquaro, S., Magnani, M., Perno, C.F., Casabianca, A., and Ceccherini-Silberstein, F., *Different kinetics of viral replication and DNA integration in the main HIV-1 cellular*

- reservoirs in the presence and absence of integrase inhibitors*. Antiviral Res, **2018**. 160: p. 165-174. doi.org/10.1016/j.antiviral.2018.10.017
52. Ho, Y.C., Shan, L., Hosmane, N.N., Wang, J., Laskey, S.B., Rosenbloom, D.I., Lai, J., Blankson, J.N., Siliciano, J.D., and Siliciano, R.F., *Replication-competent noninduced proviruses in the latent reservoir increase barrier to HIV-1 cure*. Cell, **2013**. 155(3): p. 540-51. doi.org/10.1016/j.cell.2013.09.020
  53. Kuniholm, J., Coote, C., and Henderson, A.J., *Defective HIV-1 genomes and their potential impact on HIV pathogenesis*. Retrovirology, **2022**. 19(1): p. 13. doi.org/10.1186/s12977-022-00601-8
  54. Bai, R., Song, C., Lv, S., Chang, L., Hua, W., Weng, W., Wu, H., and Dai, L., *Role of microglia in HIV-1 infection*. AIDS Research and Therapy, **2023**. 20(1): p. 16. doi.org/10.1186/s12981-023-00511-5
  55. Gantner, P., Buranapraditkun, S., Pagliuzza, A., Dufour, C., Pardons, M., Mitchell, J.L., Kroon, E., Sacdalan, C., Tulmethakaan, N., Pinyakorn, S., *et al.*, *HIV rapidly targets a diverse pool of CD4(+) T cells to establish productive and latent infections*. Immunity, **2023**. 56(3): p. 653-668.e5. doi.org/10.1016/j.immuni.2023.01.030
  56. Siliciano, J.D., Kajdas, J., Finzi, D., Quinn, T.C., Chadwick, K., Margolick, J.B., Kovacs, C., Gange, S.J., and Siliciano, R.F., *Long-term follow-up studies confirm the stability of the latent reservoir for HIV-1 in resting CD4+ T cells*. Nat Med, **2003**. 9(6): p. 727-8. doi.org/10.1038/nm880
  57. Maldarelli, F., Wu, X., Su, L., Simonetti, F.R., Shao, W., Hill, S., Spindler, J., Ferris, A.L., Mellors, J.W., Kearney, M.F., Coffin, J.M., and Hughes, S.H., *HIV latency. Specific HIV integration sites are linked to clonal expansion and persistence of infected cells*. Science, **2014**. 345(6193): p. 179-83. doi.org/10.1126/science.1254194
  58. Murray, A.J., Kwon, K.J., Farber, D.L., and Siliciano, R.F., *The Latent Reservoir for HIV-1: How Immunologic Memory and Clonal Expansion Contribute to HIV-1 Persistence*. J Immunol, **2016**. 197(2): p. 407-17. doi.org/10.4049/jimmunol.1600343
  59. Richard, K. *Documentation and molecular analysis of African medicinal plants and naturally-produced chemical compounds that modulate latent HIV-1 infection*. Thesis: Simon Fraser University, **2022**
  60. HIV drug resistance: brief report 2024. Geneva: World Health Organization; 2024. Licence: CC BY-NC-SA 3.0 IGO.
  61. Gaebler, C., Nogueira, L., Stoffel, E., Oliveira, T.Y., Breton, G., Millard, K.G., Turroja, M., Butler, A., Ramos, V., and Seaman, M.S., *Prolonged viral suppression with anti-HIV-1 antibody therapy*. Nature, **2022**. 606(7913): p. 368-374. doi.org/10.1038/s41586-022-04597-1.
  62. Casazza, J.P., Cale, E.M., Narpala, S., Yamshchikov, G.V., Coates, E.E., Hendel, C.S., Novik, L., Holman, L.A., Widge, A.T., and Apte, P., *Safety and tolerability of AAV8 delivery of a broadly neutralizing antibody in adults living with HIV: a phase 1, dose-escalation trial*. Nature medicine, **2022**. 28(5): p. 1022-1030. doi.org/10.1038/s41591-022-01762-x.
  63. Mu, W., Carrillo, M.A., and Kitchen, S.G., *Engineering CAR T Cells to Target the HIV Reservoir*. Frontiers in Cellular and Infection Microbiology, **2020**. 10: p. 410. doi.org/10.3389/fcimb.2020.00410

64. Ding, J., Liu, Y., and Lai, Y., *Knowledge from London and Berlin: finding threads to a functional HIV cure*. Frontiers in Immunology, **2021**. 12. doi.org/10.3389/fimmu.2021.688747
65. Tebas, P., Jadlowsky, J.K., Shaw, P.A., Tian, L., Esparza, E., Brennan, A.L., Kim, S., Naing, S.Y., Richardson, M.W., and Vogel, A.N., *CCR5-edited CD4+ T cells augment HIV-specific immunity to enable post-rebound control of HIV replication*. The Journal of clinical investigation, **2024**. 131(7). doi.org/10.1172/JCI144486.
66. Mancuso, P., Chen, C., Kaminski, R., Gordon, J., Liao, S., Robinson, J.A., Smith, M.D., Liu, H., Sariyer, I.K., and Sariyer, R., *CRISPR based editing of SIV proviral DNA in ART treated non-human primates*. Nature communications, **2020**. 11(1): p. 6065. doi.org/10.1038/s41467-020-19821-7
67. Ahlenstiel, C.L., Symonds, G., Kent, S.J., and Kelleher, A.D., *Block and Lock HIV Cure Strategies to Control the Latent Reservoir*. Front Cell Infect Microbiol, **2020**. 10: p. 424. doi.org/10.3389/fcimb.2020.00424
68. Board, N.L., Moskovljevic, M., Wu, F., Siliciano, R.F., and Siliciano, J.D., *Engaging innate immunity in HIV-1 cure strategies*. Nature Reviews Immunology, **2022**. 22(8): p. 499-512. doi.org/10.1038/s41577-021-00649-1
69. Singh, V., Dashti, A., Mavigner, M., and Chahroudi, A., *Latency Reversal 2.0: Giving the Immune System a Seat at the Table*. Current HIV/AIDS Reports, **2021**. 18(2): p. 117-127. doi.org/10.1007/s11904-020-00540-z
70. Ngo, M.H., Pankrac, J., Ho, R.C., Ndashimye, E., Pawa, R., Ceccacci, R., Biru, T., Olabode, A.S., Klein, K., and Li, Y., *Effective and targeted latency reversal in CD4+ T cells from individuals on long term combined antiretroviral therapy initiated during chronic HIV-1 infection*. Emerging Microbes & Infections, **2024**. 13(1): p. 2327371. doi.org/10.1080/22221751.2024.2327371.
71. Wu, L., Zheng, Z., Xun, J., Liu, L., Wang, J., Zhang, X., Shao, Y., Shen, Y., Zhang, R., and Zhang, M., *Anti-PD-L1 antibody ASC22 in combination with a histone deacetylase inhibitor chidamide as a “shock and kill” strategy for ART-free virological control: a phase II single-arm study*. Signal Transduction and Targeted Therapy, **2024**. 9(1): p. 231. doi.org/10.1038/s41392-024-01943-9.
72. World malaria report 2023. Geneva: World Health Organization; 2023. Licence: CC BY-NC-SA 3.0 IGO.
73. Tu, Y., *The discovery of artemisinin (qinghaosu) and gifts from Chinese medicine*. Nature medicine, **2011**. 17(10): p. 1217-1220.
74. Bagcchi, S., *WHO's Global Tuberculosis Report 2022*. Lancet Microbe, **2023**. 4(1): p. e20. doi.org/10.1016/S2666-5247(22)00359-7
75. Robert-Koch-Institut, Bericht zur Epidemiologie der Tuberkulose in Deutschland für 2022, Berlin 2023, doi.org/10.25646/11180
76. Dartois, V. and Dick, T., *Therapeutic developments for tuberculosis and nontuberculous mycobacterial lung disease*. Nat Rev Drug Discov, **2024**. 23(5): p. 381-403. doi.org/10.1038/s41573-024-00897-5
77. Griffith, D.E., Aksamit, T., Brown-Elliott, B.A., Catanzaro, A., Daley, C., Gordin, F., Holland, S.M., Horsburgh, R., Huitt, G., and Iademarco, M.F.,

- An official ATS/IDSA statement: diagnosis, treatment, and prevention of nontuberculous mycobacterial diseases.* American journal of respiratory and critical care medicine, **2007**. 175(4): p. 367-416. doi.org/10.1164/rccm.200604-571ST
78. Abbew, E.T., Lorent, N., Mesic, A., Wachinou, A.P., Obiri-Yeboah, D., Decroo, T., Rigouts, L., and Lynen, L., *Challenges and knowledge gaps in the management of non-tuberculous mycobacterial pulmonary disease in sub-Saharan African countries with a high tuberculosis burden: a scoping review.* BMJ Open, **2024**. 14(1): p. e078818. doi.org/10.1136/bmjopen-2023-078818
  79. Pasipanodya, J.G., Ogbonna, D., Ferro, B.E., Magombedze, G., Srivastava, S., Deshpande, D., and Gumbo, T., *Systematic Review and Meta-analyses of the Effect of Chemotherapy on Pulmonary Mycobacterium abscessus Outcomes and Disease Recurrence.* Antimicrob Agents Chemother, **2017**. 61(11). doi.org/10.1128/AAC.01206-17
  80. Conradie, F., Diacon, A.H., Ngubane, N., Howell, P., Everitt, D., Crook, A.M., Mendel, C.M., Egizi, E., Moreira, J., Timm, J., et al., *Treatment of Highly Drug-Resistant Pulmonary Tuberculosis.* N Engl J Med, **2020**. 382(10): p. 893-902. doi.org/10.1056/NEJMoa1901814
  81. Kumar, K., Daley, C.L., Griffith, D.E., and Loebinger, M.R., *Management of Mycobacterium avium complex and Mycobacterium abscessus pulmonary disease: therapeutic advances and emerging treatments.* Eur Respir Rev, **2022**. 31(163). doi.org/10.1183/16000617.0212-2021.
  82. Griffith, D.E. and Daley, C.L., *Treatment of Mycobacterium abscessus Pulmonary Disease.* Chest, **2022**. 161(1): p. 64-75. doi.org/10.1016/j.chest.2021.07.035.
  83. European Centre for Disease Prevention and Control, WHO Regional Office for Europe. Tuberculosis surveillance and monitoring in Europe 2023 – 2021 data. Stockholm: European Centre for Disease Prevention and Control and Copenhagen: WHO Regional Office for Europe. 2023.
  84. Serge Marcial Bataliack et al. Health and well-being for all in the WHO African Region: a summary; Fact sheet April 2023
  85. data from 2019; [https://ec.europa.eu/eurostat/statistics-explained/index.php?title=Main\\_Page](https://ec.europa.eu/eurostat/statistics-explained/index.php?title=Main_Page); accessed on 04th September 2024
  86. Available online: <https://www.who.int/teams/global-tuberculosis-programme/tb-reports/global-tuberculosis-report-2023/tb-disease-burden/1-1-tb-incidence>; last accessed 04th September 2024
  87. Mirsaeidi, M. and Sadikot, R.T., *Gender susceptibility to mycobacterial infections in patients with non-CF bronchiectasis.* Int J Mycobacteriol, **2015**. 4(2): p. 92-6. doi.org/10.1016/j.ijmyco.2015.05.002
  88. Chan, E.D. and Iseman, M.D., *Slender, older women appear to be more susceptible to nontuberculous mycobacterial lung disease.* Gender medicine, **2010**. 7(1): p. 5-18. doi.org/10.1016/j.genm.2010.01.005.
  89. Okoi, C., Anderson, S.T.B., Antonio, M., Mulwa, S.N., Gehre, F., and Adetifa, I.M.O., *Non-tuberculous Mycobacteria isolated from Pulmonary samples in sub-Saharan Africa - A Systematic Review and Meta Analyses.* Sci Rep, **2017**. 7(1): p. 12002. doi.org/10.1038/s41598-017-12175-z

90. Winthrop, K.L., Marras, T.K., Adjemian, J., Zhang, H., Wang, P., and Zhang, Q., *Incidence and prevalence of nontuberculous mycobacterial lung disease in a large US managed care health plan, 2008–2015*. Annals of the American Thoracic Society, **2020**. 17(2): p. 178-185. doi.org/10.1513/AnnalsATS.201804-236OC.
91. Zhou, Y., Mu, W., Zhang, J., Wen, S.W., and Pakhale, S., *Global prevalence of non-tuberculous mycobacteria in adults with non-cystic fibrosis bronchiectasis 2006-2021: a systematic review and meta-analysis*. BMJ Open, **2022**. 12(8): p. e055672. doi.org/10.1136/bmjopen-2021-055672
92. Henkle, E. and Winthrop, K.L., *Nontuberculous Mycobacteria Infections in Immunosuppressed Hosts*. Clinics in Chest Medicine, **2015**. 36(1): p. 91-99. doi.org/10.1016/j.ccm.2014.11.002
93. Jain, D., Ghosh, S., Teixeira, L., and Mukhopadhyay, S., *Pathology of pulmonary tuberculosis and non-tuberculous mycobacterial lung disease: Facts, misconceptions, and practical tips for pathologists*. Seminars in Diagnostic Pathology, **2017**. 34(6): p. 518-529. doi.org/10.1053/j.semdp.2017.06.003
94. Kaya, F., Ernest, J.P., LoMauro, K., Gengenbacher, M., Madani, A., Aragaw, W.W., Zimmerman, M.D., Sarathy, J.P., Alvarez, N., and Daudelin, I., *A rabbit model to study antibiotic penetration at the site of infection for nontuberculous mycobacterial lung disease: macrolide case study*. Antimicrobial agents and chemotherapy, **2022**. 66(3): p. e02212-21. doi.org/10.1128/aac.02212-21.
95. Ramakrishnan, L., *Revisiting the role of the granuloma in tuberculosis*. Nature Reviews Immunology, **2012**. 12(5): p. 352-366. doi.org/10.1038/nri3211.
96. Lewinsohn, D.M., Leonard, M.K., LoBue, P.A., Cohn, D.L., Daley, C.L., Desmond, E., Keane, J., Lewinsohn, D.A., Loeffler, A.M., and Mazurek, G.H., *Official American Thoracic Society/Infectious Diseases Society of America/Centers for Disease Control and Prevention clinical practice guidelines: diagnosis of tuberculosis in adults and children*. Clinical Infectious Diseases, **2017**. 64(2): p. e1-e33. doi.org/10.1093/cid/ciw778.
97. Hunter, L., Hingley-Wilson, S., Stewart, G.R., Sharpe, S.A., and Salguero, F.J., *Dynamics of macrophage, T and B cell infiltration within pulmonary granulomas induced by Mycobacterium tuberculosis in two non-human primate models of aerosol infection*. Frontiers in immunology, **2022**. 12: p. 776913. doi.org/10.3389/fimmu.2021.776913.
98. Datta, M., Via, L.E., Kamoun, W.S., Liu, C., Chen, W., Seano, G., Weiner, D.M., Schimel, D., England, K., Martin, J.D., Gao, X., Xu, L., Barry, C.E., 3rd, and Jain, R.K., *Anti-vascular endothelial growth factor treatment normalizes tuberculosis granuloma vasculature and improves small molecule delivery*. Proc Natl Acad Sci U S A, **2015**. 112(6): p. 1827-32. doi.org/10.1073/pnas.1424563112
99. Van, N., Degefu, Y.N., Leus, P.A., Larkins-Ford, J., Klickstein, J., Maurer, F.P., Stone, D., Poonawala, H., Thorpe, C.M., Smith, T.C., 2nd, and Aldridge, B.B., *Novel Synergies and Isolate Specificities in the Drug Interaction Landscape of Mycobacterium abscessus*. Antimicrob Agents Chemother, **2023**. 67(7): p. e0009023. doi.org/10.1128/aac.00090-23

100. North, R.J. and Izzo, A.A., *Mycobacterial virulence. Virulent strains of Mycobacteria tuberculosis have faster in vivo doubling times and are better equipped to resist growth-inhibiting functions of macrophages in the presence and absence of specific immunity*. J Exp Med, **1993**. 177(6): p. 1723-33. doi.org/10.1084/jem.177.6.1723
101. Richards Jacob, P., Cai, W., Zill Nicholas, A., Zhang, W., and Ojha Anil, K., *Adaptation of Mycobacterium tuberculosis to Biofilm Growth Is Genetically Linked to Drug Tolerance*. Antimicrobial Agents and Chemotherapy, **2019**. 63(11). doi.org/10.1128/aac.01213-19
102. Fennelly, K.P., Ojano-Dirain, C., Yang, Q., Liu, L., Lu, L., Progulske-Fox, A., Wang, G.P., Antonelli, P., and Schultz, G., *Biofilm Formation by Mycobacterium abscessus in a Lung Cavity*. Am J Respir Crit Care Med, **2016**. 193(6): p. 692-3. doi.org/10.1164/rccm.201508-1586IM
103. Agarwal, P., Gordon, S., and Martinez, F.O., *Foam Cell Macrophages in Tuberculosis*. Front Immunol, **2021**. 12: p. 775326. doi.org/10.3389/fimmu.2021.775326
104. Roux, A.L., Viljoen, A., Bah, A., Simeone, R., Bernut, A., Laencina, L., Deramaudt, T., Rottman, M., Gaillard, J.L., Majlessi, L., et al., *The distinct fate of smooth and rough Mycobacterium abscessus variants inside macrophages*. Open Biol, **2016**. 6(11). doi.org/10.1098/rsob.160185
105. Bernut, A., Nguyen-Chi, M., Halloum, I., Herrmann, J.L., Lutfalla, G., and Kremer, L., *Mycobacterium abscessus-Induced Granuloma Formation Is Strictly Dependent on TNF Signaling and Neutrophil Trafficking*. PLoS Pathog, **2016**. 12(11). doi.org/10.1371/journal.ppat.1005986
106. Keefe, B.F. and Bermudez, L.E., *Environment in the lung of cystic fibrosis patients stimulates the expression of biofilm phenotype in Mycobacterium abscessus*. J Med Microbiol, **2022**. 71(1). doi.org/10.1099/jmm.0.001467
107. Redpath, S., Ghazal, P., and Gascoigne, N.R., *Hijacking and exploitation of IL-10 by intracellular pathogens*. Trends in microbiology, **2001**. 9(2): p. 86-92. doi.org/10.1016/s0966-842x(00)01919-3.
108. Boon, C. and Dick, T., *How Mycobacterium tuberculosis goes to sleep: the dormancy survival regulator DosR a decade later*. Future microbiology, **2012**. 7(4): p. 513-518. doi.org/10.2217/fmb.12.14.
109. Mehra, S., Foreman, T.W., Didier, P.J., Ahsan, M.H., Hudock, T.A., Kisse, R., Golden, N.A., Gautam, U.S., Johnson, A.-M., and Alvarez, X., *The DosR regulon modulates adaptive immunity and is essential for Mycobacterium tuberculosis persistence*. American journal of respiratory and critical care medicine, **2015**. 191(10): p. 1185-1196. doi.org/10.1164/rccm.201408-1502OC.
110. Simcox, B.S., Tomlinson, B.R., Shaw, L.N., and Rohde, K.H., *Mycobacterium abscessus DosRS two-component system controls a species-specific regulon required for adaptation to hypoxia*. Front Cell Infect Microbiol, **2023**. 13: p. 1144210. doi.org/10.3389/fcimb.2023.1144210
111. Belardinelli, J.M., Verma, D., Li, W., Avanzi, C., Wiersma, C.J., Williams, J.T., Johnson, B.K., Zimmerman, M., Whittel, N., Angala, B., et al., *Therapeutic efficacy of antimalarial drugs targeting DosRS signaling in*

- Mycobacterium abscessus*. Sci Transl Med, **2022**. 14(633). doi.org/10.1126/scitranslmed.abj3860
112. Wayne, L.G. and Sohaskey, C.D., *Nonreplicating persistence of Mycobacterium tuberculosis*. Annual Reviews in Microbiology, **2001**. 55(1): p. 139-163. doi.org/10.1146/annurev.micro.55.1.139.
  113. Wood, T.K., Knabel, S.J., and Kwan, B.W., *Bacterial persister cell formation and dormancy*. Appl Environ Microbiol, **2013**. 79(23): p. 7116-21. doi.org/10.1128/aem.02636-13
  114. Batyrshina, Y.R. and Schwartz, Y.S., *Modeling of Mycobacterium tuberculosis dormancy in bacterial cultures*. Tuberculosis (Edinb), **2019**. 117: p. 7-17. doi.org/10.1016/j.tube.2019.05.005
  115. Gibson, S.E.R., Harrison, J., and Cox, J.A.G., *Modelling a Silent Epidemic: A Review of the In Vitro Models of Latent Tuberculosis*. Pathogens, **2018**. 7(4). doi.org/10.3390/pathogens7040088
  116. Betts, J.C., Lukey, P.T., Robb, L.C., McAdam, R.A., and Duncan, K., *Evaluation of a nutrient starvation model of Mycobacterium tuberculosis persistence by gene and protein expression profiling*. Molecular microbiology, **2002**. 43(3): p. 717-731. doi.org/10.1046/j.1365-2958.2002.02779.x.
  117. Wayne, L.G. and Sramek, H.A., *Metronidazole is bactericidal to dormant cells of Mycobacterium tuberculosis*. Antimicrobial agents and chemotherapy, **1994**. 38(9): p. 2054-2058. doi.org/10.1128/AAC.38.9.2054.
  118. Loebel, R., Shorr, E., and Richardson, H., *The influence of foodstuffs upon the respiratory metabolism and growth of human tubercle bacilli*. Journal of bacteriology, **1933**. 26(2): p. 139-166. doi.org/10.1128/jb.26.2.139-166.1933
  119. Yam, Y.K., Alvarez, N., Go, M.L., and Dick, T., *Extreme Drug Tolerance of Mycobacterium abscessus "Persisters"*. Front Microbiol, **2020**. 11: p. 359. doi.org/10.3389/fmicb.2020.00359
  120. Berube, B.J., Castro, L., Russell, D., Ovechkina, Y., and Parish, T., *Novel Screen to Assess Bactericidal Activity of Compounds Against Non-replicating Mycobacterium abscessus*. Front Microbiol, **2018**. 9: p. 2417. doi.org/10.3389/fmicb.2018.02417
  121. Wayne, L.G. and Hayes, L.G., *An in vitro model for sequential study of shiftdown of Mycobacterium tuberculosis through two stages of nonreplicating persistence*. Infect Immun, **1996**. 64(6): p. 2062-9. doi.org/10.1128/iai.64.6.2062-2069.1996
  122. Lanni, A., Borroni, E., Iacobino, A., Russo, C., Gentile, L., Fattorini, L., and Giannoni, F., *Activity of Drug Combinations against Mycobacterium abscessus Grown in Aerobic and Hypoxic Conditions*. Microorganisms, **2022**. 10(7). doi.org/10.3390/microorganisms10071421
  123. Gengenbacher, M., Rao, S.P., Pethe, K., and Dick, T., *Nutrient-starved, non-replicating Mycobacterium tuberculosis requires respiration, ATP synthase and isocitrate lyase for maintenance of ATP homeostasis and viability*. Microbiology, **2010**. 156(1): p. 81-87. doi.org/10.1099/mic.0.033084-0.
  124. Lee, J., Ammerman, N., Agarwal, A., Naji, M., Li, S.Y., and Nuermberger, E., *Differential In Vitro Activities of Individual Drugs and Bedaquiline-*

- Rifabutin Combinations against Actively Multiplying and Nutrient-Starved Mycobacterium abscessus*. Antimicrob Agents Chemother, **2021**. 65(2). doi.org/10.1128/AAC.02179-20
125. Martins, O., Lee, J., Kaushik, A., Ammerman, N.C., Dooley, K.E., and Nuermberger, E.L., *In Vitro Activity of Bedaquiline and Imipenem against Actively Growing, Nutrient-Starved, and Intracellular Mycobacterium abscessus*. Antimicrob Agents Chemother, **2021**. 65(12): p. e0154521. doi.org/10.1128/AAC.01545-21.
  126. Wayne, L.G. and Lin, K.Y., *Glyoxylate metabolism and adaptation of Mycobacterium tuberculosis to survival under anaerobic conditions*. Infect Immun, **1982**. 37(3): p. 1042-9. doi.org/10.1128/iai.37.3.1042-1049.1982
  127. Jakkala, K. and Ajitkumar, P., *Hypoxic Non-replicating Persistent Mycobacterium tuberculosis Develops Thickened Outer Layer That Helps in Restricting Rifampicin Entry*. Front Microbiol, **2019**. 10: p. 2339. doi.org/10.3389/fmicb.2019.02339
  128. Khan, A. and Sarkar, D., *A simple whole cell based high throughput screening protocol using Mycobacterium bovis BCG for inhibitors against dormant and active tubercle bacilli*. J Microbiol Methods, **2008**. 73(1): p. 62-8. doi.org/10.1016/j.mimet.2008.01.015
  129. Cho, S.H., Warit, S., Wan, B., Hwang, C.H., Pauli, G.F., and Franzblau, S.G., *Low-oxygen-recovery assay for high-throughput screening of compounds against nonreplicating Mycobacterium tuberculosis*. Antimicrob Agents Chemother, **2007**. 51(4): p. 1380-5. doi.org/10.1128/AAC.00055-06
  130. Taneja, N.K. and Tyagi, J.S., *Resazurin reduction assays for screening of anti-tubercular compounds against dormant and actively growing Mycobacterium tuberculosis, Mycobacterium bovis BCG and Mycobacterium smegmatis*. Journal of antimicrobial chemotherapy, **2007**. 60(2): p. 288-293. doi.org/10.1093/jac/dkm207.
  131. Global tuberculosis report 2023. Geneva: World Health Organization; 2023. Licence: CC-BY-NC-SA 3.0 IGO
  132. Chiang, C.-H., Tang, P.-U., Lee, G.H., Chiang, T.-H., Chiang, C.-H., Ma, K.S.-K., and Fang, C.-T., *Prevalence of Nontuberculous Mycobacterium Infections versus Tuberculosis among Autopsied HIV Patients in Sub-Saharan Africa: A Systematic Review and Meta-Analysis*. The American Journal of Tropical Medicine and Hygiene, **2021**. 104(2): p. 628-633. doi.org/10.4269/ajtmh.20-0973
  133. Murray, C.J.L., Ikuta, K.S., Sharara, F., Swetschinski, L., Robles Aguilar, G., Gray, A., Han, C., Bisignano, C., Rao, P., Wool, E., et al., *Global burden of bacterial antimicrobial resistance in 2019: a systematic analysis*. The Lancet, **2022**. 399(10325): p. 629-655. doi.org/10.1016/S0140-6736(21)02724-0
  134. Boyce, J.M., Cookson, B., Christiansen, K., Hori, S., Vuopio-Varkila, J., Kocagöz, S., Öztop, A.Y., Vandenbroucke-Grauls, C.M.J.E., Harbarth, S., and Pittet, D., *Meticillin-resistant Staphylococcus aureus*. The Lancet Infectious Diseases, **2005**. 5(10): p. 653-663. doi.org/10.1016/S1473-3099(05)70243-7



135. taken from the website of global health issue on 21 june 2024; access through <https://www.globalforumhealth.org/About/10-90-gap/>
136. Stevens, P., *Diseases of poverty and the 10/90 Gap in: Fighting the Diseases of Poverty* (eds). **2008**.
137. Baker, S., *North-south publishing data show stark inequities in global research*. *Nature*, **2023**. 624(7991): p. S1. doi.org/10.1038/d41586-023-03901-x
138. Chirikure, N. and Naumann, L. *Imbalance of Power Towards Genuine Collaboration in International Research*. **2024**.
139. Bringmann, G., Menche, D., Kraus, J., Mühlbacher, J., Peters, K., Peters, E.-M., Brun, R., Bezabih, M., and Abegaz, B.M., *Atropo-Enantioselective Total Synthesis of Knipholone and Related Antiplasmodial Phenylanthraquinones*. *The Journal of Organic Chemistry*, **2002**. 67(16): p. 5595-5610. doi.org/10.1021/jo020189s
140. Van Duuren, B.L., Segal, A., Tseng, S.S., Rusch, G.M., Loewengart, G., Maté, U., Roth, D., Smith, A., Melchionne, S., and Seidman, I., *Structure and tumor-promoting activity of analogues of anthralin (1,8-dihydroxy-9-anthrone)*. *J Med Chem*, **1978**. 21(1): p. 26-31. doi.org/10.1021/jm00199a005
141. Ntie-Kang, F., Onguéné, P.A., Fotso, G.W., Andrae-Marobela, K., Bezabih, M., Ndom, J.C., Ngadjui, B.T., Ogundaini, A.O., Abegaz, B.M., and Meva'a, L.M., *Virtualizing the p-ANAPL Library: A Step towards Drug Discovery from African Medicinal Plants*. *PLOS ONE*, **2014**. 9(3). doi.org/10.1371/journal.pone.0090655
142. Hartkoorn, R.C., Sala, C., Neres, J., Pojer, F., Magnet, S., Mukherjee, R., Uplekar, S., Boy-Rottger, S., Altmann, K.H., and Cole, S.T., *Towards a new tuberculosis drug: pyridomycin - nature's isoniazid*. *EMBO Mol Med*, **2012**. 4(10): p. 1032-42. doi.org/10.1002/emmm.201201689
143. Franzblau, S.G., DeGroote, M.A., Cho, S.H., Andries, K., Nuermberger, E., Orme, I.M., Mdluli, K., Angulo-Barturen, I., Dick, T., Dartois, V., and Lenaerts, A.J., *Comprehensive analysis of methods used for the evaluation of compounds against Mycobacterium tuberculosis*. *Tuberculosis (Edinb)*, **2012**. 92(6): p. 453-88. doi.org/10.1016/j.tube.2012.07.003
144. Habtemariam, S. and Dagne, E., *Differential cytotoxic and prooxidant activity of knipholone and knipholone anthrone*. *Planta Med*, **2009**. 75(09): p. SL5. doi.org/10.1055/s-0029-1234260
145. Basco, L.K. and Le Bras, J., *In vitro activity of artemisinin derivatives against African isolates and clones of Plasmodium falciparum*. *Am J Trop Med Hyg*, **1993**. 49(3): p. 301-7. doi.org/10.4269/ajtmh.1993.49.301
146. Coates, A., Hu, Y., Bax, R., and Page, C., *The future challenges facing the development of new antimicrobial drugs*. *Nat Rev Drug Discov*, **2002**. 1(11): p. 895-910. doi.org/10.1038/nrd940
147. Wu, M.-L., Aziz, D.B., Dartois, V., and Dick, T., *NTM drug discovery: status, gaps and the way forward*. *Drug discovery today*, **2018**. 23(8): p. 1502-1519. doi.org/10.1016/j.drudis.2018.04.001.
148. Parker, C.A., *Anaerobiosis with iron wool*. *Aust J Exp Biol Med Sci*, **1955**. 33(1): p. 33-7. doi.org/10.1038/icb.1955.4

149. Lang, M., Ganapathy, U.S., Mann, L., Abdelaziz, R., Seidel, R.W., Goddard, R., Sequenzia, I., Hoenke, S., Schulze, P., Aragaw, W.W., Csuk, R., Dick, T., and Richter, A., *Synthesis and Characterization of Phenylalanine Amides Active against Mycobacterium abscessus and Other Mycobacteria*. J Med Chem, **2023**. 66(7): p. 5079-5098. doi.org/10.1021/acs.jmedchem.3c00009
150. Seidel, R.W., Goddard, R., Lang, M., and Richter, A., *Nalpa-Aroyl-N-Aryl-Phenylalanine Amides: A Promising Class of Antimycobacterial Agents Targeting the RNA Polymerase*. Chem Biodivers, **2024**. 21(6). doi.org/10.1002/cbdv.202400267
151. Beuchel, A., Robaa, D., Negatu, D.A., Madani, A., Alvarez, N., Zimmerman, M.D., Richter, A., Mann, L., Hoenke, S., Csuk, R., Dick, T., and Imming, P., *Structure-Activity Relationship of Anti-Mycobacterium abscessus Piperidine-4-carboxamides, a New Class of NBTI DNA Gyrase Inhibitors*. ACS Med Chem Lett, **2022**. 13(3): p. 417-427. doi.org/10.1021/acsmedchemlett.1c00549
152. Negatu, D.A., Beuchel, A., Madani, A., Alvarez, N., Chen, C., Aragaw, W.W., Zimmerman, M.D., Laleu, B., Gengenbacher, M., and Dartois, V., *Piperidine-4-carboxamides target DNA gyrase in Mycobacterium abscessus*. Antimicrobial agents and chemotherapy, **2021**. 65(8). doi.org/10.1128/aac.00676-21
153. Kamariza, M., Keyser, S.G.L., Utz, A., Knapp, B.D., Ealand, C., Ahn, G., Cambier, C.J., Chen, T., Kana, B., Huang, K.C., and Bertozzi, C.R., *Toward Point-of-Care Detection of Mycobacterium tuberculosis: A Brighter Solvatochromic Probe Detects Mycobacteria within Minutes*. JACS Au, **2021**. 1(9): p. 1368-1379. doi.org/10.1021/jacsau.1c00173
154. Mann, L., Siersleben, F., Lang, M., and Richter, A., *Determination of bactericidal activity against 3HC-2-Tre-labelled Mycobacterium abscessus (Mycobacteroides abscessus) by automated fluorescence microscopy*. J Microbiol Methods, **2024**. 224: p. 107002. doi.org/10.1016/j.mimet.2024.107002
155. Van, N., Degefu, Y.N., and Aldridge, B.B., *Efficient Measurement of Drug Interactions with DiaMOND (Diagonal Measurement of N-Way Drug Interactions)*. Methods Mol Biol, **2021**. 2314: p. 703-713. doi.org/10.1007/978-1-0716-1460-0\_30.
156. Courbon, G.M., Palme, P.R., Mann, L., Richter, A., Imming, P., and Rubinstein, J.L., *Mechanism of mycobacterial ATP synthase inhibition by squaramides and second generation diarylquinolines*. The EMBO Journal, **2023**. 42(15): p. e113687. doi.org/10.15252/emj.2023113687
157. Tantry, S.J., Markad, S.D., Shinde, V., Bhat, J., Balakrishnan, G., Gupta, A.K., Ambady, A., Raichurkar, A., Kedari, C., and Sharma, S., *Discovery of imidazo [1, 2-a] pyridine ethers and squaramides as selective and potent inhibitors of mycobacterial adenosine triphosphate (ATP) synthesis*. Journal of medicinal chemistry, **2017**. 60(4): p. 1379-1399. doi.org/10.1021/acs.jmedchem.6b01358
158. Rominski, A., Roditscheff, A., Selchow, P., Böttger, E.C., and Sander, P., *Intrinsic rifamycin resistance of Mycobacterium abscessus is mediated by ADP-ribosyltransferase MAB\_0591*. Journal of Antimicrobial Chemotherapy, **2017**. 72(2): p. 376-384. doi.org/10.1093/jac/dkw466.

159. Aziz, D.B., Low, J.L., Wu, M.-L., Gengenbacher, M., Teo, J.W., Dartois, V., and Dick, T., *Rifabutin is active against Mycobacterium abscessus complex*. Antimicrobial agents and Chemotherapy, **2017**. 61(6): p. 10.1128/aac.00155-17. doi.org/10.1128/AAC.00155-17.
160. Xie, M., Ganapathy, U.S., Lan, T., Osiecki, P., Sarathy, J.P., Dartois, V., Aldrich, C.C., and Dick, T., *ADP-ribosylation-resistant rifabutin analogs show improved bactericidal activity against drug-tolerant M. abscessus in caseum surrogate*. Antimicrob Agents Chemother, **2023**. 67(9). doi.org/10.1128/aac.00381-23
161. Sarathy, J., Dartois, V., Dick, T., and Gengenbacher, M., *Reduced drug uptake in phenotypically resistant nutrient-starved nonreplicating Mycobacterium tuberculosis*. Antimicrobial agents and chemotherapy, **2013**. 57(4): p. 1648-1653. doi.org/10.1128/AAC.02202-12.
162. Du, P., Sohaskey, C.D., and Shi, L., *Transcriptional and Physiological Changes during Mycobacterium tuberculosis Reactivation from Non-replicating Persistence*. Front Microbiol, **2016**. 7: p. 1346. doi.org/10.3389/fmicb.2016.01346
163. Mulyukin, A.L., Recchia, D., Kostrikina, N.A., Artyukhina, M.V., Martini, B.A., Stamilla, A., Degiacomi, G., and Salina, E.G., *Distinct Effects of Moxifloxacin and Bedaquiline on Growing and 'Non-Culturable' Mycobacterium abscessus*. Microorganisms, **2023**. 11(11). doi.org/10.3390/microorganisms11112690



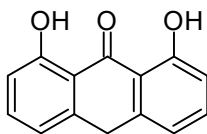
## 6) Appendices

### 6.1) Experimental part of unpublished results

#### 6.1.1) *Synthesis and chemical characterization of compounds*

All synthesized compounds were described in literature before. We therefore compared chemical characteristics with reported values to confirm their structure and abstained from additional high-resolution mass spectrometry determination.

Melting points were determined using a hot-stage microscopy system from Boëtius and are reported as uncorrected values.  $^1\text{H}$ -NMR experiments were recorded on a Varian Gemini 2000 (400 MHz für  $^1\text{H}$ -NMR) or on a Varian Inova 500 (500 MHz für  $^1\text{H}$  NMR). APCI mass spectrometry was done using an Advion Expression<sup>S</sup> (CMS) mass spectrometer (Advion, Inc., Ithaca, NY, USA). The compounds were dissolved in methanol and measured with the ASAP measuring unit. ESI mass spectrometry was measured using an LCQ-Classic-Spectrometer from Thermo Finnigan (San Jose, CA, USA). For the measurements a capillary temperature of 220°C, a voltage of 4.5 kV and a scan range from 50-2000 were used. The compounds were dissolved in methanol prior to measurement. Thin-layer chromatography was done for the determination of  $R_f$  values on ALUGRAM® SIL G/UV254-plates from Merck or Macherey-Nagel (that were coated with 0.2 mm of silica gel 60) and detected with a UV lamp at 254 nm or 365 nm or in an iodine chamber.

1,8 dihydroxy-9-(10*H*)-anthrone (anthralin, **AN1**)

2.1 mmol chrysazin/**AQ1** (danthron, sigma Aldrich) (500 mg) were dissolved in 60 mL acetic acid and refluxed. A solution of 39.2 mmol SnCl<sub>2</sub> (7.4 g) in 37 % HCl (15.5 mL) was added over a period of 3 h using a dropping funnel. The solution was allowed to cool down over night while yellow crystals crushed out. The precipitate was separated by filtration and the remaining solution was further concentrated to allow further precipitation of **AN1**. The combined batches of **AN1** were dried in a desiccator using phosphor pentoxide.

yellow solid

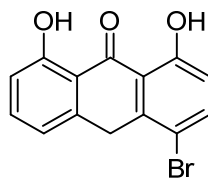
yield 466 mg (95 %)

melting point: 178-181°C

<sup>1</sup>H-NMR (400 MHz, CDCl<sub>3</sub>): δ 12.28 (s, 2H), 7.48 (t, *J* = 8.0 Hz, 2H), 6.94 – 6.86 (m, 4H), 4.35 (d, *J* = 1.4 Hz, 2H)

MS (APCI) *m/z* 227,1 [M+H]<sup>+</sup>

R<sub>f</sub>(dichloromethane): 0.58

4-Bromo-1,8-dihydroxyanthrone (4-bromoanthralin, **AN2**)

8.84 mmol of **AN1** (2 g) were dissolved in a mixture of acetic acid, chloroform and ethanol (160 mL + 30 mL + 30 mL) and cooled to 0-5°C using an ice bath. 7.07 mmol bromine (0.35 mL) were dissolved in 10 mL of chloroform and slowly (drop by drop) added to dissolved **AN1** with a dropping funnel. Reaction mixture color should have turned to light orange, indicating less bromine in the mixture before adding more bromine. The solution was allowed to stir over night and the precipitate was removed from the supernatant by filtration. Remaining bromine in the filtrate was reduced by adding an aqueous solution of Na<sub>2</sub>S<sub>2</sub>O<sub>3</sub>. The aqueous phase was extracted three times with chloroform, the organic phases combined and dried with MgSO<sub>4</sub>. The obtained organic phases were concentrated using a rotary evaporator and the precipitate was allowed to form in the cold. Filtration yielded a mixture of **AN1** and **AN2** that were separated by repeated column chromatography (silica gel, heptane). Because separation of **AN1** and **AN2** was difficult, only 20 % could be obtained in sufficient purity.

bright yellow solid

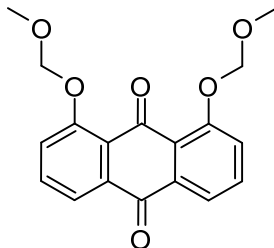
yield 550 mg (20 %)

melting point: 166-169°C

<sup>1</sup>H-NMR (400 MHz) δ 12.52 (s, 1H), 12.13 (s, 1H), 7.71 (d, *J* = 8.9 Hz, 1H), 7.54 (t, *J* = 8.0 Hz, 1H), 6.99 (dq, *J* = 7.5, 1.1 Hz, 1H), 6.93 (dq, *J* = 8.4, 0.9 Hz, 1H), 6.88 (dt, *J* = 8.9, 0.8 Hz, 1H), 4.29 – 4.24 (m, 2H)

MS (APCI) *m/z* 304.9 [M(<sup>79</sup>Br)+H]<sup>+</sup>

R<sub>f</sub> (heptane/ethyl acetate 8:2): 0.49

1,8-bis-(methoxymethoxy)-anthraquinone (AQ2)

1 mmol chrysazine/**AQ1** (danthrone, Sigma Aldrich) (240 mg) were dispersed in 6 mL of chloroform. 18 mmol of *N,N*-diisopropylethylamine (DIPEA, abcr chemicals) (3 mL) and 12 mmol of chloromethyl methyl ether (1 mL) were added. The mixture was refluxed for 22 h and subsequently allowed to cool down. The organic solution was washed three times with 1 M NaOH and one time with brine. The combined organic phases were dried with MgSO<sub>4</sub>, filtrated and the filtrate concentrated using a rotary evaporator. The obtained solid was washed again using 1 M NaOH and pure ethanol and subsequently dried in a desiccator using P<sub>2</sub>O<sub>5</sub>.

yellow solid

yield 290 mg (88 %)

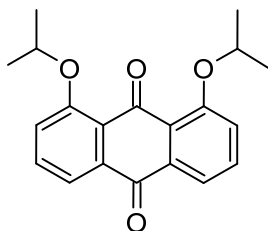
melting point: 149-153°C

<sup>1</sup>H-NMR (400 MHz, CDCl<sub>3</sub>) δ 7.92 (dd, *J* = 7.5, 1.3 Hz, 2H), 7.62 (dd, *J* = 8.4, 7.5 Hz, 2H), 7.56 (dd, *J* = 8.4, 1.3 Hz, 2H), 5.38 (s, 4H), 3.57 (s, 6H)

MS (ESI) *m/z* 351.80 [M+Na]<sup>+</sup>

R<sub>f</sub> (heptane/ethyl acetate 8:3): 0.15



1,8-diisopropoxyanthracene-9,10-dione, **AQ3**

12.5 mmol chrysazin/**AQ1** (danthron, Sigma Aldrich) (3 g) were suspended in a mixture of anhydrous acetone and DMF (60 mL + 20 mL). 56 mmol (18.2 g) anhydrous  $\text{Cs}_2\text{CO}_3$  and 43 mmol (4.3 mL) 2-iodopropane were added. The mixture was refluxed for 2 days under argon while the apparatus was covered with alumina foil to protect the reaction mixture from light. Thereafter, the mixture was filtrated to separate unreacted danthron from the filtrate. The precipitate was washed twice with acetone. Combined filtrates were then concentrated using a rotary evaporator and further purified by column chromatography (heptane/ ethyl acetate 5-20 %).

yellow fibrous solid

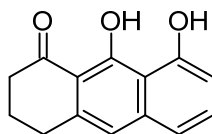
yield: 2.07 g (51 %)

melting point: 95-100°C

$^1\text{H}$  NMR (400 MHz,  $\text{CDCl}_3$ )  $\delta$  7.81 (dd,  $J$  = 7.7, 1.1 Hz, 2H), 7.56 (dd,  $J$  = 8.3, 7.7 Hz, 2H), 7.29 (ddd,  $J$  = 8.4, 4.3, 1.1 Hz, 2H), 4.61 (p,  $J$  = 6.1 Hz, 2H), 1.44 (d,  $J$  = 6.0 Hz, 12H).

MS(APCI)  $m/z$  325.2  $[\text{M}+\text{H}]^+$

$R_f$  (heptane/ethyl acetate 8:2): 0.25

8,9 dihydroxy-3,4-dihydro-2H-anthracen-1-on **AC1**

13.3 mmol **AN1** (3 g) were dissolved in 50 mL of 4 % aqueous NaOH and 4 g of Raney-Nickel (50 % w/w, Sigma Aldrich) were added. The mixture was hydrated with molecular hydrogen at 50 psi (3.5 bar) over night. The mixture was filtered using a small amount of silica gel and the precipitate was recrystallized with ethyl acetate.

brown solid

yield: 752 mg (24.8 %)

melting point: 123°C

$^1\text{H-NMR}$  (400 MHz,  $\text{CDCl}_3$ ):  $\delta$  9.76 (d,  $J$  = 0.8 Hz, 1H), 7.46 (t,  $J$  = 7.9 Hz, 1H), 7.12 (dd,  $J$  = 8.1, 1.0 Hz, 1H), 7.00 – 6.95 (m, 1H), 6.82 (dd,  $J$  = 7.8, 1.0 Hz, 1H), 2.97 (ddd,  $J$  = 7.4, 5.7, 1.3 Hz, 2H), 2.76 (dd,  $J$  = 6.8, 6.1 Hz, 2H), 2.12 (tt,  $J$  = 7.1, 5.6 Hz, 2H)

MS (ESI)  $m/z$  227.5  $[\text{M-H}]^-$

R<sub>f</sub> (DCM/heptane 1:1): 0.48

### **6.1.2) Agar Diffusion Test as a First Determination of Anti-Infective Activities on Different Microorganisms**

Agar diffusion tests were performed at the Hans-Knöll-Institute in Jena under the supervision of DR. VOIGT. The procedure followed a German microbiological guideline (DIN-Norm 58940-8, 2002). In brief, holes were pinched into sterile agar plates and filled with a stock solution of the desired compound. The desired microorganism was spread onto the plate and plates were incubated according to conditions for the respective species. After the specified time, plates were analyzed for zones of inhibition around the holes and interpreted following the cut off values in the guideline. Values > 15 mm (diameter of zone of inhibition) were designated as active, those < 15 mm as inactive.

### **6.1.3) Experiments on Starvation Models**

Working stocks were handled as described in **publication IV**. A culture in exponential growth phase was washed twice with PBS containing 0.05 % tyloxapol (6500 rpm, 5 min) and then incubated in a sufficient amount of PBS supplemented with 0.05 % tyloxapol for 24 h to use up any remaining glucose. Thereafter an inoculum of  $5 \times 10^5$  CFU/mL was prepared using the desired volume of PBS supplemented with 0.05 % tyloxapol and distributed in a microtiter plate. The plate was incubated at 37 °C in aerobic conditions (5 % CO<sub>2</sub>) for six days. Thereafter, all wells were well mixed and 2 µL of each well were transferred to a microtiter plate containing 198 µL of 7H9 suppl. with 10 % ADS and incubated at 37 °C in aerobic conditions (5 % CO<sub>2</sub>). At certain points in time, 2 µL of a 10 mM DMSO solution of the dye (see **publication IV**) were added to indicated wells, mixed very well and incubated further for 2.5 h. Thereafter, stained wells were mixed again and 2 µL were transferred into a microtiter plate containing 198 µL PFA and evaluated by automatic object count using the method described in **publication IV**.

To combine starvation and hypoxia in one experiment, the procedure described above was adjusted in the following aspects. The microtiter plate containing the distributed inoculum in PBS supplemented with 0.5 % tyloxapol was incubated for six days in the hypoxic chamber described in **publication IV** instead. All other steps were kept the same.

## 6.2) Supplementary Information Publication I

### Supplementary Materials

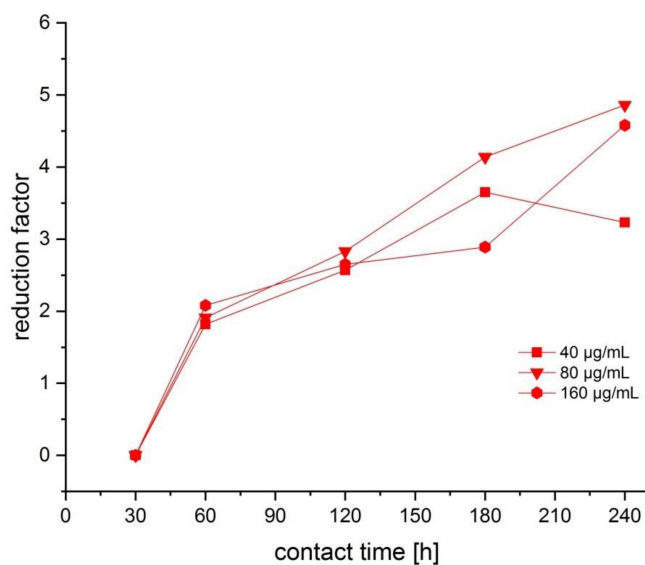


**Figure S1.** Effect of GTE on reduction factor of MSSA ATCC 43300 at tested concentrations.

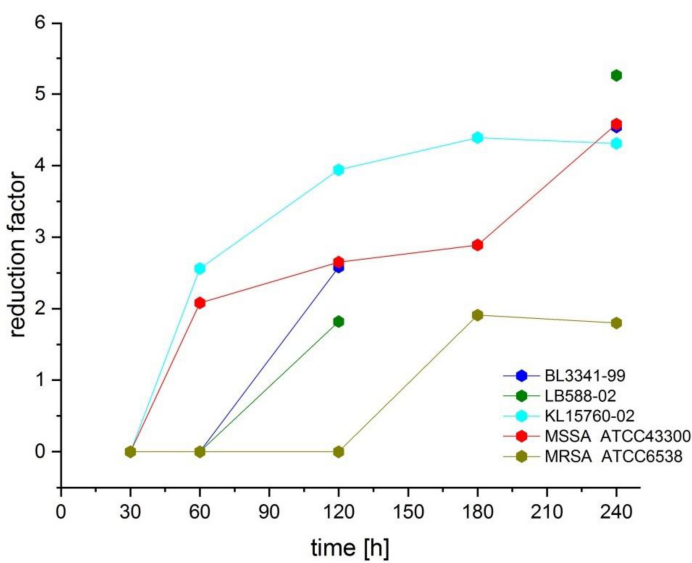


**Figure S2.** Time-kill-plot for GTE with 160 µg/mL EGCG content for the tested strains.

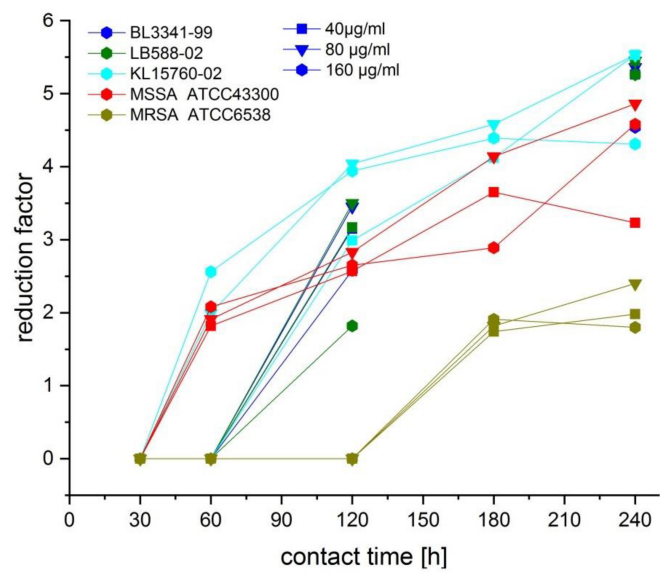
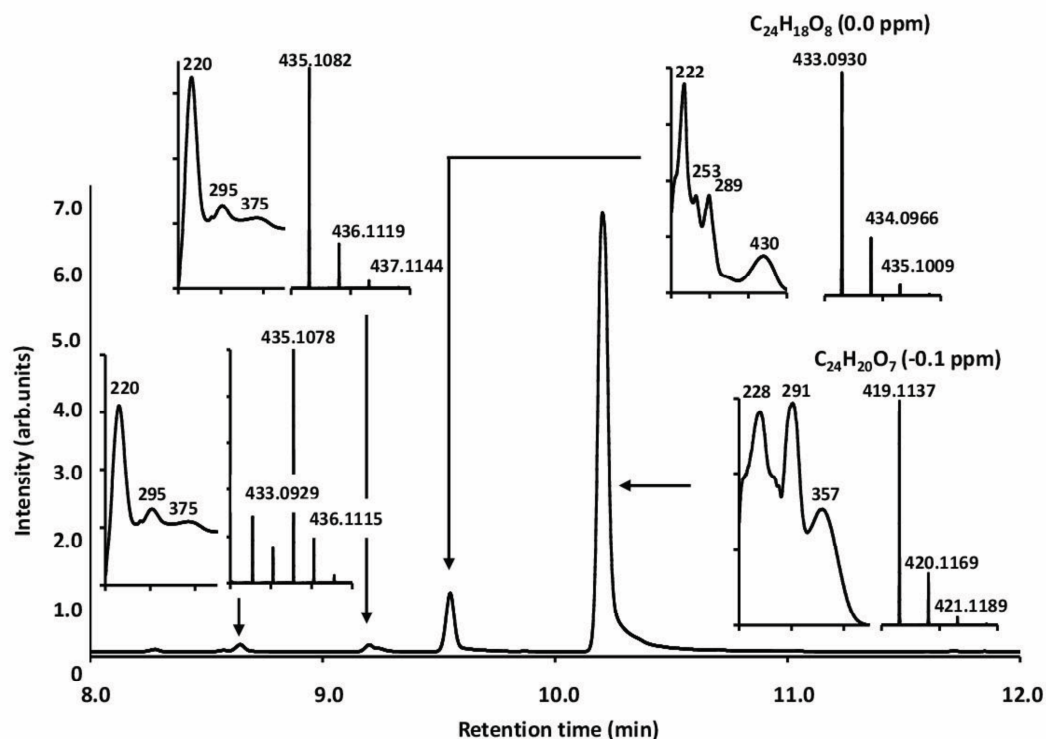
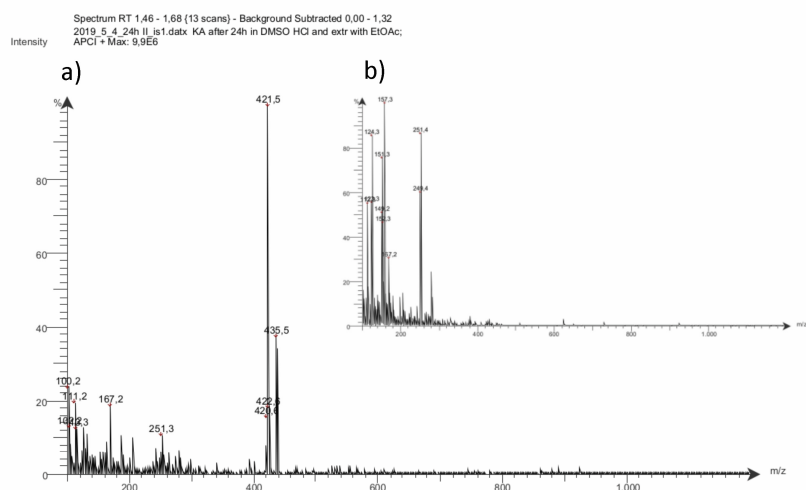


Figure S3. Overview of results for the time-kill-plot experiment.





**Figure S2:** UHPLC-ESI-QqTOF-MS of knipholone anthrone (**2**) used in this work



**Figure S3:** a) APCI-MS spectrum of knipholone anthrone (**2**) after 24 h incubation in DMSO and kept in the dark (extracted with ethyl acetate after addition of 1 N HCl). Minor peaks arise from solvent impurities: see b) APCI-MS spectrum of ethyl acetate used for extraction

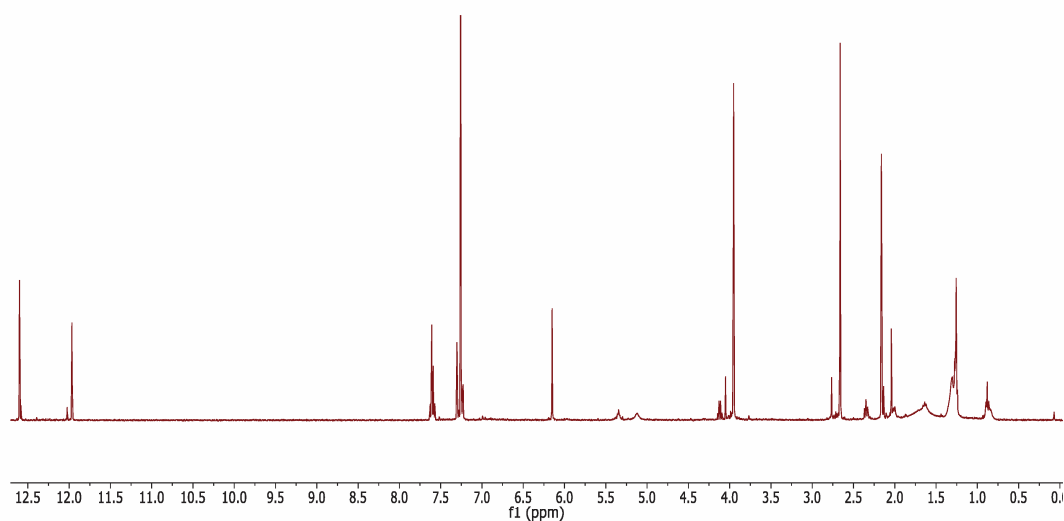


**Figure S4:**  $^1\text{H}$  NMR (400 MHz, Chloroform- $d$ ) of knipholone (**1**)

$\delta_{\text{H}}$  12.60 (s, 1H), 11.97 (s, 1H), 7.64 – 7.56 (m, 2H), 7.30 (d,  $J = 1.0$  Hz, 1H), 7.23 (d,  $J = 2.0$  Hz, 1H), 6.15 (s, 1H), 3.95 (s, 3H), 2.66 (s, 3H), 2.16 (d,  $J = 0.8$  Hz, 3H).

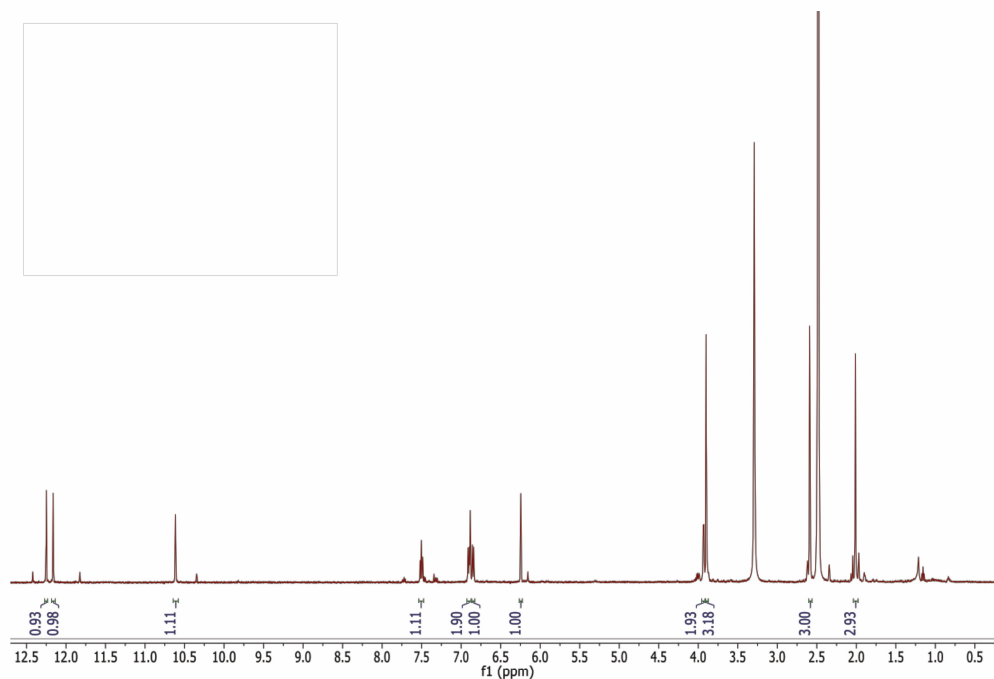


**Figure S5:**  $^1\text{H}$  NMR (500 MHz, DMSO- $d_6$ ) of knipholone anthrone (**2**)

$\delta_{\text{H}}$  12.25 (s, 1H), 12.16 (s, 1H), 10.62 (s, 1H), 7.50 (t,  $J = 7.9$  Hz, 1H), 6.93 – 6.88 (m, 2H), 6.87 – 6.83 (m, 1H), 6.25 (s, 1H), 3.93 (d,  $J = 4.7$  Hz, 2H), 3.90 (s, 3H), 2.59 (s, 3H), 2.01 (s, 3H).



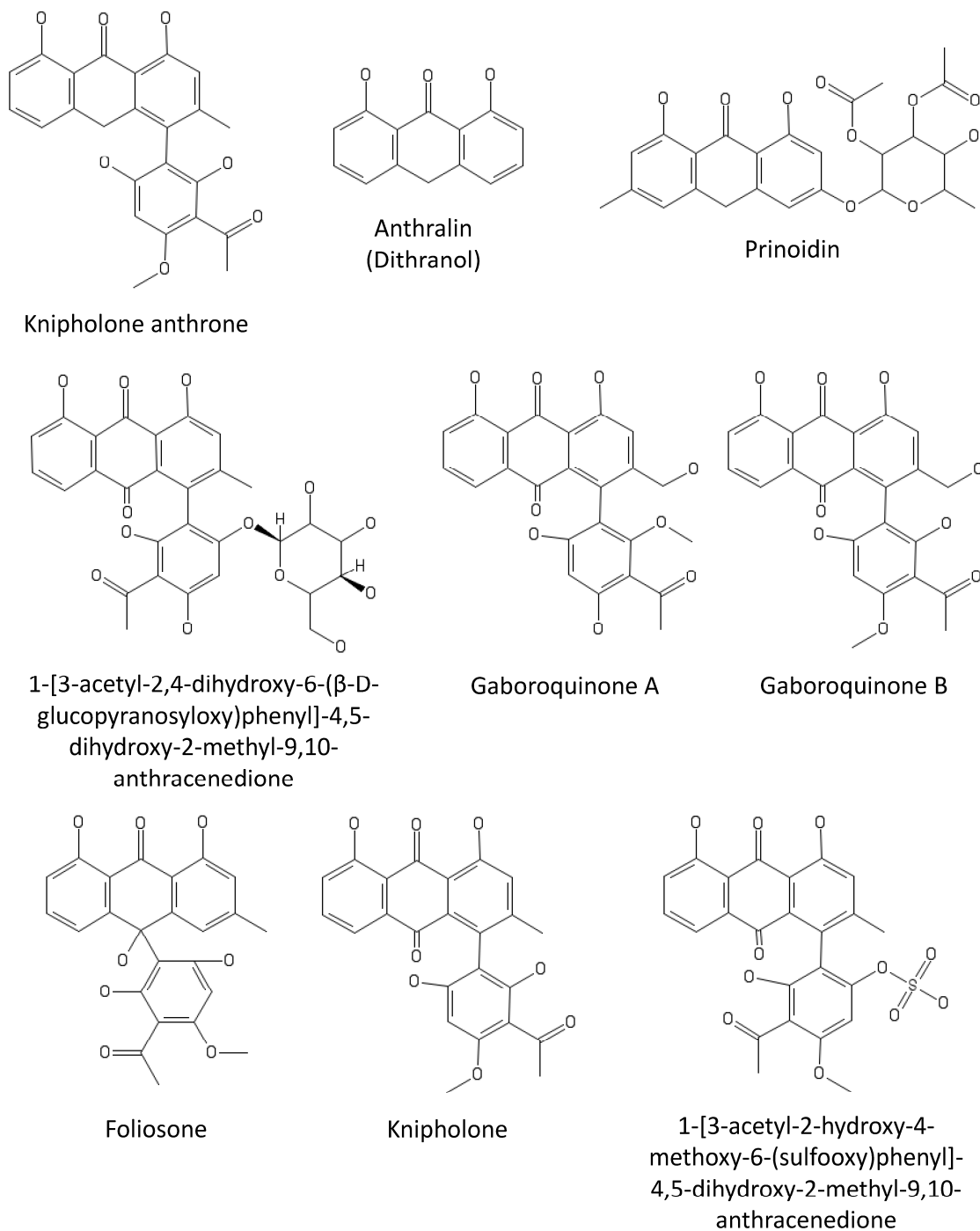
***UHPLC-ESI-QqTOF-MS***: The samples (2  $\mu$ L) were loaded on an Acquity UPLC<sup>®</sup> reversed phase BEH<sup>™</sup> column (C<sub>18</sub>-phase, ID 0.1 mm, length 50 mm, particle size 1.7  $\mu$ m, Waters GmbH, Eschborn, Germany) under isocratic conditions (3% eluent B, 1 min) and separated in a linear gradient from 3 to 95% eluent B in 15 min. Separation was performed on an ACQUITY UPLC I-Class UHPLC System (Waters GmbH, Eschborn, Germany) with a flow rate of 0.3 mL/min and 50 °C column temperature. The eluents A and B were water and acetonitrile with 0.1% (v/v) formic acid, respectively. The column effluent was introduced on-line into a photodiode array detector (PDA, 190 – 600 nm, sampling rate 20 Hz with a single wavelength acquisition at 290 nm) and further in a TripleTOF 6600 QqTOF mass spectrometer equipped with a DuoSpray ESI/APCI ion source, operating in negative ion mode and controlled by the Analyst TF 1.7.1 software (AB Sciex GmbH, Darmstadt, Germany). The spectra were acquired in the  $m/z$  range of 100 to 1000 (accumulation time 50 ms) with an ion spray voltage of 5.5 kV and 450 °C source temperature. Nebulizer and drying gases were set to 60 and 70 psi, respectively, whereas the curtain gas was set to 55 psi. Declustering (DP) and collision (CE) potentials were 35 and 10 V, respectively. The data were evaluated by Peak View 1.2.0.3 software (AB Sciex GmbH, Darmstadt, Germany).

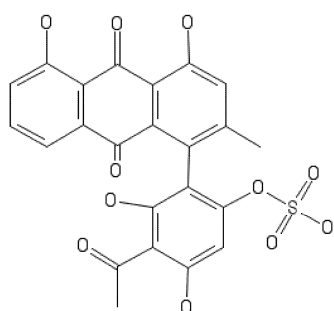
## 6.4) Supplementary Information Publication III

**Supplemental Table 1.** Absolute copies of HIV RNA per million cells, estimated number of cells assessed per qPCR reaction, and limit of detection of *ex vivo* studies in Figure 8B, as determined by qPCR of viral RNA and 18S housekeeping gene and normalized to copy number standards.

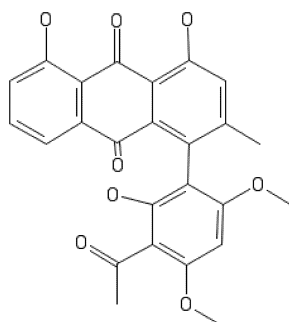
Donor	Treatment	Absolute copies of HIV RNA per million cells	Total # of cells analyzed	Limit of detection
1	0.1% DMSO	< 76	13,124	76
	100 ng/mL PMA + 0.1 µg/mL ionomycin	< 50	20,075	50
	10 µM prostratin	< 54	18,687	54
	10 µM KA	8633	14,630	68
2	0.1% DMSO	626	27,953	36
	100 ng/mL PMA + 0.1 µg/mL ionomycin	1008	30,172	33
	10 µM prostratin	1181	35,139	28
	10 µM KA	846	28,836	35
3	0.1% DMSO	602	279,932	4
	100 ng/mL PMA + 0.1 µg/mL ionomycin	672	732,347	1
	10 µM prostratin	1514	308,599	3
	10 µM KA	617	400,645	2
Average ± SD	0.1% DMSO	435 ± 311		
	100 ng/mL PMA + 0.1 µg/mL ionomycin	576 ± 486		
	10 µM prostratin	916 ± 765		
	10 µM KA	3365 ± 4563		

**Supplemental Figure 1.** Structures of all anthrones assessed for in vitro HIV latency reversal.

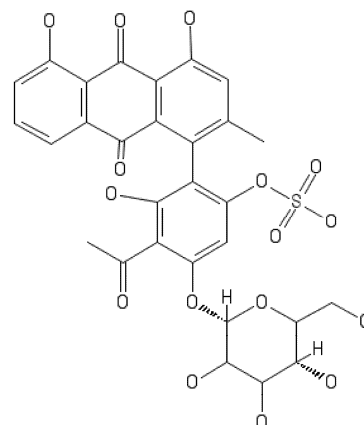




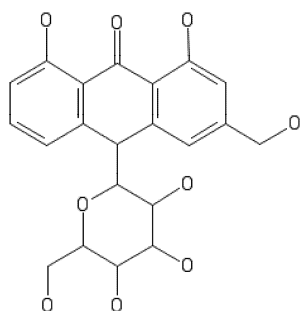
1-[3-acetyl-2,4-dihydroxy-6-(sulfooxy)phenyl]-4,5-dihydroxy-2-methyl-9,10-anthracenedione



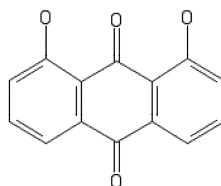
Knipholone 6'-methyl ether



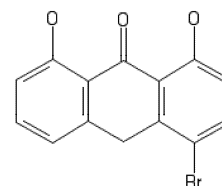
1-[3-acetyl-4-(β-D-glucopyranosyloxy)-2-hydroxy-6-(sulfooxy)phenyl]-4,5-dihydroxy-2-methyl-9,10-anthracenedione



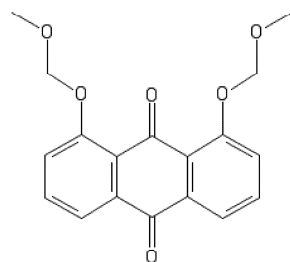
Aloin



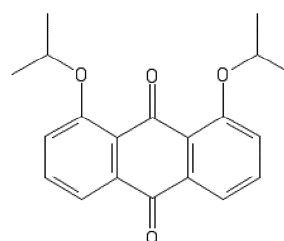
Danthron



4-Bromo-1,8-dihydroxy-10H-anthracen-9-one



1,8-Bis(methoxy)anthracene-9,10-dione



1,8-Diisopropoxyanthracene-9,10-dione

## 6.5) Supplementary Information Publication IV

### A simple *in vitro* method to determine bactericidal activity against *Mycobacterium abscessus* under hypoxic conditions

#### Supplementary Information

Ruth Feilcke, Robert Eckenstaler, Markus Lang, Adrian Richter<sup>1</sup>, Peter Imming<sup>2</sup>

Institut für Pharmazie, Martin-Luther-Universität Halle-Wittenberg, Wolfgang-Langenbeck-Straße 4  
06120 Halle

<sup>1</sup>corresponding author [adrian.richter@pharmazie.uni-halle.de](mailto:adrian.richter@pharmazie.uni-halle.de)

<sup>2</sup>corresponding author [peter.imming@pharmazie.uni-halle.de](mailto:peter.imming@pharmazie.uni-halle.de)

#### Table of content

Figure S1: Picture of *M. abscessus* LOP assay set up in a common anaerobic pot.

Figure S2: Picture of *M. abscessus* LOP assay set up in hypoxic box in our laboratory.

Figure S3: Oxygen levels in aerobe medium and different parts of the hypoxic set up.

Figure S4: Representative selection of *M. abscessus* cells incubated under aerobe (A) and hypoxic (B) conditions.



Figure S 1: Hypoxic chamber for the investigation on *M. abscessus* LOPs in an anaerobic pot, commonly used in culturing anaerobic bacteria on solid medium. Due to the round shape, the set up needs to be performed in a lying position and vials with indicator (top, right side) and carbonate solution (bottom, right side) are placed in a tray to avoid tipping over. The activated iron wool is placed in an extra tray (to prevent contamination by oxidation products) on top of the microtiter plates. Due to the unfavourable shape, this set up takes up a lot of space, but it can be used if no other airtight boxes are available.

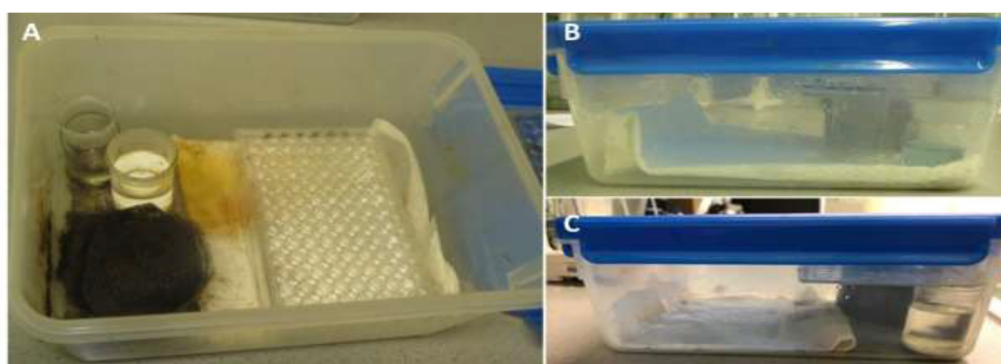


Figure S 2: Set up for *M. abscessus* LOP assay in our laboratory. A square plastic box with a "lock-n-lock" lid (equipped with rubber to ensure airtight sealing) is used as hypoxic chamber. (A) A microtiter plate, a glass vial with stabilized MB solution (top left), a glass vial with saturated carbonate solution (middle left) and activated iron wool (bottom left), placed in a crystallizing dish to hold the access copper sulphate solution, are placed next to each other in the box. If several plates are investigated at once, these can be stacked on each other. (B) Hypoxic chamber immediately after closing (MB still blue). (C) Hypoxic chamber after onset of hypoxic conditions (MB decolorized). The lid on top of the glass vials and the iron wool is a protection to prevent contamination of the microtiter plates by the oxidation products of the activated iron wool, in case of plates being stacked on top of the vials as well. A maximum of 6 microtiter plates can be examined simultaneously.

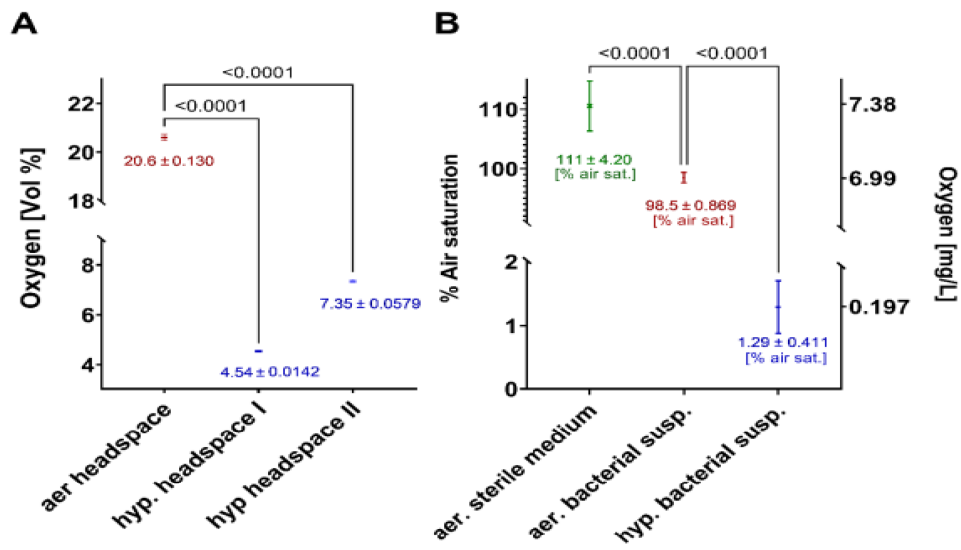


Figure S3: Determined oxygen levels in (A) headspace [Vol%] and (B) culture medium [% air saturation], measured each under aerobic and hypoxic conditions. Stabilized methylene blue solution was employed to survey oxygen conditions before measuring. In graph B, oxygen [mg/L] is displayed together with % air saturation to enable comparison with literature studies. These values were calculated using a calculation sheet free of charge of the manufacturer of the oxygen measurement equipment (available at: <https://www.presens.de/support-services/download-center/tools-utilities> - Oxygen Unit Calculation (Excel Sheet)). The recorded temperatures during measurements were included in the calculation.

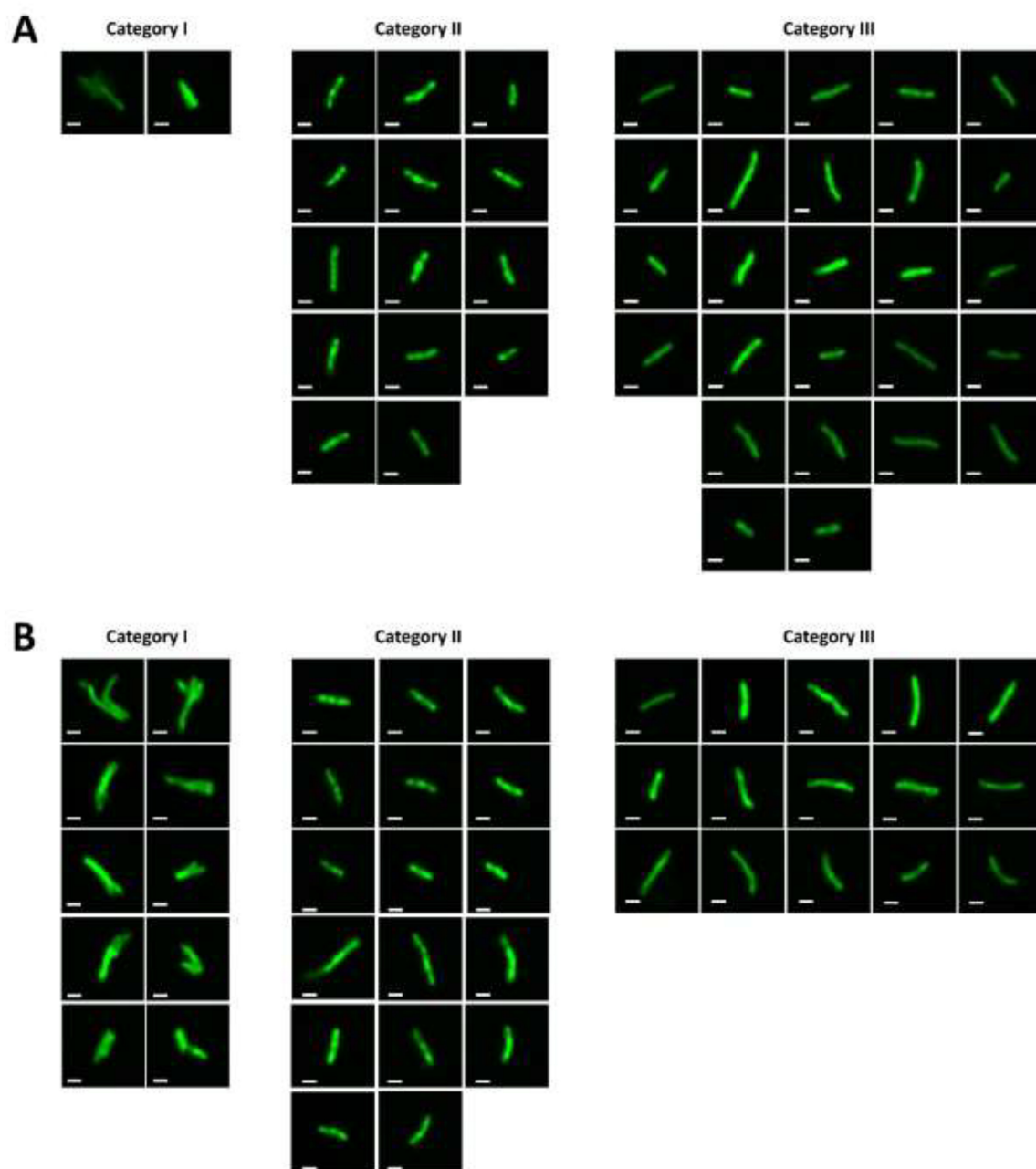


Figure S 4: Representative selection of *M. abscessus* cells pre-treated under two different conditions that were afterwards stained with compound 1 and analyzed by confocal laser scanning microscopy. Pictures are sorted by their morphological appearance into three different categories as explained within the publication. (A) Cells from LOP-culture incubated in hypoxic box and (B) cells from aerobic culture incubated in 5 % CO<sub>2</sub>, scale bar 1 μm.



## Publication list

### Scientific articles in peer reviewed journals

**Feilcke R**, Eckenstaler R, Lang M, Richter A, Imming P.  
*A Simple In Vitro Method to Determine Bactericidal Activity Against Mycobacterium abscessus Under Hypoxic Conditions.*  
Antibiotics (MDPI). **2025** Mar 13; 14(3): 299  
doi: 10.3390/antibiotics14030299

**Feilcke R**, Bär V, Wendt C, Imming P.  
*Antibacterial and Disinfecting Effects of Standardised Tea Extracts on More than 100 Clinical Isolates of Methicillin-Resistant Staphylococcus aureus.*  
Plants (MDPI). **2023** Sep 29; 12(19):3440  
doi: 10.3390/plants12193440

**Feilcke R**, Arnouk G, Raphane B, Richard K, Tietjen I, Andrae-Marobela K, Erdmann F, Schipper S, Becker K, Arnold N, Frolov A, Reiling N, Imming P, Fobofou SAT.  
*Biological activity and stability analyses of knipholone anthrone, a phenyl anthraquinone derivative isolated from Kniphofia foliosa Hochst.*  
J Pharm Biomed Anal. **2019** Sep 10; 174:277-285.  
doi: 10.1016/j.jpba.2019.05.065

Richard K, Schonhofer C, Giron LB, Rivera-Ortiz J, Read S, Kannan T, Kinloch NN, Shahid A, **Feilcke R**, Wappler S, Imming P, Harris M, Brumme ZL, Brockman MA, Mounzer K, Kossenkov AV, Abdel-Mohsen M, Andrae-Marobela K, Montaner LJ, Tietjen I.  
*The African natural product knipholone anthrone and its analogue anthralin (dithranol) enhance HIV-1 latency reversal.*  
J Biol Chem. **2020** Oct 9; 295(41):14084-14099  
doi: 10.1074/jbc.RA120.013031

**Feilcke R**, Goddard R., Imming P, Seidel R.W.  
*A structural study of seven N-acylindolines and their Pd(II)-mediated intramolecular oxidative coupling reactions for the synthesis of pyrrolophenanthridone alkaloids*  
J Mol Struc. **2019** Feb 15; 341-351  
doi:10.1016/j.molstruc.2018.10.031

### Scientific article in a non-peer reviewed journal

Ilchmann, R.  
Unterschiede in Gehalt und Zusammensetzung der Flavonoide in Moringa-Arten  
Deutsche Apotheker Zeitung, **2014** April 02, 155. Jahrg. Nr 14

Poster presentations

HIPS Symposium 2024 on pharmaceutical sciences devoted to infection research

16.05.2024, Saarbrücken

Poster on LOPs assay development

Gordon Research Conference Tuberculosis Drug Discovery and Development 2023

23.07.-28.07.2023, Castelldefels, Spain

Poster on LOPs assay development

Pharma Research Day 2023

University of Halle-Wittenberg, 07.2023, Halle

Poster on preliminary results regarding LOPs assay

DPhG – Doktorandentagung

01.-03.03.23, Bonn, Germany

Poster on the knipholone anthrone study

EMBO Conference on Tuberculosis - Interdisciplinary research on tuberculosis and pathogenic mycobacteria

19.-23.09.2016 Paris, Institute Pasteur, France

Poster on synthetic routes to hippadine like alkaloids

Oral Presentation

Research Symposium “Targets and inhibitors of Mycobacteria including Non-Tuberculous Mycobacteria” - Three-day conference at the University of Toronto, 8-9 July 2024

30 min talk about microbiological assay development

# Curriculum Vitae

<b>Name</b>	Ruth Feilcke, geb. Ilchmann	
<b>Education</b>	06.07	Allgemeine Hochschulreife (Aloys-Henhöfer-Schule Kleinsteinbach)
	04.09-10.13	Pharmacy studies (Johannes-Gutenberg-University Mainz)
	11.13-04.14	Diploma student under the supervision of Prof. Dr. Dr. h.c. Reinhard Neubert (Martin-Luther-University Halle-Wittenberg and Addis Abeba University) Titel of the diploma thesis “Comparative study of Flavonoids in Moringa stenopetala and Moringa oleifera” Awarded with the UniDAZ Wissenschaftspreis 2015
	05.14-11.14	Pharmacy trainee in a public pharmacy “Phoenix Apotheke Silberhöhe”, Halle
	12.14	Approbation as pharmacist
<b>Doctoral thesis</b>	since 01.15	PhD student under the supervision of Prof. Dr. Peter Imming (Martin-Luther-University Halle-Wittenberg)
	09.17-11.20 and 02.21-07.22	Maternity and parental leave
<b>Voluntary time</b>	08.06-08.07	Teacher for German students in a home-schooling- program in Awassa, Ethiopia

# Eidesstattliche Erklärung

Hiermit erkläre ich, dass ich die vorliegende Dissertationsschrift gemäß der Promotionsordnung der Naturwissenschaftlichen Fakultät I (Biowissenschaften) der Martin-Luther-Universität Halle-Wittenberg selbstständig und ohne fremde Hilfe angefertigt habe. Insbesondere habe ich beim Schreiben der Arbeit keinen Gebrauch von künstlicher Intelligenz gemacht. Das Übersetzungsprogramm DeepL ([www.deepl.com](http://www.deepl.com)) diene als Hilfestellung beim Umformulieren mancher Sätze und beim Finden von alternativen Vokabeln. Alle verwendeten Quellen sowie die wörtliche oder inhaltliche Wiedergabe derselben wurden kenntlich gemacht. Alle von anderen Personen erbrachten Leistungen (z.B. im Rahmen einer Kooperation) wurden in der Arbeit als solche gekennzeichnet.

Die Dissertation wurde ausschließlich der Naturwissenschaftlichen Fakultät I der Martin-Luther-Universität Halle-Wittenberg vorgelegt und an keiner anderen universitären Einrichtung weder im Aus- noch im Inland, zur Erlangung des Doktorgrades eingereicht. Ich habe bisher keine früheren erfolglosen Promotionsversuche unternommen.

---

Datum, Ort

---

Ruth Feilcke